Functioning of a 4-chlorosalicylate degrading bacterial consortium: understanding responses to environmental challenges

Von der Fakultät für Lebenswissenschaften

der Technischen Universität Carolo-Wilhelmina

zu Braunschweig

zur Erlangung des Grades eines

Doktors der Naturwissenschaften

(Dr. rer. nat.)

genehmigte

D i s s e r t a t i o n

von Filip Jakub Kaminski

aus Lodz / Polen

1. Referent: apl. Professor. Dr. Dietmar H. Pieper
2. Referent: Privatdozent Dr.-Ing. Max Schobert
eingereicht am: 21.12.2011
mündliche Prüfung (Disputation) am: 24.04.2012

Druckjahr 2013

Vorveröffentlichungen der Dissertation

Teilergebnisse aus dieser Arbeit wurden mit Genehmigung der Fakultät für Lebenswissenschaften, vertreten durch den Mentor der Arbeit, in folgenden Beiträgen vorab veröffentlicht:

Publikationen

Cámara, B., Bielecki, P., **Kaminski, F.**, Santos, V. D., Plumeier, I., Nikodem, P. and Pieper, D. H. A gene cluster involved in degradation of substituted salicylates via ortho cleavage in Pseudomonas sp. strain MT1 encodes enzymes specifically adapted for transformation of 4-methylcatechol and 3-methylmuconate. Journal of Bacteriology 189: 1664-1674 (2007).

Table of contents

RESULTS

Acknowledgments

I would like to express my gratitude to all those who gave me the possibility to complete this thesis. Above all I want to thank my supervisor Prof. Dr. Dietmar Pieper for his excellent and committed guidance as well as his outstanding insight into the research project.

I would like to thank Prof. Dr. Dietmar Schomburg and PD Dr. Max Schobert for taking part in my PhD Committee.
I would also like to thank my initial supervisor Dr. Vitor Martins dos Santos for providing me with the subject for this dissertation.

Numerous people shared with me kindly their time and expertise what helped me to master many techniques from areas of microbiology and molecular biology. I would like to mention here: Iris Plumeier for her assistance with mating experiments, Patrizia Nikodem for her guidance with enzymatic activity assays, Steffi Tillmann and Birgit Jung for introduction into the immunofluorescence, Peter Golyshin and Tatyana Chernikova for plenty of useful tips on constructing genomic phage libraries. The DNA sequencing of inserts from genomic libraries would never be accomplished on time without excellent work of Anette Krüger and Brigitta Happe. Roberto Bobadilla, Beatriz Camara, Massimo Strocchi, Marcelo Comini and Miguel Godinho are all much appreciated for hours-long discussions that were both helpful in designing experiments and often thought-provoking. I truly enjoyed working in the friendly and supportive environment.

Many thanks I would like to direct to Dr. Heinrich Lünsdorf and Dr. Faiza Rharbaoui for introducing me to epifluorescent microscope and uncovering secrets of flow cytometry, respectively.
I have enormous debt of gratitude to Dr. Helena Sztajer who supported me in the most difficult moments and was always ready to share her know-how, friendship and advice.

I want to thank my Family, especially my wife Renata and our son Mikolaj, and all my Friends for being always so supportive and encouraging.
I would also like to express my sincere gratitude to Prof. Ian Graham, Dr. Thilo Winzer and all my colleagues from CNAP at the Univeristy of York for their generous support, encouragement and understanding.

Finally, I would also like to thank once again my supervisor Prof. Dr. Dietmar Pieper for putting up with me and being wonderfully kind human being.

Abbreviations

2,4,5-T	2,4,5-trichlorophenoxyacetate
2,4-D	2,4-dichlorophenoxyacetate
4-CC	4-chlorocatechol
4-CS	4-chlorosalicylate
5-CS	5-chlorosalicylate
AOB	ammonium oxidizing bacteria
bp	base pairs
BSA	bovine serum albumin
cDNA	complementary DNA
CFU	colony-forming units
CIAP	calf intestine alkaline phosphatase
CoA	Coenzyme A
D	dilution rate
DAPI	4',6-diamidine-2'-phenylindole
DIG	digoxigenin
DNA	deoxyribonucleic acid
dNTP	deoxynucleotide triphosphates (equimolar mix of dATP, dCTP, dGTP & dTTP)
EDTA	ethylene diamine tetraacetate (disodium salt)
EPPS	4-(2-hydroxyethyl)piperazine-1-propanesulfonic acid
FCM	flow cytometry
F*IS*H	Fluorescent *In Situ* Hybridisation
FRET	Fluorescence Resonance Energy Transfer
g	gravity of Earth (acceleration, equal to 9,81 m/s^2)
HPLC	High Performance/Pressure Liquid Chromatography
IPTG	isopropyl-1-thio-β-D-galactopyranoside
K_S	affinity constant (for substrate)
LB	Luria-Bertani medium
M	molar
MALDI	Matrix Assisted Laser Desorption-Ionisation
MCPA	2-methyl-4-chlorophenoxyacetic acid
MCI	muconate cycloisomerase
MS/MS	tandem Mass Spectrometry
MT1	*Pseudomonas reinekei* MT1
MT1/MT3	binary culture of *P. reinekei* MT1 and *A. xylosoxidans* MT3
MT1/MT4	binary culture of *P. reinekei* MT1 and *P. veronii* MT4
MT2	*Empedobacter brevis* MT2
MT3	*Achromobacter xylosoxidans* MT3
MT4	*Pseudomonas veronii* MT4
NADH	nicotinamide dinucleotide
ND	not determined
OD_{600}	optical density at a wavelength of 600 nm
ORF	open reading frame
PBS	phosphate buffered saline

PCR	polymerase chain reaction
PEG	polyethylene glycol
pfu	plaque-forming units
RNA	ribonucleic acid
rRNA	ribosomal RNA
RT	room temperature
RW10	*Pseudomonas moorei* RW10
SDS	sodium dodecyl sulfate
S_{min}	minimum concentration of substrate
SSC	saline-sodium citrate buffer (sodium chloride and trisodium citrate)
TOF	time-of-flight
U	unit
UV	ultraviolet light
vvm	aeration rate (gas volume flow per unit of liquid volume per minute)
w/v	weight per final volume
X-gal	5-bromo-4-chloro-3-indolyl-β-D-galactoside
μ	specific growth rate
μ_{max}	maximum specific growth rate

SUMMARY

Biodegradation of recalcitrant xenobiotic pollutants, such as chlorinated aromatics, which pose a significant threat to human health, is a complex process that often involves the coordinated action of complex microbial communities. In this work, the functioning of a four-membered bacterial consortium consisting of *Pseudomonas reinekei* MT1, *Empedobacter brevis* MT2, *Achromobacter xylosoxidans* MT3 and *Pseudomonas veronii* MT4, that had been isolated for its capability to grow on 4-chlorosalicylate (4-CS), was studied.

Genetic and biochemical analysis of the possible contribution of the different community members identified two gene clusters in the genome of strain MT1, the only consortium strain that can grow on 4-CS as monoculture and is thus assumed as being responsible for shaping the community, as encoding enzymes relevant for the degradation of aromatic and chloroaromatic compounds. The *sal* gene cluster encodes a salicylate 1-hydroxylase of broad substrate specificity, including 4-CS, as well as a catechol 1,2-dioxygenase and a muconate cycloisomerase ($C12O_{salD}$ and MCI_{salC}) that are specialized for converting methylsubstituted derivatives but also crucial for 4-CS degradation. Genes from the *pca* cluster encode enzymes of the protocatechuate branch of the 3-oxoadipate pathway crucial for channeling of 3-oxoadipate derived from 4-CS degradation into the central metabolism. Evidence was accumulated that MT3 is capable of degrading the *cis*-dienelactone metabolite.

To be capable to study the robustness of the microbial consortium, its efficiency under changing environmental conditions like variation in temperature and oxygen supply and availability of carbon source, a rapid, reproducible and accurate F*IS*H-flow cytometry enumeration technique was developed, which allowed a detailed characterisation of the community composition over time.

Typically, in addition to MT1, strain MT3 was identified as an abundant member of the consortium under continuous culture conditions, as supported by binary culture experiments, providing evidence that this strain significantly share metabolites produced by MT1, even though growth on the critical metabolite 4-chlorocatechol could not be observed in pure culture. MT4 as well as MT2 constituted only minor community members, as also evidenced by a MT1/MT4 binary culture.

The consortium was capable of growth and efficient mineralization of 4-CS at temperatures between 12 and 30°C in agreement with the temperature range of growth of its crucial member *P. reinekei* MT1. 4-Chlorocatechol was identified as critical metabolite obviously negatively influencing growth at higher temperatures. Anaerobiosis had a detrimental effect on the functioning of the consortium, where the accumulation of toxic 4-chlorocatechol produced by MT1 resulted in severe alterations of the community composition, specifically negatively affecting the producing organism. Remarkably, under favourable conditions the community was capable to rapidly recover both its primary structure and degradative function. An increase in dilution rate resulted in a remarkable increase in biomass and in alterations in community composition, with strain MT3 becoming the predominant community member. Thus, the efficiency of assimilation of carbon from 4-CS depends on the composition of the community and is positively correlated with the content of MT3. Overall, these experiments indicate MT3 to be responsible for preventing and overcoming environmental perturbations and sharing significant amount of substrate carbon processed by MT1, probably by assimilating 4-chlorocatechol and *cis*-dienelactone.

Zusammenfassung

Der Abbau xenobiotischer Schadstoffe, z.B. von chlorierten Aromaten, welche eine signifikante Gefahr für die menschliche Gesundheit darstellen, ist ein komplexer Prozess, der oft ein koordiniertes Zusammenspiel verschiedener Mitglieder komplexer mikrobieller Gemeinschaften erfordert. In der vorliegenden Arbeit wurde die Funktion einer mikrobiellen Gemeinschaft untersucht, die aus *Pseudomonas reinekei* MT1, *Empedobacter brevis* MT2, *Achromobacter xylosoxidans* MT3 und *Pseudomonas veronii* MT4 besteht, und welche aufgrund ihrer Fähigkeit 4-Chlorsalicylat (4-CS) abzubauen isoliert wurde.

Die genetische und biochemische Analyse möglicher Beiträge der Gemeinschaftsmitglieder zum Abbau führte zur Identifizierung von zwei für den Chloraromaten- und Aromatenabbau wichtigen Genclustern im Stamm MT1. Dieser ist als einziger Stamm der Gemeinschaft befähigt, 4-CS in Monokultur zu verwerten und wird somit als verantwortlich für die Zusammensetzung der Gemeinschaft angenommen. Das *sal* Gencluster kodiert für eine Salicylat 1-Hydroxylase mit breiter Substratspezifität, als auch für eine Catechol 1,2-Dioxygenase und eine Muconat Cycloisomerase welche speziell an den Abbau methylsubstituierter Derivative angepasst, aber auch für den Abbau von 4-CS wichtig sind. Die Gene des *pca* Clusters kodieren für Enzyme des Protocatechuat-Astes des 3-Oxoadipat-Abbauweges und sind entscheidend für das Einleiten von 3-Oxoadipat als Metabolit des 4-CS-Abbaus in den zentralen Stoffwechsel. Zudem wurden Hinweise dafür gewonnen, dass MT3 den Metaboliten *cis*-Dienlacton abbauen kann.

Um die Robustheit des mikrobiellen Konsortiums, und seine Effizienz unter veränderten Umweltbedingungen (Temperaturschwankungen, Sauerstoffversorgung, Verfügbarkeit von Kohlenstoffquellen) untersuchen zu können, wurde eine schnelle und reproduzierbare Durchflusszytometrie/F*IS*H Technik entwickelt, die eine detaillierte Charakterisierung der Zusammensetzung der Gemeinschaft über die Zeit erlaubt.

Typischerweise konnte in kontinuierlicher Kultur neben dem Stamm MT1 auch Stamm MT3 als anteilsmäßig häufiges Gemeinschaftsmitglied nachgewiesen werden. Dies wurde auch in binärer Kultur beobachtet und weist darauf hin, dass MT3 in signifikantem Ausmaß durch MT1 produzierte Metabolite verwertet, obwohl z.B. ein Wachstum mit 4-Chlorcatechol als zentralem Metaboliten in Reinkultur nicht beobachtet werden konnte. Im Gegensatz dazu waren MT4 und nur untergeordnete Gemeinschaftsmitglieder.

Das Konsortium wuchs mit 4-CS und zeigte eine effiziente Mineralisierung bei Temperaturen zwischen 12 and 30°C, was in Einklang mit der Wachstumstemperatur von MT1 steht. 4-Chlorcatechol konnte als kritischer Metabolit, welcher das Wachstum bei höheren Temperaturen beeinträchtigt, nachgewiesen werden. Anaerobiose erwies sich als schädlich für die Funktionsfähigkeit des Konsortiums, da durch den Stamm MT1 produziertes 4-Chlorocatechol zu erheblichen Veränderungen in der Zusammensetzung führte, und insbesonders den produzierenden Stamm MT1 negativ beeinflusste. Bemerkenswerterweise war die Gemeinschaft unter günstigen Bedingungen zu einer raschen Erholung befähigt und erlangte ihre ursprüngliche Zusammensetzung und Funktion. Eine Steigerung der Verdünnungsrate führte zu einem aussergewöhnlichen Anstieg der Biomasse und Veränderungen in der Zusammensetzung der Gemeinschaft, dahingehend, dass MT3 das dominierendes Mitglied darstellte. Somit ist die Effizienz der Assimilierung von Kohlenstoff aus 4-CS von der Gemeinschaftszusammensetzung abhängig und positiv mit dem Anteil an MT3 korreliert. Zusammenfassend deuten die Experimente darauf hin, dass MT3 für die Prävention und Überwindung von Störeinflüssen wichtig ist, und einen signifikanten Anteil des von MT1 prozessierten Substrates verwertet, möglicherweise durch die Assimilierung von 4-Chlorcatechol und *cis*-Dienlacton.

1. INTRODUCTION

1.1. The importance of microbial communities

Pure cultures were classically considered as essential for studies in microbiology. Until recently only pure cultures allowed to get insights into the genetics, biochemistry and physiology of microbes. However, the cultivation-dependent microbiology did not take into consideration that microorganisms in nature almost exclusively exist in the form of complex communities (Madigan & Martinko, 2005). Furthermore, physiological studies in axenic culture disregard the influence of the biotic environment. Finally, appropriate conditions for growth of pure cultures are currently known only for a small fraction of all microorganisms.

Habitats like aquifers, terrestrial ecosystems or the guts of higher organisms are populated by complex microbial communities in which individual species interact in various ways, both harmful and beneficial (Madigan & Martinko, 2005). These interactions can be described as a constant chemical cross-talk as the metabolites produced by one microorganism may interfere with the growth of other populations. However, as it will be dissected further, these interactions in communities are usually quite complex, forming elaborate and diverse networks.

The importance of microbial communities was largely overlooked until the realisation that the vast majority of microorganisms from the environment has never been cultivated (for instance: Wagner *et al.*, 1993). Knowledge on the phylogenetic diversity, the quantitative structure of the communities as well as unravelling the processes that take place within communities may help to understand how the ecosystems really work on the microscale. This information may also hold a paramount diagnostic value and may open up possibilities for improving biologically-mediated processes, e.g. bioremediation. The emerging interest in microbial communities together with the rapid progress in DNA sequencing technologies uncovered various ‘community genomes’ or so-called meta-genomes. For instance, oceanic microbial diversity in the Sargasso Sea was assessed by the whole-genome shotgun sequencing of the filtered seawater samples (Venter *et al.*, 2004). Similarly, through large-scale DNA sequencing it was established that among ammonia-oxidizing microorganisms in soil those of archeal origin greatly outnumber their proteobacterial counterparts (Leininger *et al.*, 2006). The on-going Human Microbiome Project aiming to describe microbial communities associated with the human body might be perceived as a logical consequence of the recognition that ‘bacterial societies’ gain from the microbiologists (Turnbaugh *et al.*,

2007, Dethlefsen *et al.*, 2007). Some of the reasons why microbial communities have attracted so much attention are illustrated with examples below.

1.1.1. The role of microbial communities in the cycling of carbon

Bacterial and archeal communities that are involved in carbon cycling under anoxic conditions stand out as an example of relatively well-studied microbial associations. Constant circulation of carbon in anaerobic habitats would not be possible without the activities of certain highly specialized communities (Fig. 1.1.).

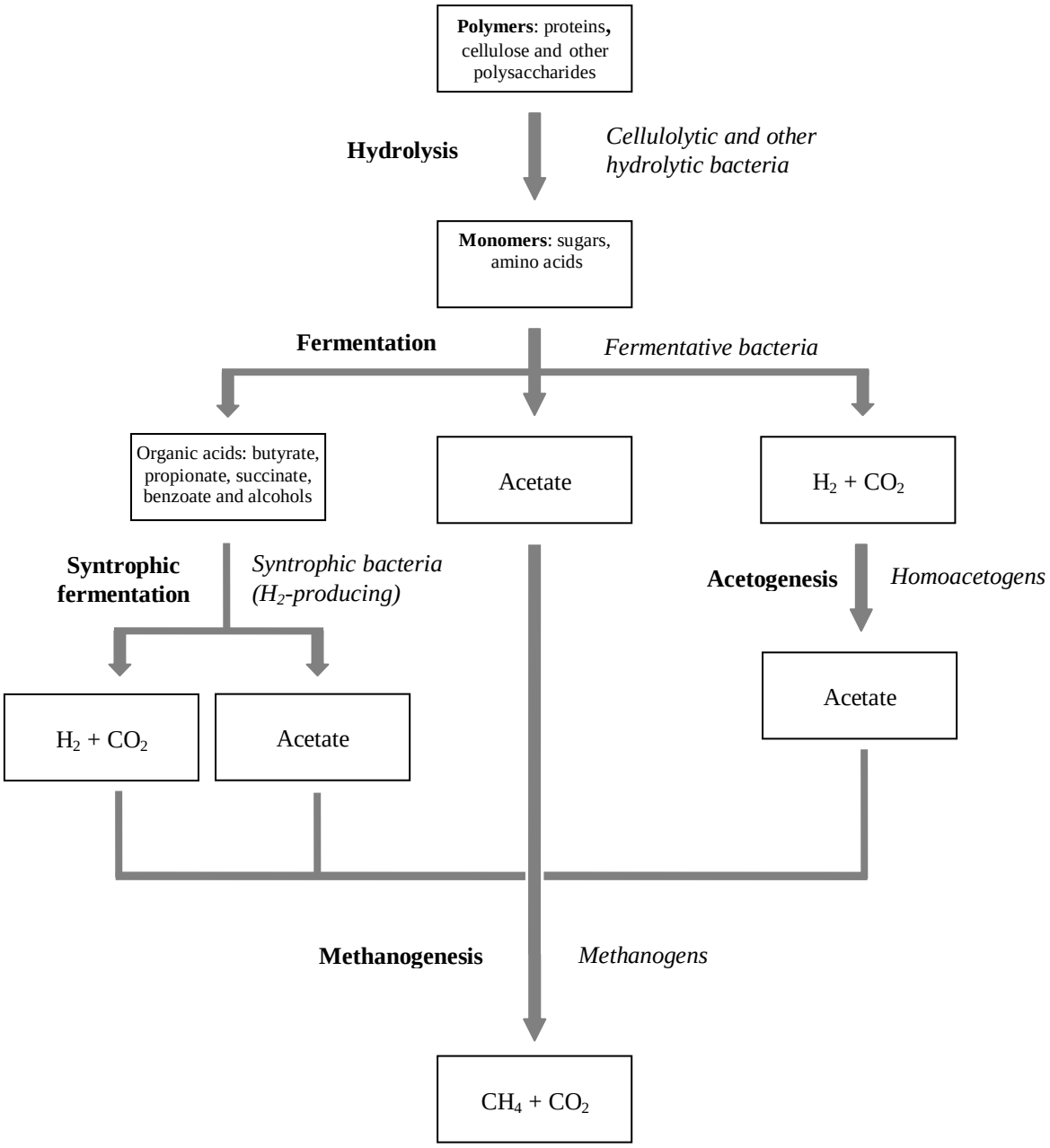

Figure 1.1. Decomposition and carbon flow under anoxic conditions.

Interactions between the particular community members that allow some of the partners to extract the energy from the otherwise endergonic processes demonstrate both simplicity and ingenuity of evolutionary solutions.

The vast majority of bioprocesses that result in decomposition of organic matter in the freshwater sediments and sewage occurr under anoxic conditions. Conversion of polymeric substances like polysaccharides, proteins and lipids ultimately into methane (CH_4) and carbon dioxide (CO_2) requires cooperation of several physiologically unique groups of procaryotes (Madigan & Martinko, 2005). As soon as the hydrolysis of biopolymers results in the corresponding monomers – sugars, amino acids and fatty acids – this pool of substrates enters the fermentative metabolism of a group of bacteria termed *primary fermenters*. Glucose, originating from the decomposition of cellulose and starch, is fermented to the variety of products but mainly to acetate, propionate, butyrate, succinate, alcohols, H_2 and CO_2. Hydrogen produced in the primary fermentation process is used by methanogenic and homoacetogenic microorganisms or by sulfate-reducing bacteria. Acetate formed by the breakdown of sugars or from CO_2 and H_2 *via* acetogenesis belongs to the very few substrates that can be directly converted into methane by certain methanogens (*Methanosaeta*, *Methanosarcina*). However, the fermentation results in a large number of alcohols and fatty acids that cannot be directly metabolised into CH_4 and CO_2. Alcohols and fatty acids are converted to CH_4 and CO_2 by *secondary fermenters* termed syntrophs. Syntrophs typically ferment their specific substrates such as C_4-C_8 fatty acids (*Syntrophomonas wolfei*), propionate (*Syntrophobacter wolinii*) or aromatic compounds like benzoate (*Syntrophus gentianae*) into acetate, CO_2 and H_2. However, extracting the energy from *secondary fermentation* would not be possible without the activity of methanogenic archea that instantly remove the produced hydrogen. Elimination of hydrogen from the environment causes significant shifts in the free-energy values for syntrophic conversions as shown in the Table 1.1.

Interestingly, the symbiotic relationship of secondary fermenters with their methanogenic partners, that is indispensable for converting fatty acids and alcohols into CH_4 and CO_2 under anoxic conditions, is not obligatory for syntrophs. When other substrates become available many syntrophs can thrive and generate energy in an independent way, without the presence and activity of methanogenes.

On the molecular level, the interactions between syntrophs and methanogens are governed by the transfer of molecular hydrogen. It was historically assumed that this transfer from syntrophic bacteria to methanogenic archea proceeds through a common hydrogen pool in their microenvironment. Studies of Conrad and colleagues (1985) were later confirmed by

MacLeod and colleagues (1990) suggesting a need for physical interactions between syntrophs and methanogens.

Table 1.1. Substrates for some major anoxic conversions, including syntrophic fermentations, their fermenters and corresponding free-energy values (Zinder, 1984; Madigan & Martinko, 2005).

Substrate (products)	Microorganisms	ΔG^0 [kJ][a]	ΔG [kJ][b]
glucose (acetate, H_2, CO_2)	primary fermenters	-207	-319
glucose (butyrate, H_2, CO_2)	primary fermenters	-135	-284
H_2 and CO_2 (methane)	methanogens	-136	-3,2
H_2 and CO_2 (acetate)	homoacetogens	-105	-7,1
butyrate (acetate, H_2)	*Syntrophomonas wolfei*	+48,2	-17,6
propionate (acetate, CO_2, H_2)	*Syntrophobacter wolinii*	+76,2	-5,5
ethanol (acetate, H_2)	*"Methanobacillus omelianskii"*	+19,4	-37
benzoate (acetate, CO_2, H_2)	*Syntrophus gentianae*	+70,1	-18

(a) ΔG^0 – standard conditions of 1 M solutes and 1 atm of gases; (b) ΔG for anoxic freshwater ecosystem: 10 μM glucose, 1 mM fatty acids, 20 mM HCO_3^-, 0,6 atm methane and 10^{-4} atm H_2.

As for every product of primary fermentations like alcohols or fatty acids a pair of syntrophs and methanogens can be found that is able to break it into CH_4 and CO_2 thus these cross-species microbial interactions facilitate circulation of carbon in the ecosystem under anoxic conditions. Close interspecies cooperation in the syntrophic fermentation ensures that both parties share the free-energy generated from two consecutive transformations. Molecular mechanisms of these interactions are so intimate as to demand the physical contact of both microbial partners for the direct hydrogen transfer.

1.1.2. Interactions in the microbial community inhabiting human oral cavity

The oral microflora (dental plaque) belongs to the most complex microbial communities in the human body with over 700 identified bacterial species (Aas *et al.*, 2005; Paster *et al.*, 2001 & 2006; Kroes *et al.*, 1999). Microbial communities residing in the supragingival plaque are dominated by gram-positive streptococci (*Streptococcus sanguinins, S. oralis, S. mutans, S. mitis, S. gordonii, S. salivarius*) and contain lower amount of *Actinomyces* spp., *Eikenella* spp., *Haemophilus* spp., *Prevotella* spp., *Propionibacterium* spp. and *Veillonella* spp. (Nyvad & Kilian, 1987). The subgingival tissues, on the other hand, are mainly colonized by gram-

negative and often anaerobic bacteria such as: *Tannerella forsythia, Actinobacillus actinomycetemcomitans, Capnocytophaga* spp., *Fusobacterium nucleatum, Campylobacter* spp., *Porphyromonas gingivalis, Prevotella intermedia* and *Treponema denticola* (Aas *et al.*, 2005; Paster *et al.*, 2001). Due to the fact that they play an important role in the development of dental caries and periodontitis, the interactions between bacteria in the dental plaque are relatively well studied (Marsh, 2005; Kuramitsu *et al.*, 2007).

Spatial cell-to-cell recognition in the form of coaggregation and coadhesion is essential for retention of bacteria in the constantly flowing environment of the oral cavity (Whittaker *et al.*, 1996; Bos *et al.*, 1996). The formation of complex biofilms of the dental plaque is not merely a stochastic process but involves collaboration of different groups of bacteria. Among them 'early colonizers' (mainly streptococci) are able to bind to the receptors on surfaces of teeth and periodontal tissues, the 'late colonizers' adhere to the primary colonizers and bring to the biofilm useful metabolic and competitive advantages, while some other bacteria like *F. nucleatum* act as coaggregating bridges (Kolenbrander *et al.*, 1989; Kolenbrander *et al.*, 1990; Kolenbrander, 2000).

The intense exchange of metabolites observed in the microbial oral community may have either symbiotic or competitive character. For instance, *S. mutans* produces lactic acid that inhibits many acid-sensitive anaerobes and some oral streptococci like *S. sanguinis* but at the same time it promotes growth of *Veillonellae* sp. that can convert it into less potent acetic acid (Mikx *et al.*, 1975 & van der Hoeven *et al.*, 1978). On the other hand, *S. sanguinis* produces hydrogen peroxide that acts antagonistically towards oxidant-sensitive *S. mutans* (Kreth *et al.*, 2005) and many anaerobic bacteria (Ihalin *et al.*, 2001). Both *F. nucleatum* and *P. intermedia* ferment aspartic and glutamic acid from saliva and crevicular fluid generating ammonia which locally neutralizes the pH and enables survival of acid-sensitive species like *P. gingivalis* in the dental plaque (Takahashi, 2003).

Another mechanism exploited by bacteria that increases their chance of survival in the dental plaque involves exchange of DNA. Natural genetic transformation by the uptake of chromosomal or plasmid DNA has been shown for many oral streptococci in planktonic cultures (Lunsford 1998; Mercer *et al.*, 1999 & Mercer *et al.*, 2001). Genetic exchange in *S. mutans* is mediated through the competence-stimulating peptide (CSP) signalling system (Havarstein *et al.*, 1996 & Lunsford 1998) and was shown to enhance induction of competence and uptake of a variety of plasmid or chromosomal donor DNAs by 10 to 600 times as compared with planktonic cells (Li *et al.*, 2001).

Microorganisms in the dental plaque influence or control their immediate biotic environment by secretion of virulence factors – bacteriocins. Among bacteria in the dental

plaque streptococci are by far the most potent bacteriocins producers (Nes *et al.*, 2007) with *S. mutans* excreting at least five different mutacins (I-V) (Chikindas *et al.*, 1995; Qi *et al.*, 1999 & 2001). Beside streptococci, many other oral bacteria like *P. gingivalis*, *P. intermedia*, *Prevotella nigrescens* (Teanpaisan *et al.*, 1998), *A. actinomycetemcomitans* (Hammond *et al.*, 1987) or *F. nucleatum* (Gaetti-Jardim & Avila-Campos, 1999) use specific bacteriocins to outcompete other strains.

Yet another avenue of interactions exploited by oral bacteria is the interference with signalling systems. In particular, the susceptibility of *S. mutans* to endogenous antimicrobial agents found in saliva (histatins) is modulated by the presence of *S. gordonii* (Matsumoto-Nakano & Kuramitsu, 2006). As it was demonstrated, *S. gordonii* may inactivate the CSP of *S. mutans* by the proteolytic action of challisin and compromise several quorum-sensing mechanisms of the latter strain (Wang & Kuramitsu, 2005).

From the diverse mechanisms of communication between bacteria in the dental plaque it might be perceived that the ability to interact efficiently in the mutualistic or competitive way with other microorganisms is an element of a successful evolutionary strategy of survival in a microbial community.

1.1.3. Microbial consortia in biodegradation of contaminants and 4-chlorosalicylate degrading consortium

In several instances microbial consortia were isolated from the environment by selective enrichment based on their capability to use xenobiotic or natural substrates for growth. Barreiros and colleagues (2003) proposed three distinct types of cooperation that may occur between microorganisms in consortia during biodegradation: metabolic deficiency, metabolic association and metabolite detoxification. In case of **metabolic deficiency** the degradation performed by one microorganism is promoted or enhanced by secondary strains providing specific nutritional factors. For instance, Sørensen and colleagues (2002) observed that the degradation rate of the herbicide isoproturon by *Sphingomonas* sp. SRS2 could be significantly enhanced by the coculture with a soil bacterium termed SRS1. The authors further established that the mechanism of synergy for degradation of isoproturon by SRS2 involves the supply of a specific mixture of amino acids, and particularly methionine, by the strain SRS1. A similar mechanism of metabolic deficiency was suggested to explain why a triclosan-degrading strain *Sphingomonas* sp. Rd1 was unable to grow on the substrate in pure culture but was able to mineralize it in a microbial consortium (Hay *et al.*, 2001). **Metabolic association** is probably the most common form of cooperation in microbial consortia and is

characterised by the cross-feeding of metabolites from the degradation pathway within the members of the community. As an example, the mineralization of chlorinated dibenzofurans can be successfully performed by mixed cultures. Arfmann *et al.* (1997) showed mineralization of 4-chlorodibenzofuran by a consortium consisting of *Sphingomonas* sp. RW1, that attacks the unchlorinated aromatic ring and releases 3-chlorosalicylate, and *Ralstonia* sp. JWS, that is capable to mineralize the latter compound. Also 2- and 3-chlorodibenzofuran were reported to be mineralized in a similar manner by a mixed culture where 4- and 5-chlorosalicylate are excreted by *Sphingomonas* sp. RW16 and further utilized by *Pseudomonas moorei* RW10 (Wittich *et al.*, 1999). Interestingly, some natural compounds are degraded by microbial consortia, as demonstrated for cocaine that was hydrolyzed by *Comamonas acidovorans* MBLF into benzoate and ecgonine methyl ester. *Pseudomonas fluorescens* MBER was capable of growing on both hydrolysis products, but shared the benzoate formed with *C. acidovorans* MBLF (Lister *et al.*, 1996). In **metabolite detoxification**, that can be regarded as a special case of metabolic association, a toxic or inhibitory metabolite produced by the microorganism initiating the degradation is removed by the action of other consortium members (Barreiros *et al.*, 2003). According to this principle, the degradation of 4-aminobenzenesulfonate by a mixed culture is achieved through the combined action of *Hydrogenophaga palleronii* S1, which oxidatively desaminates the substrate into toxic catechol-4-sulfonate which is predominantly excreted into the medium, and *Agrobacterium radiobacter* S2, which efficiently mineralizes this metabolite (Feigel & Knackmuss, 1993).

A microbial consortium capable of degrading 4-chlorosalicylate that was studied in this work also represents an example of interactions that rely primarily on metabolite detoxification (Pelz *et al.*, 1999). A four-membered MT bacterial consortium was isolated from the sediment of the highly polluted Spittelwasser creek (Lower Sachsony, Germany) through selective enrichment in a chemostat using 4-chlorosalicylate (4-CS) as a sole carbon source (Faude, 1995). By a series of experiments applying ^{13}C-labelled isotope tracers, it could be established that the cooperation in the consortium has a metabolic character (Pelz *et al.*, 1999). The authors observed that only *P. reinekei* MT1, the strain dominating the four-membered consortium, is capable of degrading 4-CS, however with the excretion of 4-chlorocatechol and protoanemonin as toxic intermediates which are assimilated by *A. xylosoxidans* MT3 and *P. veronii* MT4, respectively (Pelz *et al.*, 1999). A schematic view of the carbon flow within the consortium, as proposed by Pelz and colleagues (1999) and modified according to biochemical evidence (Nikodem, 2004; Camara *et al.*, 2009), is shown in Figure 1.2.

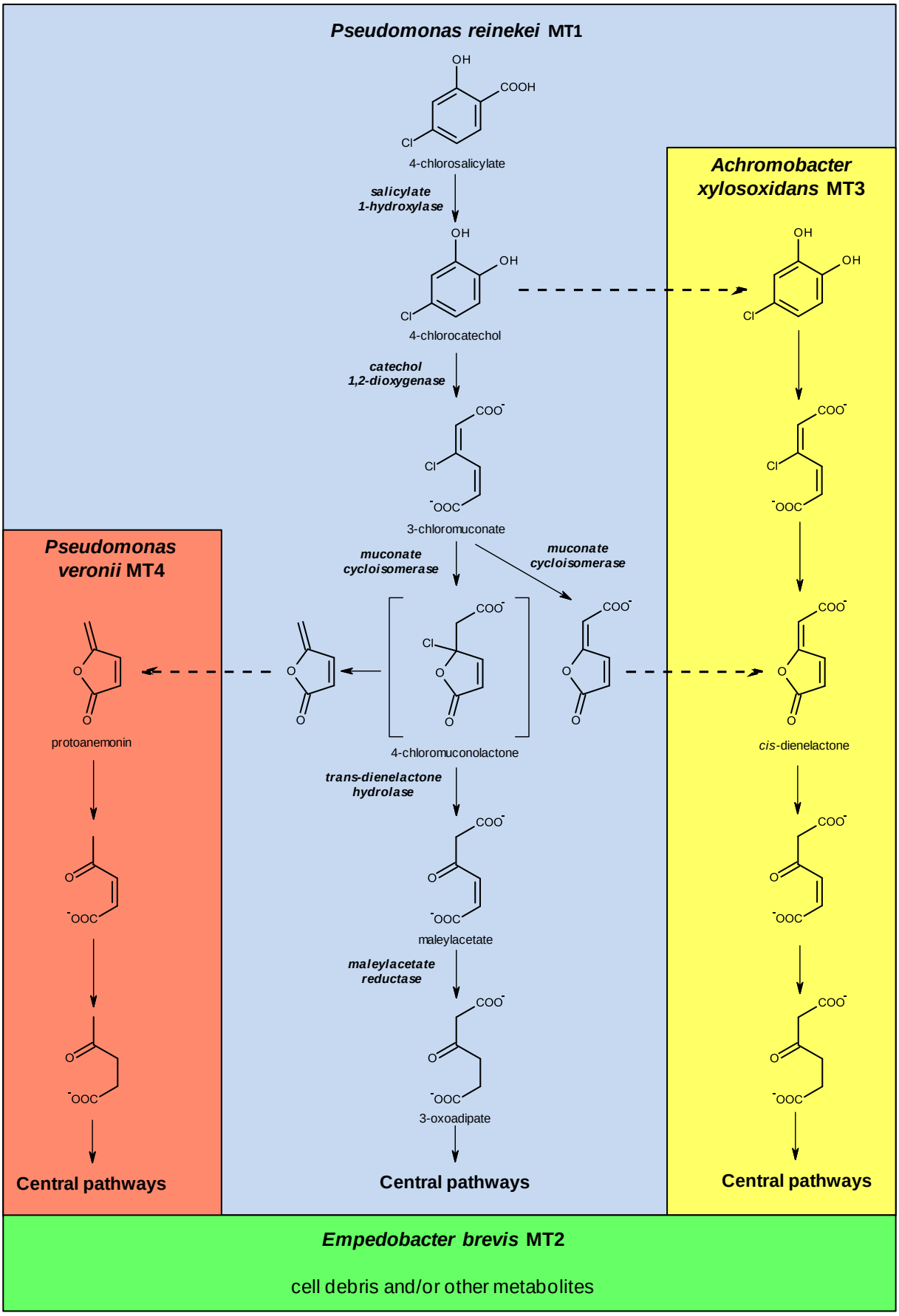

Figure 1.2. Current view on the carbon flow in a 4-chlorosalicylate degrading bacterial consortium (modified after Pelz *et al.*, 1999; Nikodem, 2004; Camara *et al.*, 2009).

Elucidation of the metabolic route of 4-CS degradation by MT1 identified a novel pathway, where 4-CS is transformed by a salicylate 1-hydroxylase to 4-chlorocatechol, which is subject to intradiol cleavage by a catechol 1,2-dioxygenase. However, in contrast to previously described pathways for 4-chlorocatechol degradation, which involve the cycloisomerization of intermediate 3-chloromuconate by a chloromuconate cycloisomerase exclusively to *cis*-dienelactone followed by a dienelactone hydrolase forming maleylacetate, *cis*-dienelactone was only a minor metabolite formed during cycloisomerization of 3-chloromuconate by MT1, which was not further transformed (Nikodem *et al.*, 2003). In contrast, evidence was given, that 3-chloromuconate was transformed by a muconate cycloisomerase activity with 4-chloromuconolactone as central intermediate. 4-Chloromuconolactone in turn may spontaneously decarboxylate and dechlorinate, resulting in protoanemonin as highly toxic intermediate (Blasco *et al.*, 1995). However, in MT1 a *trans*-dienelactone hydrolase hydrolyzes 4-chloromuconolactone to form maleylacetate, which is further reduced by a maleylacetate reductase giving 3-oxoadipate. The action of *trans*-dienelactone hydrolase, a novel type of zinc-dependent hydrolases acting on 4-chloromuconolactone and *trans*-dienelactone, but not on *cis*-dienelactone (Camara *et al.*, 2008), reduces but does not completely prevent the formation of protoanemonin, which is a dead-end metabolite for MT1. Genes encoding enzymes of this pathway were identified on two gene clusters termed *sal* and *cca*, whereas enzymes of the catechol pathway, that are typically encoded on the chromosome of *Pseudomonas* strains, were not involved in the degradative pathway (Camara *et al.*, 2007). The *sal* gene cluster, which will be described in this work, encodes salicylate 1-hydroxylase, catechol 1,2-dioxygenase and muconate cycloisomerase activities, which are highly adapted for the transformation of methylsubstituted substrates (Camara *et al.*, 2007), whereas the *cca* cluster encodes novel types of catechol 1,2-dioxygenase and muconate cycloisomerase as well as *trans*-dienelactone hydrolase and maleylacetate reductase crucial for chloroaromatic degradation by MT1 (Camara *et al.*, 2009). A fourth gene cluster termed *mml* was described as essential for the further metabolism of 4-methylmuconolactone formed from 4- and 5-methylsalicylate by enzymes encoded by the *sal* cluster (Marin *et al.*, 2010).

In effort to create a proteome reference map for *P. reinekei* MT1 118 different proteins could be identified (Bobadilla, 2006). The proteome was then analysed in pure cultures of MT1 as well as in mixed cultures of MT1 with MT3 to characterise the specific responses to shock loads of 4-CS and high concentrations of the toxic metabolites 4-chlorocatechol and protoanemonin. The comparative proteomic study showed remarkable differences in the

composition of the outer membrane of MT1 when grown in pure versus mixed culture (Bobadilla, 2006), possibly indicating a reduction of stress through the action of MT3.

In earlier work, Rabenau (2004) compared the growth of MT1 on 4-CS with that of the whole consortium, however, only negligible differences in growth rate were observed. The same author studied the influence of various biotic and abiotic perturbations on the community. As expected, the addition of a second carbon source to a consortium growing on 4-CS resulted in significant changes in the community structure, where MT4 was highly adapted to grow on histidine and MT2 to grow on nutrient broth. Reduced aeration in the continuous culture was reported not to have a major effect on the degradation of 4-CS and on the composition of the consortium, however, the expression of an alternative 4-chlorocatechol *meta*-cleavage pathway was observed, which resulted in the accumulation of the yellow colored ring-cleavage product (Rabenau, 2004). It may be speculated that this transformation is due to the expression of enzymes of a 2,3-dihydroxybenzoate degradative pathway which was recently identified in MT1 (Marin *et al.*, unpublished).

However, despite the years of extensive studies not much is hitherto known about the influence of parameters that are often crucial for *in situ* bioremediation like temperature, substrate supply and aeration on the fine-scale structure and functioning of the 4-CS-degrading consortium.

1.2. The chemostat as a model system for investigation of microbial communities

Since the time of its invention by Novick & Szilard (1950a) and Monod (1950), cultivating microorganisms in a chemostat or 'bactogène' contributed enormously to the understanding of microbial growth, physiology, genetics or ecology. In principle, the chemostat is a culture vessel having an input aperture for the influx of sterile nutrient medium and an overflow aperture for the efflux of exhausted medium, living cells and cellular debris (Dykhuizen & Hartl, 1983). More sophisticated set-ups used both in the laboratory and in industrial practice contain one or several detectors (electrodes) plus external devices that allow to measure and precisely control physicochemical factors like temperature, pH, and oxygen concentration. An exemplary chemostat system, that was used in this study for analysing the 4-CS degrading community is shown in Figure 1.3.

In the chemostat the growth of biomass is equal to and limited by the rate at which the culture is being diluted (D). Under steady-state conditions the concentration of biomass in the

vessel is constant and the growth rate of a given microorganism $\mu = D$ can be adjusted within its specific limits ($0 < \mu \leq \mu_{max}$). If the dilution rate exceeds the maximum specific growth rate of the microorganisms under the given conditions ($D > \mu_{max}$) the culture is washed out.

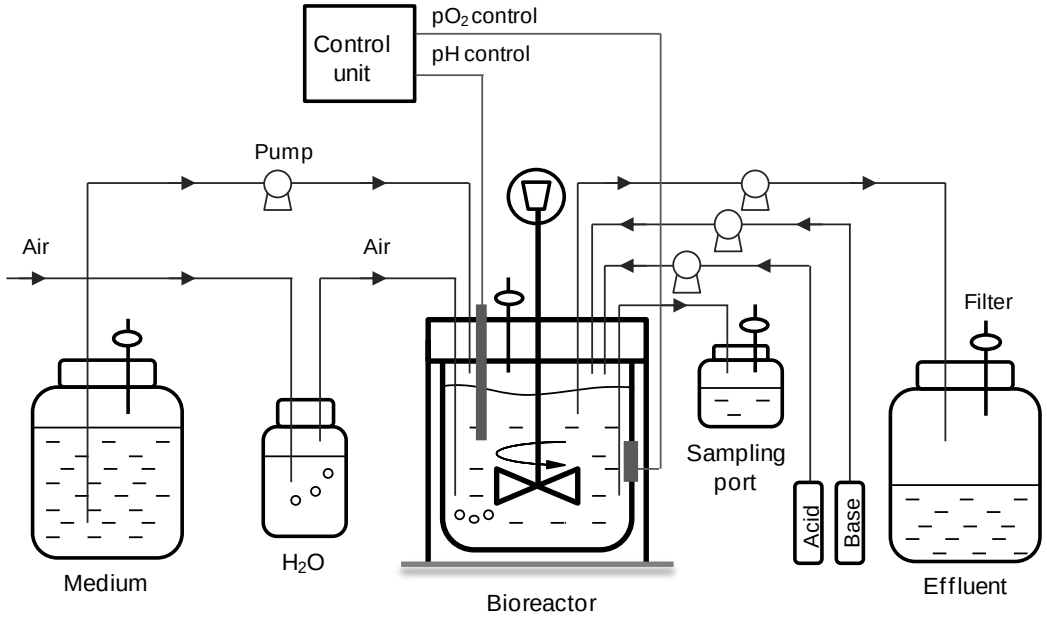

Figure 1.3. Schematic view of the chemostat system used for study over the 4-CS degrading consortium.

Although it was initially thought as a vehicle to maximize productivity of bacterial cells (Monod, 1950) or to study the rate of mutations (Novick & Szilard, 1950b), the chemostat almost instantly gained popularity in the fields of microbial physiology, biochemistry and microbial ecology. The main reasons for its success were: (i) the possibility of obtaining large biomass of metabolically uniform cells grown under defined conditions and (ii) its simplicity in controlling microbial growth that allowed the chemostat to outcompete other methods of continuous cultivation like the turbidostat (Bryson & Szybalski, 1952) or the pH auxostat (Martin & Hempfling, 1976).

Cultivation in the chemostat provided mathematical descriptions of microbial growth kinetics for various combinations of microorganisms and substrates (K_s, μ_{max} and s_{min}) and helped to understand the correlation between the specific growth rate (μ) and the concentration of substrate (s). It, however, also revealed various novel phenomena. For instance, it was found that cells in the chemostat could be 'trained' to increase their specific growth rate (μ_{max}) (Dean & Hinshelwood, 1966) or affinity towards the substrate (decreased K_s) (Senn *et al.*, 1994). Another important observation concerns the ability of heterotrophic microorganisms to simultaneously assimilate different carbon sources under carbon-limited

conditions. When faced with a mixture of potential carbon sources, each one at a concentration of only a few µg/l many heterotrophic microorganisms support their growth by simultaneous utilization of many substrates (mixed-substrate growth). As an example, *P. aeruginosa* was reported to grow on a mixture of 45 different carbon substrates supplied in the tap water at a concentration of 1 µg of carbon per liter whereas none of the compounds could serve as a growth substrate on its own at this concentration (van der Kooji *et al.*, 1982). Such substrate utilization pattern contrasts diauxic growth that is typically observed for many bacteria in liquid culture.

Apart from the impact on the characterisation of the kinetics of microbial growth, the chemostat was also instrumental in studies on evolution and in microbial ecology. It was continuous cultivation under substrate-limiting conditions that allowed to enrich selectively from the environment many xenobiotic-degrading microorganisms such as *Pseudomonas* strains capable to degrade naphthalenesulfonates (Brilon *et al.*, 1981), 1,2-dichlorobenzene (Haigler *et al.*, 1988), or 1,2,4-trichlorobenzene (van der Meer *et al.*, 1987). On the other hand, the possibility of relatively long cultivation in the chemostat was exploited to study mechanisms of evolution on the molecular level (Hartl & Dykhuizen, 1979; Wiebe *et al.*, 1994 and Notley-McRobb & Ferenci 1999).

The recent renaissance of the cultivation of microbes in chemostats could be attributed to the ability of providing large amount of physiologically uniform cells (Hoskisson & Hobbs, 2005). Characterisation of a given microorganism at the molecular level using post-genomic methods requires minimisation of the bias incurred through dynamic cultivation conditions. Here the chemostat provides an optimal experimental system that allows the comparative proteome analysis of e.g. *S. cerevisiae* grown on glucose and ethanol (Kolkman *et al.*, 2005) or the comparison of global gene expression profile during growth under different conditions (Hayes *et al.*, 2002; Boer *et al.*, 2003 and Wu *et al.*, 2004). The reproducibility achieved even by interlaboratory comparison of transcriptomic data analyses of chemostat cultures of *S. cerevisiae* testifies the suitability of this cultivation technique for gathering genome-wide insights into physiology of microorganisms (Piper *et al.*, 2002).

1.2.1. Conditions for microbial growth in the chemostat and in the environment

Little controversy exists that the constant physicochemical parameters as obtained in the chemostat together with ideal mixing, do not reflect growth conditions that occurr in nature (Kovar-Kovarova & Egli, 1998, Jannasch & Egli, 1993). The situation of a given microorganism in the environment probably remains somewhere between the ‘closed’ batch

culture and 'open' continuous culture. Notably, the ecosystems of the oral cavity or the gut might be considered as approaching the principles of a chemostat (Hoskisson & Hobbs, 2005). Despite that discrepancy between growth conditions in the environment and in the chemostat, the continuous culture represents probably the most appropriate experimental set-up for studying microbial kinetics and physiology (Kovarova-Kovar & Egli, 1998). The strictly controlled environmental millieu in the continuous chemostat culture is superior to the batch culture in providing cells at the same physiological state which in turn is a prerequisite for obtaining precise, reproducible and statistically sound experimental data (Senn *et al.*, 1994; Kovarova *et al.*, 1997).

For a long time the chemostat system was deemed unsuitable for ecologically relevant studies of microbial communities as it displays strong selective enrichment effect toward the fastest growing microorganism under given cultivation conditions (Jannasch & Egli, 1993). Several solutions were proposed to maintain heterogeneity of the original inoculum and counteract the undesired enrichment in the chemostat, like e.g. growth of communities either under conditions of discontinuous flow and incomplete mixing (Jannasch, 1974; Jannasch & Egli, 1993) or in the multistage continuous flow cultures with several connected vessels run at different dilution rates (Herbert, 1961). Contrary to the theoretical predictions, many microbial consortia were isolated from the environment under standard chemostat cultivation conditions with various xenobiotic compounds used as sole carbon source, e.g. Mecoprop (Lappin *et al.*, 1985), bromobenzene (Sperl & Harvey, 1988), linear alkylbenzene sulfonate (Jimenez *et al.*, 1991), 4-CS (Faude, 1996), phenol (Watanabe *et al.*, 1998) or triclosan (Hay *et al.*, 2001).

1.2.2. Studies of bacterial communities in the chemostat

Cultivations in the chemostat found numerous applications in studies of microbial communities degradating recalcitrant pollutants. As an example, Lappin and colleagues (1985) selectively enriched a five-membered bacterial community containing *Alcaligenes* sp., *Flavobacterium* sp., *Acinetobacter calcoaceticus* and two species of *Pseudomonas* from the rhizosphere soil of wheat root by continuous culture with the herbicide Mecoprop as sole carbon source. This community remained stable in the chemostat for over 2 months and preserved not only its structure and function but was also shown to break down structurally related herbicides 2,4-D and MCPA. In another study, selective enrichment in the chemostat helped to isolate a four-membered bacterial consortium capable for complete mineralization of a common anionic surfactant linear alkylbenzene sulfonate (LAS). Even though, LAS is

completely degraded to CO_2 in the aquifiers or activated sludge, single species with this capability are not available. Mineralization thus far necessitates a two-membered community, where one organism oxidizes the side-chain generating sulfophenylcarboxylates, which serve as substrate for a second organism (Schleheck *et al.*, 2004). Watanabe and collaborators (1998) aimed on characterising the dominant phenol-degrading bacteria in activated sludge and reported that those could be isolated and identified by direct plating and chemostat enrichment, whereas batch culture enrichment selected for minor community members.

Cultivation in the chemostat was also instrumental in analysing artificially composed defined microbial mixed cultures and in dissecting the interactions between oral bacteria. Already decades ago, continuous culture experiments helped in elucidating the interactions between oral streptococci and *Veillonellaceae*, where short-chain fatty acids produced from sugars by the former group were shown to support the growth of the latter (Mikx and van der Hoeven, 1975). Subsequently, many other pairs of closely interacting microorganisms were identified among members of the dental plaque by their growth in corresponding mixed culture chemostats such as *F. nucleatum* and *P. gingivalis* (Diaz *et al.*, 2002) or *P. gingivalis* and *T. denticola* (Grenier & Mayrand, 1986).

1.2.2.1. Response of isolates and communities to changing environmental conditions

The chemostat is also an important tool to analyse the response of single strains or communities to changes in environmental conditions, be it biotic or abiotic perturbation. In this case, the role of the chemostat is to provide cells under steady state conditions, thus removing transient growth effects and allowing assessment of the influence of a single medium component or other single factors on the overall metabolic network (Hoskisson & Hobbs, 2005). Avignone-Rosa and colleagues (2002) examined the effect of different growth rates on the antibiotic production by *Streptomyces*. The authors observed that an increased growth rate resulted in an increased flux through the glycolytic and pentose phosphate pathways and consequently in a decreased rate of biosynthesis of undecylprodigiosin and actinorhodin. Accordingly, other researchers postulated that metabolic flux analysis should be feasible for defined, metabolically-interacting consortia grown under chemostat conditions (Lovley, 2003). Thus, it was assumed that a perturbation and response analysis supported by *in silico* modelling could help to determine the most relevant 'environmental' stresses and lead to better and more efficient strategies for *in situ* bioremediation (Lovley, 2003).

One of the first examples of using the stress and response strategy to understand community behavior was the study of a nine-species mixed culture representing the oral microbial community (Bradshaw *et al.*, 1989). The authors pulse-fed the steady-state mixed

chemostat culture with glucose for ten days at regular time intervals and recorded pH-driven shifts in the populational structure of the community. They observed that the percentage of viable *Streptococcus mutans* and *Lactobacillus casei* in the perturbed community increased respectively to 18,9% and 36,1% when compared to the reference pulse-fed and pH-controlled chemostat (1,0% and 0,2%, respectively). In contrast, the counts of *Fusobacterium nucleatum* and *Treponema intermedia* decreased from 9,5% to $2 \cdot 10^{-5}$ % and from 5,6% to $6 \cdot 10^{-4}$ %, respectively (Bradshaw *et al.*, 1989). The evident success of this approach simulating community responses *in vivo* prompted authors to test the influence of fluoride (Marsh & Bradshaw, 1990), sugar substitutes such as xylitol (Bradshaw & Marsh, 1994) and chlorhexidine antibiotics (Kinniment *et al.*, 1996) on the nine-species oral community in a similar chemostat set-up.

1.3. Advances in F*IS*H-flow cytometry for analysing microbial communities

Despite many years of intense research monitoring growth of subpopulations in microbial communities is still problematic. Quantification of microorganisms in the mixed cultures might be complicated for the following reasons: (i) different growth rates of particular members, (ii) their wide taxonomic diversity (*Eubacteria, Archea, Eucaryota*), (iii) various cell morphologies (single cells, aggregates, filamentous growth, etc.), (iv) presence of dormant cells and endospores, (v) differences in the physiological state of individual cells, and (vi) the need to monitor growth both under laboratory conditions and *in situ* in the environment. The advent of enumeration techniques based on molecular biology broadened the spectrum of available methods of quantification. However, the complexity inherent to microbial communities often requires individually tailored solutions.

The divergence of 16S ribosomal RNA sequences defines the outline of a modern, natural classification system of microorganisms (Woese *et al.*, 1985; Woese, 1987). Richness and depth of the 16S rRNA data deposited in the public domain that originate from various 16S screening programs is a sound indicator of prokaryotic diversity on Earth as it also accounts for not-yet-cultivated microorganisms. Fluorescent *In Situ* Hybridisation (F*IS*H) is one of the molecular methods used for exploring and exploiting the diversity of microbial 16S rRNA sequences. In this technique, whole microbial cells, following their prior fixation (dehydration) and subsequent permeabilization of their cellular envelopes, are hybridised to fluorescently labeled oligonucleotide probes of typically 18-30 bp length and visualized under an epifluorescent microscope (DeLong *et al.*, 1989; Amann *et al.*, 1990b). Usual targets for

F*IS*H probes in the cell are abundant rRNA molecules such as 16S rRNA and 23S rRNA. Since the 16S rRNA contains domains of various degree of conservation, the probes could be designed to ensure the desired taxonomic specificity. Specificity of the F*IS*H probe may span from single species or even cultivars up to the entire kingdom (Amann *et al.*, 1995).

Due to its undisputed advantages, F*IS*H quickly earned widespread acceptance and popularity. Stoffels and colleagues (1998) used it to study bacterial community dynamics during degradation of Solvesso100 which is a mixture of polyalkylated aromatic compounds. The authors used probes of broad specificity and observed that the sample of wastewater that served as original inoculum was dominated by α- and β-Proteobacteria (16% and 11%, respectively) with only a negligible content of γ-Proteobacteria (<0,1%). Interestingly, propagation of the community in the Solvesso100-fed chemostat resulted in the reversal of the community structure with γ-Proteobacteria accounting for 80% of the population. After transferring the culture adapted in the chemostat into a trickle-bed bioreactor, the community returned to its initial state with α- and β-*Proteobacteria* being dominant. Further insights into the community structure using F*IS*H probes of narrow specificity revealed that 83% of the β-Protebacteria were related to *Burkholderia cepacia* and *B. vietnamensis*, respectively while the members of the γ-Proteobacteria were almost exclusively related to *Pseudomonas putida* and *P. mendocina* (Stoffels *et al.*, 1998).

F*IS*H is specifically useful in studies where the localization of a given group of bacteria should be confirmed and for instance it helped to establish the presence of *Tannerella forsythia* in the subgingival plaque samples from patients affected by serious periodontitis (Gersdorf *et al.*, 1993). Other environments where F*IS*H was used for detection, quantification and localization of microorganisms included soil samples (Hahn *et al.*, 1992), marine aquatic habitats (Glöckner *et al.*, 1996), bioaerosols (Lange *et al.*, 1997), fecal samples (Zoetendal *et al.*, 2002), microbial flocs (Tay *et al.*, 2002) and activated sludge (Wagner *et al.*, 1994).

Already at the advent of F*IS*H, DeLong and colleagues (1989) realised that the content of probe targets, ribosomes, varies in the cell and thus might reflect microbial activity. However, detailed studies on different organisms from various habitats led to the now widely accepted conclusion that a correlatation of F*IS*H-conferred fluorescence with cellular activity requires prior knowledge on the correlation between growth rate and ribosome content for a given organism (Licht *et al.*, 1999; Molin & Givskov, 1999).

F*IS*H proved to be compatible with many other techniques. For instance, Lee and colleagues (1999) combined F*IS*H with microautoradiography to study the uptake of organic and inorganic radiolabeled substrates by probe-defined populations in activated sludge. In another study, the use of F*IS*H and microelectrodes sensing concentration of O_2 and NO_3^-

helped to establish that in the biofilm composed of ammonia-oxidizing *Nitrosomonas* and nitrite-oxidizing *Nitrobacter* the process of nitrification is actually limited to its top narrow zone (Schramm *et al.*, 1996).

Like all empirical techniques, F*IS*H is not devoid of limitations such as frequently reported difficulties with permeabilisation of cells, poor accessibility of target sites, insufficient sensitivity in case of low rRNA content or background fluorescence. Many solutions were proposed that help to overcome above mentioned problems, however, the use of F*IS*H in studies on complex and diverse microbial communities may still be a challenge.

1.3.1. Flow cytometry and FISH-flow cytometry in microbiology

In principle, flow cytometers might be considered as equivalent to a microscope, but designed for handling liquid samples. In fact, the first cytometric instrument built for the purpose of studying bacteria used the microscope optics coupled to a photomultiplier tube and a multichannel analyser (Steen & Lindmo, 1979). In the flow cytometer, small objects like bacterial cells that are suspended in a stream of flowing liquid pass the light emitted by a laser or arc-lamp. Upon illumination, individual particles scatter the light at small angle (forward scatter) and large angle (side scatter). The intensity of light scattered at small angle depends strongly on the object's size and refractive index while the intensity of side scatter correlates with the surface roughness and the density of the cellular matrix (granularity). Since the flow cytometers are routinely equipped with various filters and dichroic mirrors, it is also feasible to record the intensity of fluorescence emitted by an object at different wavelengths. Staining the cells prior to analysis with appropriate fluorescent reagents or probes provides the opportunity to determine their various extrinsic parameters. The power of the cytometric approach lies in the acquisition of multiparametric data on the single-cell level in a digital form that greatly facilitates handling and multivariate analysis. This becomes even more important if one considers that modern flow cytometers offer a speed of analysis up to more than 1000 events per second. Additionally, many modern instruments have the capability to effectively sort cells according to the desired parameter. From a mixed population of cells only those displaying a given feature can be identified and physically separated for further analysis (Fuchs *et al.*, 2000) or for application in an enrichment culture (Nebe-von-Caron *et al.*, 2000).

Already at the moment of its invention, flow cytometry was predicted to find multiple applications in bacteriology (Gucker *et al.*, 1947), however, it remained a completely uncharted territory for microbiologists until the late 1970s, when the improvements in optics and the development of new generations of fluorescent dyes fostered its application. Bailey *et*

al. (1977) analysed cytometrically the protein and nucleic acid content in cells of a batch culture of *Bacillus subtilis*. The authors used fluorescein to stain cellular proteins and propidium iodide to stain nucleic acids and observed a reduction in the amount of both cellular components when the culture approached stationary phase. As cytometry allows single-cell analysis, it was rapidly adopted by microbial ecologists to study bacterial communities. Already in 1990 the high throughput flow cytometric approach was combined with F*IS*H in order to enumerate specific cells in mixed bacterial cultures (Amann *et al.*, 1990). Using a similar approach activated sludge from a wastewater treatment plant was analysed for the abundance of α-, β- and γ- *Proteobacteria* and specifically for *Acinetobacter* spp. Cytometric enumerations were generally in good agreement with microscopic counts, except that the abundance of the members of the α-Proteobacteria and of *Acinetobacter* were underestimated (Wallner *et al.*, 1995). The observed discrepancies between cytometric and microscopic counts are probably due to the occurrence of flocs in the case of α-*Proteobacteria* or chains as the case for *Acinetobacter* spp. (Wallner *et al.*, 1995) which illustrates well the previously discussed limitations of F*IS*H. By using multiparametric flow cytometry the authors were also able to characterise cell size (forward scatter) and DNA content (Hoechst-conferred fluorescence) distribution within specific groups. They observed that within β-*Proteobacteria* two subpopulations could be discerned: large single and double rods (1,0 by 1,5 to 1,5 by 2,5 µm) showing strong activity and less active smaller rods (0,4 by 1,0 to 1,5 µm) (Wallner *et al.*, 1995). Due to the increased throughput of cytometric detection and thus increased sensitivity, Lange and colleagues (1997) were able to enumerate even low abundant F*IS*H-labeled bacteria in bioaerosols.

All the unique properties of the flow cytometry that were only briefly mentioned above indicate the potential of this technique to become a routine analytical tool in microbiological laboratories worldwide.

1.4. Aerobic degradation of aromatic and chlorinated aromatic compounds in the post-genomic era

1.4.1. Phylogenomics of aerobic degradation of aromatics

The sequencing of hundreds of microbial genomes over the last decade had enormous impact on all aspects of microbiology including increasing our knowledge on the degradation of natural and xenobiotic compounds. The constantly growing resources of genomic sequence information together with slower but steady progress in biochemical characterisation of novel

metabolic pathways added a new exciting perspective of getting a phylogenomic insight into biodegradation. Elucidation of degradation pathways of aromatic compounds under aerobic conditions was based on selecting the key catabolic functions to probe the database of sequenced genomes which was then followed by refining positive scores (Perez-Pantoja *et al.*, 2010b). As authors demonstrated, phylogenomic analysis of 822 available microbial genomes was not only suitable for determining the catabolic abilities among certain groups of bacteria but could also be instrumental in defining new enzyme families, suggesting new putative functions and proposing evolutionary links among different groups of sequences.

Genome database search using representative gene sequences as catabolic markers revealed that the distribution of aromatic catabolic pathways is not uniform among different bacterial phyla with the members of Proteobacteria and Actinobacteria accounting for the majority of positive hits (Perez-Pantoja *et al.*, 2010b). The absence of catabolic pathways for degradation of aromatics in certain phyla could be explained either by the lifestyle of their representatives like in strictly anaerobic *Chlorobi* or typically obligate parasitic *Chlamydia*, or by the small number of genomes available for search like in case of *Fusobacteria* (2), *Planctomycetes* (3) or *Thermotogae* (6). The members of *Bacteroidetes*, *Chloroflexi* and particularly *Firmicutes* (*Bacilli*) locate on the other side of the spectrum as being well-equipped for degradation of aromatics with gentisate, homogentisate and anthranilate pathways being relatively frequently observed (Perez-Pantoja *et al.*, 2010b). This is hardly surprising as the capability of *Bacillus* species to degrade aromatics such as biphenyl, guaiacol or coumarate is known since the pre-genomic era (Shimura *et al.*, 1999; Peng *et al.*, 2003). Both in case of Actinobacteria and Proteobacteria the distribution of aromatic pathways was not uniform among families. For instance, none of the sequenced members of *Cellulomonadaceae*, *Microbacteriaceae* or *Bifidobacteriaceae* contain a single metabolic route for aromatics while *Micrococcaceae*, *Corynebacteriaceae*, and specifically *Nocardiaceae* seem to be endowed with a broad metabolic potential (Perez-Pantoja *et al.*, 2010b). Inside the Proteobacteria, the β-Proteobacteria (families of *Burkholderiaceae* and *Commamonadaceae*) harbor all known major pathways for degradation of aromatics what could be expected, as their metabolic potential was often the rationale behind corresponding genome sequencing projects. Genomes of α- and γ-Proteobacteria seem to be less well equipped for the breakdown of aromatics, although in the families *Bradyrhizobiaceae* and *Sphingomonadaceae* or *Pseudomonadaceae* and *Enterobacteriaceae*, respectively, a broad catabolic potential could be observed. Many of the α-proteobacterial families (*Rikettsiales*, *Bartonellaceae* or *Erythrobacteraceae*) and γ-proteobacterial families (*Francisellaceae*,

Coxiellaceae) as well as majority of δ- and all ε-Proteobacteria seem to be completely devoid of aerobic aromatic degradation pathways (Perez-Pantoja *et al.*, 2010b).

Another use of phylogenomic analysis was shown by probing evolutionary relationships among different intradiol dioxygenases – enzymes that catalyze central oxygenolytic cleavage reaction in the metabolism of various aromatics. By using multiple alignments of corresponding protein sequences followed by dendrogram construction, seven discrete clusters comprised of hydroxybenzoquinol dioxygenases, actinobacterial and proteobacterial catechol 1,2-dioxygenases, chlorocatechol 1,2-dioxygenases and α- and β-subunits of protocatechuate 3,4-dioxygenases were identified. The function of enzymes grouped in a remaining cluster has to be elucidated and indicates the possibility of novel aromatic ring-cleavage reactions (Perez-Pantoja *et al.*, 2010b).

Importantly, the phylogenetic approach might contribute to correcting misannotations that are still frequent in databases. From a nearly 100 genes in bacterial genomes that were annotated as encoding salicylate 1-hydroxylases the detailed phylogenetic analysis against proteins of validated salicylate 1-hydroxylase function confirmed only nine. All other enzymes annotated as salicylate hydroxylases showed highest similarity to other flavoprotein monooxygenases like 6-hydroxynicotinate 3-monooxygenase or 3-hydroxybenzoate 6-hydroxylase (Perez-Pantoja *et al.*, 2010b).

1.4.2. In-depth analysis of degradative pathways within a genome

Among almost thousand bacterial genomes that have been sequenced, several were selected on the basis of the extraordinary degradative capabilities displayed by particular strains like e.g. *Pseudomonas putida* KT2440 (Nelson *et al.*, 2002), *Burkholderia xenovorans* LB400 (Chain *et al.*, 2006), *Rhodococcus jostii* RHA1 (McLeod *et al.*, 2006) and *Cupriavidus necator* JMP134 (Lykidis *et al.*, 2010). Analysis of genomes of these bacteria provided pivotal information about their potential for the degradation of natural and xenobiotic aromatic compounds.

For instance, the genomic analysis of *P. putida* KT2440 helped to establish that in this strain catabolic genes for channeling different aromatics into a common central pathway are not organized in a supraoperonic structure. Two gene clusters were identified in the KT2440 genome as putatively involved in the catabolism of N-heterocyclic aromatic compounds (*nic*) or central meta cleavage pathway (*pcm*) as well as numerous genes encoding enzymes of peripheral pathways for *p*-hydroxybenzoate (*pob*), benzoate (*ben*), quinate (*qui*) and natural polyprenoids (*fcs*, *ech*, *vdh*, *cal*, *van*, *acd*, and *acs*) (Jimenez *et al.*, 2002).

Even more spectacular insights were gained from the metabolic reconstruction done on the genome of *C. necator* JMP134 (Perez-Pantoja *et al.*, 2008). In the reported work, authors linked *in silico* predicted catabolic abilities from the complete genome sequence analysis with the range of compounds supporting growth of this bacterium. Out of 140 aromatic substrates that were tested, 60 could serve as sole carbon and energy source for growth of *C. necator* JMP134. This number included approximately 40 compounds that have not been previously reported as growth substrates (Perez-Pantoja *et al.*, 2008). Indeed, *C. necator* JMP134 seems to be endowed with exceptional capabilities for degradation of aromatics as it harbors in the genome determinants for almost all known main ring-cleavage pathways, both those proceeding *via* oxygenolytic reaction and those being initiated by the formation of CoA-derivatives, together with a broad spectrum of peripheral reactions that funnel substituted aromatics into this ring cleavage pathways. The observed gene redundancy may play a significant role in the catabolic potential of this strain (Perez-Pantoja *et al.*, 2008) and provides foundations for designing future experiments.

1.4.3. Mechanisms of aerobic degradation of aromatics and chloroaromatics

The wealth of aromatic hydrocarbons in the environment derives primarily from the plant biomass where they constitute a significant part of lignin (Kirk & Farrell, 1987) and to a lesser extent from the ubiquitous presence of aromatic amino acids like phenylalanine and tyrosine. Xenobiotic aromatics, and particularly chloro-substituted aromatics that are extensively used in industrial processes and agriculture, additionally contribute to the pool of these compounds in the environment. Recalcitrance of aromatic compounds due to the thermodynamic stability of the benzene ring is well known. However, microorganisms evolved diverse strategies to degrade aromatics efficiently both under aerobic and anoxic conditions that allow them to extract carbon and energy and to close the biogeochemical cycle of carbon in nature.

Under aerobic conditions degradation of aromatics is initiated by activation of the benzene ring, typically through oxygenation to form di- or tri-hydroxy derivatives which are then subjected to oxygenolytic ring-cleavage or alternatively by formation of the corresponding CoA thioesters (Perez-Pantoja *et al.*, 2010a). In the oxygenolytic route, the initial peripheral reactions that prepare aromatic hydrocarbons for ring cleavage are catalyzed by enzymes that belong to one of three different families: Rieske non-heme iron oxygenases, soluble diiron monooxygenases and flavoprotein monooxygenases. Rieske non-heme iron oxygenases typically mediate the incorporation of two oxygen atoms into the aromatic ring to form the corresponding *cis*-dihydrodiols that are subsequently dehydrogenated to give

(substituted) catechols. Enzymes of this family are involved for instance in the degradation of benzoate (Reiner & Hegeman, 1971), benzene, toluene, naphthalene, biphenyl (Gibson & Parales, 2000) or anthranilate (Bundy *et al.*, 1998). Soluble diiron monooxygenases catalyze hydroxylation of benzene or toluene to phenol or xylenes and phenols to catechols (Leahy *et al.*, 2003). One of the best characterised examples of this class is the phenol hydroxylase of *Pseudomonas stutzeri* OX1 that is capable of transforming both benzene and toluene although with much slower rates (Cafaro *et al.*, 2004). Enzymes of the third group of flavoprotein monooxygenases also catalyze the incorporation of a single oxygen atom (Ballou *et al.*, 2005). Single-component salicylate 1-hydroxylase that carries out oxidative decarboxylation of salicylate into catechol was the first characterised enzyme of this family (Yamamoto *et al.*, 1965). Notably, a homologous salicylate 1-hydroxylase of strain MT1 that displays a broad substrate specificity including chloro- and methyl-substituted salicylates also belongs to the family of flavin monooxygenases (Camara *et al.*, 2007).

Side chains present in substituted aromatic compounds are typically oxidized, such as the oxidation of methyl groups to carboxylic moieties like in the oxidative pathway of toluene degradation *via* benzoate (Assinder & Williams, 1990), eliminated by *o*-demethylations such as the methoxy substituent in vanillate degradation (Buswell & Ribbons, 1988) or eliminated by non-oxidative (reductive) decarboxylations as in the metabolism of phthalate (Nakazawa & Hayashi, 1978).

Further metabolism of central hydroxylated intermediates in the oxygenolytic routes proceeds *via ortho* (intradiol) ring-cleavage or through one of the various meta-cleavage (extradiol) pathways. The 3-oxoadipate pathway, named after a further central intermediate formed from both protocatechuate and catechol after intradiol cleavage, is fairly ubiquitous among soil bacteria. Its two branches – the catechol and protocatechuate branch serve to channel a large spectrum of aromatics to the central metabolism (Fig. 1.4.). The metabolism of catechol is initiated by *ortho*-cleavage catalyzed by catechol 1,2-dioxygenase resulting in the formation of *cis,cis*-muconate that is subsequently transformed into muconolactone by the action of muconate cycloisomerase. Isomerization of muconolactone carried out by muconolactone isomerase yields 3-oxoadipate-enol-lactone that constitutes the convergence point for the catechol and protocatechuate branches of the 3-oxoadipate pathway. In the protocatechuate branch, protocatechuate is cleaved by protocatechuate 3,4-dioxygenase to form 3-carboxy-*cis,cis*-muconate that is converted by carboxymuconate cycloisomerase into 4-carboxymuconolactone. Carboxymuconolactone decarboxylase transforms the latter compound into 3-oxoadipate enol-lactone that is hydrolyzed by an enol-lactone hydrolase to give 3-oxoadipate. A distinct intradiol ring-cleavage route is the hydroxybenzoquinol pathway

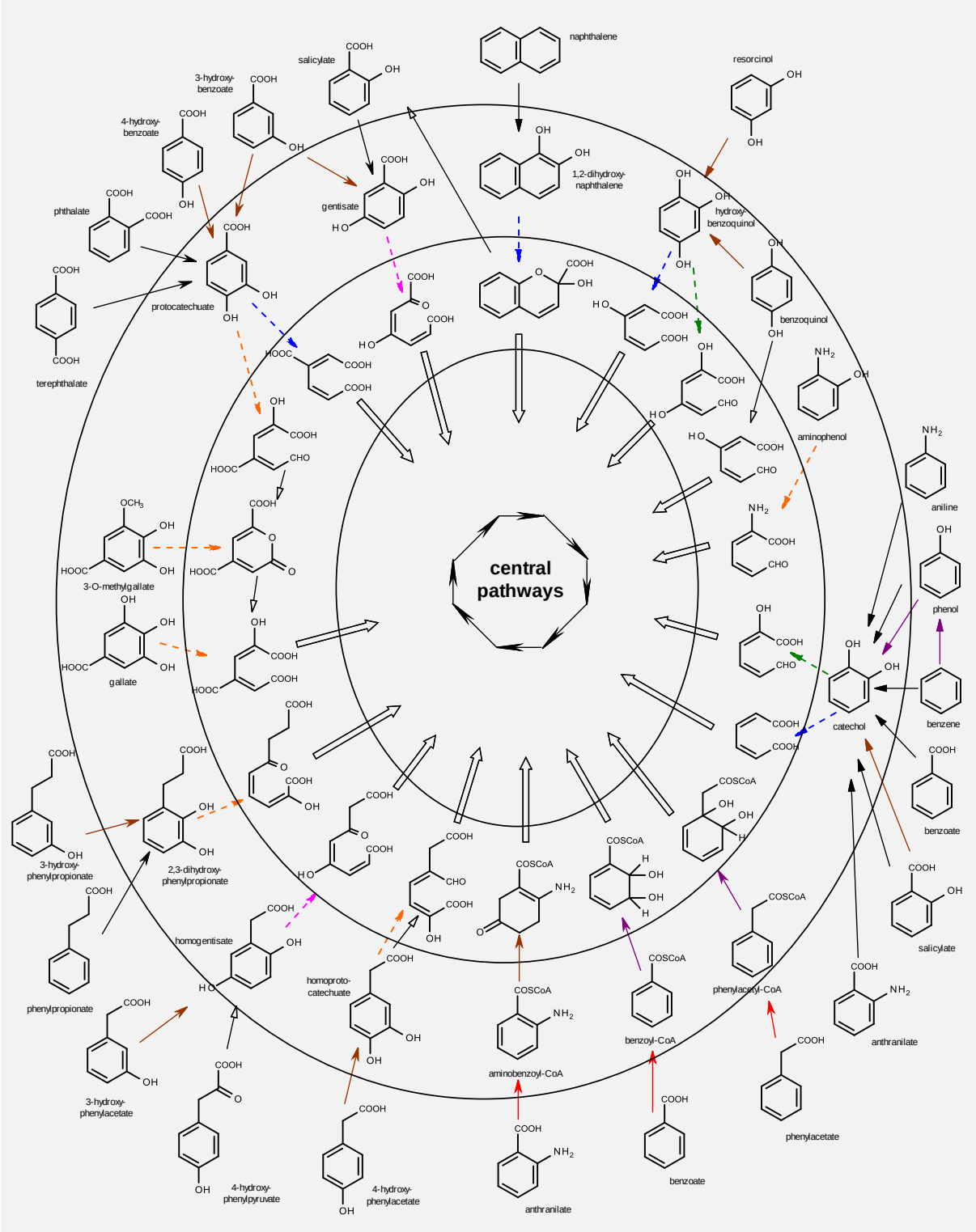

Figure 1.4. Aerobic metabolism of aromatic compounds *via* di- or trihydroxylated intermediates and *via* CoA-derivatives. Reactions catalyzed by Rieske non-heme iron oxygenases (black arrows), flavoprotein monooxygenases (brown arrows), soluble diiron oxygenases (violet arrows), CoA ligases (red arrows), intradiol dioxygenases (dashed blue arrows), extradiol dioxygenases (dashed green arrows), LigB superfamily proteins (dashed orange arrows), cupin superfamily proteins (dashed pink arrows), or other family proteins (open-head arrows) are indicated. Block arrows denote conversions to the intermediates of central pathways.

used for the breakdown of natural aromatic hydrocarbons like resorcinol (Huang *et al.*, 2006) but also for many recalcitrant xenobiotics such as 2,4,5-T (Daubaras *et al.*, 1996), 4-chlorophenol (Nordin *et al.*, 2005) or *p*-nitrophenol (Jain *et al.*, 1994). The key enzyme in this pathway is hydroxybenzoquinol 1,2-dioxygenase that catalyzes intradiol cleavage of 1,2,4-trihydroxybenzene to form 3-hydroxy-*cis,cis*-muconate being in tautomeric equilibrium with maleylacetate. Maleylacetate reductase performs the subsequent reduction of the carbon-carbon double bond resulting in the formation of 3-oxoadipate.

Another route for metabolizing hydroxylated central intermediates involves cleaving the carbon-carbon bond of the aromatic ring in the position adjacent to the hydroxyl groups (extradiol). Several compounds are degraded by *meta*-cleavage pathways. However, whereas intradiol dioxygenases all belong to the same superfamily, members of three distinct superfamilies have thus far been reported to catalyze extradiol cleavage (Perez-Pantoja *et al.*, 2010b). For instance, the *meta*-cleavage of catechol or 2,3-dihydroxybiphenyl is catalyzed by members of the vicinal chelate superfamily, the cleavage of gallate, protocatechuate or homoprotocatechuate by enzymes of the LigB superfamily while the transformation of gentisate, homogentisate or 3-hydroxyanthranilate is mediated by enzymes of the cupin superfamily (Perez-Pantoja *et al.*, 2010b).

In the second general scenario, aromatic compounds under aerobic conditions may be activated through the formation of the corresponding CoA thioesters. The existence of such pathways has been reported for the degradation of phenylacetate (Olivera *et al.*, 1998), benzoate (Altenschmidt *et al.*, 1993), anthranilate (Altenschmidt & Fuchs, 1992) and even salicylate (Ishiyama *et al.*, 2004). In case of benzoate, benzoyl-CoA formed by the action of benzoate-CoA ligase is transformed to 2,3-dihydro-2,3-dihydroxybenzoyl-CoA by benzoyl-CoA oxygenase/reductase (Zaar *et al.*, 2004). In contrast to oxygenolytic routes, the ring of dihydrodiol is not re-aromatized but subjected to fission catalyzed by dihydrodiol lyase resulting in formation of 3,4-dehydroadipyl-CoA semialdehyde (Gescher *et al.*, 2005). The sequence of further reactions involves oxidations by corresponding dehydrogenases and probable steps of isomerisation and hydratation leading ultimately to 3-oxoadipyl-CoA that can be incorporated into the central metabolism (Zaar *et al.*, 2004).

Incorporation of chlorine atom(s) into the aromatic ring significantly modifies the physicochemical and biochemical properties of the compound and directly contributes to its increased persistence in the environment. Mineralization of chlorinated aromatic compounds presents microorganisms with an additional challenge as dechlorination need to be performed (Pieper *et al.*, 2010). In analogy to the pathways described above, microbial degradation of chloroaromatics is typically initiated by activation of the aromatic nucleus through

oxygenation reactions forming a few central intermediates such as chlorinated catechols, protocatechuates, gentisates,or hydroxybenzoquinols. These peripheral reactions are often catalyzed by the enzymes functioning in the degradation of aromatic compounds which exhibit relaxed substrate specificity and tolerate lower chlorinated substrate analogs (Reineke, 2001). Further degradation of hydroxylated chloroaromatics involves oxygenolytic ring cleavage followed by transformations of the ring-cleavage products often by highly specialized enzymes that allow channeling the products into central metabolism (Pieper *et al.*, 2010). Interestingly, dehalogenation of chloroaromatics may occur at different stages of the pathway, for instance: (i) during peripheral reactions like in the degradation of 2-chlorobenzoate by *Burkholderia cepacia* 2CBS (Fetzner *et al.*, 1992), (ii) during structural rearrangements of intermediates like by the action of chloromuconate cycloisomerases in the chlorocatechol pathway (see below), or (iii) at terminal stages before channeling intermediates into central metabolism as is the case with 2-chloromaleylacetate resulting from (chloro)catechol or (chloro)benzoquinol pathways, which is dechlorinated by the action of maleylacetate reductase, first to maleylacetate and further to 3-oxoadipate (Kaschabeck & Reineke, 1992). Biodegradation of highly-chlorinated aromatics like lindane or pentachlorophenol requires additional dehalogenation steps that are carried out by specific dehalogenases (Miyauchi *et al.*, 1998; Nagata *et al.*, 2007).

1.4.4. Degradation of chlorocatechols by intradiol cleavage pathways

In contrast to unsubstituted catechol that can be degraded *via* wide-spread *ortho* or *meta*-cleavage routes, the degradation of chlorocatechols necessitates specific pathways (Fig. 1.5.).

In most Proteobacteria that were isolated thus far for their capability to degrade chloroaromatics *via* chlorocatechols as central intermediates, chlorocatechols are degraded by the specialized chlorocatechol pathway (Reineke, 2001). Intradiol ring fission in this pathway is catalyzed by broad specificity chlorocatechol 1,2-dioxygenase and results in the formation of 2- or 3-chloromuconate (from 3- and 4-chlorocatechol, respectively).

Chlorinated muconates are subjected to reactions of cyclisation and dehydrochlorination performed by the chloromuconate cycloisomerase that is the key enzyme of the pathway. Cycloisomerisation of 2-chloromuconate results in the formation of preferentially 5-chloromuconolactone, which is dehalogenated to *trans*-dienelactone, as abstraction of the proton for dehalogenation requires rotation of the lactone ring in the catalytic center (Schell *et al.*, 1999). In contrast, cycloisomerisation and dehydrochlorination seem to proceed concomitantly for 3-chloromuconate and result in the formation of *cis*-isomer of dienelactone (Kaulmann *et al.*, 2001). Both *cis*- and *trans*-dienelactone are converted by dienelactone

hydrolases into maleylacetate (Schmidt & Knackmuss, 1980). Maleylacetate reductase, an enzyme that is also present in the hydroxyquinol pathway, transforms maleylacetate into 3-oxoadipate that is channeled into the central metabolism (Kaschabek & Reineke, 1992).

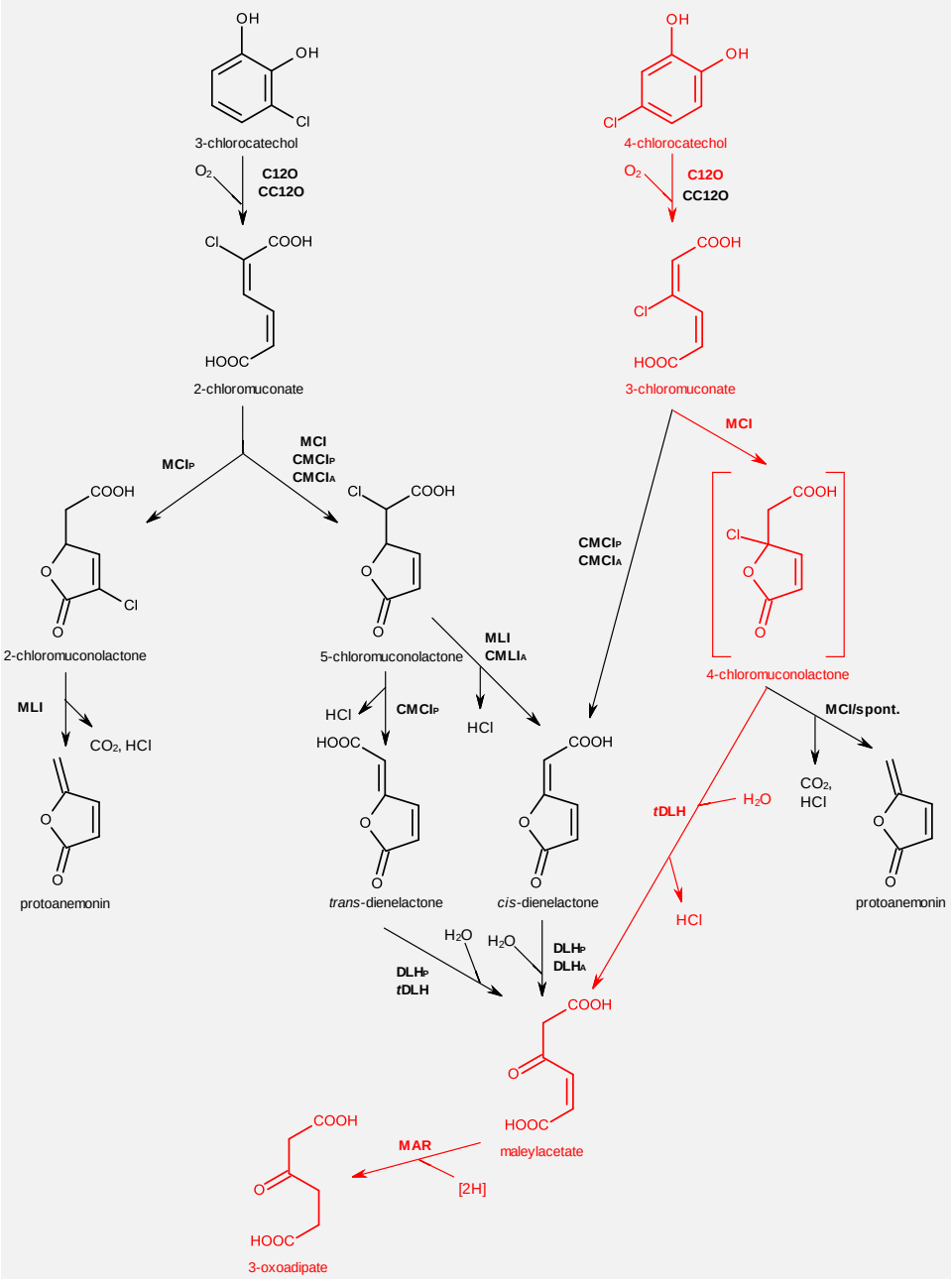

Figure 1.5. Pathways for the degradation of 3- and 4-chlorocatechols *via* intradiol ring-cleavage in Proteobacteria and Actinobacteria. The route in *P. reinekei* MT1 is marked red. C12O, catechol 1,2-dioxygenase; CC12O, chlorocatechol 1,2-dioxygenase; MCI, muconate cycloisomerase; MCI_P, proteobacterial muconate cycloisomerase; $CMCI_{A/P}$, actinobacterial and proteobacterial chloromuconate cycloisomerase; MLI, muconolactone isomerase; $CMLI_A$, actinobacterial chloromuconolactone isomerase; $DLH_{A/P}$, actinobacterial and proteobacterial dienelactone hydrolase; *t*DLH, trans-dienelactone hydrolase; MAR, maleylacetate reductase (after: Pieper *et al.*, 2010, modified).

Chlorocatechol pathways have also been identified in Actinobacteria, for instance in *Rhodococcus opacus* 1CP, but corresponding enzymatic activities, particularly chloromuconate cycloisomerase and dienelactone hydrolase, differ significantly from their proteobacterial counterparts (Figure 1.5.) (Moiseeva *et al.*, 2002). Most importantly, 2-chloromuconate formed from 3-chlorocatechol is not dehalogenated by chloromuconate cycloisomerase, but only transformed to 5-chloromuconolactone, which is dehalogenated by a muconolactone isomerase to *cis*-dienelactone.

Microorganisms possessing the chlorocatechol pathway typically encode also enzymes of the catechol branch of 3-oxoadipate pathway and concomitant expression of enzymes from both routes may pose additional complications in the degradation of chlorocatechols. In the case of 3-chlorocatechol subsequent transformation of 2-chloromuconate by muconate cycloisomerase and muconolactone isomerase *via* 2-chloromuconolactone as intermediate may result in the formation of a toxic metabolite – protoanemonin. Breakdown of 4-chlorocatechol may also lead to the formation of protoanemonin as 3-chloromuconate is converted by muconate cycloisomerase into 4-chloromuconolactone that undergoes spontaneous dehalogenation and decarboxylation (Blasco *et al.*, 1995; Nikodem *et al.*, 2003). However, enzymes of the catechol branch of the 3-oxoadipate pathway can in some cases be accommodated in a functional 4-chlorocatechol mineralization route as described for *P. reinekei* MT1 (Nikodem *et al.*, 2003). In this strain degradation of 4-CS and 5-CS occurs via 4-chlorocatechol and 3-chloromuconate. However, in contrast to the proteobacterial chlorocatechol pathway, where 3-chloromuconate is degraded by chloromuconate cycloisomerase and *via cis*-dienelactone as intermediate, degradation in MT1 proceeds *via* the unstable 4-chloromuconolactone. This intermediate is converted into maleylacetate by the action of a *trans*-dienelactone hydrolase which prevents formation of protoanemonin (Nikodem *et al.*, 2003). Maleylacetate reductase, that is located in the same transcriptional unit as *trans*-dienelactone hydrolase (Camara *et al.*, 2009), transforms maleylacetate into 3-oxoadipate similar as in the chlorocatechol pathway. Metabolic efficiency of this alternative pathway for the degradation of 4-chlorocatechol in MT1 is limited and growth of the strain under conditions of high substrate (4-CS) concentrations requires additional mechanisms for detoxification of 4-chlorocatechol and protoanemonin. In the case of MT1, which was isolated as a member of a four-species chlorosalicylate degrading community, and which constitute the object of the current study, such detoxifying capabilities are assumed to be supplied by the other community members (Pelz *et al.*, 1999).

1.5. Goals of the project

A four-membered bacterial consortium termed MT comprising of *Pseudomonas reinekei* MT1, *Empedobacter brevis* MT2, *Achromobacter xylosoxidans* MT3 and *Pseudomonas veronii* MT4 was isolated from the sediment of Spittelwasser creek for its ability to degrade 4-chlorosalicylate in a symbiotic fashion. Understanding the way how complex microbial communities react to challenges posed by constantly changing environmental milieu could contribute to designing more efficient bioremediation strategies. Thus, the influence of parameters that are crucial for aerobic bioremediation processes such as temperature, substrate supply and aeration on the functioning and structure of MT consortium grown on 4-chlorosalicylate was studied in detail in fed-batch and continuous culture.

The effect of microbial community composition on the degradation of 4-chlorosalicylate was evaluated by comparing the performance of the entire MT consortium and two binary cultures containing strains MT1 and MT3 or MT1 and MT4, respectively, under identical cultivation conditions in the chemostat.

In order to frequently monitor the community composition of the consortium and binary cultures a rapid, accurate and reliable quantification technique was developed that combined Fluorescent *In Situ* Hybridisation (F*IS*H) with a high-throughput flow cytometric counting of labeled cells.

Genomic phage libraries of individual consortium members were prepared and subjected to various screening procedures to reveal the genetic determinants of 4-chlorosalicylate degradation by the consortium and specifically by MT1. This part of the project contributed to a larger research programme, dedicated to discovering and characterising genes involved in the degradation of aromatic and chloroaromatic compounds.

2. MATERIALS AND METHODS

2.1. Appliances

Analytical balance:	BP210S and R160P, Sartorius AG, Göttingen, Germany
Autoclave:	Tecnoclav 50, Tecnomara AG, Zürich, Switzerland
	Sauter 464, Sulgen, Switzerland
CCD Camera:	INTRAS, Infors AG
Climate chamber:	RUMED 3500, Rubbarth Apparate, Germany
Centrifuge:	RC3C and RC5C Sorvall Instruments, Du Pont, USA
Cooling centrifuge:	Biofuge Primo R, Heraeus
	Biofuge Fresco, Heraeus
Developing machine:	Curix 60, Agfa, Leverkusen
DNA Sequenator:	ABI PRISM System 3730 and 3100 Genetic Analyzer, Applied Biosystems, CA, USA
Electroporation system:	Gene Pulser II Plus, Bio-Rad, USA
Epifluorescence microscope:	Axiophot Zeiss, Jena
Flow cytometer:	FACS Calibur, Becton Dickinson, San Jose, CA, USA
	MoFlo II, Dako Cytomation Inc., USA
French Press:	Aminco, American Instrument Comp., Silver Spring, USA
Gel electrophoresis chambers:	Horizon 58 and Horizon 11.14, Gibco BRL, Eggenstein
	Wide Mini-Sub Cell, Bio-Rad, Italy
Gel documentation system:	E.A.S.Y. System, Herolab, Wiesloch
	Pixel Room CP580, BioSciTec GmbH, Germany with Nicon Coolpix 4500 digital camera, Tokyo, Japan
HPLC:	Waters Alliance 2690 Separation Module, Milford, USA
	Waters PDA 996 Detector, Waters GmbH, Eschborn
Hybridisation oven:	Techne Hybridiser HB-1D, Techne Ltd., Cambridge, UK
Incubator:	Infors Multitron, Infors AG, Bottmingen, Switzerland
	Innova 4300 Incubator Shaker, New Brunswick Scientific, Nürtingen, Germany
Magnetic stirrer:	Ikamag RET, IKA-Labortechnik, Staufen, Germany
Microcentrifuge:	Biofuge Pico, Heraeus
Microscope:	Axioskop and Axiotech 25HD, Carl Zeiss, Jena, Germany
Microwave oven:	Dimension 4, Panasonic, Japan
PCR Thermocycler:	Landgraf Thermocycler, Langenhagen, Germany
	Whatman Biometra T3 and Personal Cycler, Biotron GmbH, Göttingen, Germany
	Personal Cycler 48, Biometra
Peristaltic pump:	Abimed Miniplus 3, Gilson, Villiers, France
	VerderFlex 2010, Germany
	Watson Marlow 505U and 501U, Watson-Marlow Ltd, Falmouth, UK

pH meter:	Orion 920A, Orion Research Inc., Boston, MA, USA HI 9017 Microprocessor pH meter, Hanna Instruments, Portugal
Power supply:	GPS 200/400, Pharmacia LKB, Sweden
Rotary Evaporator:	Rotavapor R-114, Büchi, Switzerland
Rotary shaker:	Pilot-shake RC-6-U, Adolf Kühner AG, Basel, Switzerland
Spectrophotometer:	UV 2100, Shimadzu Corp., Kyoto, Japan Spectronic 601, Milton Roy Comp., USA Ultrospec Plus, Pharamcia LKB, LKB Biochrom, England Ultrospec 3000, Pharmacia Biotech Ltd., Cambridge, UK
Swinging platform:	DuoMax 1030, Heidolph Instruments, Germany
Table universal shaker:	Certomat U, R and C, B.Braun, Melsungen AG, Germany
Thermomixer:	Thermomixer 5437 and Thermomixer Comfort 5355 P, Eppendorf, Hamburg
Ultracentrifuge:	Beckman L7-65 and LE-80, Beckman Instruments Inc., Palo Alto, CA, USA
UV-Crosslinker:	UV Stratalinker 1800, Stratagene, CA, USA
UV-Transilluminator:	TFP-M/WL, BioSciTec GmbH, Germany
Vortex:	Genie 2, Scientific Industries Inc., Bohemia NY, USA
Vacuum concentrator:	DNA Speedvac 120, Thermo Savant, USA
Waterbath:	Köttermann 3043, Uetze-Hänigsen, Germany GFL 1083, Gesellschaft für Labortechnik GmbH, Burgwedel, Germany

2.2. Materials

2.2.1. Chemicals

Chemicals were purchased from Fluka AG, Merck AG, Riedel-de-Haen and Sigma-Aldrich and were in general of the highest purity available. Solvents for HPLC analyses were from J.T.Baker (Philipsburgh, NJ, USA). 4-Chlorosalicylate and 4-chlorocatechol were obtained from TCI (Tokyo, Japan). 3-Chloro-*cis,cis*-muconate was prepared *in situ* from 4-chlorocatechol by transformation with chlorocatechol 1,2-dioxygenase from *P. chlororaphis* RW71 in 50 mM Tris-HCl buffer containing 2 mM $MnCl_2$ (pH 7,5). *Cis*-dienelactone was synthesized chemically and generously donated by Walter Reineke (Bergische Universität – Gesamthochschule Wuppertal, Germany) and Stefan Kaschabeck (TU Bergakademie, Freiberg, Germany). Protoanemonin was obtained from 4-chlorocatechol by its transformation with crude cell extracts of salicylate-grown cells of *Pseudomonas* sp. RW10 as described previously (Blasco *et al.*, 1995). *trans*-Dienelactone was prepared as previously described (Reineke and Knackmus, 1984). Maleylacetate was prepared *in situ* from *cis*-dienelactone by

alkaline hydrolysis (Seibert *et al.*, 1993). *cis*-Acetylacrylate was obtained by UV light-mediated isomerization of its corresponding *trans*-isomer (Lancaster Synthesis, Morecambe, UK) as described previously (Schlömann *et al.*, 1990a).

4',6-Diamidine-2'-phenylindole dihydrochloride (DAPI) and the chemiluminescent substrate for alkaline phosphatase (CDP-Star) were purchased from Roche Diagnostics GmbH (Mannheim, Germany).

Formamide for *in situ* hybridisation was supplied by Applichem GmbH (Germany).

2.2.2. Enzymes

Restricton endonucleases were purchased from New England Biolab or MBI Fermentas. Enzymes were used in buffers and at reaction conditions recommended by the manufacturers. T4 DNA ligase was purchased from Stratagene (La Jolla, CA, USA), Klenow enzyme from Roche (Mannheim, Germany) and *Taq* polymerase from Qiagen (Hildesheim, Germany).

2.2.3. Vectors

Products of PCR reactions were routinely cloned in plasmid pCR®2.1 of the TOPO cloning system (Invitrogene). Genomic libraries were created by cloning of partially-digested DNA in ZAP Express® phage vector (Stratagene).

Excision of the pBK-CMV phagemid from the ZAP Express® phage was carried out with ExAssist® interference-resistant helper phage.

Plasmid pSPM100 carrying *xylXYZL* genes that are necessary for transformation of 4-chlorobenzoate into 4-chlorocatechol was used for transconjugation experiments.

Table 2.1. Brief characteristic of all vectors used in this study.

Vector	Description	Source/Reference
pCR®2.1-TOPO®	Ap^R, Km^R, *lacZα*, lac^p, pUC *ori*, f1 *ori*, T7 promoter	Invitrogen (Groningen, The Netherlands)
ZAP Express®	Neo^R, Km^R, pUC *ori*, f1 *ori*, *lacZα*, lac^p, bla^p, *SV40* promoter, *CMV* promoter	Stratagene (La Jolla, CA, USA)
ExAssist®	f1 *ori*, *lacZ'*	Stratagene (La Jolla, CA, USA)
pSPM100	Ap^R, Tel^R, *Pm xylXYZL* inserted into *Sfi*I site of pUTTcTel*xylS*	(Panke & de Lorenzo, unpubl.)

2.2.4. Bacteria

Bacterial strains that were studied in this work or used for various purposes are listed in Table 2.2.

Table 2.2. Bacterial strains used in this study.

Strain	Genotype/Description	Source
Pseudomonas moorei RW10	environmental isolate	(Wittich *et al.*, 1999)
Pseudomonas reinekei MT1	environmental isolate	(Faude, 1995)
Empedobacter brevis MT2	environmental isolate	(Faude, 1995)
Pseudomonas veronii MT4	environmental isolate	(Faude, 1995)
Achromobacter xylosoxidans MT3	environmental isolate	(Faude, 1995)
Escherichia coli XL1-Blue MRF'	Δ(*mcr*A)183 Δ(*mcr*CB-*hsd*SMR-*mrr*)173 *end*A1 *sup*E44 *thi-1 rec*A1 *gyr*A96 *rel*A1 *lac* [F' *pro*AB *lac*I^q ZΔM15 Tn*10* (Tet^r)]	Stratagene (La Jolla, CA, USA)
Escherichia coli XLOLR	Δ(*mcr*A)183 Δ(*mcr*CB-*hsd*SMR-*mrr*)173 *end*A1 *thi-1 rec*A1 *gyr*A96 *rel*A1 *lac* [F' *pro*AB *lac*I^q ZΔM15 Tn*10* (Tet^r)] Su^- (nonsupressing) λ^r (lambda resistant)	Stratagene (La Jolla, CA, USA)
Escherichia coli One Shot® TOP10 Electrocomp	F^-*mcr*A Δ(*mrr-hsd*RMS-*mcr*BC) Φ*80lac*ZΔM15 Δ*lac*X74 *deo*R *rec*A1 *ara*D139 Δ(ara-leu)7697 *gal*U *gal*K *rps*L (Str^R) *end*A1 *nup*G	Invitrogen (Carlsbad, CA, USA)
Escherichia coli One Shot® TOP10F'	F' {*lac*I^q Tn*10* (Tet^R)} *mcr*A Δ(*mrr-hsd*RMS-*mcr*BC) Φ*80lac*ZΔM15 Δ*lac*X74 *deo*R *rec*A1 *ara*D139 Δ(ara-leu)7697 *gal*U *gal*K *rps*L (Str^R) *end*A1 *nup*G	Invitrogen (Groningen, The Netherlands)
Escherichia coli SM100	Δ(*ara-leu*) *ara*D Δ*lac*X74 *gal*E *gal*K *pho*A20 *thi*-1 *rps*E *rpo*B *arg*E(Am) *rec*A1 λ*pir* Lysogen, contains pSPM100 {*Pm xyl*XYZL (Ap^R) (Tel^R)}	(Panke & de Lorenzo, unpubl.)
Escherichia coli HB101	*rec*A *thi pro leu hsd*RM^+ (Sm^R)	(Kessler *et al.*, 1992)

2.2.5. Media

Consortium strains were grown in batch cultures and in the chemostat on mineral medium G4. 4-Chlorosalicylate and other compounds used as substrates were added as sole carbon source at a concentration between 1 and 10 mM.

Transconjugants obtained after mating were selected on M9 minimal agar medium prepared according to Sambrook *et al.* (1989).

Mineral medium G4

Phosphate buffer solution (10×M9)	100 ml	
Magnesium sulphate solution	0,67 ml	
Trace elements solution	1,33 ml	
Fe-EDTA solution	4 ml	
Carbon source	1-10 mM	(autoclaved / steril-filtered)
Yeast extract (for MT2 strain only)	0,05 %	(autoclaved)
$H_2O_{dist.}$	ad 1000 ml	

Phosphate buffer solution (10×M9):

$Na_2HPO_4 \cdot 2H_2O$	87,78 g	
KH_2PO_4	30,00 g	
$(NH_4)_2SO_4$	12,37 g	
$H_2O_{dist.}$	ad 1000 ml	(autoclaved)

Magnesium sulphate solution:

$MgSO_4 \cdot 7H_2O$	246,48 g	
$H_2O_{dist.}$	ad 1000 ml	(sterile-filtered)

Trace elements solution:

MgO	10,75 g	
$FeSO_4 \cdot 7H_2O$	4,50 g	
$CaCO_3$	2,00 g	
$ZnSO_4 \cdot 7H_2O$	1,44 g	
$MnSO_4 \cdot 2H_2O$	0,87 g	
$CoSO_4 \cdot 7H_2O$	0,28 g	
$CuSO_4 \cdot 5H_2O$	0,25 g	
H_3BO_3	0,06 g	
HCl (37%)	51,3 ml	
$H_2O_{dist.}$	ad 1000 ml	(sterile-filtered)

Fe-EDTA solution:

$FeSO_4 \cdot 7H_2O$	3,20 g	
EDTA	12,37 g	
$H_2O_{dist.}$	ad 1000 ml	(sterile-filtered)

E. coli strains used in this study were cultivated in complex media or on respective agar often with addition of supplements (see: Table 2.3.). Tryptone, yeast extract and agar were purchased from Difco Laboratories (Detroit, MI, USA), agarose from Roth (Germany). Antibiotics, IPTG, X-gal and NZ amine (casein hydrolysate) were from Sigma (St. Louis, MO, USA).

LB (Luria-Bertani) Broth:

NaCl	10 g	
tryptone	10 g	
yeast extract	5 g	
agar	15 g	(for **LB Agar** only**)**
agarose	7 g	(for **LB Top Agar** only**)**
$H_2O_{dist.}$	ad 1000 ml	pH 7,0 (autoclaved)

NZY Broth:

NaCl	5 g	
$MgSO_4 \cdot 7H_2O$	2 g	
yeast extract	5 g	
NZ amine (casein hydrolysate)	10 g	
agar	15 g	(for **NZY Agar** only**)**
agarose	7 g	(for **NZY Top Agar** only**)**
$H_2O_{dist.}$	ad 1000 ml	pH 7,5 (autoclaved)

SOC Broth:

NaCl	0,58 g	
KCl	0,18 g	
$MgCl_2$	0,95 g	
$MgSO_4$	1,20 g	
glucose	3,60 g	(steril-filtered)
tryptone	20 g	
yeast extract	5 g	
$H_2O_{dist.}$	ad 1000 ml	(autoclaved)

Table 2.3. Antibiotics and other media supplements used in this study.

Abbreviation	Antibiotic/Component	Final Concentration
Km	kanamycin sulphate	50-100 µg/ml
Tc	tetracycline hydrochloride	12,5 µg/ml
Cm	chloramphenicol	30 µg/ml
Te	potassium tellurite (K_2TeO_3)	40 µg/ml
IPTG	isopropyl-1-thio-β-D-galactopyranoside	2,5 mM
X-gal	5-bromo-4-chloro-3-indolyl-β-D-galactoside	0,5% (w/v)
maltose	maltose	0,2% (w/v)
$MgSO_4$	magnesium sulphate	10 mM

2.2.6. Buffers

The composition of routinely used buffers is shown below.

SM buffer:
100 mM NaCl
8 mM $MgSO_4$
50 mM Tris-HCl (pH 7,5)
0,01 % (w/v) gelatin
$H_2O_{dist.}$ ad 1000 ml (autoclaved)

PBS buffer (Phosphate Buffered Saline):
137 mM NaCl
2,7 mM KCl
10 mM Na_2HPO_4
1,8 mM KH_2PO_4
$H_2O_{dist.}$ ad 1000 ml pH 7,4 (autoclaved)

2.3. Methods

2.3.1. Cultivation of bacteria

2.3.1.1. Growth on agar plates

Bacteria grown on LB agar were used as standard inoculating material. Plating on rich nonselective media was also carried out to control the purity of the chemostat culture and for CFU determinations. Bacteria on LB agar were grown at 30ºC for a period of 1-2 days.

Minimal agar media with single carbon sources (typically 2 mM) were used to determine the degradative capacity of strains MT1-MT4. In this case bacteria were incubated on plates for at least 7 days at 30ºC.

2.3.1.2. Growth in continuous chemostat culture

Mixed cultures were grown in a 4-chlorosalicylate-limited chemostat with regulated substrate inflow rate, pH and aeration. Bioreactors were inoculated with cells pregrown separately on mineral medium G4 with appropriate substrates. All chemostats were supplied with mineral medium G4 which contained 10 mM of 4-chlorosalicylate. Unless specified otherwise, the cultures were grown at 30ºC in vessels aerated through the membrane filter (Sartorius AG, Göttingen, Germany) and equipped with a stirring system. The pH of the culture media was controlled and adjusted to 7,2 either automatically or manually. Samples from the continuous cultures were taken with the use of a sampling device that was independently connected to the main reactor vessel.

2.3.1.3. Growth in batch cultures

Cells were grown in baffled Erlenmeyer flasks filled up to a maximum of 25% of its total volume with appropriate minimal medium containing 1-10 mM of carbon source. Substrates known for their toxicity or low water solubility like chlorobenzene, chlorophenols or dichlorobenzenes were supplied in vapours from a device held in the cap of the flask. Unless stated otherwise all cultures were incubated at 30ºC with 120 rpm shaking.

2.3.2. Analytical techniques

2.3.2.1. HPLC analyses

Concentration of substrates and metabolites in the cultures was determined with High-Performance Liquid Chromatograpy (HPLC). Bacterial cells were removed from the sample by centrifugation at 15000×g for 8 min at RT prior to HPLC analysis. Supernatants were either directly analysed or stored over short time periods at -20ºC.

Compounds present in the sample were separated in a Waters 2690 (Milford, USA) separation module equipped with a Nucleosil 100 C-18 column (Macherey-Nagel, Germany) and detected with a photodiode array PDA 996 detector (Waters GmbH, Eschborn, Germany). Water:methanol with 0,1% v/v H_3PO_4 was used as mobile phase at a flow rate of 250 µl/min and its composition changed in the gradient from 80:20 (t = 0 min) through 78:22 (t = 12 min) up to 20:80 (t = 30 min). Separated compounds were detected in the effluent at 210 nm UV light wavelengths (4-chlorocatechol, 4-CS, 5-CS, 4-chlorobenzoate, maleylacetate, *cis*-acetylacrylate) or at 260 nm (protoanemonin, *cis*- and *trans*-dienelactone, and 3-chloro-*cis,cis*-muconate). Compounds were identified by comparison of their retention volumes and their absorption spectra recorded in the UV-range by *Millenium* software (Waters) with those of authentic standards. Retention volumes observed for authentic standards under above conditions were as follows: 0,64 ml for maleylacetate, 0,8 ml for *trans*-dienelactone, 0,83 ml for *cis*-acetylacrylate, 1,15 ml for protoanemonin, 1,4 ml for *cis*-dienelactone, 4,21 ml for 4-chlorocatechol, 6,40 ml for 4-chlorobenzoate, and 6,79 ml for 4-chlorosalicylate. Concentrations of metabolites were calculated from the corresponding peak areas using appropriate calibration curves.

2.3.2.2. Nucleic acid analysis

DNA concentration and purity was determined spectrophotometrically (Sambrook *et al.*, 1989).

2.3.2.3. Bacterial counts

Growth of bacteria was routinely measured turbidimetrically at λ = 600 nm (OD_{600}) with cell-free medium as a reference.

Colony forming units (CFU) were determined by plating serial dilutions on LB agar medium. Counting was performed after 36 h of incubation.

Total cell numbers were determined microscopically by counting the DAPI-stained bacteria on the surface of a 0,22 µm filter or cytometrically by counting propidium iodide-fluorescent bacteria.

2.3.3. Fluorescent In Situ Hybridisation (FISH)

2.3.3.1. Fixation

Three volumes (typically 1,5 ml) of ice-cold 4% (w/v) paraformaldehyde in 1×PBS (pH 7,2) fixative solution were added to one volume (0,5 ml) of cell suspension and thoroughly mixed by inverting the tube a few times. Fixation was carried out for 2 h at 4ºC, and then cells were pelleted by centrifugation at 9500×g for 2 min. The pellet was washed in 1 ml PBS buffer by vigorous mixing on the vortex and centrifuged at 4600×g for 2 min. After removing the supernatant, washing and centrifugation steps were repeated once again. Finally, cells were resuspended in a 1:1 (v/v) mixture of PBS and absolute ethanol (routinely 200 µl). Fixed cells were stored at -80ºC.

2.3.3.2. Hybridisation on microscopic slides

Hybridisation on microscopic slides was carried out in 10 µl of F*IS*H hybridisation buffer containing 30% formamide (v/v) and 50 ng of fluorescent probe while the excess of unbound probe was washed off with F*IS*H washing buffer as described by Manz *et al.* (1993). Bacteria in the sample were counterstained with DAPI according to Porter & Feig (1980).

F*IS*H hybridisation buffer:
30% (v/v) formamide
0,9 M NaCl
0,02 M Tris-HCl (pH 8.0)
0,01% (w/v) of SDS (or 0,005% for FISH-FCM)
in sterile milliQ H_2O

F*IS*H washing buffer:
0,102 M NaCl
0,02 M Tris-HCl (pH 8.0)
0,005 M EDTA
0,01% (w/v) SDS
in sterile milliQ H_2O

Fluorescent probes used in this study are listed in Table 2.4. Oligonucleotide probes were synthesized and labelled by IBA (Göttingen, Germany) or MWG (Germany).

Table 2.4. F*IS*H probes used in this study.

Probe	Sequence (5'→3')	Fluorescent Dye
MT1	GAA TTC AGG AGC AAG CTC CT	5'-Cy3
Main_MT1	GCC GCT GAA TTC AGG AGC AA	5'-Cy3
MT1_green	GAA TTC AGG AGC AAG CTC CT	5'-AlexaFluor 488
MT1_red	GAA TTC AGG AGC AAG CTC CT	5'-Bodipy 630/650
MT1_420	AAG CTC CTG TCA TCC GCT CG	5'-AlexaFluor 488
MT2	TAA TCC TCC TTT CGA AGG GC	5'-Cy3
MT2_blue	TAA TCC TCC TTT CGA AGG GC	5'-AlexaFluor 350
MT2_Cy5	TAA TCC TCC TTT CGA AGG GC	5'-Cy5
MT2_mega	TAA TCC TCC TTT CGA AGG GC	5'-Dy 485 XL
MT2_double405	TAA TCC TCC TTT CGA AGG GC	5'- and 3'-AlexaFluor 405
MT3	ATA TCG GCC GCT CTA ATA GT	5'-Cy3
MT3_blue	ATA TCG GCC GCT CTA ATA GT	5'-AlexaFluor 350
MT3_green	ATA TCG GCC GCT CTA ATA GT	5'-AlexaFluor 488
helper_MT3	TAC CCC ACC AAC TAG CTA AT	3'-AlexaFluor 546
MT3_Alexa647	ATA TCG GCC GCT CTA ATA GT	5'-AlexaFluor 647
MT3_mega	ATA TCG GCC GCT CTA ATA GT	5'-Dy 485 XL
MT3_FRET	ATA TCG GCC GCT CTA ATA GT	5'-6-FAM, dT_{12}-Alexa546
MT4	CTC AAG AGA AGC AAG CTT CT	5'-Cy3
New_MT4	GCC GCT CTC AAG AGA AGC AA	5'-Cy3
Add_MT4	AAG CTT CTC TCT ACC GCT GC	5'-Cy3
MT4_red	AAG CTT CTC TCT ACC GCT CG	5'-Bodipy 630/650
MT4_orange	AAG CTT CTC TCT ACC GCT CG	5'-AlexaFluor 546
MT4_Alexa594	AAG CTT CTC TCT ACC GCT CG	5'-AlexaFluor 594
FC [a,1]	AGG TAC CCC CAG CTT CCA TGG CT	5'-Cy3
BPA [a,2]	GTG TGC CGG TTC TCT TTC GAG CAC	5'-Cy3
P(I) [a,3]	ATT TCA GCC TAC CAC CTT AA	5'-Cy3
EUB338 [b,4]	GCT GCC TCC CGT AGG AGT	5'-Cy3
EUB338_green [b,4]	GCT GCC TCC CGT AGG AGT	5'-AlexaFluor 488
Non_EUB338 [c,5]	ACT CCT ACG GGA GGC ACG	5'-Cy3

[a] (Kenzaka *et al.*, 1998); [b] (Amann *et al.*, 1990b); [c] (Wallner *et al.*, 1993).

[1] specific to *Flavobacterium-Cytophaga*; [2] specific to *Burkholderia-Pseudomonas* (rRNA III)-authentic *Alcaligenes* ; [3] specific to *Pseudomonas* (rRNA I) ; [4] specific to *Eubacteria* ; [5] antisense of the EUB338 probe.

2.3.3.3. Hybridisation in solution

Aliquots of fixed cells corresponding to 50 µl of bacterial suspension with an OD_{600} of 0,3 were centrifuged at 4600×g for 4 min. The supernatant was carefully discarded and replaced by 90 µl of hybridisation buffer prewarmed to 46ºC. Cells were prehybridised at 46ºC for 15 min. After the probes were added to final concentration of 5 ng/µl, the sample volume was adjusted to 100 µl with sterile milliQ H_2O. Hybridisation was carried out at 46ºC for 2 h. Afterwards, cells were pelleted by 3 min of centrifugation at 4600×g and washed with 1 ml of washing buffer at 48ºC for 15 min. Following a second identical washing step, cells were resuspended in 400 µl of ice-cold 1×PBS and incubated at 4ºC for 30 min. 200 µl of this suspension were directly analysed on a flow cytometer whereas the remaining portion of sample was counterstained with propidium iodide (47 µM final concentration), incubated at RT for 10 min and then subjected to cytometric analysis.

2.3.4. Indirect immunofluorescence

For the purpose of comparing various direct and indirect methods of enumeration MT1-MT4 cells were visualized and quantified following their staining with fluorescent antibodies. Mono- and polyclonal sera raised in mice were used as primary strain-specific antibodies (Tesar *et al.*, 1996) while the fluorescence immunodetection resulted from binding of the DTAF-conjugated rabbit anti-mouse secondary antibody (Table 2.5.).

Table 2.5. Antibodies used in this study.

Antibody	Description	Dilution	Source
3G8	Anti-MT1 mouse monoclonal AB	1:20	(Tesar *et al.*, 1996)
4C2	Anti-MT2 mouse polyclonal serum	1:8	(Tesar *et al.*, 1996)
1A3	Anti-MT3 mouse polyclonal serum	1:8	(Tesar *et al.*, 1996)
170	Anti-mouse rabbit DTAF conjugate	1:80000	Sigma

5-8 µl of cells fixed in PFA solution (see: 2.3.3.1.) were spotted into wells of gelatine-precoated multiwell slide (Marienfeld, Germany) and air-dried at RT. Bacteria immobilized on the surface were covered with 20 µl of primary antibody solution in Roti-Block (Roth, Germany) and incubated for 30 min at RT in darkness. Excess of antibodies was removed from the slide by rinsing with a 1% (v/v) aqueous solution of Roti-Block. After the slide was dried at RT, a solution of fluorescently labeled secondary antibody was applied to the wells and incubated for 30 min at RT. Excess of antibodies was flushed away from the slide with

Roti-Block solution. Slides were air-dried at RT in the darkness and bacterial cells were counterstained with 10 µl of DAPI (1 µg/ml) for 10 min on ice. After rinsing with Roti-Block solution slides were air-dried, covered with Moviol (Hoechst, Germany), topped with coverslips, sealed with nail varnish and observed under the microscope.

2.3.5. Molecular techniques

2.3.5.1. Agarose gel electrophoresis

DNA fragments were analysed following their electrophoretical separation in 0,4-2,5% (w/v) agarose gels in 1×TAE buffer (Sambrook *et al.*, 1989). Nucleic acids present in the gel were stained with ethidium bromide (1 µg/ml) or SYBR Gold (Molecular Probes, Eugene, OR, USA) solution for 10 or 30 min, respectively. Bands were visualized under UV light and their sizes were judged by the position of fragments of a 1 Kb DNA ladder or λ mono-cut DNA marker (both Invitrogen, Groningen, The Netherlands).

2.3.5.2. Plasmid isolation

Plasmids and phagemids were isolated with *NucleoSpin® Plasmid Mini Kit* (Macherey-Nagel, Düren, Germany) according to the manufacturer's manual and routinely eluted with milliQ H_2O.

2.3.5.3. Restriction enzyme digestion

Restriction digests were routinely carried out in 20 µl reaction volume according to the conditions recommended by the manufacturer and with an excess of enzyme. Where appropriate, residual enzyme activity after digestion was inactivated by 20 min incubation at 65ºC.

2.3.5.4. Cloning

Purified PCR products were cloned with the TOPO TA Cloning® Kit (Invitrogen) according to manufacturer's manual:

4 µl of amplified PCR product
1 µl of Salt Solution
1 µl of TOPO vector

Components were combined, mixed, incubated for 30 min at RT and transformed into *E. coli* One Shot® TOP10F' cells by a 30 sec heat-shock at 42ºC. Transformants were

recovered in SOC medium at 37ºC for 1 h and plated on LB agar supplemented with kanamycin, X-gal and IPTG. Plates were incubated overnight at 37ºC. Up to 10 white colonies were picked, grown in LB broth supplemented with kanamycin and subjected to plasmid isolation. Presence of insert was verified by restriction digest and electrophoresis.

2.3.5.5. Purification of DNA fragments from agarose gels

DNA fragments in bands excised from agarose gels were purified with QIAEX II Gel Extraction Kit (Qiagen, Hilden, Germany) according to the manufacturer's protocol.

2.3.5.6. Purification of DNA from solutions

PCR products for further manipulations were purified with QIAquick PCR Purification Kit (Qiagen, Hilden, Germany).

Purification of high-molecular DNA fragments and concentration of nucleic acids in the sample was performed by precipitation with ethanol and sodium acetate (Sambrook *et al.*, 1989).

2.3.5.7. Polymerase Chain Reaction (PCR)

Fragments of target genes were amplified from total genomic or vector DNA by PCR (Saiki *et al.*, 1985; Mullis *et al.*, 1986) using the conditions below:

Component	**Final concentration**
PCR reaction buffer (10×)	1×
dNTPs	200 µM
forward primer	0,5 µM
reverse primer	0,5 µM
DNA template	0,1-1,0 µg
Taq polymerase (5 U/µl)	2,5 U

The standard amplification program included:

	2 min	initial denaturation	94°C,
then 30 cycles of:	60 s	denaturation	94ºC
	60 s	annealing	40-60ºC
	60 s	elongation	72ºC
	10 min	final extension	72°C

The quality of amplification was routinely controlled by agarose gel electrophoresis.

Both degenerate and sequence-specific primers used for amplification are listed in the Tables 2.6 and 2.7, respectively. Oligonucleotide primers were purchased from Invitrogen (Groningen, The Netherlands).

Table 2.6. Degenerate primers used in this study.

Primer	Sequence (5'→3')	Target (source)
MT1:MCI_F1	CTI GAY GCC IAR GGC AAR CG	MT1 muconate
MT1:MCI_F2	GGI MTI GAA AGY GCS ITG CTC	cycloisomerase,
MT1:MCI_R	CRT CCC AIT AYT GRT TIA CGT C	*salD* (this study)
MT1:CARB_F1	GGI GCS ACC AGY CAG GAY G	Carboxymuconate
MT1:CARB_F2	CGN ACC TGG YTS CAR CAI GC	cycloisomerase
MT1:CARB_F3	SCT GCA RTT CGG CGG TGC	from MT1, *pcaB*
MT1:CARB_R1	TTI CGC TTR TGY GGC ATG GT	(this study)
MT1:CARB_R2	GTT TCC CAY TCI GCA TGC CA	
CCD(G-)_F	ATC GAY RTS TGG CAY TCS ACI C	Chlorocatechol
CCD(G-)_R	TCR AAG TAG TAY TGS GTS GTC AI	1,2-dioxygenase [a,1]
C12D_pbF1	GCI ATI SAG GGI CCI TAC T	Catechol
C12D_pbR2	TGC ASI TGM GCI GGA CGC CA	1,2-dioxygenase [a,2]
CMCI_F72	TAC AGC AAI TGI TGC CAC ITS TTC G	Chloromuconate
CMCI_F86	CCA CIT STT CGT ITC GAT ACI CTA GC	cycloisomerase;
CMCI_F483	GCI GCI GTG TTI GCS AAG TTC	Generic for
CMCI_R744	GTC ICT CGA STC CGA IAG IAG CCG	Gram(-) *Eubacteria*
CMCI_R818	GGI GGG TAC AAC GTI TCG AAS TC	(this study)
CDLH_F1	AAG GCT TAT CTA TCG ATG CG	*cis*-Dienelactone
CDLH_F2	GCT GAC TGA AGG CTT ATC TA	Hydrolase
CDLH_R1	TGA TGA GTT GTC TGG CCT CC	Generic for
CDLH_R2	ATT GGT GAT GAG TTG TCT GG	Gram(-) *Eubacteria*
CDLH_R3	CTT CAG CAT TTC CAG CGT GC	(this study)
DLH_pbF1	TGI TSG GIT ATT GYI TIG GSG G	*cis*-Dienelactone
DLH_pbR2	CCK IGC GAA CGA RTG ICC IRC	hydrolase [a]
DLH_pbR3	IGC IAR GAA ICC RTG ICC IGC	(Bielecki, unpubl.)
MR_F335	CCG CCI CCI AGI YGG TAG CCI GA	Maleylacetate
MR_F350	CCI AGI TGR TAG CCI GAG CGI TTC	reductase [a]
MR_R747	CAI ACC GTI TCG AAC ACY ACG T	(this study)
MR_pbF2	GCS ATT GGI GGI GGI TCD AC	Maleylacetate
MR_pbF3	NTI CCV ACI ACI TAT GCV GG	reductase [a]
MR_pbR1	AGC TTI TGR TGC ARK ICC AT	(Bielecki, unpubl.)

[a] generic primers for Gram-negative *Eubacteria*; [1] (Thiel & Schlömann, 2000); [2] (Bielecki, unpubl.)

2.3.5.8. DNA Sequencing

DNA fragments were sequenced with the dideoxy-termination method using DYEnamic ET Terminator Cycle Sequencing kit (Amersham Biosciences) or BigDye Terminator 1.1 Cycle Sequencing Kit (Applied Biosystems) on ABI PRISM 3730 and 3100 Genetic Analyzer (Applied Biosystems) according to the recommendations of the manufacturer.

Following amplification, DNA was purified either by precipitation with ethanol and sodium acetate (Sambrook *et al.*, 1989) or with DyeEx 2.0 Spin kit (Qiagen, Hilden, Germany).

Table 2.7. Universal sequencing primers used in this study.

Primer	Sequence (5'→3')	T_m [ºC]
16F27	AGA GTT TGA TCM TGG CTC AG	59
16F357	ACT CCT ACG GGA GGC AGC AG	66
16R518	CGT ATT ACC GCG GCT GCT GG	66
16R1087	CTC GTT GCG GGA CTT AAC CC	64
16R1492	TAC GGY TAC CTT GTT ACG ACT T	63
T3	AAT TAA CCC TCA CTA AAG GG	56
T7	GTA ATA CGA CTC ACT ATA GGG C	64
M13	GAC GTT GTA AAA CGA CGG CCA G	68
rM13	CAC AGG AAA CAG CTA TGA CCA TG	68

Sequences were analysed with the BioEdit software package v.7.0.5.3 (Hall, 1999), and by using BLAST (Altschul *et al.*, 1990, 1997) provided by National Center for Biotechnology Information (NCBI).

2.3.6. Biochemical methods

2.3.6.1. Preparation of cell-free extracts

Bacteria for preparation of cell-free extracts were grown in G4 mineral medium with a single carbon source in a minimum volume of 500 ml. Cells during late exponential growth phase were harvested by centrifugation at 9000×g for 10 min at 4ºC. Then, bacteria were washed in 40 ml of appropriate buffer (100 mM sodium/potassium phosphate buffer of pH 7,4 or 50 mM Tris-HCl + 2 mM $MnCl_2$ of pH 7,5), centrifuged and finally resuspended in 3 ml of ice-cold buffer. After addition of DNase I, bacteria were disrupted by passing the suspension twice through a French press at 10000 lb/in^2. Cellular debris were removed by ultracentrifugation at 100000×g for 35 min at 4ºC. The decanted clear supernatant was used as crude cell-free extract.

2.3.6.2. Determination of protein concentrations

Protein concentrations in cell-free extracts were determined according to the method of Bradford (Bio-Rad Protein Assay, Hercules, CA, USA) using bovine serum albumin as a standard.

2.3.6.3. Enzymatic activities

Enzymatic activities were determined by following changes of absorption due to the depletion of substrate or the formation of product upon addition of cell-free extract. Reactions were carried out in 1 ml quartz cuvettes. Absorption changes in the reaction mixture without cell extract were subtracted from the values obtained for enzymatic transformations.

Activity of **salicylate 1-monooxygenase** (salicylate hydroxylase) was measured by following the oxidation of NADH (ε_{340nm} = 6220 $l \cdot M^{-1}$ cm^{-1}) in the reaction mixture (Bosch *et al.*, 1999):

50 mM Tris-HCl (pH 8.0)
1 mM EDTA
0,2 mM NADH
0,2 mM salicylate/4-chlorosalicylate

Background NADH-oxidizing activity of cell-free extracts in the absence of salicylate was recorded and subtracted from the activity in the presence of substrate.

Chloro/catechol 1,2-dioxygenase activity was determined by measuring the rate of formation of muconate (ε_{260nm} = 16800 $l \cdot M^{-1}$ cm^{-1}) and 3-chloromuconate (ε_{260nm} = 12400 $l \cdot M^{-1}$ cm^{-1}) from catechol or 4-chlorocatechol, respectively (Dorn and Knackmuss, 1978):

50 mM Tris-HCl (pH 8,0)
1,3 mM EDTA
0,2 mM catechol/4-chlorocatechol

The rate of formation of 2-hydroxymuconic semialdehyde (ε_{375nm} = 36000 $l \cdot M^{-1} cm^{-1}$) from catechol was used to assay **catechol 2,3-dioxygenase** activity (Mars *et al.*, 1997):

50 mM sodium/potassium phosphate buffer (pH 7,4)
0,2 mM catechol

Activity of **muconate cycloisomerase** was measured as the decrease in the concentration of muconate (ε_{260nm} = 16800 $l \cdot M^{-1}$ cm^{-1}) according to Dorn and Knackmuss (1978):

33 mM Tris-HCl (pH 7.5)
2 mM $MnCl_2$
0,1 mM muconate

Dienelactone hydrolase activity was measured with both *cis*- and *trans*-dienelactone isomers (ε_{280nm} = 17000 $l \cdot M^{-1}$ cm^{-1} and ε_{280nm} = 15625 $l \cdot M^{-1}$ cm^{-1}, respectively) by monitoring the decay rate of substrate in the following mixture (Schmidt and Knackmuss, 1980; Schlömann *et al.*, 1990b):

10 mM histidin-HCl buffer (pH 6,5)
50 µM *cis*-dienelactone or *trans*-dienelactone

Gentisate 1,2-dioxygenase activity was assayed by following the formation of maleylpyruvate (ε_{334nm} = 10800 $l \cdot M^{-1}$ cm^{-1}) according to Crawford *et al.* (1975):

100 mM sodium/potassium phosphate buffer (pH 7,4)
0,1 mM gentisate

Maleylacetate reductase activity was determined according to Seibert *et al.* (1993) from the rate of NADH oxidation (ε_{340nm} = 6220 $l \cdot M^{-1}$ cm^{-1}) coupled to the reduction of substrate:

50 mM Tris-HCl (pH 7,5)
200 µM NADH
50 µM maleylacetate

NADH oxidation by cell extracts in the absence of maleylacetate was recorded and subtracted from the activity displayed in the presence of substrate.

2.3.7. Resting cell assays

Bacteria for resting cell assays were grown in G4 minimal medium with a single carbon substrate (succinate, acetate or salicylate) in a minimum volume of 500 ml. Genes encoding enzymes of the chlorocatechol pathway were induced by addition of 0,1-0,5 mM 4-chlorocatechol 4 h prior to harvest. Cells from the late exponential phase were pelleted by centrifugation at 9000×g for 15 min at 4ºC, washed and finally resuspended in 5-10 ml of physiological salt solution. Bacterial suspensions were dispensed to Erlenmeyer flasks which contained minimal medium with substrate to give an OD_{600} of 0,5-2,0. Suspensions were incubated at 30ºC with 120 rpm shaking for up to 10 h. Samples for HPLC analyses and cell density measurements were taken in regular time intervals. Incubation of the substrate without cells was used as negative control.

2.3.8. Transconjugation

Plasmid pSPM100 containing a minitransposon carrying *xylXYZL* genes (encoding toluate 1,2-dioxygenase and 1,2-dihydro-1,2-dihydroxytoluate dehydrogenase) from plasmid pWW0 and a tellurite resistance gene was transformed by mating into MT3 and MT4 in an attempt to extend the degradative capabilities of these strains to grow on 4-chlorobenzoate. Donor and helper *E. coli* strains were grown at 37ºC in LB broth supplemented with the appropriate antibiotics. The recipient strains MT3 and MT4 were grown at 30ºC in LB broth. Cells were inoculated to LB broth without supplements and were further cultivated at 30ºC or 37ºC until they reached an OD_{600} of approx. 1,0. Aliquots of donor, helper and recipient strains were mixed to achieve an 1:1:1 ratio. Approximately 1-1,5 ml of this suspension was harvested by centrifugation at 10000×g for 3 min, resuspended in 80 µl of fresh LB broth and transferred onto sterile 0,22 µm membrane filter (Sartorius, Germany) placed on the surface of an LB agar plate. The plates were incubated at 30ºC for at least 12 h. Afterwards, the cells grown on the membrane were thoroughly resuspended in 1 ml of sterile 50 mM $MgSO_4$ and plated on M9 agar medium containing 2 mM 4-chlorobenzoate or benzoate as carbon source and potassium tellurite as selective marker. Plates were incubated at 30ºC for up to 2 weeks until black colonies of transconjugants were visible. Suspensions of the recipient strain and the mixture of donor and helper strains treated identically served as negative controls.

2.3.9. Construction and screening of genomic libraries

2.3.9.1. Isolation of total genomic DNA

Cells of MT1, MT2, MT3 and MT4 grown on acetate in G4 minimal medium were harvested during late exponential growth phase by centrifugation at 10000×g for 5 min. Total genomic DNA was extracted from bacteria with the GNOME kit (BIO101, La Jolla, CA, USA) according to the protocol recommended by the manufacturer. Finally, the isolated bacterial genomic DNA was dissolved in 100-200 µl of sterile milliQ H_2O.

2.3.9.2. Partial digestion of gDNA with *Sau*3AI and cloning into the phage vector

Genomic DNA was fragmented by partial digestion with *Sau*3AI restriction endonuclease. The ratio of enzyme to DNA was optimized to yield primarily fragments of 4-12 kbp in length. The reaction was carried out at 37ºC for 1 h and was halted by addition of EDTA to a final concentration of 50 mM.

100-200 µg of partially digested genomic DNA was fractionated by size through ultracentrifugation in the sucrose gradient at 100000×g for 22 h (Sambrook *et al.*, 1989).

Fractions of 300 µl volume were collected from the top of the tube immediately after centrifugation and DNA was recovered by precipitation with PEG 6000 as described by Sambrook *et al.* (1989). Finally, DNA was dissolved in 10-12 µl of milliQ H_2O and its quality was controlled by electrophoresis in 0,4% agarose gels.

DNA from the fractions that contained mainly 4-12 kbp long fragments was ligated into Bam*HI*-cut and CIAP-treated ZAP Express phage vector at 4ºC for minimum of 12 h in the following reaction mixture:

1,0 µl of the ZAP Express vector (1 µg/µl)
0,5 µl of 10×ligase buffer (containing 10 mM rATP)
4,0 µl of DNA solution (fractionated)
0,5 µl of T4 DNA ligase (2 U)

Following incubation, 4 µl of the ligation mixture was packaged as functional phage particles with Gigapack III Gold Packaging Extract (Stratagene, La Jolla, CA, USA) strictly according to the manufacturer's protocol. The supernatant obtained from the packaging reaction was treated as the primary phage library.

2.3.9.3. Titration, quality control and amplification of primary phage libraries

The efficiency of the packaging reaction (titer) was determined as plaque-forming units per milliliter (pfu/ml) by counting the plaques formed on the bacterial lawn of *E. coli* XL1-Blue MRF' cells infected with 1 µl of serial dilutions from the primary phage library in SM buffer. Infection and plating were carried out as recommended by manufacturer (Stratagene).

The DNA ligation efficiency into the phage vector was estimated from the ratio of colourless (recombinant) plaques to blue (nonrecombinant) plaques and in case of all four libraries it was found higher than 95%.

To determine the average insert size, up to 20 random colonies were picked and tested following mass excision (see: 2.3.9.4.) and conversion of phages into phagemids. Isolated phagemids were digested with Eco*RI*, Bam*HI* and Hind*III* and obtained fragments were analysed by agarose gel electrophoresis. Average insert size varied between 4,1 kbp and 6,5 kbp for all four libraries.

Primary phage libraries were amplified using a small-scale liquid culture method to obtain large, stable and high titer stock according to the method of Leder *et al.* (1977) with modifications described by Sambrook *et al.* (1989). The decanted supernatant obtained from

this protocol was titrated and stored at 4ºC for up to 12 months as stable amplified library stock that served for all screening procedures.

2.3.9.4. Plating the library, recovery of phages, single-clone and mass *in vivo* excision

Serial dilutions of the genomic library were plated on NZY agar/top agarose and grown at 37ºC for 10-12 h. Only plates where individual distinct plaques formed were taken for further manipulations.

Single plaques were cored from the top agar layer with a Pasteur pipette and transferred to 500 µl of SM buffer containing 20 µl of chloroform. After vigorous mixing, the suspension was incubated overnight at 4ºC and released phage particles were treated as phage stocks that could be stored for up to 6 months.

Excision of phage particles both from single recombinants and from the whole library (mass excision) were carried out with ExAssist helper phage exactly as described in the manufacturer's manual (Stratagene). After dilution, excised phagemids were used to transduce XLOLR *E. coli* cells at 37ºC for 15 min. Following recovery, bacteria were plated on selective LB agar with kanamycin and grown at 30ºC or 37ºC overnight.

2.3.9.5. Library screening by plaque hybridisation

Plaque hybridisation was used for screening MT1 and MT4 genomic libraries for genes involved in the biodegradation of chloroaromatic and aromatic compounds. For this purpose, genomic libraries were plated on NZY agar/top agarose at a density of 1000-1500 pfu per 121 cm^2 plate and grown at 37ºC until distinct plaques were formed (at least 10 h).

Plates with the freshly grown library (plaque diameter < 2 mm) were chilled at 4ºC for 2 h to harden. Bacteria and phages from the surface of the top agarose were transferred onto a positively-charged nylon membrane (Hybond N+, Amersham Biosciences) for 1 min. After the membrane was carefully lifted, the DNA bound to it was denatured, neutralised and rinsed as described by the manufacturer's manual (Stratagene). Following rinsing, the membrane was blotted on Whatman paper and air-dried for 15 min at RT. DNA was crosslinked to the membrane by illumination with UV light at 120000 µJ for 2 min. Membranes with linked DNA were stored at RT and the original agar plates at 4ºC.

Gene fragments of carboxymuconate cycloisomerase (Bobadilla, 2006) and muconate cycloisomerase (Nikodem *et al.*, 2003) were used as probes for screening the MT1 genomic library. A fragment of the gene encoding a putative maleylacetate reductase, which was obtained by PCR with degenerate primers and confirmed by DNA sequencing, constituted a probe for screening the MT4 library. Probes for plaque hybridisation were synthesized by

PCR with DIG-Labeling Mix (Roche, Mannheim, Germany) containing DIG-labeled dUTP in the following reaction conditions:

Component	**Final concentration**
10×PCR buffer (Qiagen, Hilden)	1×
PCR DIG labeling mix (Roche, Mannhein)	200 µM (each)
forward primer	0,25 µM
reverse primer	0,25 µM
DNA template	0,1-1,0 µg
Taq polymerase (Qiagen, Hilden)	5 U

The standard PCR amplification program was as below:

	2 min	initial denaturation	94ºC,
then 30 cycles of	60 s	denaturation	94ºC
	60 s	annealing	45-50ºC
	60 s	elongation	72ºC
	10 min	final extension	72ºC

The quality and quantity of obtained PCR products were controlled electrophoretically. The reaction mixture was treated as the probe solution without further purification.

Membranes with covalently-linked single stranded DNA were prehybridised in 50 ml hybridisation solution for 2 h at 68ºC. Hybridisation was carried out at 68ºC overnight with 20 ml of fresh hybridisation solution containing 50 µl of denatured probe. The stringency of the hybridisation solution was individually optimised (see: below).

Hybridisation solution (low-stringent):
5×SSC
1% (w/v) of blocking reagent (Roche)
0,1% (w/v) of N-sodiumlaurylsarcosine
0,02% (w/v) of SDS

Hybridisation solution (medium-stringent):
5×SSC
2% (w/v) of blocking reagent (Roche)
0,1% (w/v) of N-sodiumlaurylsarcosine
0,02% (w/v) of SDS

Following hybridisation, membranes were subjected to a series of low and high stringency washing steps. Further processing involved: blocking of unhybridised DNA, incubation with a conjugate of anti-DIG antibody and alkaline phosphatase, rinsing,

equilibrating and application of CDP-Star (substrate for alkaline phosphatase). All steps were performed exactly as recommended by the manufacturer (Roche, Mannheim, Germany). After removing the excess of liquid, membranes were sealed in polypropylene bags and stored in the dark.

Chemiluminescence from the probe-bound DNA on the membrane was recorded on a photographic film (X-Omat AR-5 or BioMax MR, Kodak) after exposition for 30 s up to 1 h. Films were developed automatically with the Curix 60 system (Agfa, Leverkusen, Germany). Plaques from phages that were identified as positive were captured after superimposing the membrane, photographic film and the original agar plate on the surface of a visible light transilluminator.

In order to ensure error-free plaque assignment and to minimize the risk of selecting transformants infected with multiple phages the whole procedure was repeated with the stocks of selected positive phages as starting material.

2.3.9.6. Plating the library and screening for enzymatic activity

Genomic libraries of MT3 and MT4 were screened directly on plates for 4-chlorocatechol and *cis*-dienelactone transforming activities. In both cases the enzymatic activity assay was based on the formation of a strong acid (chloromuconate and maleylacetate, respectively) from the neutral or weakly acidic substrate. Local acidification around the recombinant plaques was visualized by the colour change displayed by the pH indicator present in the mixture. For the purpose of screening the enzymatic activities, *E. coli* XL1-Blue MRF' cells were infected with phage libraries ensuring a density of 10000-50000 pfu per 534 cm^2 of screening plate, mixed with substrate, pH indicator and top agar and plated on NZY agar.

Screening substrate-indicator mixture I:
48 ml of LB or NZY top agar
250 mg of sodium bisulfite
5 mg of p-rasaniline (pH indicator)
7 mg of 4-chlorocatechol (substrate)

Plates were incubated at 37ºC for a minimum of 12 h in the dark and observed yellow or brownish zones surrounding the plaques were indicative for recombinants exhibiting 4-chlorocatechol transforming activity.

In a second variant of the method, libraries were plated as described above but without substrate and pH indicator and incubated overnight at 37ºC until well-formed plaques could

be seen. The plates were then overlaid with 40 ml of substrate-indicator mixture II and incubated further at 30ºC in the dark. The appearance of brownish, orange or yellow zones was monitored periodically over the next 8 h. Recombinants showing 4-chlorocatechol or *cis*-dienelactone transforming activity were identified by a local change of colouration and collected.

Screening substrate-indicator mixture II:
2 mM EPPS (buffering agent)
0,5 mM phenol red (pH indicator)
1-2 mM substrate (*cis*-dienelactone or 4-chlorocatechol)
0,5% (w/v) agarose

2.3.9.7. Sequencing of inserts from identified recombinant phages

Phages identified as positive in the screening tests were collected and converted to phagemids by single-clone *in vivo* excision as described by the manufacturer (Stratagene). Inserts from the phagemids were sequenced by primer walking or through subsequent restriction digest, subcloning and primer walking. The complete list of primers used for sequencing of inserts from different clones is shown in the Table A.1. of the Appendix.

3. RESULTS

In order to understand how a microbial consortium using 4-chlorosalicylate as its sole carbon and energy source and consisting of *Pseudomonas reinekei* MT1, *Empedobacter brevis* MT2, *Achromobacter xylosoxidans* MT3 and *Pseudomonas veronii* MT4 may respond to changing conditions in the environment a basic knowledge about the degradative potential of individual strains is needed. This knowledge was acquired from a series of experiments which included growth tests of the corresponding pure cultures on various substates, resting cell assays, and determination of enzymatic activities. Further on, the influences exerted by temperature shifts and varying amounts of substrate on the degradation of 4-CS by consortium were studied in batch, fed-batch, and continuous culture. The effect of temporary interrupted aeration (anaerobiosis) on functioning and structure of the community in the chemostat was tested.

Following the dynamics of community structure in mixed bacterial cultures demands adequate enumeration techniques. This challenge was met by developing a multicolour F*IS*H-flow cytometry approach that allowed quantification of individual bacterial populations in the community in an efficient, accurate and reproducible way.

By cultivating three different mixed cultures, the four-membered consortium, a binary culture of MT1 with MT3 and a binary culture of MT1 with MT4 under identical chemostat conditions the influence of community members on the process of 4-chlorosalicylate degradation was evaluated.

The ability of two chlorosalicylate-degrading strains, *P. reinekei* MT1 and *P. moorei* RW10, to coexist and function as the members of the complex microbial community was compared during growth of their corresponding mixed cultures on 4-CS and 5-CS in the fed-batch mode.

Some of the genetic elements that contribute to the aromatics and chloroaromatics degradative potential of strains MT1 and MT4 were identified through screening of the corresponding genomic libraries.

3.1. Characterisation of the physiological capacity and the enzymatic equipment of individual consortium members

All four consortium members are heterotrophic microorganisms and depend in their growth on the availability of carbon substrate. The physiological capabilities of individual

strains were tested with various compounds as sole carbon and energy source for two purposes: (i) to explain their behaviour in mixed cultures upon certain perturbations like alteration of the type or amount of supplied substrate and (ii) to provide rational guidelines for elucidation of the biochemistry and genetics essential for supporting the 4-CS breakdown by consortium members MT2, MT3 and MT4.

3.1.1. Identification of carbon substrates supporting growth of consortium members

Selective enrichment of environmental samples on aromatic or haloaromatic substrates frequently results in isolating strains belonging to the families of *Burkholderiaceae* and *Pseudomonadaceae* of the β- and γ-*Proteobacteria*. This phenomenon might reflect the general preference of currently used methods for isolation of particular groups of bacteria. However, from the broad phylogenomic study of 822 sequenced bacterial genomes an unequal distribution of aromatic catabolic pathways is evident with families of *Nocardioidaceae* (*Actinobacteria*), *Bradyrhizobiaceae* (α-*Proteobacteria*), *Burkholderiaceae*, *Comamonadaceae* (both β-*Proteobacteria*) and *Pseudomonadaceae* (γ-*Proteobacteria*) as being endowed with a particularly broad metabolic potential (Perez-Pantoja *et al.*, 2010b). Individual members of the 4-CS degrading consortium were cultivated with single carbon substrate primarily to probe their central catabolic pathways for degradation of aromatics or haloaromatics. Even though only a few compounds out of the whole range of (halo)aromatics were tested, the results of the metabolic reconstruction of degradation potential of *C. necator* JMP134 suggest that the number and diversity of functional central pathways may also be indicative of the wealth of peripheral pathways (Perez-Pantoja *et al.*, 2008).

3.1.1.1. Substrates utilized by pure cultures of consortium strains

Selection of compounds that were tested as sole carbon and energy substrates for consortium strains aimed to: (i) determine their ability to metabolize simple carbon sources (acetate, succinate), (ii) identify functional central pathways (protocatechuate, gentisate), and (iii) probe the spectrum of chloroaromatics that can be degraded (chlorosalicylates, chlorobenzoates, chloro- and dichlorobenzenes, 2,4-D).

The ability of bacteria to grow at the expense of a given compound was indicated by an increase of the optical density (OD_{600}) in liquid culture and by the formation of colonies on agar plates with minimal medium containing the mentioned substrate as sole carbon source.

P. reinekei MT1 could use benzoate, salicylate and protocatechuate but not gentisate as sole carbon substrates for its growth. This indicates the presence of both protocatechuate and catechol central pathways as salicylate is likely to be degraded *via* catechol and not through

gentisate in this strain. MT1 grew in mineral medium at the expense of 4-CS and 5-CS but none of the other tested chlorinated aromatics could be used as growth substrate. Since many of these compounds are degraded through chlorocatechol derivatives it may suggest that MT1 is devoid of corresponding peripheral pathways. However, some of the substrates like chlorobenzene or 3-chlorobenzoate are typically transformed by peripheral pathways to 3-chlorocatechol, which cannot be degraded by MT1. Moreover, the strain does not have the potential to mineralize dichlorosubstituted catechols.

Table 3.1. Growth of consortium strains on various compounds as sole carbon substrates

Substrate	*P. reinekei* MT1	*E. brevis* MT2	*A. xylosoxidans* MT3	*P. veronii* MT4
acetate	+	–	+	+
succinate	+	–	+	+
laevulinate	+	–	+	+
benzoate	+	–	+	+
salicylate	+	–	+	–
protocatechuate	+	–	–	+
gentisate	–	–	+	–
3-chlorosalicylate	–	–	–	–
4-chlorosalicylate	+	–	–	–
5-chlorosalicylate	+	–	–	–
3,5-dichlorosalicylate	–	–	–	–
3-chlorobenzoate	–	–	–	–
4-chlorobenzoate	–	–	–	–
chlorobenzene	–	ND	–	–
1,2-dichlorobenzene	–	ND	–	–
1,3-dichlorobenzene	–	ND	–	–
1,4-dichlorobenzene	–	ND	–	–
4-chlorophenol	–	–	–	–
2,4-dichlorophenoxyacetate	–	–	–	–

(+) – growth both in liquid medium and on agar plates; (–) – no growth; ND – not determined.

Cultivation of *E. brevis* MT2 was not possible in mineral medium with any of the tested compounds. However, supplementation of the mineral medium with 0,01% (w/v) of yeast extract resulted in growth of the strain with acetate and succinate, as indicated by a higher increase of the optical density compared to growth on yeast extract only. Obviously, MT2 depends on growth factors present in yeast extract. Whereas benzoate and 4-chlorobenzoate did not disturb growth of MT2, already 1 mM of salicylate, chlorosalicylates, or 2,4-D in the

mineral medium completely inhibited its growth on yeast extract. MT2 could be easily cultivated in rich media like LB, NB or YM.

A. xylosoxidans MT3 could grow on benzoate, salicylate and gentisate but not on protocatechuate what indicates the absence of the protocatechuate pathway and presence of both a catechol and a gentisate pathway. Thus, MT3 may degrade salicylate *via* gentisate or catechol. MT3 was not capable to grow on any of the chlorinated aromatics tested.

P. veronii MT4 used benzoate and protocatechuate as sole carbon substrates but not salicylate or gentisate. This may be indicative of the presence of functional protocatechuate and catechol pathways and an absence of gentisate pathway. Similarly to MT3, MT4 was not able to degrade any of the tested halogenated substrates.

Interestingly, incubation of individual consortium members for one week in mineral medium without carbon source resulted in a sharp drop of the optical density in the MT1 culture, whereas the optical density of cultures of MT2, MT3 and MT4 remained unaffected.

3.1.1.2. Growth of consortium strains on metabolites of the 4-CS pathway

Initial hypotheses assumed that 4-CS degradation by MT1 results in the excretion of some intermediates and dead-end metabolites that could be cross-fed to other consortium members like MT3 and MT4 (Pelz *et al.*, 1999). Growth of MT1, MT3, and MT4 on intermediates (4-chlorocatechol) or dead-end metabolites (*cis*-dienelactone) of the 4-CS breakdown as sole carbon source was tested in liquid culture. Additionally, *cis*-acetylacrylate and laevulinate, that were postulated as intermediates of 4-CS degradation pathway in MT1 by Pelz and coworkers (1999), were used as growth substrates in a similar set-up.

Table 3.2. Growth of pure cultures of the consortium members on substrates, intermediates and metabolites of chlorosalicylate pathway of *P. reinekei* MT1.

Substrate	***P. reinekei* MT1**	***A. xylosoxidans* MT3**	***P. veronii* MT4**
4-chlorosalicylate	+	–	–
5-chlorosalicylate	+	–	–
4-chlorocatechol	–	–	–
cis-dienelactone	+	+	+
cis-acetylacrylate	–	+/–	–
laevulinate	+	+	+

(+) – growth in liquid medium; (–) – no growth; (+/–) – results inconclusive.

Unfortunately, several other intermediates and metabolites of 4-CS pathway could not be tested due to their relative instability in the mineral medium (3-chloromuconate and maleylacetate) or due to their insufficient availability (*trans*-dienelactone, protoanemonin).

4-Chlorocatechol, the first intermediate of the 4-CS degradation pathway by MT1 was not used as growth substrate by any of the tested bacteria. This observation agrees with findings that catecholic and halocatecholic compounds are unsuitable substrates for microbial cultures under aerobic conditions due to their prominent toxicity (Schweigert *et al.*, 2001) and liability to undergo radical oxidative polymerisation (Haller & Finn, 1979). Indeed, incubation of 0,5-1,0 mM of 4-chlorocatechol in mineral medium at 30ºC resulted in rapid formation of a brown pigment. It is likely that the relatively high concentration of substrate (0,5 mM) was responsible for inhibiting growth of bacteria, even in the case of strain MT1 known to be capable of mineralizing of 4-chlorocatechol.

cis-Dienelactone is the common intermediate in the chlorocatechol degradation pathway (Schmidt & Knackmuss, 1980) but notably it was found as dead-end metabolite in case of 4-CS breakdown by MT1 (Nikodem et al, 2003; Nikodem, 2004). When strains MT1, MT3 or MT4 were cultivated in the medium with *cis*-dienelactone as sole carbon source the concentration of substrate decreased fastest in the MT3 culture (Fig. 3.1.). Since maleylacetate, that usually results from the hydrolysis of *cis*-dienelactone, was not detected in the culture supernatant it remains an open question whether and on which way the substrate was hydrolyzed.

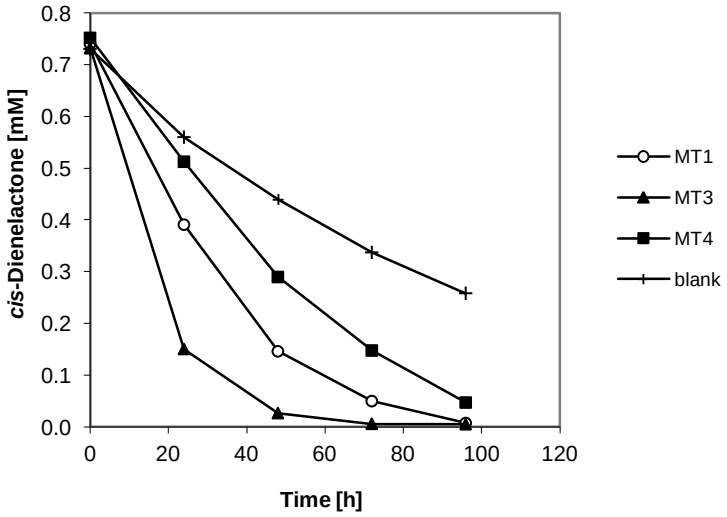

Figure 3.1. Breakdown of *cis*-dienelactone by pure cultures of MT1, MT3 and MT4.

Conversion of *cis*-acetylacrylate into biomass was detected only in the culture of *A. xylosoxidans* MT3 but even in this case the growth could not always be reproduced.

Laevulinate, which was shown previously to be formed from *cis*-acetylacrylate by the action of maleylacetate reductase from MT1 (Pieper *et al.*, 2002; Nikodem, 2004), was used as sole carbon source by MT1, MT3 and MT4. Although all tested strains could be cultivated in the mineral medium with 1-5 mM of laevulinate, in each case the growth phase was preceded by a prolonged adaptation phase that lasted up to 4 days.

3.1.2. Transformation of 4-CS metabolites by resting cells of MT3 and MT4

Resting cell assays provide an excellent tool to study metabolic conversions of compounds that are either tolerated by cells only at low concentration like protoanemonin or that have very limited stability in the corresponding culture medium like 4-chlorocatechol. A series of assays with resting cells of MT3 and MT4 were carried out in order to test the ability of both strains to transform 4-chlorocatechol and protoanemonin.

3.1.2.1. Transformation of 4-chlorocatechol by resting cells of MT3 and MT4

MT3 and MT4 cells were pregrown on succinate in mineral medium, separated from the supernatant by centrifugation and resuspended to an OD_{600} = 1-1,6 in mineral medium containing between 50 μM and 3 mM of 4-chlorocatechol. Transformation of substrate was followed by HPLC analysis over a period of 8-10 h with corresponding cell-free solutions of 4-chlorocatechol serving as controls (Fig. 3.2.).

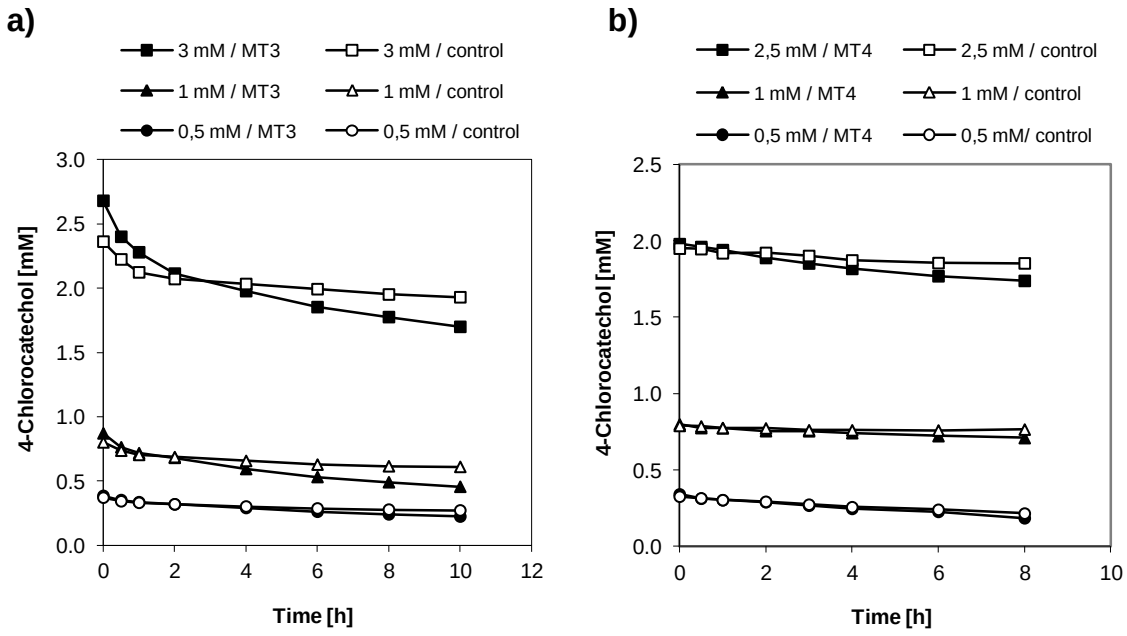

Figure 3.2. Transformation of 4-chlorocatechol by resting cells of *A. xylosoxidans* MT3 **(a)** and *P. veronii* MT4 **(b)**.

Neither MT3 nor MT4 alone showed any 4-chlorocatechol-transforming activity in the resting cell assays exceeding the spontaneous autooxidation rate observed for control samples. None of the expected intermediates of chlorocatechol metabolism like 3-chloromuconate, *cis*-/*trans*-dienelactone or maleylacetate could be detected in the medium supernatant.

3.1.2.2. Transformation of protoanemonin in the presence of 4-chlorocatechol by resting cells of MT3 and MT4

In order to replicate conditions from the 4-CS-fed continuous culture, MT3 and MT4 cells pregrown on succinate were resuspended to an OD_{600} = 0,6-1,2 in the mineral medium containing up to 40 µM protoanemonin and 0,5 mM of 4-chlorocatechol. Transformation of protoanemonin by resting cells at 30ºC was followed by HPLC over 10 h with the cell-free solutions as reference controls (Fig. 3.3.).

As in the experiment described above (3.1.2.1.), resting cells of MT3 and MT4 did not display any 4-chlorocatechol transforming activity. Depletion of this compound in the medium supernatant resulted from its autooxidation as indicated by the similar rate of decrease in the cell-free reference controls.

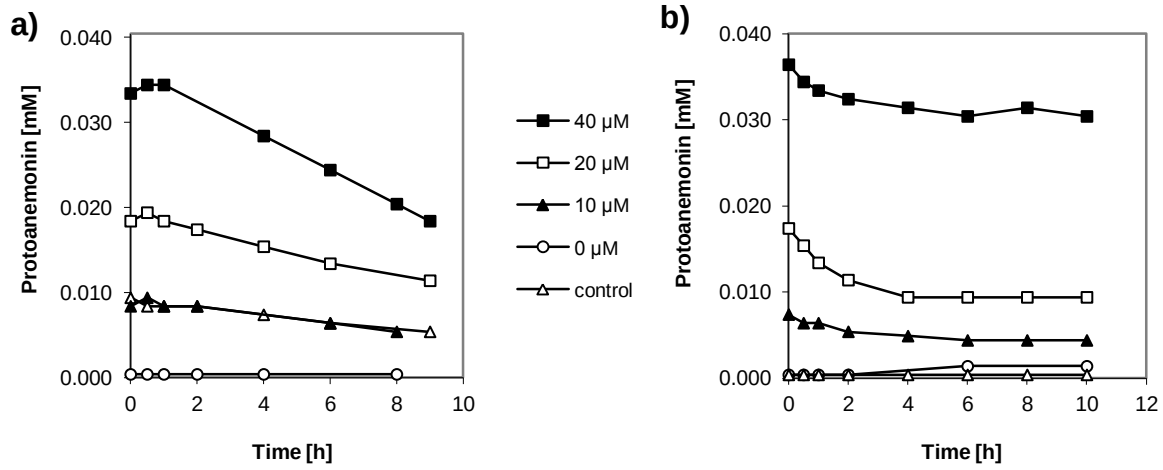

Figure 3.3. Transformation of protoanemonin in the presence of 4-chlorocatechol by resting cells of *A. xylosoxidans* MT3 (**a**) and *P. veronii* MT4 (**b**).

The concentration of protoanemonin in the medium decreased with time and this effect was particularly prominent in the first 2 hours of incubation with MT4 resting cells (Fig. 3.3b). However, since no product of protoanemonin transformation could be detected in the supernatant it is impossible to decide whether the compound was hydrolysed and degraded or just sequestered by bacterial cells. When MT3 resting cells were incubated with protoanemonin the decrease of its concentration was gradual and could be attributed solely to

the chemical decomposition as judged from its rate of decay in the reference control (Fig. 3.3a).

3.1.3. Enzymatic activities in cellular extracts of A. xylosoxidans MT3 and P. veronii MT4

Analysis of enzymatic activities in cell extracts of the whole consortium, as well as of MT1 grown on 4-CS in the chemostat, had shown the presence of chlorocatechol 1,2-dioxygenase and maleylacetate reductase in the community (Pelz *et al.*, 1999; Pelz, 1999). These enzymatic activities may be indicative of the novel chlorocatechol pathway. In order to determine which member of the consortium may contribute to the chlorocatechol degradation pathway and to probe further into central pathways for degradation of aromatics cellular extracts of MT3 and MT4 were analysed. For this purpose strains were grown on succinate and induced with 4-chlorocatechol (MT3 and MT4) or on salicylate and gentisate (MT3 only) and the following enzymatic activities were measured in the crude cell-free extracts: salicylate hydroxylase, catechol 1,2-dioxygenase (catechol intradiol-ring cleavage and chlorocatechol pathway), muconate cycloisomerase (catechol pathway), catechol 2,3-dioxygenase (catechol *meta*-cleavage pathway), dienelactone hydrolase (chlorocatechol pathway) and gentisate dioxygenase (gentisate pathway).

Table 3.3. Specific enzymatic activities in the cellular extracts of *A. xylosoxidans* MT3 and *P. veronii* MT4 grown on different carbon sources.

Enzyme	Substrate	Specific activity [U/g protein] after growth with:		
		MT4 (Succinate)	**MT3 (Succinate)**	**MT3 (Salicylate)**
salicylate hydroxylase	salicylate	<2	<2	15
catechol 1,2-dioxygenase	catechol	<2	<2	<2
	4-chlorocatechol	<2	<2	ND
catechol 2,3-dioxygenase	catechol	<1	<1	<1
	4-chlorocatechol	ND	ND	ND
gentisate dioxygenase	gentisate	ND	ND	828[a]
muconate cycloisomerase	muconate	<1	<1	ND
dienelactone hydrolase	*cis*-dienelactone	ND	<1	28

Cells were grown on succinate and induced with addition of 0,5 mM of 4-chlorocatechol 4 h prior to harvest. MT3 cells grown on salicylate were not induced; [a] – cells grown on gentisate (activity of gentisate dioxygenase was not measured for salicylate grown MT3 cells).

Cell extracts of succinate grown MT3 and MT4 showed no measurable activity for any of the tested enzymes. In particular, no activity was observed for (chloro)catechol 1,2-dioxygenase and dienelactone hydrolase that were selected as markers for the chlorocatechol pathway. The absence of measurable activity for enzymes of the chlorocatechol pathway could result from their insufficient induction as it is known that usually chlorinated muconates rather than catechols act as inducers (McFall *et al.*, 1998). In contrast to these findings, low activities of salicylate hydroxylase and dienelactone hydrolase was detected in cell extracts of salicylate grown MT3. Salicylate 5-hydroxylase that probably serves in channeling salicylate into the gentisate pathway in MT3 is a multicomponent protein for which activity measurements are problematic unless the enzyme is significantly overexpressed (Zhou *et al.*, 2002). On the other hand, low activity of dienelactone hydrolase observed in cell-free extracts of MT3 does not constitute sufficient evidence for the presence of a chlorocatechol pathway in MT3. As expected, cellular extracts of gentisate grown MT3 exhibited high level of gentisate dioxygenase activity. Gentisate dioxygenase is probably also expressed in bacteria cultivated on salicylate but this activity was not determined in the course of the experiment.

3.1.4. Incorporation of novel metabolic features in MT3 and MT4 through mating

Heterologous genes for catabolic enzymes could be incorporated into genomes of bacterial strains in order to successfully broaden the spectrum of degraded substrates as demonstrated by the concept of patchwork assembly (Reineke, 1998). This principle was used to bring activities of toluate 1,2-dioxygenase and 1,2-dihydro-1,2-dihydroxytoluate dehydrogenase (encoded by *xylXYZL*) into MT3 and MT4. The genetic cassette containing *xylXYZL* from the catabolic plasmid pWW0 and the gene for resistance to tellurite on a minitransposon was incorporated into the genomes of MT3 and MT4 by transconjugation. Engineered variants were expected to acquire the ability to convert 4-chlorobenzoate into 4-chlorocatechol and thus to grow on 4-chlorobenzoate as sole carbon source if they harbour enzymes for the 4-chlorocatechol mineralization. Single colonies of transformants were selected on mineral agar medium with benzoate as a sole carbon source and potassium tellurite. Recombinants were examined for their ability to degrade 4-chlorobenzoate in liquid mineral medium. Genetically improved variants of MT3 and MT4 were intended to serve as model systems for further studies on enzymatic activities in the chlorocatechol pathway.

However, none of the approximately one hundred tested recombinants of MT3 and MT4 demonstrated the ability to grow on 4-chlorobenzoate as carbon source in mineral medium. Resuspending the transconjugants pregrown on benzoate with tellurite to an OD_{600} = 0,6

(resting cells) and incubation with 4-chlorobenzoate at concentrations of 50 µM to 1 mM resulted in the the accumulation of 4-chlorocatechol in the medium supernatant. Alterations of the culture medium, which turned from colourless to violet and then to dark-brown indicated that 4-chlorocatechol formed from 4-chlorobenzoate was further oxidized. None of the intermediates of the chlorocatechol pathway could be detected in the culture supernatant. The lack of a 4-chlorobenzoate degrading phenotype among the *xylXYZL*-positive recombinants was possibly due to the absence of a chlorocatechol pathway in either MT3 or MT4 or due to deficient regulatory mechanisms between heterologous peripheral pathway and their native central chlorocatechol pathway.

3.2. Identification of genetic elements involved in the degradation of aromatic and chloroaromatic compounds by consortium strains

The search for genes encoding enzymes that could be involved in the breakdown of 4-CS by consortium strains was carried out by two different strategies. The first approach used the wealth of information available in GeneBank on homologous genes and proteins of chlorocatechol pathways and included PCR amplification with degenerate primers followed by cloning and sequencing. In the second approach, genomic phage libraries were constructed for individual consortium members and these were subsequently screened with the use of both sequence-dependent and sequence-independent strategies.

3.2.1. Identification of genes encoding enzymes of the chlorocatechol pathway in the consortium genome

Genes encoding proteins with a given function may be retrieved from genomes by PCR primers covering conserved gene regions as it was shown for instance for alkane monooxygenases (Smits *et al.*, 1999). Fragments of genes encoding chlorocatechol 1,2-dioxygenase, catechol 1,2-dioxygenase, chloromuconate cycloisomerase, dienelactone hydrolase and maleylacetate reductase were attempted to be amplified by PCR with genomic DNA from consortium bacteria as template using degenerate primers designed in-house (Tab. 2.6.) or retrieved from the literature (Thiel & Schlömann, 2000). PCR with degenerate primers resulted in amplification of fragments of the expected length for genes encoding maleylacetate reductase (MT4 and MT1, see: Fig. 3.4.), dienelactone hydrolase (MT3) and chlorocatechol dioxygenase (MT3 and MT4). None of the tested primer combinations for fragments of chloromuconate cycloisomerase and catechol 1,2-dioxygenase encoding genes

produced amplicons of expected size. Obtained fragments of the expected length were cloned into the pCR2.1-TOPO® plasmid vector, sequenced, and their identity was established by comparison with the NCBI sequence depository through blastx searches (Tab. 3.4.).

As shown in Fig. 3.4., PCR amplification with MT4 genomic DNA as template with two combinations of primers targeting maleylacetate reductase encoding genes resulted in products of the expected size of approx. 450 and 380 bp, respectively. Subsequent cloning and sequencing confirmed that both amplicons covered overlapping fragments of the same gene. Comparison of the encoded protein with those deposited in public databases through blast searches revealed high homology with maleylacetate reductases (Tab 3.4.). The actual origin and function of this putative maleylacetate reductase from *P. veronii* MT4 is discussed further in section 3.2.2.1.

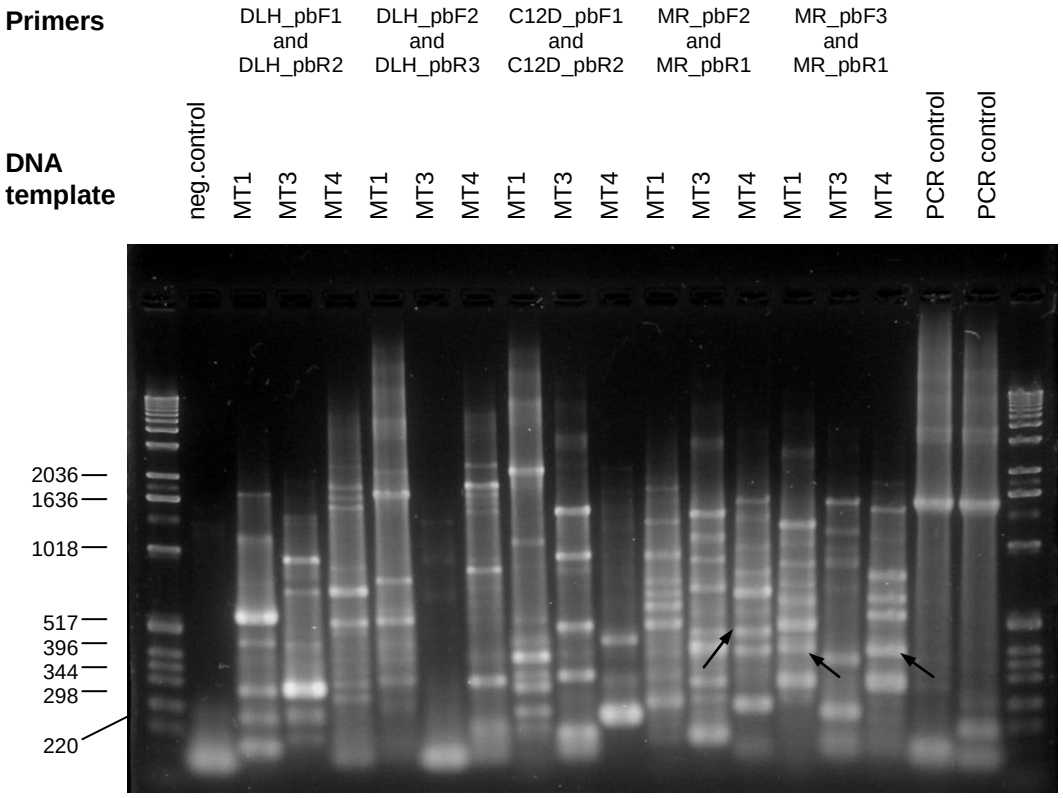

Figure 3.4. Results of PCR amplification on genomic DNA of consortium strains with selected combinations of degenerate primers. Arrows indicate amplicons of expected size that were obtained for maleylacetate reductase encoding gene.

In case of all other PCR products that were of the expected length, subsequent cloning, sequencing and blast searches revealed them to be derived from non-related and non-targeted genes (Tab. 3.4.).

Table 3.4. PCR products obtained with degenerate primers and gene products of their homologues

Organism	PCR product / related gene product	Function	% aa identity	Accession no.
***Pseudomonas veronii* MT4**	**452 bp-long PCR product obtained with primers MR_pbF2 and MR_pbR1**			
Pseudomonas sp. PDS-7	putative maleylacetate reductase	-	85	gb|ABW99095.1
Pseudomonas aeruginosa PA7	maleylacetate reductase	-	83	gb|ABR86468.1
Burkholderia cepacia	maleylacetate reductase	+[a]	66	sp|Q45072
***Pseudomonas veronii* MT4**	**380 bp-long PCR product obtained with primers MR_pbF3 and MR_pbR1**			
Pseudomonas sp. PDS-7	putative maleylacetate reductase	-	84	gb|ABW99095.1
Pseudomonas aeruginosa PA7	maleylacetate reductase	-	82	gb|ABR86468.1
Pseudomonas sp. P51	maleylacetate reductase	+[b]	65	sp|P27101
***P. reinekei* MT1**	**385 bp-long PCR product obtained with primers MR_pbF3 and MR_pbR1**			
Pseudomonas fluorescens Pf-1	cysteine synthase A	-	90	gb|AAY90802.1
Pseudomonas aeruginosa PAO1	cysteine synthase A	-	84	gb|AAG06097.1
Synechococcus elongatus	cysteine synthase, (O-acetylserine sulfhydrylase)	+[c]	76	sp|Q59966
***Achromobacter xylosoxidans* MT3**	**543 bp-long PCR product obtained with primers CDLH_F1 and CDLH_R1**			
Bordetella bronchiseptica	putative membrane protein	-	87	emb|CAE31315.1
Bordetella parapertussis	putative membrane protein	-	87	emb|CAE40139.1
***Achromobacter xylosoxidans* MT3**	**240 bp-long PCR product obtained with primers CCD(G-)F and CCD(G-)R**			
Bordetella parapertussis	malonyl CoA-acyl carrier protein transacylase	-	86	emb|CAE38591.1
Bordetella bronchiseptica	malonyl CoA-acyl carrier protein transacylase	-	86	emb|CAE35731.1
Escherichia coli	malonyl CoA-acyl carrier protein transacylase	+[d]	61	sp|P0AAI9.2
***Pseudomonas veronii* MT4**	**254 bp-long PCR product obtained with primers CCD(G-)F and CCD(G-)R**			
Xanthomonas campestris	putative IcmO-like type IV secretion system protein	-	67	emb|CAJ19855.1
Legionella pneumophila	hypothetical protein	-	57	emb|CAH11660.1

[a] (Daubaras *et al.*, 1995); [b] (van der Meer *et al.*, 1991); [c] (Nicholson *et al.*, 1995); [d] (Verwoert *et al.*, 1992).. Alignments were produced with **blastx** (search of protein databases using translated nucleotide query)

3.2.2 Identification of gene clusters encoding enzymes involved in the degradation of aromatics and haloaromatics by screening genomic libraries of consortium strains

Various enzymes of the 4-chlorosalicylate degradation pathway in MT1 have been isolated, purified and characterised (Nikodem, 2004; Camara; 2007) during the preparation of the current thesis. It was anticipated that an extensive gene discovery program in degradation of aromatics and chloroaromatics by MT1, carried out by the group of Prof. Pieper (Nikodem, 2004; Camara, 2006; Marin *et al.*, 2010; this work), will contribute to understanding principles of carbon-sharing in the 4-CS degrading consortium. Partial protein sequences obtained after purification of enzymes to homogeneity (Nikodem, 2004) or from comparative proteomic expression profiling (Bobadilla, 2006 & Strocchi, unpublished) served as starting points for sequence-based screenings of the MT1 genomic library (Fig. 3.5.). Hybridisation of the MT1 genomic library with corresponding probes led to identification of clones that carried salicylate (*sal*) and protocatechuate (*pca*) gene clusters, which are presumably involved in the degradation of methyl- and chloro-substituted salicylates and protocatechuate, respectively.

The genomic library of *P. veronii* MT4 was screened through DNA-hybridisation for clones carrying the putative maleylacetate reductase encoding gene identified previously by the degenerate PCR approach (see: 3.2.1., Tab. 3.4., and Fig. 3.4.).

Genes that encode enzymes catalyzing reactions involved in chlorocatechol degradation by *A. xylosoxidans* MT3 were searched for in the corresponding library by an alternative approach based on activities exhibited by encoded proteins (Fig. 3.5.). Recombinants expressing activity towards 4-chlorocatechol and *cis*-dienelactone were attempted to be identified by acidification of the medium resulting from the production of 3-chloromuconate or maleylacetate, respectively. Thus, clones carrying such activity should produce visible halos on the surface of screening agar plate resulted from the change of colour displayed by an appropriate pH-indicator.

3.2.2.1. The *mar* gene cluster from *P. veronii* MT4 encompassing maleylacetate reductase encoding gene

Maleylacetate reductase catalyzes the reduction of maleylacetate into 3-oxoadipate. Beside being involved in the chlorocatechol pathway (Kaschabek & Reineke, 1992) maleylacetate reductase activity was also identified as crucial for the degradation of nitroaromatic (Katsivela *et al.*, 1999), sulfoaromatic (Contzen & Stolz, 2000) and natural aromatic compounds (Perez-Pantoja *et al.*, 2010b).

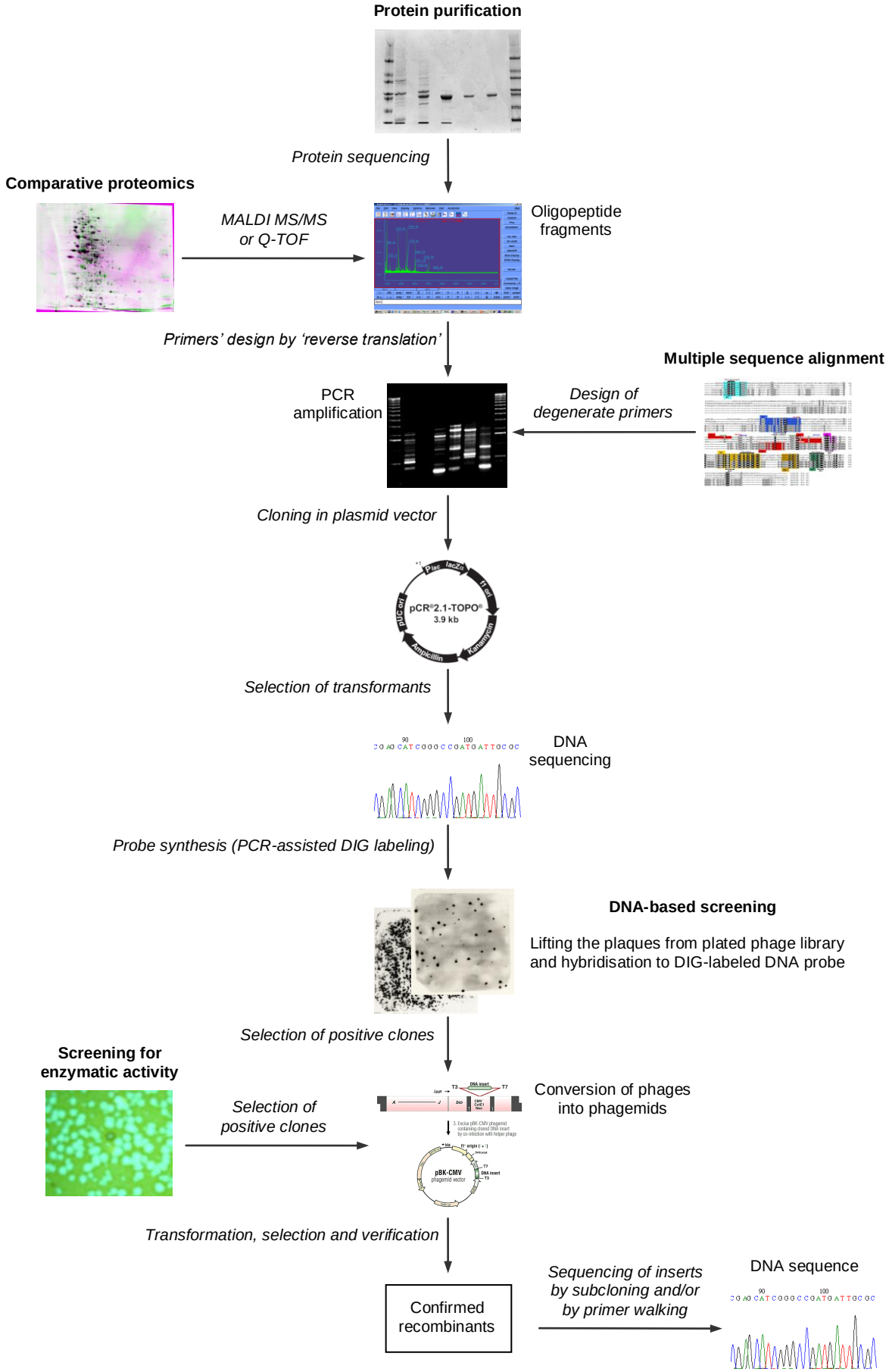

Figure 3.5. Strategy for the screening of genomic libraries and retrieving sequence information from selected recombinants.

Screening of a MT4 genomic library with a DIG-labelled 452-bp long PCR amplicon, encoding part of a putative maleylacetate reductase, obtained with MR_pbF2 and MR_pbR1 primers resulted in one positive clone showing hybridisation. Conversion of the positive recombinant phage into a phagemid and sequencing of the 7639-bp insert revealed the presence of 8 ORFs (Fig.3.6.).

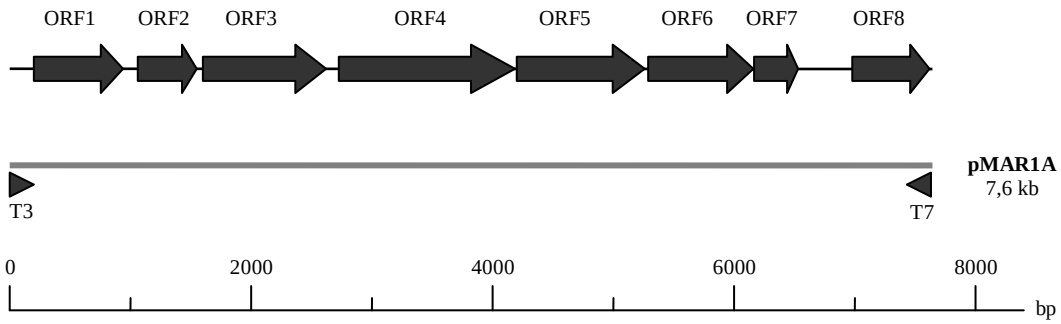

Figure 3.6. Physical map of the neighbouring region of gene coding for maleylacetate reductase in *P. veronii* MT4 (ORF5). Position and size of cloned insert is indicated below the line representing the consensus sequence. Arrowheads indicate orientation of the insert in the phagemid in relation to flanking primer sequences.

Proteins encoded by ORFs 1-8 were identified through blast searches to entries from SwissProt and NCBI/EMBL/DDBJ protein databases to find their orthologous counterparts (Tab. 3.5.).

Five out of eight identified ORFs showed homology to enzymes of aromatic degradation pathways, while the remaining three ORFs encode transcriptional regulators. The protein encoded by ORF2 and ORF3 resembles two subunits of the recently described and characterised hydroquinone dioxygenase of the non-heme-iron(II)-dependent dioxygenases family (Moonen *et al.*, 2008a). This enzyme is involved in a 4-hydroxyacetophenone pathway and cleaves hydroquinone to 4-hydroxymuconic semialdehyde. Products of ORF 4 and 5 show high amino acid identity with downstream enzymes 4-hydroxymuconic semialdehyde dehydrogenase and maleylacetate reductase, respectively (Moonen *et al.*, 2008b). The protein encoded by ORF6 belongs to the superfamily of intradiol dioxygenases. As recently described by Perez-Pantoja (2010a) proteins of this subfamily can be grouped into 5 clusters. The ORF6 encoded protein clearly belongs to the cluster of hydroxyquinol 1,2-dioxygenases (Fig.3.7). Interestingly, Moonen and colleagues (2008b) did not propose any function for the hydroxyquinol dioxygenase in the 4-hydroxyacetophenone catabolic pathway.

Table 3.5. Genes and their corresponding products related to ORFs in a 7639-bp long sequenced DNA region of *P. veronii* MT4.

Gene	Position in insert	Function in strain MT4	Related protein	Function	Organism	% aa identity	Accession no.
ORF1 (*marA*)	211-924	LysR family transcriptional regulator	LysR family transcriptional regulator	-	*Pseudomonas aeruginosa* PA7	80	gb|ABR82395.1
			LysR family transcriptional regulator	-	*Burkholderia phymatum*	70	gb|EAU95814.1
			LysR family transcriptional regulator	-	*Burkholderia multivorans*	69	gb|EAV65389.1
ORF2 (*marB*)	1056-1547	Hydroquinone dioxygenase	hydroquinone dioxygenase (α subunit)	-	*Pseudomonas putida* DLL-E4	90	gb|ACN43569.1
			hydroquinone dioxygenase (α subunit)	-	*Pseudomonas* sp. NyZ402	88	gb|ACZ51386.1
			hydroquinone dioxygenase (small sub.)	+[a]	*Pseudomonas fluorescens* ACB	73	gb|ACA50457.2
ORF3 (*marC*)	1602-2618	Hydroquinone dioxygenase	hydroquinone dioxygenase (large sub.)	-	*Pseudomonas* sp. WBC-3	91	gb|ABU50916.1
			hydroquinone dioxygenase (β subunit)	-	*Pseudomonas putida* DLL-E4	86	gb|ACN43570.2
			hydroquinone dioxygenase (large sub.)	+[a]	*Pseudomonas fluorescens* ACB	80	gb|ACA50458.2
ORF4 (*marD*)	2711-4171	4-hydroxymuconic semialdehyde dehydrogenase	γ-hydroxymuconic semialdehyde dehydrogenase	-	*Pseudomonas* sp. 1-7	95	gb|ADB81388.1
			4-hydroxymuconic semialdehyde dehydrogenase	-	*Pseudomonas putida* DLL-E4	86	gb|ACN43571.2
			4-hydroxymuconic semialdehyde dehydrogenase	-	*Pseudomonas fluorescens* ACB	83	gb|ACA50459.1
ORF5 (*marE*)	4129-5247	Maleylacetate reductase	putative maleylacetate reductase	-	*Pseudomonas* sp. WBC-3	92	gb|ABU50914.1
			maleylacetate reductase	-	*Pseudomonas* sp. 1-7	91	gb|ACO53215.2
			maleylacetate reductase tftE	+[b]	*Burkholderia cepacia*	56	sp|Q45072
			maleylacetate reductase	+[c]	*Sphingobium japonicum*	55	dbj|BAD66863.1
ORF6 (*marF*)	5287-6156	Hydroxyquinol 1,2-dioxygenase	1,2,4-benzenetriol 1,2-dioxygenase	-	*Pseudomonas* sp. 1-7	88	gb|ACO53214.1
			hydroxyquinol 1,2-dioxygenase	-	*Pseudomonas* sp. WBC-3	88	gb|ABU50913.1
			hydroxyquinol 1,2-dioxygenase	+[d]	*Pseudomonas putida* DLL-E4	77	pdb|3N9T|A
			hydroxyquinol 1,2-dioxygenase	+[e]	*Sphingomonas* sp. RW1	51	emb|CAA51371.1
ORF7 (*marG*)	6163-6471	YciI-family protein	hypothetical protein	-	*Pseudomonas* sp. WBC-3	82	gb|ABU50912.1
			YciI-related protein	-	*Pseudomonas putida* DLL-E4	75	gb|ACN43574.1
			YciI-related domain-containing protein	-	*Pseudomonas aeruginosa* PA7	68	gb|ABR82085.1
ORF8	6959-7639	Transcriptional regulator	transcriptional regulatory protein	-	*Bradyrhizobium japonicum*	36	dbj|BAC50548.1
			regulatory protein IclR	-	*Ralstonia eutropha* JMP134	35	gb|AAZ59651.1
			Mhp operon transcriptional activator	+[f]	*Escherichia coli*	33	sp|P77569

[a] (Moonen *et al.*, 2008a); [b] (Daubaras *et al.*, 1995); [c] (Endo *et al.*, 2005); [d] (Shen *et al.*, 2010); [e] (Armengaud *et al.*, 1999); [f] (Spence *et al.*, 1996).

Figure 3.7. Dendrogram showing relatedness of protein product of ORF6 (*mar*F) encoded by the *mar* cluster of *P. veronii* MT4. Coloured yellow are proteobacterial catechol 1,2-dioxygenases, brown - actinobacterial catechol 1,2-dioxygenases, green - chlorocatechol 1,2-dioxygenases and red - hydroxybenzoquinol dioxygenases.

Activities of hydroxyquinol dioxygenase and subsequent maleylacetate reductase were frequently observed in the aerobic degradation pathways for nitrophenols (Jain *et al.*, 1994; Shen *et al.*, 2010), chlorophenols (Nordin *et al.*, 2005), 2,4,6-trichlorophenol (Latus *et al.*, 1995), 2,4,5-trichlorophenoxyacetate (2,4,5-T) (Daubaras *et al.*, 1996), and some natural compounds like resorcinol (Perez-Pantoja *et al.*, 2010a). The enzymatic functions of proteins encoded by ORF5 and ORF6 were proposed basing on physiological activities of their closest functionally-characterised relatives (Fig.3.8.). However, further and more detailed study is

required in order to understand the physiological role of proteins encoded by ORF5 and ORF6 from the *mar* gene cluster in MT4 in the metabolism of aromatics.

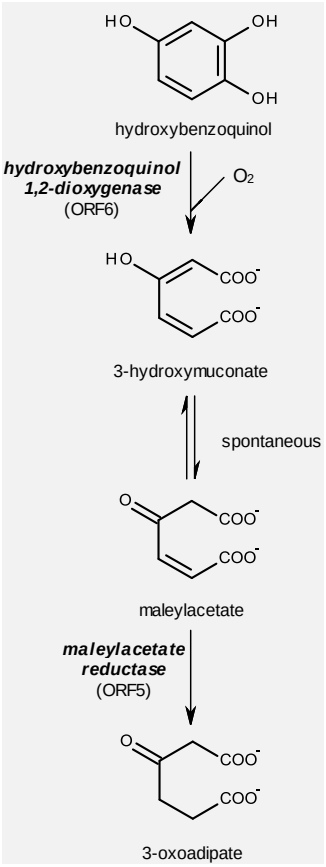

Figure 3.8. Proposed enzymatic functions of proteins encoded by ORF5 (MarE) and ORF6 (MarF) from the *mar* cluster in *P. veronii* MT4.

The role and function of transcription factors encoded by ORFs 1, 7 and 8 remains unclear and it would likely require prior characterisation of the entire metabolic pathway.

The structure of *mar* gene cluster identified in the strain MT4 closely resembles the organization of *hapCDEFGHIBA* cluster from *P. fluorescens* ACB encoding proteins of the 4-hydroxyacetophenone degradation pathway (Moonen *et al.*, 2008b), the *pnp* gene cluster for degradation of *p*-nitrophenol in *P. putida* DLL-E4 (Shen *et al.*, 2010) and several hitherto uncharacterised clusters from *P. aeruginosa* PA7, *Burkholderia* sp. 383 and *Photorhabdus luminescens* TTO1 (Moonen *et al.*, 2008b).

3.2.2.2. *Sal* gene cluster from *P. reinekei* MT1

A novel muconate cycloisomerase displaying unique substrate preference and kinetic properties was purified from *P. reinekei* MT1 to homogeneity and partially sequenced by Nikodem (2004). SGLESALLDAKGKR and VDVNQYWDEAQALR oligopeptides obtained

from protein sequencing were used for designing primers through reverse translation. PCR amplification on MT1 genomic DNA with primers MT1:MCI_F1 and MT1:MCI_R (Tab. 2.6.) yielded a 279-bp long product that was used as hybridisation probe for screening the MT1 genomic library. Sequencing of inserts from three selected clones covered a nearly 10 kb-long DNA region containing seven complete and two partial open reading frames (Fig. 3.9.).

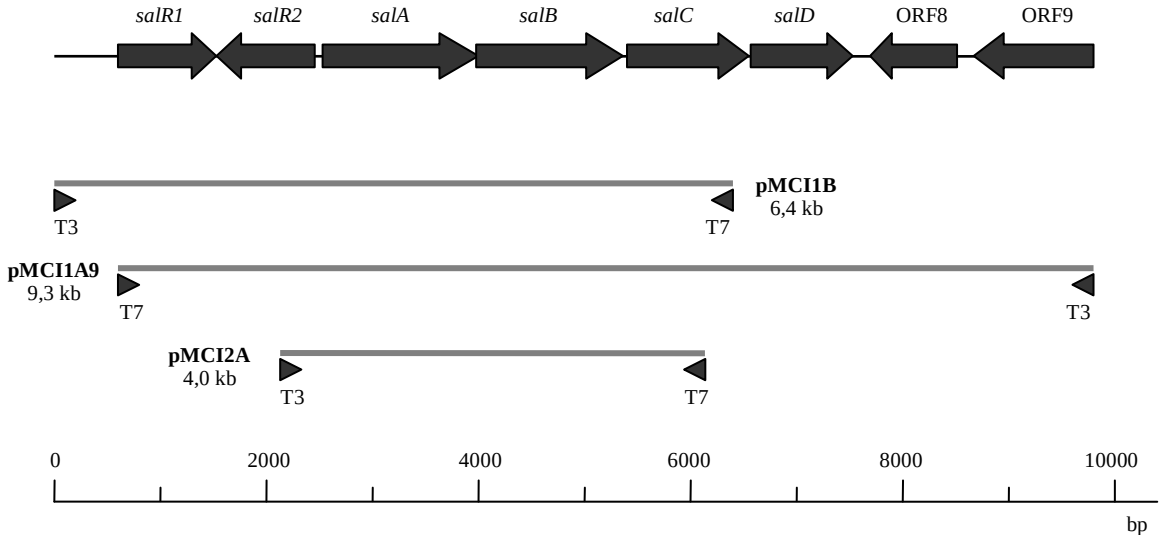

Figure 3.9. Genetic organization of a 9886-bp region from *P. reinekei* MT1 containing the *sal* gene cluster. Positions and sizes of inserts are shown below the line representing the consensus sequence. Arrowheads indicate orientation of inserts in the phagemids in relation to flanking primer sequences.

ORF4 (*salA*) from the cluster termed further as *sal* was identified as encoding a salicylate 1-hydroxylase. This enzyme catalyzes the initial step of degradation of salicylate, that is decarboxylation and hydroxylation. Phylogenetic analysis showed that SalA shared 68-71% amino acid identity with monooxygenases transforming salicylate into catechol from the naphthalene degradation pathway like NahG (Camara *et al.*, 2007). The protein encoded by ORF7 (*salD*) belongs to the superfamily of intradiol dioxygenases and shows highest homology to catechol 1,2-dioxygenases. Catechol 1,2-dioxygenase catalyzes transformation of catechol into muconate by oxygenolytic cleavage of aromatic ring. Muconate cycloisomerase was identified as the product of ORF6 (*salC*) and this enzyme usually carries out the subsequent reaction in the central catechol pathway by converting muconate into muconolactone. However, as established by Nikodem and coworkers (2003) SalC from MT1 differs from its homologues by showing preference to 3-chloromuconate rather than muconate and transforming chlorinated analog into 4-chloromuconolactone.

Table 3.6. Genes and their protein products from the *sal* cluster and its neighbouring region in the genome of *P. reinekei* MT1.

Gene	Position in sequence	Function in strain MT1	Related protein	Function	Organism	% aa identity	Accession no.
ORF1	483-1 (truncated)	Dehydrogenase	putative dehydrogenase/oxidoreductase	-	*Burkholderia xenovorans*	50	gb|ABE31831.1
			putative dehydrogenase	-	*Achromobacter xylosoxidans*	48	emb|CAI47836.1
ORF2 (*salR1*)	598-1521	LysR family transcriptional regulator	LysR-type transcriptional regulator	-	*Achromobacter xylosoxidans*	57	emb|CAI47838.1
			unknown protein	-	*Pseudomonas aeruginosa* JB2	55	gb|AAC69490.1
			LysR-type transcriptional regulator NahR	+[a]	*Pseudomonas fluorescens*	38	gb|AAM18544.1
ORF3 (*salR2*)	2444-1542	LysR family transcriptional regulator	LysR-type transcriptional regulator NahR	+[a]	*Pseudomonas fluorescens*	74	gb|AAM18544.1
			LysR-type transcriptional regulator	-	*Pseudomonas* sp. KB35B	73	gb|ABB72205.1
			HTH-type transcriptional activator NahR	+[b]	*Pseudomonas putida*	73	sp|P10183
ORF4 (*salA*)	2549-3982	Salicylate 1-hydroxylase	salicylate hydroxylase NahG	-	*Pseudomonas stutzeri*	69	gb|AAD02146.1
			salicylate hydroxylase NahG	-	*Pseudomonas putida*	70	gb|AAM09538.1
			salicylate 1-monooxygenase	+[c]	*Pseudomonas putida*	71	sp|P23262
ORF5 (*salB*)	3967-5337	Transporter protein	major facilitator superfamily MFS_1	-	*Pseudomonas putida*	67	gb|EAZ66973.1
			benzoate transporter protein	-	*Pseudomonas* sp. ND6	66	gb|AAP44250.1
			permease of the major facilitator family	-	*Magnetospirillum magneticum*	58	dbj|BAE53281.1
ORF6 (*salC*)	5381-6499	Muconate cycloisomerase	muconate cycloisomerase	-	*Pseudomonas putida* KT2440	81	gb|AAN69312.1
			muconate cycloisomerase	-	*Pseudomonas entomophila*	81	emb|CAK15905.1
			cis,cis-muconate cycloisomerase CatB	+[d]	*Pseudomonas* sp. CA10	82	dbj|BAB32456.1
ORF7 (*salD*)	6571-7503	Catechol 1,2-dioxygenase	catechol 1,2-dioxygenase α chain	-	*Pseudomonas* sp. ND6	65	gb|AAP44248.1
			catechol 1,2-dioxygenase	+[e]	*Pseudomonas putida*	65	dbj|BAA07036.1
			catechol 1,2-dioxygenase	-	*Pseudomonas fluorescens*	66	gb|ABA74070.1
ORF8	8523-7696	Hydroxymuconic semialdehyde hydrolase	2-hydroxymuconic semialdehyde hydrolase	-	*Alcaligenes faecalis*	63	gb|ABV30923.1
			2-hydroxymuconic semialdehyde hydrolase	+[f]	*Delftia tsuruhatensis*	62	gb|AAX47253.1
			2-hydroxymuconic semialdehyde hydrolase	+[g]	*Pseudomonas putida*	59	dbj|BAF02459.1
ORF9	9885-8677 (truncated)	Probable RND transporter	probable transporter	-	*Pseudomonas putida* KT2440	66	gb|AAN68810.1
			probable transporter	-	*Azoarcus* sp. EbN1	68	emb|CAI09396.1

[a] (Park *et al.*, 2002); [b] (You *et al.*, 1988); [c] (You *et al.*, 1990 and 1991); [d] (Nojiri *et al.*, 2002); [e] (Nakai *et al.*, 1995); [f] (Liang *et al.*, 2005); [g] (Keil *et al.*, 1985).

The protein product of ORF5 (*salB*) belongs to the MFS superfamily of transporter proteins while both ORF2 (*salR1*) and ORF3 (*salR2*) encode transcriptional regulators of the LysR family. A fragment of a gene coding for a putative 3-hydroxybutyrate dehydrogenase (ORF1) was identified upstream of the *sal* cluster.

Downstream, the *sal* cluster is flanked by divergently transcribed genes coding for 2-hydroxymuconic semialdehyde hydrolase (ORF8) and a putative transporter protein (ORF9). Interestingly, 2-hydroxymuconic semialdehyde hydrolase constitute a part of the alternative catechol *meta*-cleavage pathway in the degradation of aromatics (Perez-Pantoja *et al.*, 2010a). Recent analysis indicates this gene to be part of a cluster of genes encoding enzymes for 2,3-dihydroxybenzoate degradation (Marin et al, unpublished).

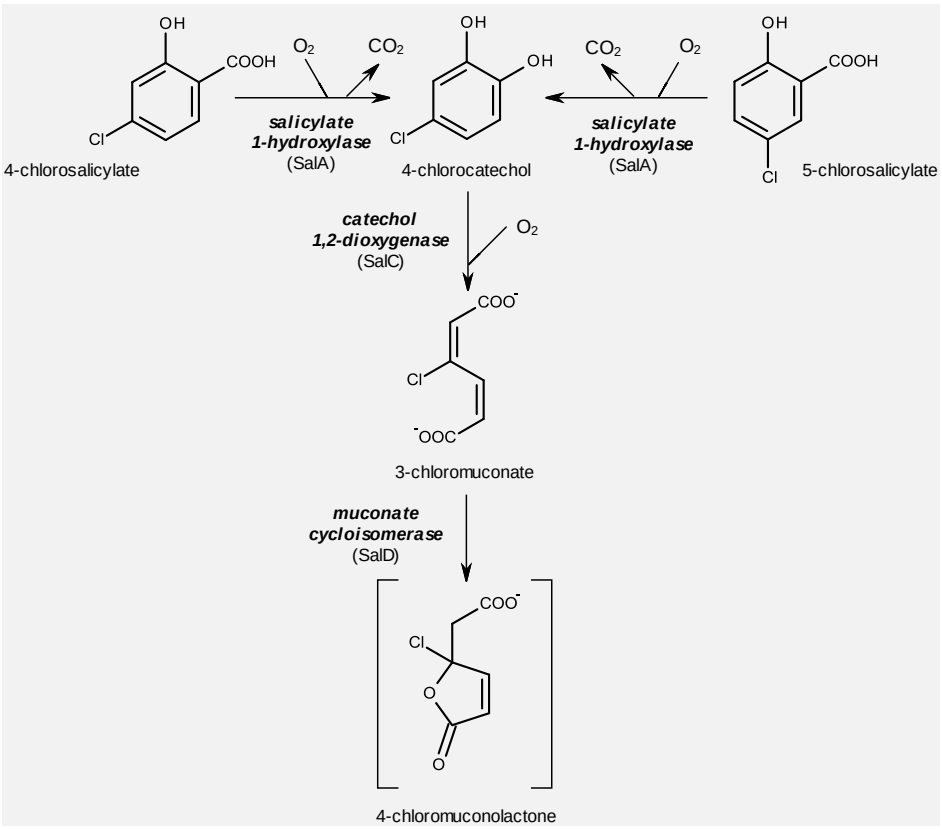

Figure 3.10. Catabolic activities of the *sal*-encoded enzymes in the breakdown of 4- and 5-chlorosalicylate by *P. reinekei* MT1.

Three features make the *sal* gene cluster unique among other gene clusters involved in the degradation of salicylate and catechol that were previously reported. First, breakdown of salicylate *via* catechol usually proceeds through extradiol cleavage by catechol 2,3-dioxygenases with further steps catalyzed by the enzymes of catechol *meta*-cleavage pathway (Yen & Serdar, 1988; Bosch *et al.*, 1999; Dennis & Zylstra, 2004). Second, a gene encoding muconolactone isomerase (*catC*) typically located in close proximity to genes coding for

catechol 1,2-dioxygenase (*catA*), muconate cycloisomerase (*catB*) and transcriptional regulator (*catR*) within canonical *catRBCA* catechol-degrading units in *Pseudomonas* (Nojiri *et al.*, 2002; Jimenez *et al.*, 2002; Stover *et al.*, 2004) is absent from the *sal* cluster. Third, the catabolic genes in the *sal* cluster are preceded not by one but by two different and divergently transcribed transcriptional regulators.

Based on protein sequence homology, the enzymatic function in the breakdown of 4- and 5-CS could be identified for catabolic proteins encoded by the *sal* gene cluster. From the Figure 3.10. it is evident that mineralization of 4- and 5-CS by MT1 can not be achieved solely by *sal* cluster encoded enzymes. It seems likely that genes coding for other enzymes that are crucial for breakdown of chlorinated salicylates are located in other clusters and that their expression is regulated in the concerted manner during growth on the substrate.

3.2.2.3. The *pca* gene cluster from *P. reinekei* MT1 encoding enzymes for degradation of protocatechuate

Comparative proteome analysis of MT1 grown on 4-CS and acetate revealed many proteins being significantly upregulated or exclusively expressed on the former substrate (Bobadilla, 2006). MALDI MS/MS fragmentation pattern analysis showed that enzymes of the protocatechuate pathway like 3-carboxymuconate cycloisomerase were significantly overexpressed during growth on this compound (Bobadilla, 2006). Oligopeptide fragments of 3-carboxymuconate cycloisomerase from MALDI MS/MS analysis were used to design degenerate primers (MT1:CARB_F1 and MT1:CARB_R2; Tab. 2.6.) A 612-bp long PCR product amplified with these primers with MT1 genomic DNA as template served as a hybridisation probe to screen the corresponding genomic library. Inserts from four selected clones, that were recovered from phages after converting them into phagemids, spanned an over 10,5 kb-long region of the MT1 genome which contained ten complete open reading frames (Fig. 3.11. and Tab. 3.7.).

Although the *pca* cluster of MT1 contains the majority of genes encoding enzymes of protocatechuate degradation pathway observed in different Proteobacteria its overall structure is unique. The gene order in the *pca* cluster of MT1 resembles most closely that observed in *P. putida* PRS2000 (Reineke, 1998) but unlike in PRS2000, where genes are scattered on the chromosome, all identified ORFs are located together in close proximity as observed for instance in *A. calcoaceticus* (Harwood & Parales, 1996).

Table 3.7. Genes and gene products in the sequenced region of *P. reinekei* MT1 containing *pca* cluster

Gene	Position in sequence	Function in strain MT1	Related protein	Function	Organism	% aa identity	Accession no.
ORF1 (*pcaI*)	240-1094	3-Oxoadipate: succinyl-CoA transferase, s. A	3-oxoadipate:succinyl-CoA transferase A subunit	-	*Pseudomonas fluorescens*	96	gb|AAY90602.1
			3-oxoadipate:succinyl-CoA transferase A subunit	-	*Pseudomonas syringae*	92	gb|AAZ34550.1
			3-oxoadipate:succinyl-CoA transferase subunit A	+[a]	*Pseudomonas knackmussii*	88	gb|AAL02405.1
ORF2 (*pcaJ*)	1097-1873	3-Oxoadipate: succinyl-CoA transferase, s. B	3-oxoadipate:succinyl-CoA transferase B subunit	-	*Pseudomonas fluorescens*	94	gb|AAY90603.1
			3-oxoadipate:succinyl-CoA transferase B subunit	-	*Pseudomonas syringae*	91	gb|AAO57759.1
			3-oxoadipate:succinyl-CoA transferase subunit B	+[a]	*Pseudomonas knackmussii*	88	gb|AAL02406.1
ORF3 (*pcaF*)	1876-3075	3-Oxoadipyl-CoA thiolase	β-ketoadipyl CoA thiolase	-	*Pseudomonas fluorescens*	95	gb|AAY90604.1
			β-ketoadipyl CoA thiolase	+[b]	*Pseudomonas putida*	90	sp|Q51956
ORF4 (*pcaH*)	3116-3817	Protocatechuate 3,4-dioxygenase β subunit	protocatechuate 3,4-dioxygenase, β subunit	-	*Pseudomonas fluorescens*	91	gb|AAY90605.1
			protocatechuate 3,4-dioxygenase, β subunit	-	*Ralstonia metallidurans*	73	gb|ABF10881.1
			protocatechuate 3,4-dioxygenase β chain	+[c]	*Burkholderia cepacia*	59	sp|P15110
ORF5 (*pcaG*)	3822-4385	Protocatechuate 3,4-dioxygenase α subunit	protocatechuate 3,4-dioxygenase, α subunit	-	*Pseudomonas fluorescens*	89	gb|AAY90606.1
			protocatechuate 3,4-dioxygenase, α subunit	-	*Ralstonia metallidurans*	55	gb|ABF10882.1
			protocatechuate 3,4-dioxygenase α chain	+[d]	*Acinetobacter calcoaceticus*	44	pir||D35119
ORF6 (*pcaT*)	4629-5930	Transporter	dicarboxylic acid transport protein	-	*Pseudomonas fluorescens*	89	gb|AAY90607.1
			PcaT-like protein	+[e]	*Pseudomonas putida*	85	gb|AAD39560.1
ORF7 (*pcaB*)	5979-7340	3-Carboxy-*cis*,*cis*-muconate cycloisomerase	3-carboxy-*cis*,*cis*-muconate cycloisomerase	-	*Pseudomonas fluorescens*	83	gb|AAY90608.1
			3-carboxy-*cis*,*cis*-muconate cycloisomerase	-	*Pseudomonas putida*	80	gb|AAN67002.1
			3-carboxy-*cis*,*cis*-muconate cycloisomerase	+[f]	*Acinetobacter* sp. ADP1	46	sp|Q59092
ORF8 (*pcaD*)	7460-8143	3-Oxoadipate enol-lactone hydrolase	putative hydrolase	-	*Pseudomonas fluorescens*	88	gb|AAQ92186.1
			3-oxoadipate enol-lactonase	-	*Pseudomonas fluorescens*	83	gb|AAY90609.1
			3-oxoadipate enol-lactone hydrolase	+[a]	*Pseudomonas knackmussi*	68	gb|AAL02408.1
ORF9 (*pcaC*)	8187-8546	4-Carboxy-muconolactone decarboxylase	4-carboxymuconolactone decarboxylase	-	*Pseudomonas fluorescens*	94	gb|AAY90610.1
			4-carboxymuconolactone decarboxylase	-	*Pseudomonas putida*	90	gb|AAN67004.1
			4-carboxymuconolactone decarboxylase	-	*Azotobacter vinelandii*	92	gb|EAM05558.1
ORF10 (*pcaK*)	9969-8713	Probable transporter	PhaK-like protein	-	*Pseudomonas fluorescens*	91	gb|AAQ92184.1
			BenF-like porin	-	*Pseudomonas fluorescens*	86	gb|AAY90614.1

[a] (Göbel *et al.*, 2002); [b] (Harwood *et al.*, 1994); [c] (Zylstra *et al.*, 1989); [d] (Hartnett *et al.*, 1990); [e] (Ramos *et al.*, 1998); [f] (Kowalchuk *et al.*, 1994).

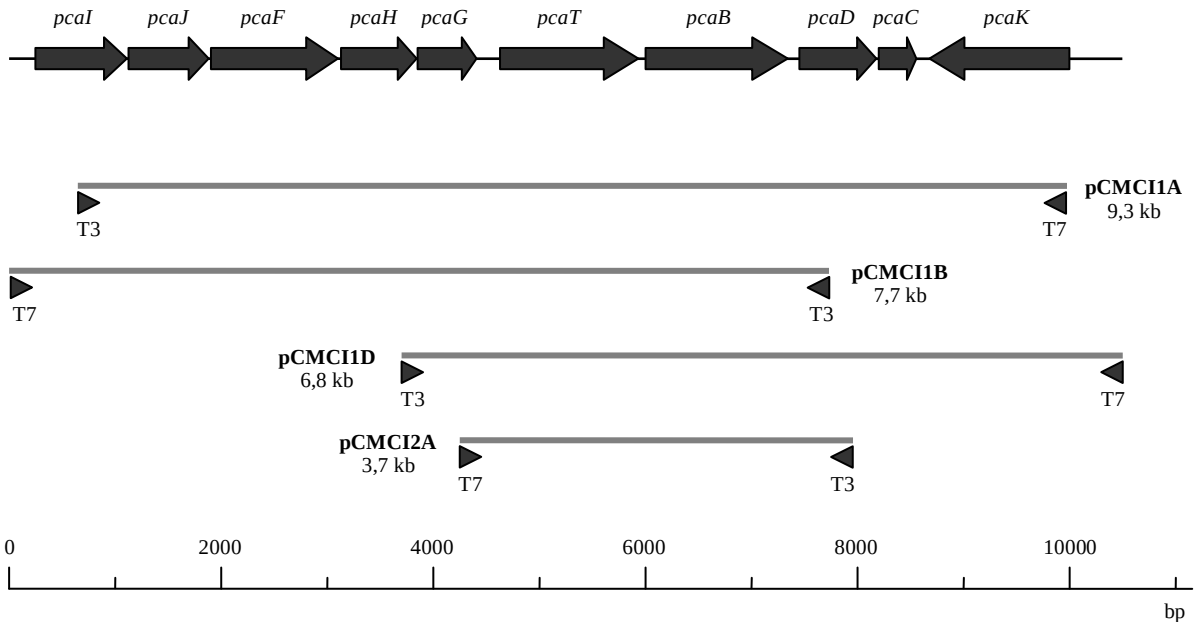

Figure 3.11. Genetic organization of a 10504-bp region containing the *pca* gene cluster of *P. reinekei* MT1. Positions and sizes of clones are indicated below the line representing consensus sequence. Arrowheads indicate orientation of inserts in the phagemids in relation to flanking primer sequences.

Based on homology, enzymes encoded by the ORFs 4-5 and 7-9 are likely to catalyze reactions of the protocatechuate branch of the 3-oxoadipate pathway whereas ORF6 encodes a transporter. ORFs 1-3 obviously encode enzymes for the transformation of 3-oxoadipate into acetyl-CoA and succinyl-CoA. The *pca* gene cluster is preceeded downstream by the divergently transcribed ORF10 which encodes a PhaK-like transporter. Among the ten ORFs in the *pca* cluster no regulatory protein could be identified. The presence of transcriptional regulators in the unsequenced region upstream to ORF1 (*pcaI*) can not be excluded as the expression of protocatechuate degradation genes in other strains is usually induced by corresponding regulatory proteins, e.g. PcaR and PcaU in *P. putida* PRS2000 (Romero-Steiner *et al.*, 1994) and PobR and PcaU in *A. calcoaceticus* (DiMarco *et al.*, 1993).

3-Oxoadipate:succinyl-CoA transferase (PcaIJ) and 3-oxoadipyl-CoA thiolase (PcaF) transform 3-oxoadipate, which is a convergence point for the catechol and protocatechuate branch of the 3-oxoadipate pathway with the chlorocatechol pathway, into succinyl-CoA and acetyl-CoA (Göbel *et al.*, 2002). The overexpression of enzymes from protocatechuate pathway, observed in proteomic analysis during growth of MT1 on 4-CS (Bobadilla, 2006), could be explained by the coordinated transcription of all genes from the *pca* cluster in response to the need of channeling 3-oxoadipate originating from the chlorocatechol pathway.

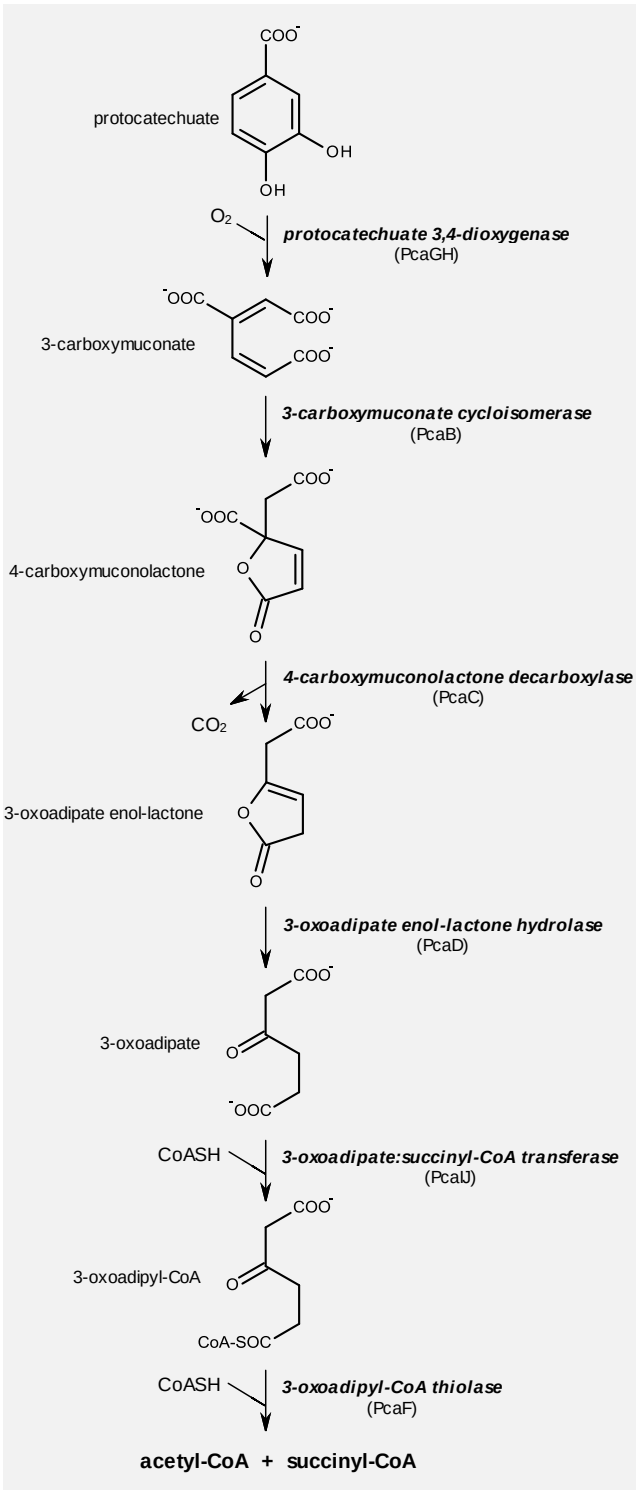

Figure 3.12. Proposed enzymatic activities of proteins encoded in the *pca* cluster of *P. reinekei* MT1.

3.2.2.4. Search for genes encoding chlorocatechol 1,2-dioxygenase and dienelactone hydrolase in *A. xylosoxidans* MT3

Due to the lack of any DNA sequence information for chlorocatechol 1,2-dioxygenase and dienelactone hydrolase encoding genes from MT3, the corresponding genes were

searched by activity-based screening of the MT3 genomic library. For this purpose MT3 proteins cloned in the library were expressed from recombinant phages in *E. coli* cells under the control of the IPTG-inducible *lac* promoter. Despite numerous rounds of screening (approx. 50000 plaques in total) for recombinant phages expressing 4-chlorocatechol transforming activity and acidifying the medium due to the formation of 3-chloromuconate no one plaque produced a positive signal. It can not be excluded that the random cloning of the MT3 genome into the phage vector resulted in a low representation or even complete omission of genes of a putative chlorocatechol pathway. Notably, however, these results are congruent with conclusions drawn from resting cell assays (Fig. 3.2.) and enzymatic activity assays (Tab. 3.3.) that MT3 does not contain a 4-chlorocatechol metabolic pathway.

cis-Dienelactone hydrolase was an enzymatic activity observed in consortium cell extracts, albeit at the very low level (Pelz *et al.*, 1999). Proteins of MT3 were expressed from recombinant phages in *E. coli* and screened for *cis*-dienelactone transforming activity. *cis*-Dienelactone hydrolyzing activity from recombinant phages was visualized by a local change of pH caused by acidification of the medium due to the formation of maleylacetate. Phage plaques producing strong positive reaction upon contact with substrate were recovered, however, the pH drop accompanying the enzymatic transformation was apparently so severe that it hindered rescueing functional infective phage particles. In accordance with the observed *cis*-dienelactone hydrolase activity in phages, activity towards *cis*-dienelactone could be detected in resting cell assays (Fig. 3.1.) as well as in cell extracts (Tab. 3.3.). Nonetheless, *cis*-dienelactone hydrolytic activity by itself can not be directly indicative of the presence of a chlorocatechol pathway as numerous lipases and esterases of microbial origin were reported to catalyze unspecific hydrolysis of lactonic compounds (e.g.: Khalameyezer *et al.*, 1999; Liu *et al.*, 2001).

3.3. Development of a high-throughput technique to determine the quantitative structure of the 4-CS degrading consortium

The availability of robust and reliable methods that allow to determine the abundance of specific subpopulations is of primary importance for studying mixed microbial cultures. In this work Fluorescent *In Situ* Hybridisation (DeLong *et al.*, 1989; Amann *et al.*, 1990b) was selected as a method of choice to discriminate between members of the bacterial consortium particularly due to its potential for automation and increasing the throughput of the measurements (Amann *et al.*, 1990a).

3.3.1. Design of strain-specific FISH oligoprobes for consortium bacteria

Virtually any kind of nucleic acids can be used as a target for F*IS*H probes, however, 16S and 23S rRNA remain by far the preferred ones for the purpose of detecting bacteria as they are present in high copy number in any viable single cell. The sequences of 23S rRNA from MT1 and MT4 are almost identical and lack sufficient variability for developing strain-specific probes (Tillmann, 2004). In this work, F*IS*H probes targeting 16S rRNA were developed in regions that showed both variability and good accessibility for hybridisation probes when tested in *E. coli* (Fuchs *et al.*, 1998). Probes for discriminating the most closely related strains in the consortium, *P. reinekei* MT1 and *P. veronii* MT4, were designed in the variable region V1: helix 6 (*E. coli* positions 66-103) of the 16S rRNA as recommended for the species of the genus *Pseudomonas* by Moore *et al.* (1996). A multiple sequence alignment of 16S DNA fragments of all four consortium strains together with the target sites for strain-specific F*IS*H probes is shown in the appendix in the Fig. A.1.

Basic principles of oligoprobe design included a length of the oligonucleotide core of 20 bp, with 45-55% G+C content and a minimum of three mismatches to the closest relative in the central region of the probe. Oligonucleotides were routinely labeled at their 5' ends, although dual labeling schemes were also tested for cytometric applications. Fluorescent dyes were selected to accommodate both cytometric and microscopic detection.

Table 3.8. F*IS*H probes suitable for discrimination of the consortium bacteria.

Probe name	Sequence (5'→3')	Dye	Detection	
			microscopy	cytometry
MT1	GAA TTC AGG AGC AAG CTC CT	5'-Cy3	+	–
MT1_420	AAG CTC CTG TCA TCC GCT CG	5'-AlexaFluor 488	+	+
MT2	TAA TCC TCC TTT CGA AGG GC	5'-Cy3	+	–
MT2_Cy5	TAA TCC TCC TTT CGA AGG GC	5'-Cy5	–	+
MT3	ATA TCG GCC GCT CTA ATA GT	5'-Cy3	+	–
MT3_Alexa647	ATA TCG GCC GCT CTA ATA GT	5'-AlexaFluor 647	–	+
MT3_green	ATA TCG GCC GCT CTA ATA GT	5'-AlexaFluor 488	+	+
Add_MT4	AAG CTT CTC TCT ACC GCT GC	5'-Cy3	+	–
MT4_orange	AAG CTT CTC TCT ACC GCT CG	5'-AlexaFluor 546	+	–
MT4_Alexa594	AAG CTT CTC TCT ACC GCT CG	5'-AlexaFluor 594	+	–
MT4_red	AAG CTT CTC TCT ACC GCT CG	5'-Bodipy 630/650	–	+

Specificity of designed probes was determined by cross-hybridisation with all consortium bacteria. Binding efficiency of the oligonucleotides to the target 16S rRNA was evaluated

microscopically as a relative brightness of fluorescent signal. Hybridisation conditions, including temperature and time of incubation as well as the content of formamide in the hybridisation buffer, were optimised individually so as to ensure both the desired specificity and high binding efficiency (Tab. 3.8). All selected strain-specifc probes showed a brightness of the fluorescent signal equal to or higher than the Eubacteria-specifc probe EUB338 (Amann *et al.*, 1990b).

In the process of designing F*IS*H oligoprobes, several fluorescent dyes were tested and for cytometric detection AlexaFluor 488 was found superior to others for excitation by the argon laser (488 nm). In contrast to this finding, Cy5, AlexaFluor 647 and Bodipy 630/650 were delivering equally bright fluorescence upon excitation with the helium laser (633 nm). Unfortunately, lasers in the cytometer and an arc-lamp in the microscope that are used as source of light for exciting fluorescence as well as optics of both instruments account for their low compatibility in terms of available fluorophores. In general, only probes labeled with AlexaFluor 488 could be used for cytometric and microscopic detection.

3.3.2. Quantification of bacteria in mixtures using direct and indirect techniques

For the purpose of cytometric analysis, consortium bacteria grown separately on acetate in mineral medium were harvested during the exponential growth phase, fixed and stained with F*IS*H probes (Tab. 3.8.). Hybridisation in solution was generally carried out according to published reports (Amann *et al.*, 1990a; Wallner *et al.*, 1995; Lange *et al.*, 1997; Fuchs *et al.*, 1998 and Fuchs *et al.*, 2000) using protocols being individually optimized to ensure reproducibility, minimum noise from cellular debris, suspension of cells without aggregates, as well as maximum specificity and intensity of the fluorescence signal. A FACS Calibur flow cytometer (Becton Dickinson, USA) was aligned with fluorescent beads of 1 µm diameter (Polybead Microspheres, Polyscience, USA) and F*IS*H-labeled cells suspended in 1×PBS buffer were passed through it with the speed of analysis not exceeding 2000 events per second. A minimum of 50000 and typically more than 100000 events were analysed in individual samples of F*IS*H stained bacteria. Recorded light signals for events within the gate that separated cells (typically > 98% of all events) from debris and electronic noise was amplified at logarithmic scale. The total counts of bacteria within the gated events were corrected after staining the sample with unspecific DNA-binding dye (propidium iodide) and repeated cytometric analysis. Results of F*IS*H-flow cytometry were analysed using dot plots and histograms with appropriate gates set up to discriminate stained and non-stained subpopulations of bacteria. Cells from mixed cultures were stained in pairs (typically MT1 + MT4 and MT3 + MT2) with appropriate probes conferring green and red fluorescence that

served both a discriminatory purpose and as hybridisation-stringency controls and were analysed after the instrument was set up with stained bacterial pure cultures.

The developed F*IS*H-flow cytometry quantification technique was compared with cultivation-dependent (CFU counting on solid agar medium) and other cultivation-independent (immunofluorescence and F*IS*H) methods of enumeration. Comparative analysis aimed primarily to assess the influence of (i) the target molecule (antigen vs. rRNA), (ii) the mode of quantification (microscopic vs. cytometric) and (iii) the principle of detection (growth-dependent *vs.* growth-independent) on the estimated values. Accuracy, sensitivity and reproducibility of all enumeration techniques was evaluated with two different mixtures of consortium bacteria. The mixtures emulated in their composition a functional consortium (a) and a perturbed consortium (b) and were prepared by blending acetate-grown pure cultures of consortium bacteria of known CFU. As discriminating colonies on solid agar medium, except for strain MT2, is practically impossible, the CFU counts were calculated from the CFUs of individual cultures and the CFUs of the mixtures. Quantification of individual bacterial strains in the mixtures was performed at least in triplicate for every method tested and the calculated mean values together with the values of standard errors are plotted in Figure 3.13.

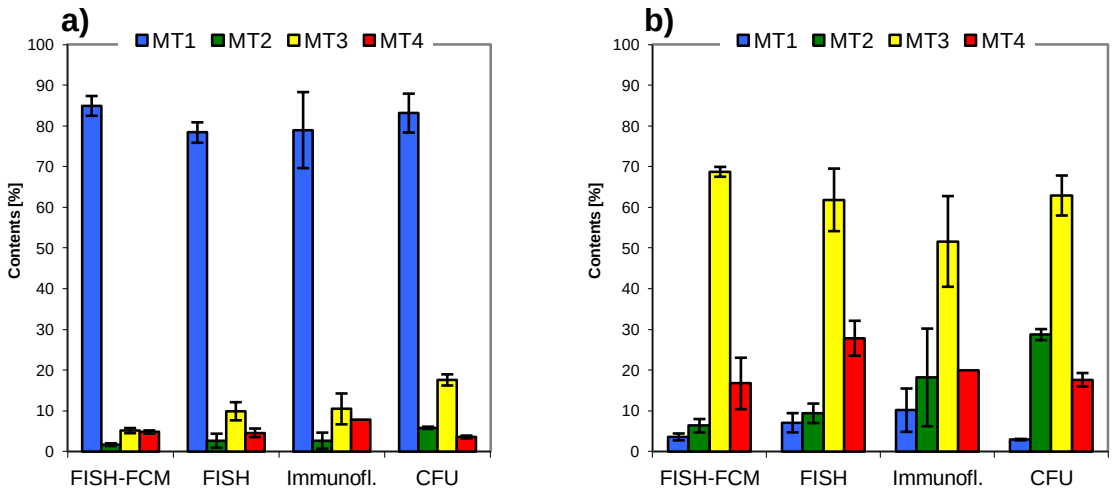

Figure 3.13. Comparison of F*IS*H-flow cytometry (F*IS*H-FCM), F*IS*H, immunofluorescence and CFU enumeration techniques for different bacterial mixtures representing: **(a)** 'functional consortium', **(b)** 'perturbed consortium'.

The composition of bacterial mixtures determined by fluorescence-based methods was generally in a good agreement with cultivation-dependent CFU counts. Observed discrepancies remained typically within the range of calculated standard errors of the mean.

Comparison of results obtained by immunofluorescent quantification and F*IS*H confirms that both antibodies and oligonucleotide probes display sufficient specificity and may be used to discriminate even the closely related consortium bacteria.

Calculated standard errors were lowest when bacterial mixtures were quantified by flow cytometry. This is hardly surprising as the number of bacterial cells counted cytometrically (here >100000) exceeded the number of cells quantified under the microscope by at least two orders of magnitude. The developed FISH-flow cytometry enumeration technique was accurate for populations that were present both in the highest and lowest content in the mixture. As expected, microscopic detection proved as the more sensitive for quantification of minor bacterial populations. Considerable reduction of time and workload needed to analyse a single sample made F*IS*H-flow cytometry superior to other tested techniques for high throughput quantification of bacteria in the 4-CS-degrading consortium.

3.4. Influence of the composition of the mixed culture on 4-CS degradation

Strains MT2, MT3 and MT4 show a remarkable ability to remain in the mixed community with MT1 when grown on 4-CS as sole carbon source in continuous culture, even though MT1 is the only strain capable of degrading 4-CS in pure culture. Although strains MT2, MT3 and MT4 are not able to attack 4-CS, they may possibly contribute to the degradation of the substrate. Three different mixed cultures were set up under chemostat conditions in order to assess the effect exerted by the presence of individual strains on the degradation of 4-CS by the microbial community. The first culture constituted of the entire four-membered consortium, while the second and third reactors were inoculated with binary cultures of MT1/MT4 and MT1/MT3, respectively. The concentration of substrate (4-CS) and of metabolites accumulating in the medium, as well as the biomass (optical density) and the community structure were analysed over time.

3.4.1. Continuous culture of the four-membered consortium with 4-chlorosalicylate as substrate

The four-membered bacterial consortium was cultivated in the standard chemostat, fed with 10 mM 4-CS at the standard dilution rate of D = 0,2 d^{-1} at 30°C, with an automatically controlled pH of 7,2 and aeration of 300 vvm. After completing three residence times the basic parameters of the culture, which are the concentration of 4-CS and metabolites in the medium, the biomass level (optical density), as well as the composition of the bacterial com-

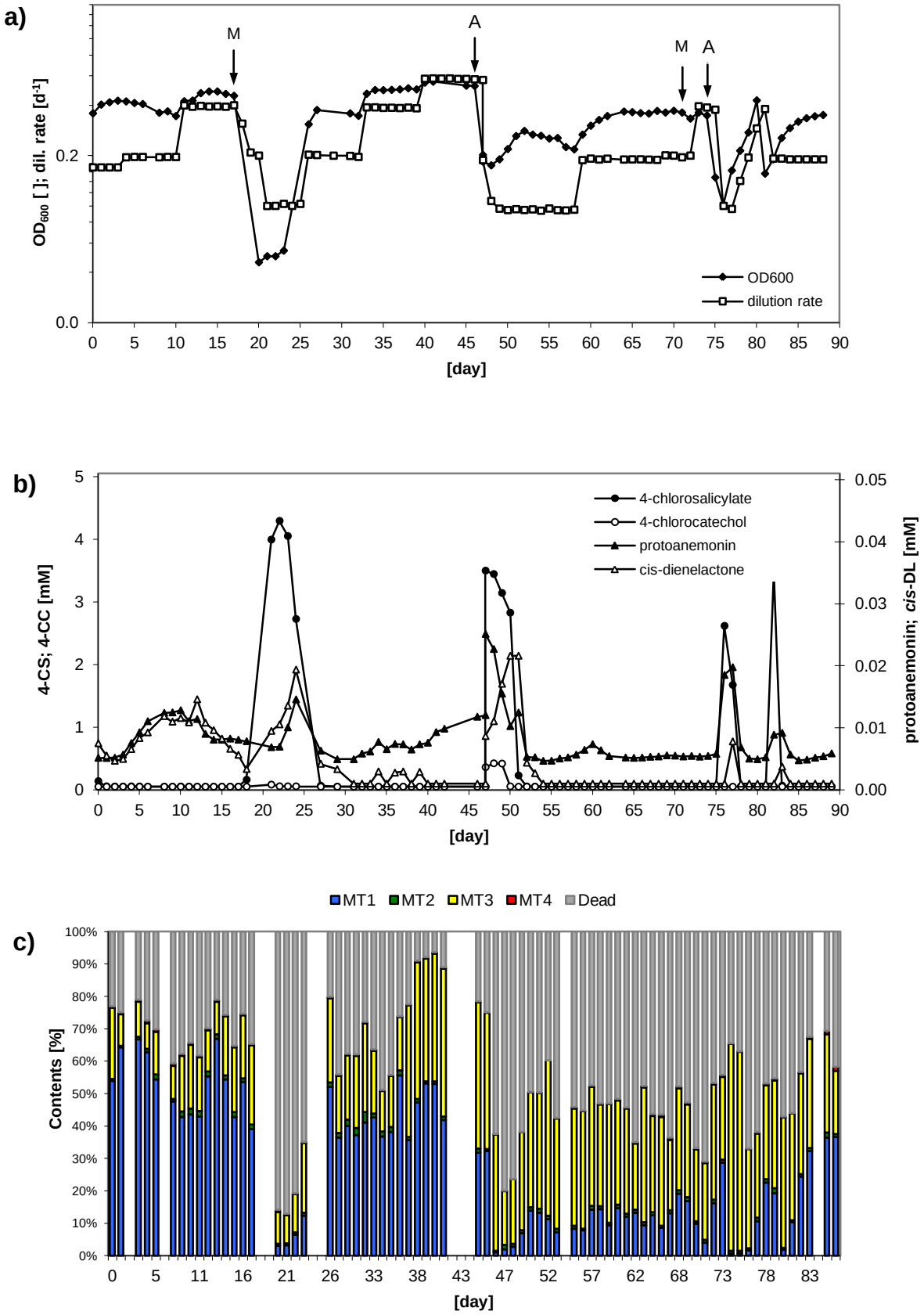

Figure 3.14. Consortium culture in the 4-chlororosalicylate chemostat: **(a)** biomass and dilution rate, **(b)** substrate and metabolite profile, and **(c)** consortium structure. Arrows denote installation of new media bottle (M) or period of anaerobiosis (A).

munity were monitored on a daily basis for nearly 90 days (Fig. 3.14.). The consortium culture was subjected to a series of perturbations which included step-wise increase of the dilution rate and transient anaerobiosis. The effects of perturbation on the consortium chemostat culture are discussed further in chapter 3.5.3.

During the first ten days of the steady-state and under standard growth conditions the consortium culture in the reactor reached on average an optical density of 0,379 ± 0,036. Degradation of 4-CS was complete as judged from its absence in the medium. The breakdown of 4-CS by the consortium resulted in the accumulation of small amounts of protoanemonin (7,1 ± 3,1 µM) and *cis*-dienelactone (5,4 ± 3,9 µM). *P. reinekei* MT1 was the dominant strain in the consortium accounting on average for 49,5 ± 10,4% of total bacteria. With an average share of 17,2 ± 6,4 % *A. xylosoxidans* MT3 represented the second most abundant population. The content of *E. brevis* MT2 and *P. veronii* MT4 in the chemostat culture was much lower with 1,5 ± 0,8% and 0,6 ± 0,2%, respectively. In terms of active (all F*IS*H-positive) bacteria, percentages of particular strains were on average as follows: 72% of MT1, 2% of MT2, 25% of MT3, and 1% of MT4.

3.4.2. Continuous culture of a MT1/MT4 consortium with 4-chlorosalicylate as substrate

Also a binary culture of *P. reinekei* MT1 and *P. veronii* MT4 was cultivated in the chemostat supplied with the medium containing 10 mM 4-CS at the dilution rate of 0,2 d^{-1}. The pH was controlled at 7,2 and aeration occurred at 300 vvm. After reaching the steady state (three residence times) the key parameters of the culture (concentration of the substrate and metabolites, biomass level and quantitative structure of the community) were monitored on a daily basis for a period of over 40 days (Fig. 3.15.).

The MT1/MT4 community could be maintained in the 4-chlorosalicylate fed chemostat under the tested conditions. The average cellular density of OD_{600} = 0,273 ± 0,030 obtained in this culture was identical to that recorded for the pure culture of MT1 grown under identical conditions with OD_{600} = 0,269 ± 0,015 (Strocchi, unpublished).

HPLC analyses of the medium supernatant confirmed quantitative depletion of 4-CS. Intermediates of the 4-CS degradation pathway like 4-chlorocatechol, 3-chloromuconate and maleylacetate could not be detected in the culture supernatant. The reported dead-end metabolites - protoanemonin and *cis*-dienelactone (Nikodem *et al.*, 2003) were present in the supernatant at levels of 5-12 µM, which is higher than the 5-7 µM concentration that was measured for the consortium culture grown under identical conditions.

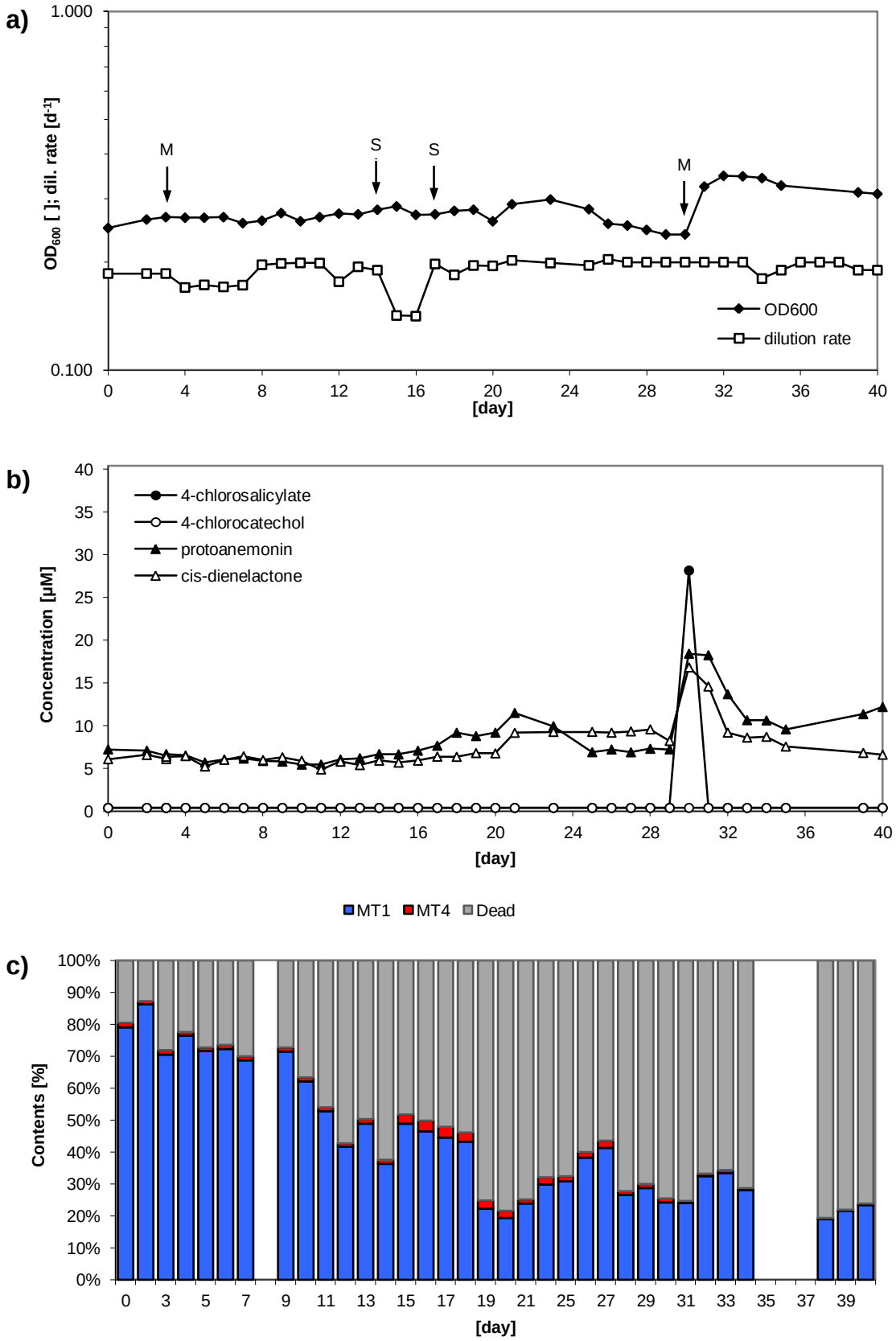

Figure 3.15. Binary culture of *P. reinekei* MT1 and *P. veronii* MT4 grown on 4-CS in the chemostat: (**a**) cellular density and dilution rate, (**b**) metabolite profile and (**c**) community structure. Arrows denote when new media bottles were installed (M) and time-points of large-volume sampling (S).

The bacterial community in the chemostat was dominated by *P. reinekei* MT1 that accounted for 94-98% of viable bacteria. The population of *P. veronii* MT4 coexisted stably with MT1 and constituted typically 2-6% of viable cells with the exception of days 18-20, where following the perturbation due to the large-volume sampling, it reached a maximum of 10%. The F*IS*H-flow cytometry determinations of the community structure indicated that the percentage of active bacteria decreased constantly with the age of the culture. This observation was confirmed by CFU counts on LB agar and for instance at the start (day 0), after 7 days and 14 days of cultivation the CFU/ml accounted for $1{,}56 \cdot 10^8$, $1{,}28 \cdot 10^8$ and $0{,}54 \cdot 10^8$, whereas the corresponding cytometric determinations showed the sum of active MT1 and MT4 to equal 80,5%, 69,9%, and 37,6% of the total bacteria, respectively. The reduced number of viable cells in the reactor could result at least partially from the formation of a biofilm occluding the substrate inlet, thus effectively decreasing the amount of substrate that entered the vessel.

3.4.3. Continuous culture of a MT1/MT3 consortium with 4-chlorosalicylate as substrate

It would be expected that a mixed culture of the two most abundant consortium species *P. reinekei* MT1 and *A. xylosoxidans* MT3 will most closely resemble the original four-membered bacterial culture. The MT1/MT3 mixed culture was grown in the chemostat supplied with 10 mM 4-chlorosalicylate at a dilution rate D = 0,2 d^{-1} at 30°C, with an automatically controlled pH of 7,2 and aeration of 250 vvm. After completing three residence times the chemostat culture reached steady state and its performance (concentration of the substrate and metabolites, biomass level and the quantitative structure of the community) was monitored for a period of over 80 days (Fig. 3.16).

During growth in continuous culture, MT1 and MT3 formed a stable community that was capable for quantitative mineralization of 4-CS. An average optical density of 0,292 ± 0,039 in the MT1/MT3 chemostat was slightly higher than the 0,269 ± 0,015 observed in the pure culture of MT1 (Strocchi, unpublished) but lower than the 0,379 ± 0,036 observed in the consortium chemostat (see: 3.4.1.). However, it has to be noted that the level of biomass in the MT1/MT3 culture vessel was heavily influenced by the formation of biofilm in the inlet tubing, as indicated by the slowly decreasing values of OD_{600} that followed installing fresh medium reservoirs (Fig. 3.16a). Bacteria that grew in the biofilm occluding the inlet tubing obviously consumed part of the carbon substrate (4-CS) from the medium, effectively reducing its concentration what contributed to a decreased level of biomass of planktonic cells. It is thus likely that the gradual decrease of optical density of the culture reflects the growth and development of a biofilm.

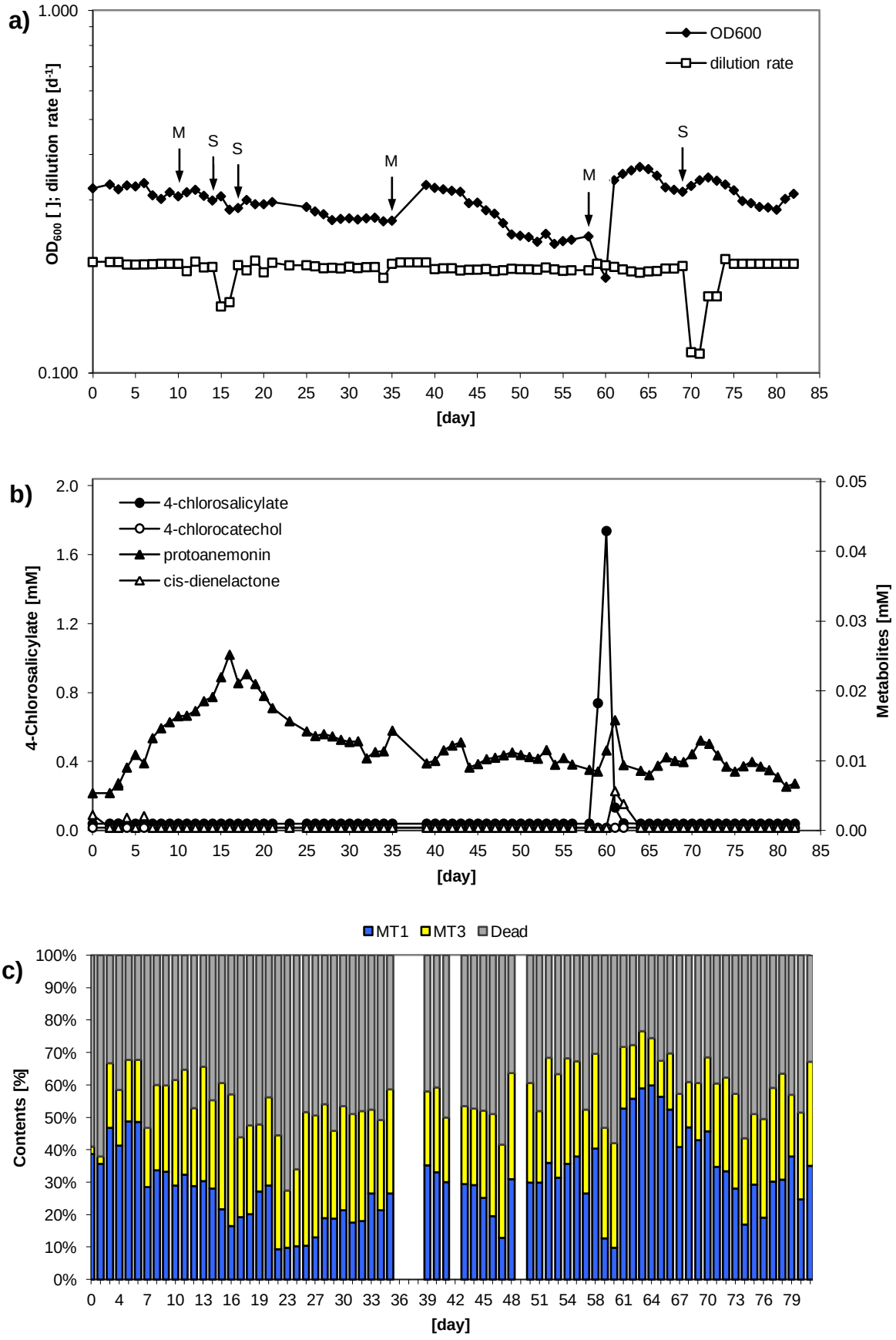

Figure 3.16. Binary culture of *P. reinekei* MT1 and *A. xylosoxidans* MT3 grown on 4-CS in the chemostat: **(a)** biomass and dilution rate, **(b)** metabolite profile, and **(c)** community structure. Arrows denote installing new medium reservoir (M) and large volume sampling (S).

The binary culture of MT1/MT3 degraded 4-chlorosalicylate completely and accumulation of intermediates in the chemostat medium was not detected at any stage of the culture except short periods after installing fresh medium reservoirs. Protoanemonin was the only compound constantly present in the culture supernatant at a level of 5-20 µM. In contrast to the MT1/MT4 binary culture and the pure culture of MT1 (Strocchi, unpublished) *cis*-dienelactone accumulation was not observed.

Community structure determinations by F*IS*H-flow cytometry showed an equilibrium between both strains with the culture comprising on average 53% of MT1 and 47% of MT3. Unlike the case in the MT1/MT4 binary culture, the content of active cells detected by F*IS*H-flow cytometry could not be unequivocally correlated with the CFU counts. The number of bacteria showing reproductive growth on LB agar plates was decreasing during cultivation while the F*IS*H-flow cytometry estimations of the sum of MT1 and MT3 fluctuated over time.

The binary culture of MT1/MT3 seems to be as capable of breaking down the 4-CS as the original four-membered bacterial consortium but it did not accumulate *cis*-dienelactone and displayed even better vigour than consortium.

3.5. Responses of the consortium to environmental perturbations

Functioning of microbial communities in the environment is influenced by both biotic and abiotic factors. This work focused mainly on understanding the impact of abiotic factors on the consortium by simulating the most likely occurring environmental disturbances, such as changes in the growth temperature, alternated supply of substrate, alterations in the type of available carbon source and temporary oxygen limitation. In order to simulate biotic changes in the environment, *P. reinekei* MT1 was substituted by another chlorosalicylate-degrading strain *P. moorei* RW10 with a view of investigating the ability of MT2, MT3 and MT4 to thrive in an alternative community.

3.5.1. Influence of temperature on the consortium structure and performance

Temperature belongs to the most powerful abiotic factors that affect functioning of any biological system. Like every other life forms, microorganisms may thrive, reproduce and exhibit their full metabolic potential only within a certain range of temperature conditions. To determine the influence of temperature on growth, degradation of substrate, as well as on the community composition, the four-membered bacterial consortium was grown on 4-CS in the batch mode and in continuous culture at temperatures ranging between 4°C and 37°C .

3.5.1.1. Growth rate of individual consortium strains at different temperature

Prior to testing a thermal optimum for the whole 4-chlorosalicylate degrading community the optimal growth temperatures were determined for individual consortium members. Bacteria were grown at temperatures ranging between 4ºC and 37ºC in mineral medium with 8 mM acetate (and yeast extract for MT2) and the optical density of the cultures was monitored at regular time intervals. Specific growth rates (μ) of the pure cultures at different temperatures were calculated and plotted in the Fig. 3.17.

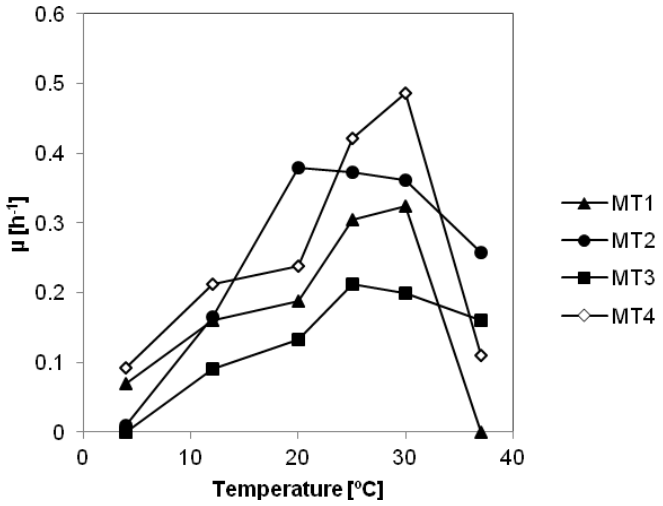

Figure 3.17. Dependence of the specific growth rate (μ) of pure cultures of MT1, MT2, MT3 and MT4 on the temperature of cultivation during growth in mineral medium supplemented with acetate.

All four consortium members were able to grow on acetate in mineral medium at temperatures between 12 and 30ºC and were generally achieving their maximum specific growth rate between 25 and 30ºC.

Significant differences between consortium strains were observed at the extreme of the temperatures tested. Notably, neither MT2 nor MT3 were able to grow under psychrophilic conditions (4ºC) while strain MT1 could not replicate at 37ºC. At 37ºC also growth of the second *Pseudomonas* strain, MT4, was severely compromised.

3.5.1.2. Growth of the consortium on 4-CS at various temperature conditions

A consortium cultivated to late exponential growth phase in mineral medium with 5-CS as sole carbon source at 25ºC in batch culture, on an orbital shaker (120 rpm), served as inoculum for this experiment. The ability of the consortium to grow on and to mineralize 4-CS was tested in batch cultures incubated at 4, 12, 20, 25, 30 and 37ºC with shaking (120 rpm). Growth of the consortium was followed by analysis of optical density.

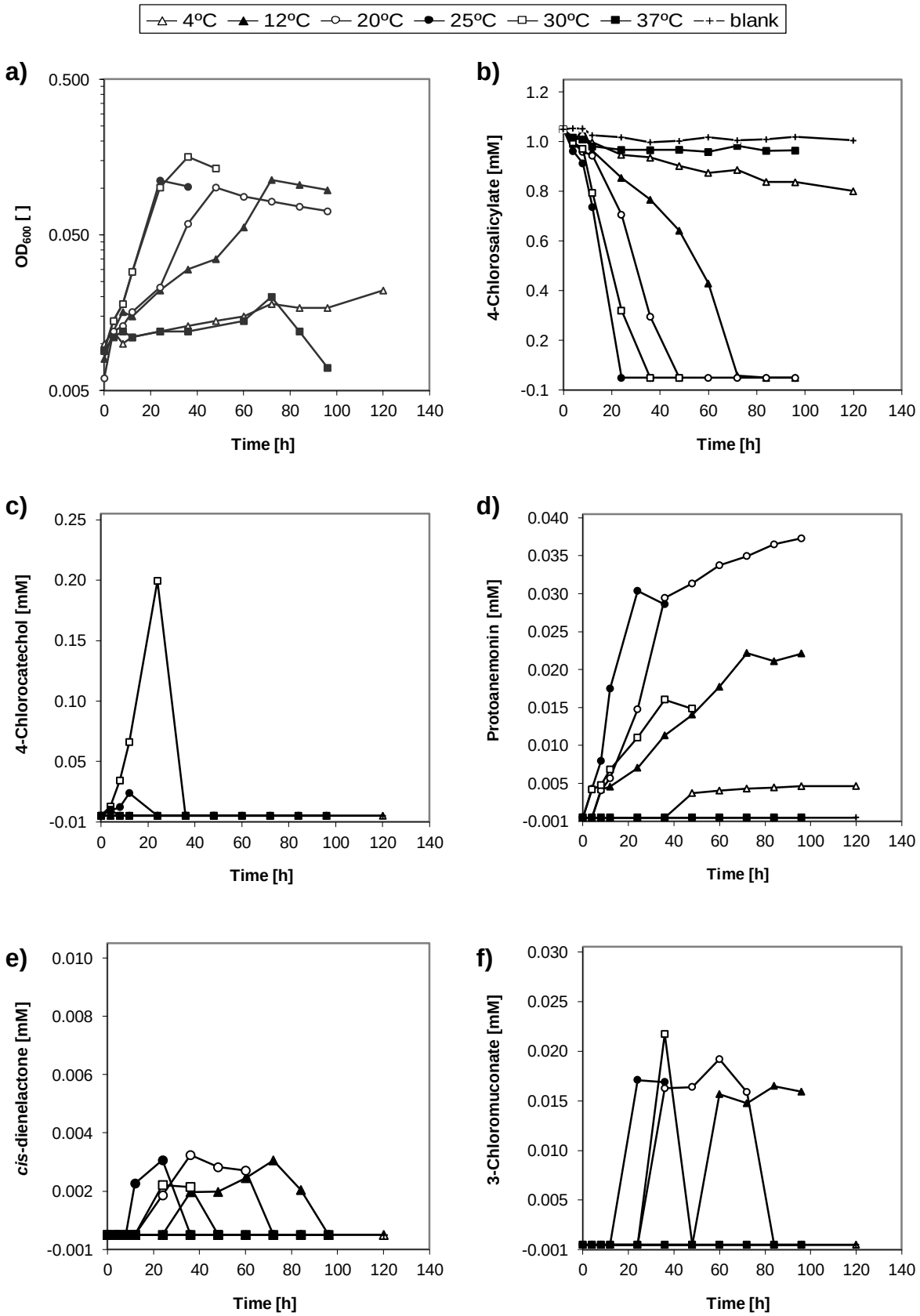

Figure 3.18. Consortium performance at temperatures ranging from 4 to 37ºC as a function of cell density **(a)**, concentration of 4-CS **(b)**, 4-chlorocatechol **(c)**, protoanemonin **(d)**, *cis*-dienelactone **(e),** and 3-chloromuconate **(f)** in the culture supernatant.

Concentration of substrate and metabolites was measured by HPLC (Fig. 3.18). The rate by which 4-CS was degraded by the consortium at different temperatures was calculated from the depletion of substrate per time interval and per OD_{600} unit of biomass.

Thus, the bacterial consortium could grow on 4-CS at temperatures ranging from 12ºC to 30ºC (Fig. 3.18a) and weak growth was also observed at 4ºC. A temperature of 37ºC proved to be too high for the 4-CS-degrading consortium, consistent with the failure of MT1 to grow at this temperature (see: 3.5.1.1. and Fig. 3.17). Bacteria showed fastest growth at 25ºC with μ equal to 0,114 h^{-1} while at 30ºC their specific growth rate was reduced to 0,078 h^{-1}. Unsurprisingly, the consortium grew slower at 20ºC and 12ºC with values of μ of 0,062 and 0,044 h^{-1}, respectively.

The rate of 4-CS breakdown correlated with the growth rate of the bacteria and was fastest at 25ºC with 0,83 mM/h·unit of OD_{600}. Accordingly, the 4-CS degradation rate was decreasing at 30ºC, 20ºC and 12ºC to 0,68, 0,42 and 0,33 mM/h·unit of OD_{600}, respectively. The consortium grown at 4ºC managed to consume only approx. 25% of substrate during six days of cultivation (Fig. 3.18b).

Interestingly, 4-chlorocatechol accumulated in the medium only when the consortium was grown at 25ºC and 30ºC, but not at 12ºC or 20ºC (Fig. 3.18c). The maximum accumulating concentration of this intermediate at 30ºC equalled to 194 μM while at 25ºC it was ten-fold lower with 19 μM. In contrast to 4-chlorocatechol, 3-chloromuconate was present in all consortium cultures between 12 and 30ºC and reached a level of 15-20 μM (Fig. 3.18f). Similarly, *cis*-dienelactone accumulated in the medium at all growth temperatures to a level of 2-4 μM (Fig. 3.18e). Both 3-chloromuconate and *cis*-dienelactone were excreted during extensive breakdown of substrate, accumulated only transiently and at the same level for all temperatures. In contrast, protoanemonin excreted by the consortium tended to accumulate in the medium without any indications of being further metabolized (Fig. 3.18d). The maximum accumulating concentration of protoanemonin in the medium depended on the temperature and reached the highest value of 38 μM at 20ºC and the lowest value of 15 μM at 30ºC.

Interestingly, at the end of the experiment, the cultures showed difference in coloration. Cell-free controls as well as cultures incubated at 4ºC, 12ºC and 37ºC remained colourless. The medium after growth of the consortium at 20ºC turned into pale yellow while at 25ºC into intense yellow, what may indicate an active *meta*-cleavage pathway. Cultures grown at 30ºC turned dark brown as a result of accumulating 4-chlorocatechol.

3.5.1.3. Effect of temperature on the structure of the consortium grown on 4-CS

The microbial consortium could grow on 4-chlorosalicylate at temperatures between 12 and 30ºC as shown above. In order to find out if and how the temperature may affect the structure of the consortium, the dynamics of subpopulations was followed during growth in batch culture at 12, 20, 25 and 30ºC (Fig. 3.19). The preparation of inoculating material and the experimental set up were identical as previously described (see: 3.5.1.2.).

As might be seen from the analyses of the consortium structure (Fig. 3.19a and b), transfer of the bacterial inoculum grown at 25ºC to lower temperatures of 12 or 20ºC had a negative effect on the amount of active bacteria in the culture. The amount of viable cells during the lag phase at 12ºC or 20ºC decreased by 50%, specifically due to a decline of viable MT1 cells, whereas this effect was completely absent for the consortium cultivated at 25ºC and 30ºC (Fig. 3.19c and d).

The dominant role of MT1 in the consortium was not affected by the temperature of cultivation during the phase of extensive 4-CS breakdown. Its share in the consortium during the exponential growth phase at 12ºC equalled to 80% of active bacteria and was even higher at higher cultivation temperatures such as 89% at 20ºC or as much as 95% at 30ºC. However, after the substrate became exhausted and the culture reached its stationary growth phase the content of MT1 showed a tendency to decrease. This effect was evident at all tested temperature conditions and for instance at 20ºC the share of MT1 dropped to 68% while at 30ºC to 81% of active bacteria.

The content of MT2 in the community does not show any correlation with the concentration of 4-CS in the medium. However, optimal conditions for this strain to thrive in the consortium seem to involve the presence of both 4-CS and large amount of organic matter derived from died and lysed bacteria. Under such conditions, for instance during the lag phase of growth at 12ºC and 20ºC the share of MT2 reached as much as 9,5% and 6,7% of all active bacteria, respectively.

In contrast to MT2, the content of MT3 in the community was strongly dependent on the growth phase. When the cultures reached their stationary growth phase, MT3 became the second most abundant consortium member accounting for 9% of active bacteria at 25ºC, 18% at 30ºC and as much as 26% at 20ºC.

The temperature of cultivation had also an effect on the content of MT4 in the consortium grown on 4-CS. During growth at 12ºC and 20ºC this strain constituted between 4% and 11% of all active bacteria. The content of MT4 in the community showed a tendency to decrease in cultures incubated at 25ºC and 30ºC to the level of 2,3% and 0,95% of all active

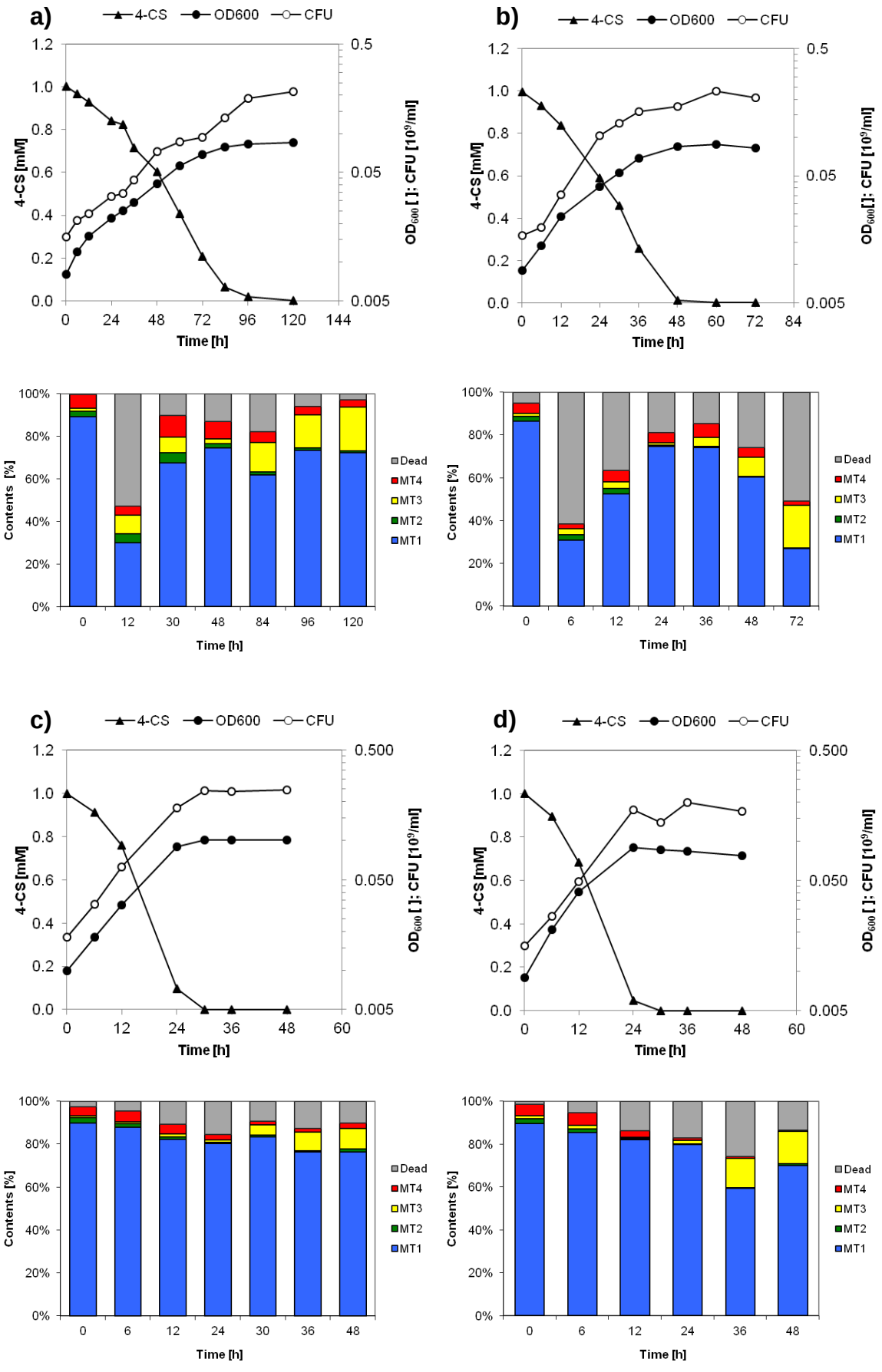

Figure 3.19. Consortium growth and community dynamics during growth on 4-CS at 12ºC **(a)**, 20ºC **(b)**, 25ºC **(c)** and 30ºC **(d)**.

bacteria, respectively. MT4 was typically more abundant during early exponental growth compared to late exponential growth.

The observed differences in the structure of the consortium during cultivation at different temperatures were masked by a strong effect of the phase of growth, as it is often characteristic for a batch culture.

3.5.1.4. Effect of temperature on the consortium structure in continuous culture

Results presented above show that consortium structure clearly depends on the growth phase in the batch culture. In order to reduce the growth phase effect, the consortium was grown in the chemostat supplied with 10 mM 4-CS at a dilution rate of 0,2 d^{-1}, pH controlled at 7,2, and 300 vvm aeration. The growth temperature was gradually decreased, first from 30ºC to 20ºC and then to 12ºC (Fig. 3.20). Each time after changing the temperature of cultivation, the chemostat was left undisturbed for a period of at least 2 weeks to achieve new steady-state conditions.

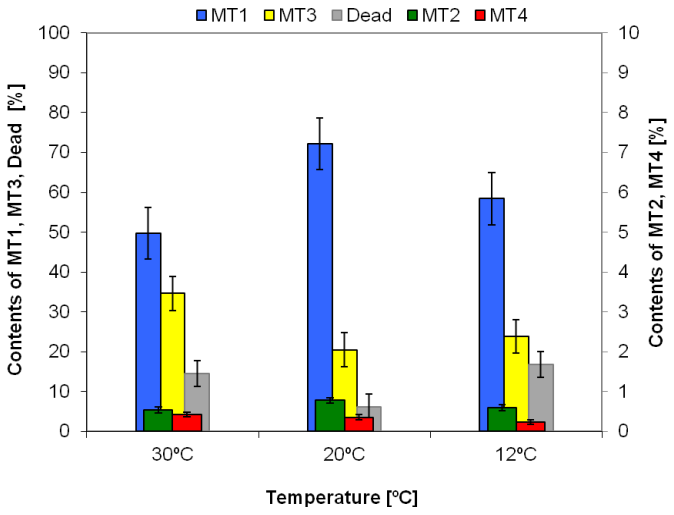

Figure 3.20. Composition of the microbial consortium grown in continuous culture on 4-CS at different temperature conditions.

Changes of the cultivation temperature did result in some shifts within the community structure. The average content of MT1 in the consortium fluctuated between 50% at 30ºC, 72% at 20ºC and 58% at 12ºC. Similarly, the average share of MT3 was highly variable with 35% at 30ºC, 20% at 20ºC and 24% at 12ºC. In contrast, the content of MT2 in the consortium did not vary significantly at different temperatures and was always 0,54-0,78%. Despite its overall low abundance in the consortium, the content of MT4 varied between 0,43% at 30ºC and 0,23% at 12ºC.

From the experiment in the continuous culture it might be concluded that the temperature has only a slight effect on the composition of the 4-CS degrading community. These results show, that the community composition is more dependent on the growth phase than on the growth temperature (see: 3.5.1.3.).

3.5.2. Comparison of 4- and 5-CS as substrates supporting growth of microbial consortia

The growth of two different microbial consortia, the original MT consortium and one where the chlorosalicylate degrading *P. moorei* RW10 is replacing *P. reinekei* MT1, were tested on 4-CS and 5-CS in batch, as well as in a fed-batch mode, in order to assess how strongly strains MT2, MT3 and MT4 are associated with specific major chlorosalicylate degraders.

3.5.2.1. Growth of the MT consortium on 4-chlorosalicylate in fed-batch culture

Individual strains were cultivated in mineral medium with 8 mM acetate as sole carbon source at 30ºC to the late exponential phase. Subsequently, cultures of MT1, MT2, MT3 and MT4 were combined in a volumetric ratio of 1:1:1:1 and this mixture served as inoculating material. The four-membered MT consortium was then grown in mineral medium containing initially 1 mM of 4-CS at 30ºC on the orbital shaker (120 rpm) with the intention of gradually increasing doses of substrate through feeding. Growth of the consortium was determined by measuring the optical density. Concentrations of 4-CS and metabolites were determined by HPLC (Fig. 3.21).

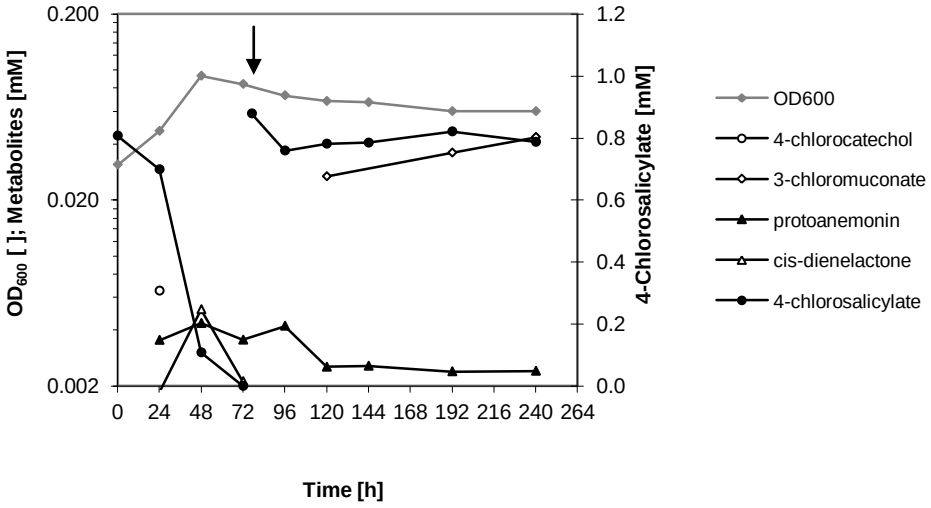

Figure 3.21. Degradation of 4-**c**hlorosalicylate by the MT consortium in the fed-batch mode. An arrow on the graph indicates the time point when feeding with 4-CS occurred.

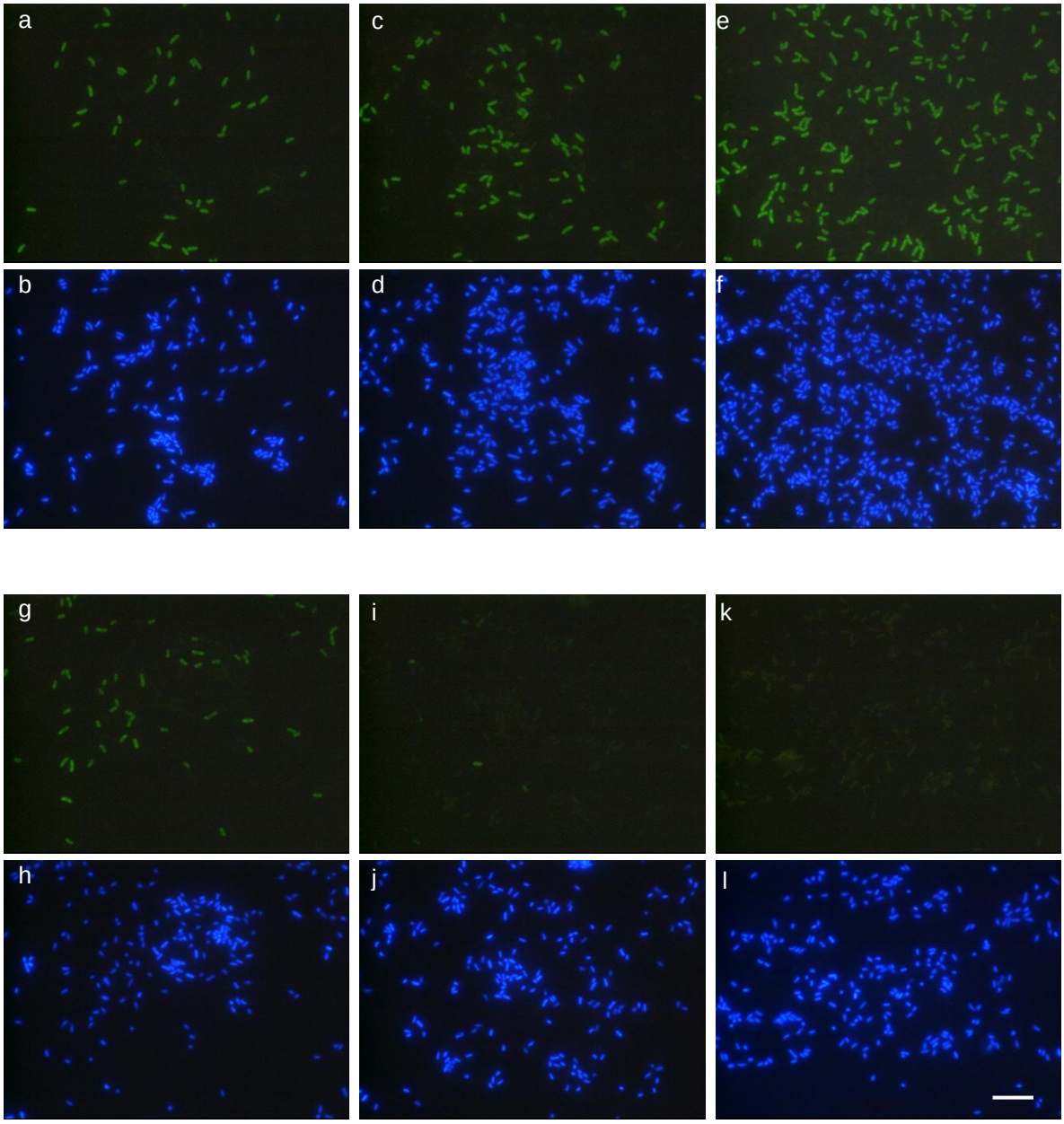

Figure 3.22. Microscopic images of F*IS*H-labeled cells of *P. reinekei* MT1 in the consortium grown on 4-chlorosalicylate. Panels: **(a-b)** at t = 0 h; **(c-d)** after 24 h; **(e-f)** after 48 h; **(g-h)** after 72 h; **(i-j)** after 96 h; **(k-l)** after 120 h. MT1 cells stained with F*IS*H probe shown in the panels **a**, **c**, **e**, **g**, **i**, and **k**. Total bacteria counterstained with DAPI presented in the panels **b**, **d**, **f**, **h**, **j**, and **l**. A bar represents 10 µm.

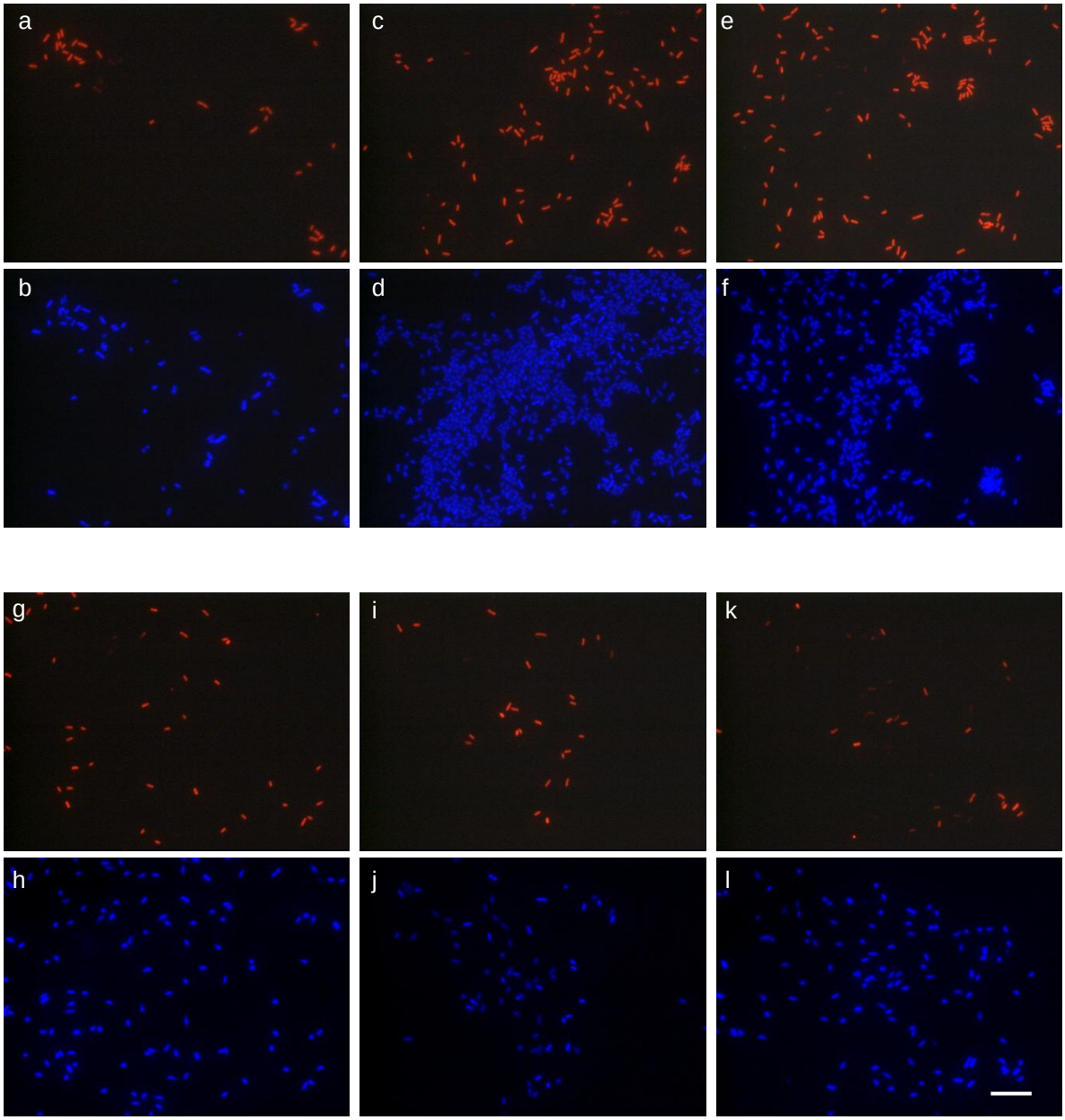

Figure 3.23. Microscopic images of F*IS*H-labeled cells of *E. brevis* MT2 in the consortium grown on 4-chlorosalicylate. Panels: **(a-b)** at t = 0 h; **(c-d)** after 24 h; **(e-f)** after 48 h; **(g-h)** after 72 h; **(i-j)** after 96 h; **(k-l)** after 120 h. MT2 cells after F*IS*H-staining shown in the panels **a**, **c**, **e**, **g**, **i**, and **k**. Total bacteria counterstained with DAPI presented in the panels **b**, **d**, **f**, **h**, **j**, and **l**. The bar represents 10 µm.

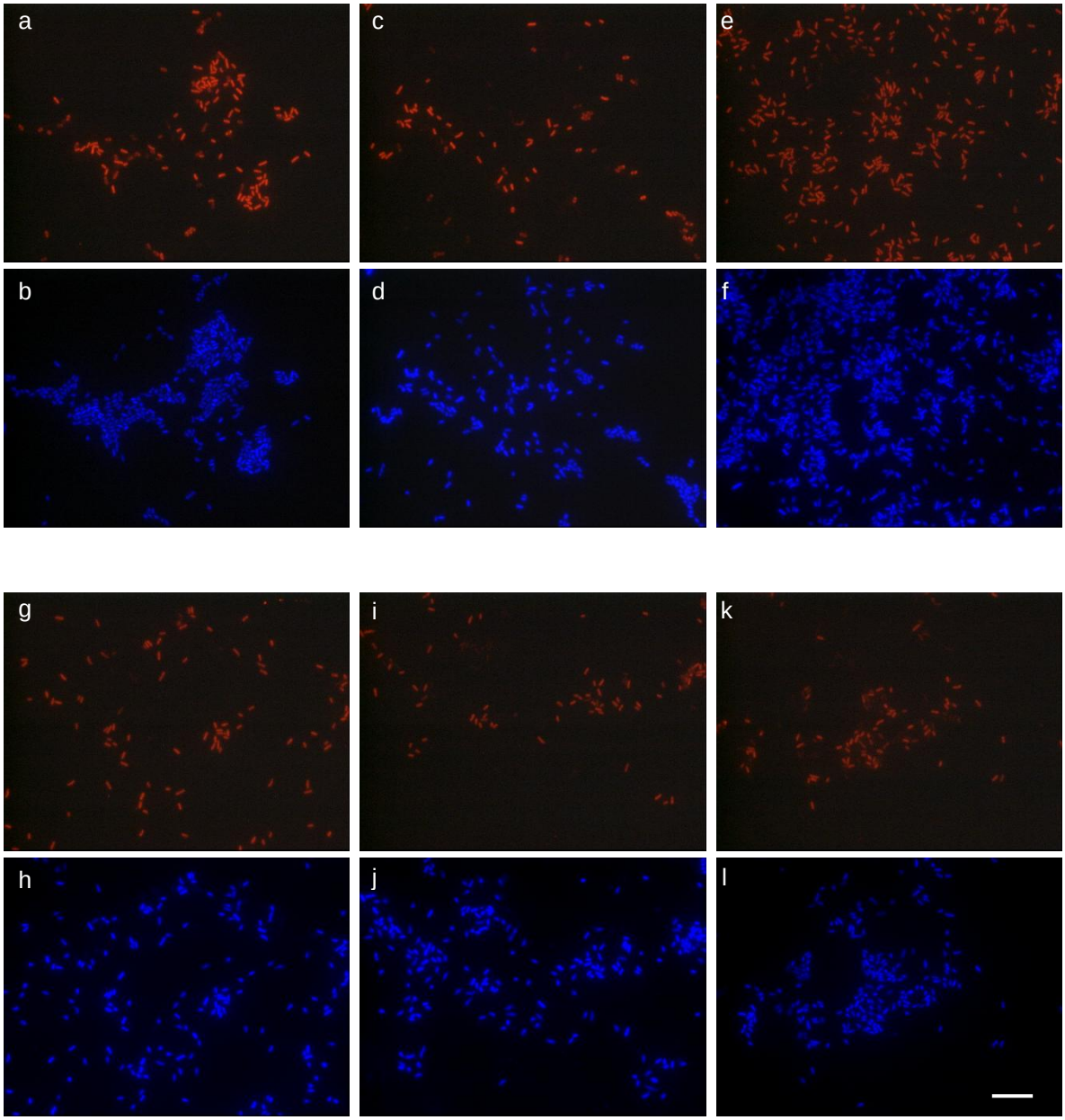

Figure 3.24. Microscopic images of F*IS*H-labeled cells of *A. xylosoxidans* MT3 in the consortium grown on 4-chlorosalicylate. Panels: **(a-b)** at t = 0 h; **(c-d)** after 24 h; **(e-f)** after 48 h; **(g-h)** after 72 h; **(i-j)** after 96 h; **(k-l)** after 120 h. F*IS*H-stained MT3 cells shown in the panels **a**, **c**, **e**, **g**, **i**, and **k**. Total bacteria counterstained with DAPI presented in the panels **b**, **d**, **f**, **h**, **j**, and **l**. The bar represents 10 µm.

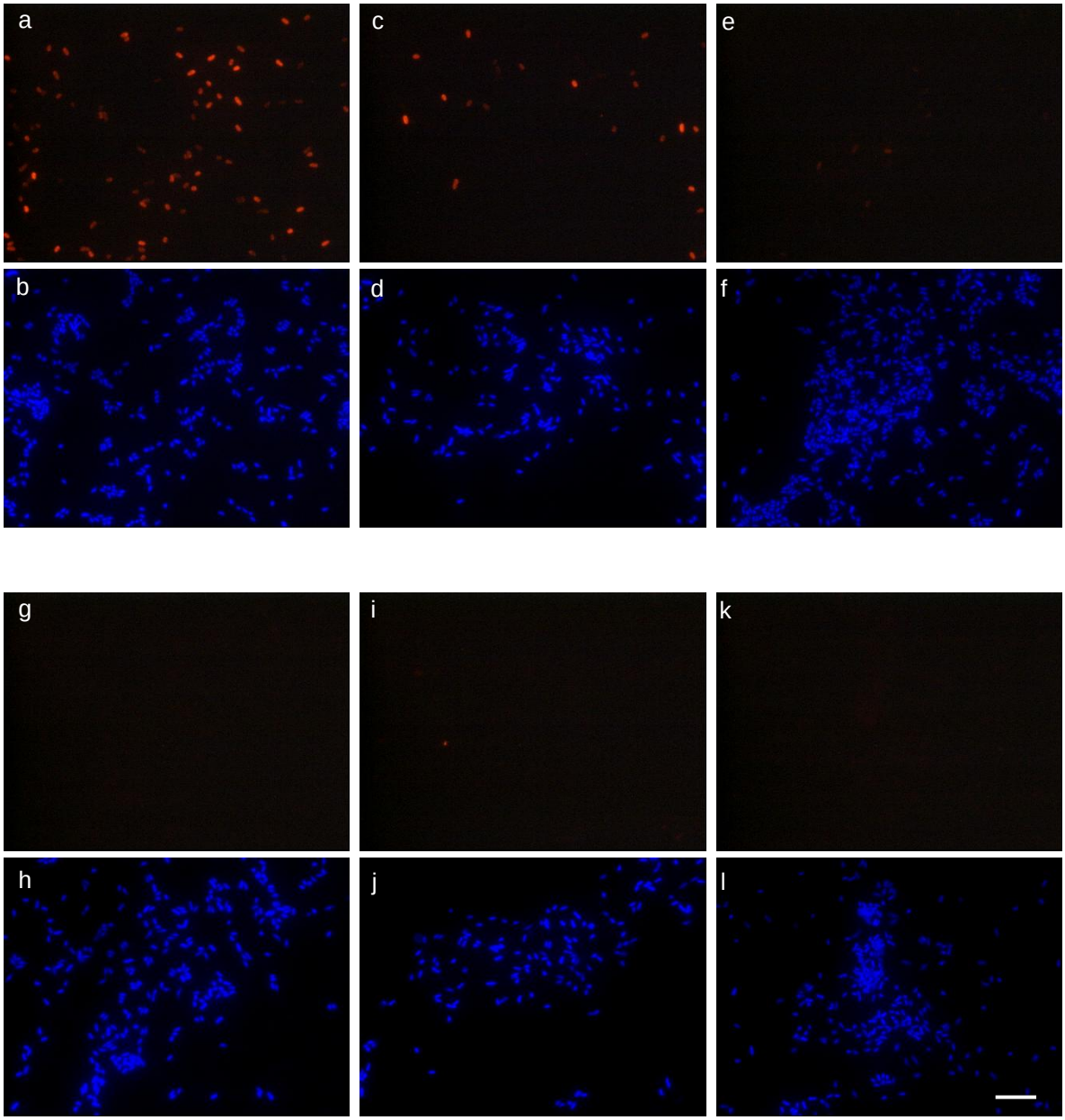

Figure 3.25. Microscopic images of F*IS*H-labeled cells of *P. veronii* MT4 in the consortium grown on 4-chlorosalicylate. Panels: **(a-b)** at t = 0 h; **(c-d)** after 24 h; **(e-f)** after 48 h; **(g-h)** after 72 h; **(i-j)** after 96 h; **(k-l)** after 120 h. MT4 cells after F*IS*H-staining shown in the panels **a**, **c**, **e**, **g**, **i**, and **k**. Total bacteria counterstained with DAPI presented in the panels **b**, **d**, **f**, **h**, **j**, and **l**. The bar represents 10 µm.

The rate of 4-CS degradation by the consortium was calculated from the depletion of substrate per unit of time and per OD_{600} unit of biomass. Changes in the community structure were followed by F*IS*H and microscopic analysis (Figs. 3.24-3.27).

The MT consortium grew on 4-CS with a rate of 0,028 h^{-1} that is lower than the value of 0,05 h^{-1} reported for the batch culture of strain MT1 (Nikodem *et al.*, 2003). 4-CS was degraded at a maximum rate of 0,35 mM/h·unit of OD_{600}. Both the specific growth rate (μ) and the 4-CS degradation rate determined here were approx. 2-3 times lower than those obtained in an identical set-up previously (see: 3.5.1.2.). This discrepancy may be due to the fact that the inoculum used here was not pre-adapted to chlorinated substrates. Breakdown of substrate was accompanied by the accumulation of 4-chlorocatechol (6 μM), protoanemonin (4 μM) and *cis*-dienelactone (5 μM) in the medium. Supplementation of the culture with additional 1 mM of 4-CS resulted in the medium turning dark brown, indicating an excessive accumulation of catecholic compounds that results in poisoning of the bacteria.

The sequence of representative microscopic images (Fig. 3.22) shows an intense proliferation of MT1 during the phase of 4-CS breakdown in the culture (panels a-h). Supplementation of the medium with additional 4-CS resulted in a sudden drop in the number of active MT1 cells that could no longer be found among the consortium bacteria after 96 h of experiment (panels i-l).

The number of initially abundant MT2 bacteria decreased gradually with time during growth on 4-chlorosalicylate (Fig. 3.23 panels a-f) but even after the breakdown of the culture following supplementation with 4-CS cells of this strain could still be detected in the consortium (panels k-l).

Similarly to MT2, MT3 represented a considerable fraction of bacteria during growth of the consortium on 4-CS (Fig. 3.24 panels a-h). Also MT3 cells could still be found in the community that ceased its functional degradative activity (panels i-l).

MT4 showed a rapid decline in the consortium during cultivation on 4-CS (Fig. 3.25 panels a-j). After 6 days of incubation, only very few MT4 cells could be visualized by F*IS*H-microscopy (panels i-l).

The sequences of microphotographs shown in Fig. 3.22-3.25 are representative of the functional breakdown of the 4-CS grown consortium not only in the batch culture as identical images were observed under the microscope for samples taken from the consortium chemostat following its response to transient anaerobiosis (described in detail in 3.5.3.2.).

3.5.2.2. Growth of the MT consortium on 5-chlorosalicylate in fed-batch culture

The inoculum used in this experiment was identical with the one described above (3.5.2.1.). The MT consortium was grown in mineral medium containing initially 1 mM of 5-CS at 30ºC on the orbital shaker (120 rpm). After the substrate became exhausted, the culture was supplemented with increasing doses of 5-chlorosalicylate to reach successively concentrations of 2 mM, 3 mM, 4 mM and finally 4,5 mM, respectively. The growth of consortium was determined by measuring the optical density. The concentrations of 5-CS and metabolites were measured by HPLC (Fig. 3.26a). The rate of 5-CS degradation by the consortium was calculated by the depletion of substrate per unit of time and per OD_{600} unit of biomass. The community dynamics was followed by F*IS*H and epifluorescent microscopy (Figs. 3.29-3.32) and the composition quantified by F*IS*H-flow cytometry (Fig. 3.26b).

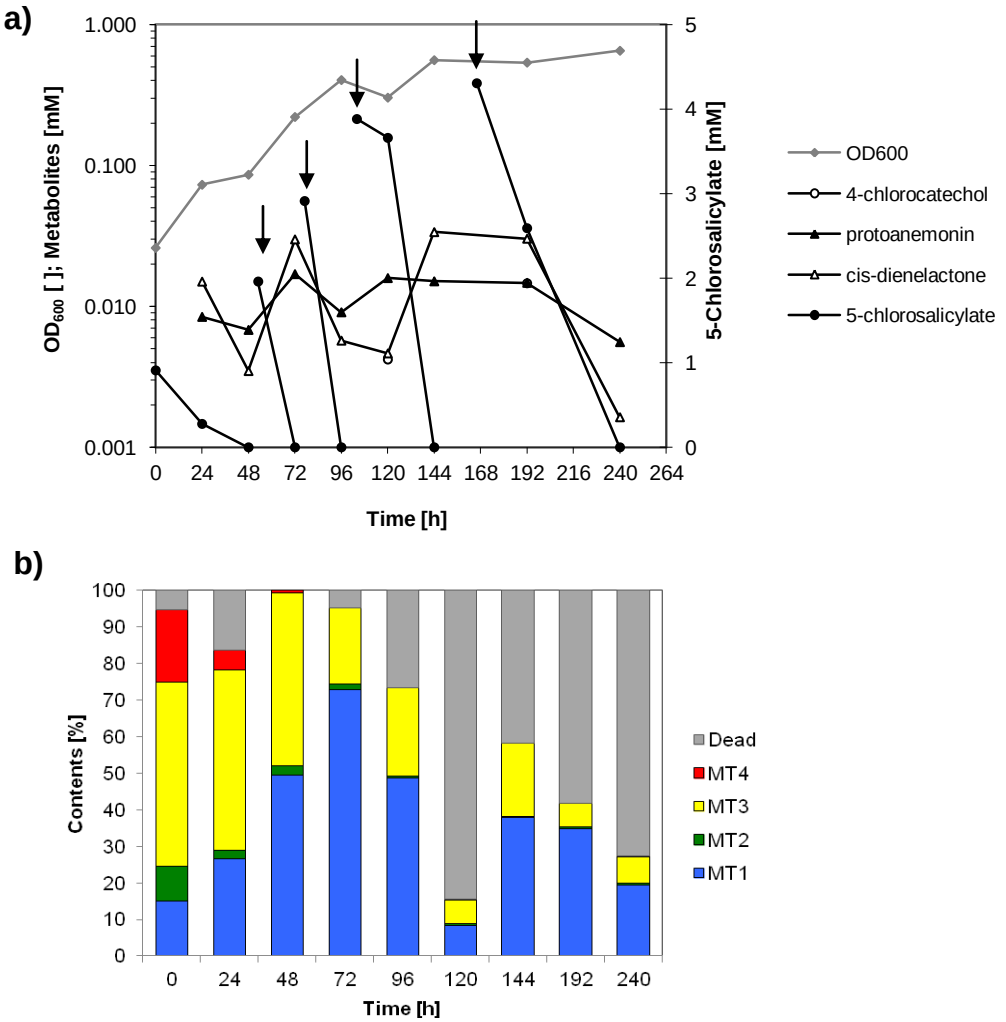

Figure 3.26. Degradation of 5-chlorosalicylate by the MT consortium in fed-batch mode: (**a**) concentration of substrate and metabolites; (**b**) consortium structure dynamics over time. Arrows on the graph indicate time points when the culture was fed with 5-CS.

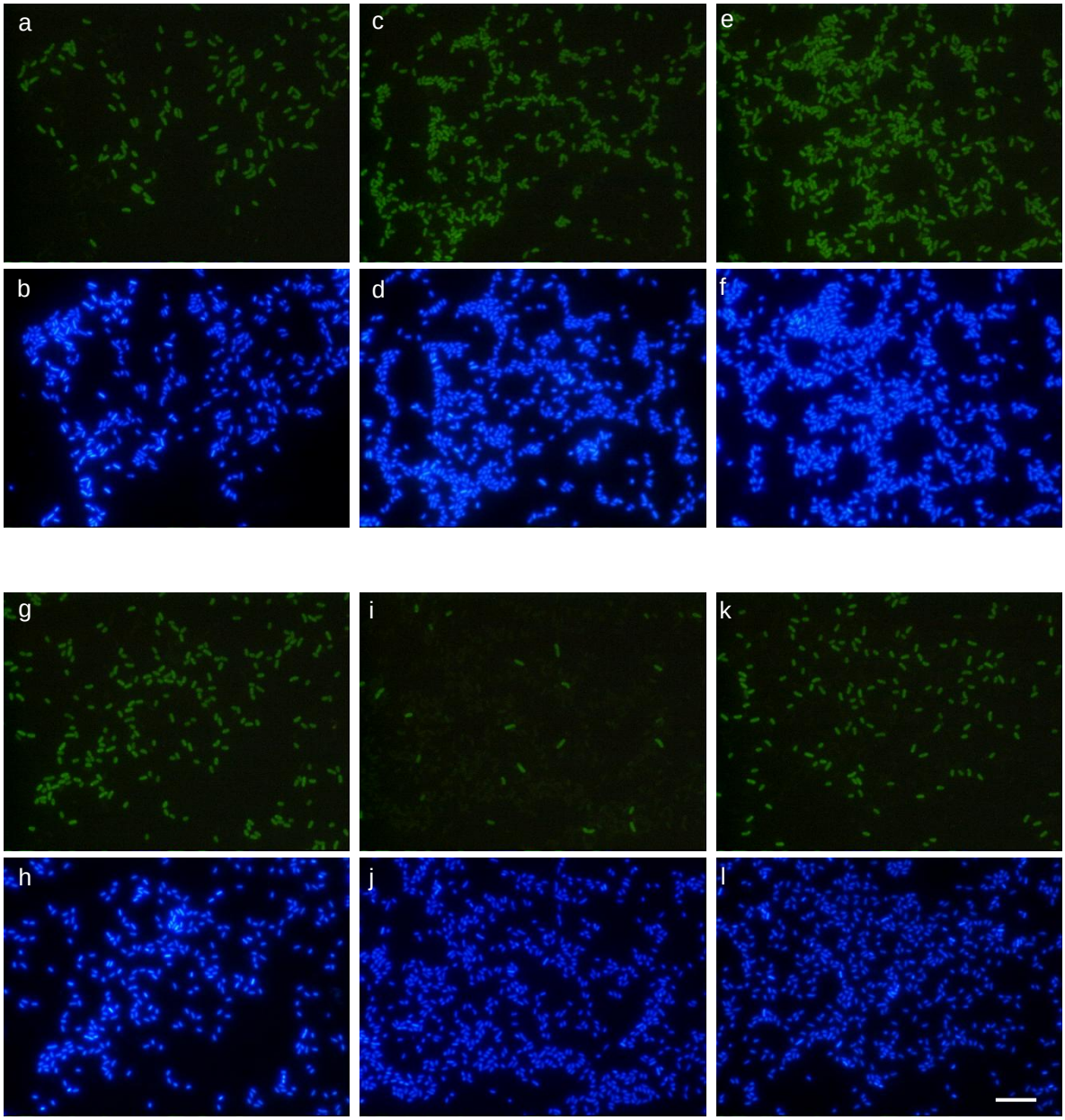

Figure 3.27. Microscopic images of F*IS*H-labeled cells of *P. reinekei* MT1 in the 5-CS grown consortium. Panels: **(a-b)** after 24 h; **(c-d)** after 48 h; **(e-f)** after 72 h; **(g-h)** after 96 h; **(i-j)** after 120 h; **(k-l)** after 144 h. MT1 cells stained with F*IS*H probe depicted in the panels **a**, **c**, **e**, **g**, **i**, and **k**. Total bacteria counterstained with DAPI presented in the panels **b**, **d**, **f**, **h**, **j**, and **l**. The bar represents 10 µm.

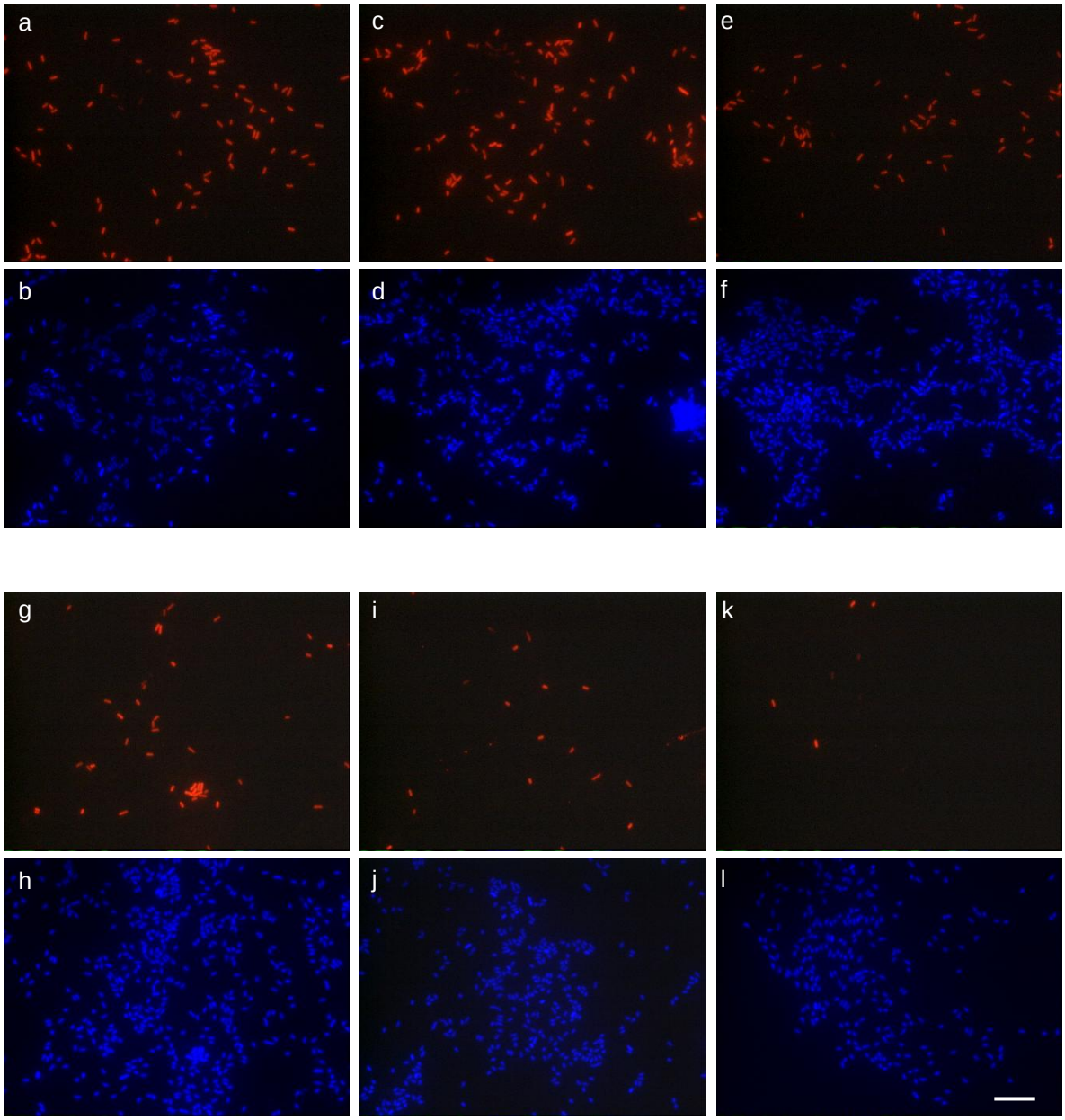

Figure 3.28. Microscopic images of F*IS*H-labeled cells of *E. brevis* MT2 in the 5-CS grown consortium. Panels: **(a-b)** after 24 h; **(c-d)** after 48 h; **(e-f)** after 72 h; **(g-h)** after 96 h; **(i-j)** after 120 h; **(k-l)** after 144 h. F*IS*H-stained MT2 cells depicted in the panels **a**, **c**, **e**, **g**, **i**, and **k**. Total bacteria counterstained with DAPI presented in the panels **b**, **d**, **f**, **h**, **j**, and **l**. The bar represents 10 µm.

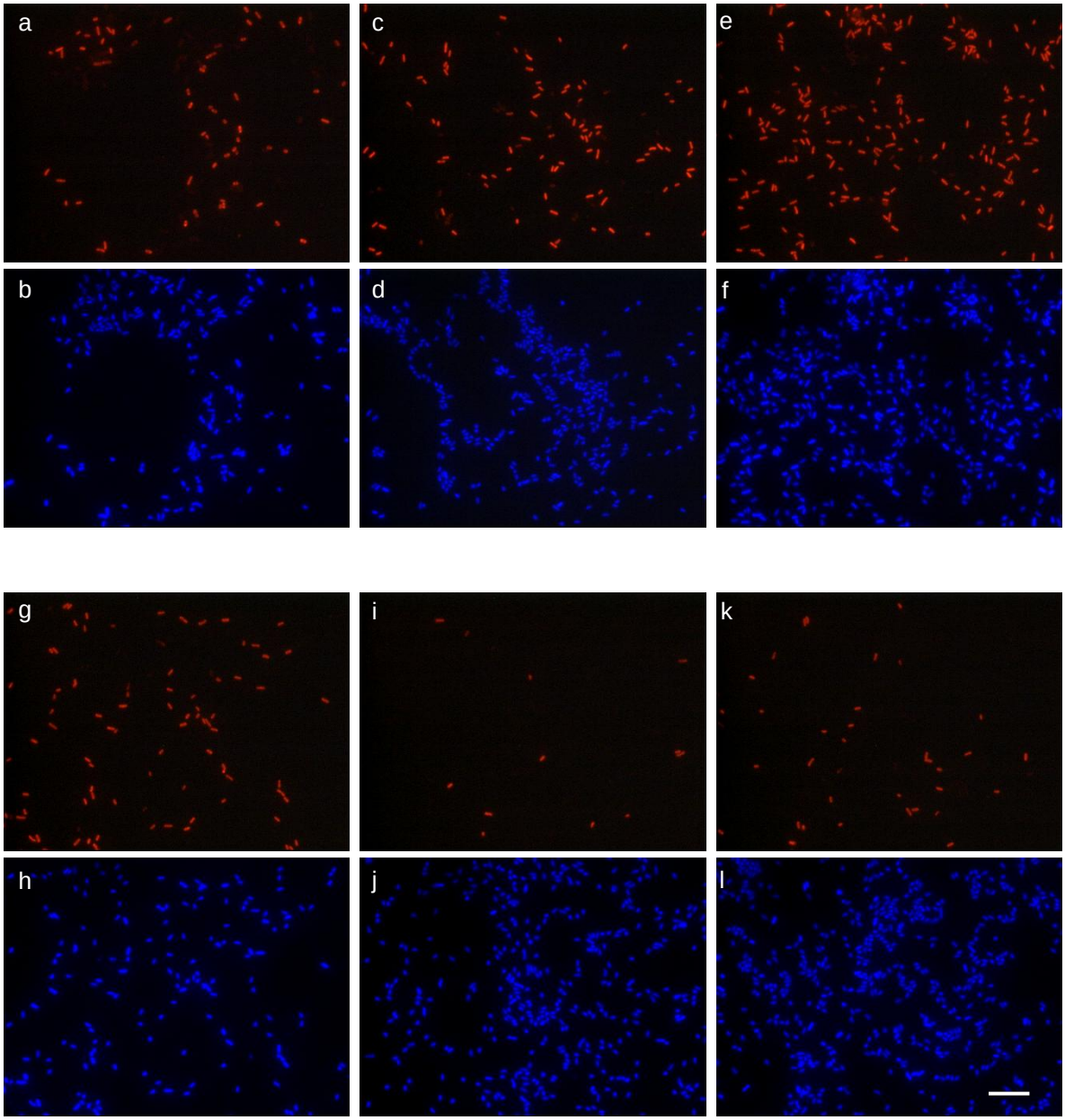

Figure 3.29. Microscopic images of F*IS*H-labeled cells of *A. xylosoxidans* MT3 in the 5-CS grown consortium. Panels: **(a-b)** after 24 h; **(c-d)** after 48 h; **(e-f)** after 72 h; **(g-h)** after 96 h; **(i-j)** after 120 h; **(k-l)** after 144 h. MT3 cells after F*IS*H-staining depicted in the panels **a**, **c**, **e**, **g**, **i**, and **k**. Total bacteria counterstained with DAPI presented in the panels **b**, **d**, **f**, **h**, **j**, and **l**. The bar represents 10µm.

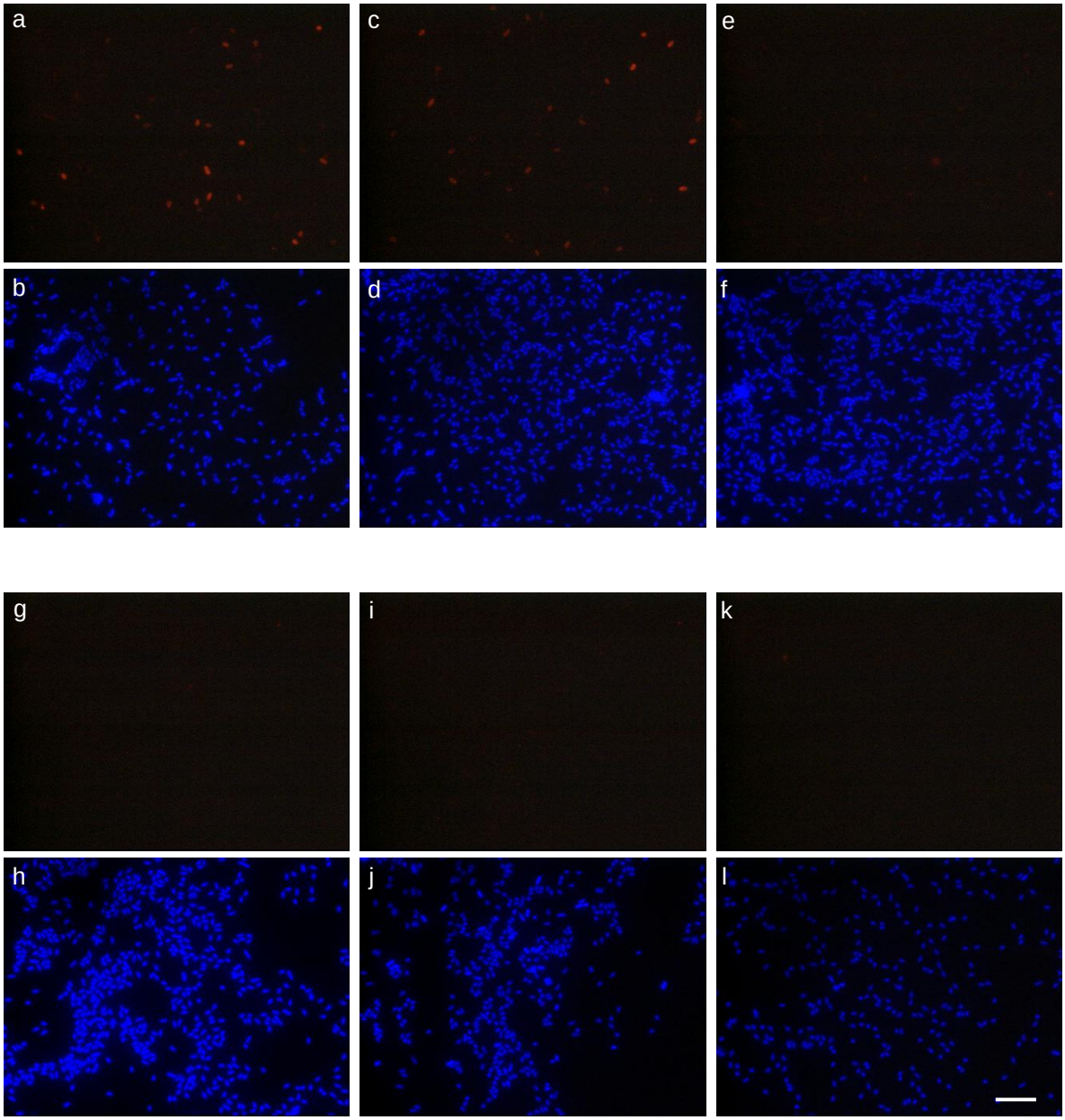

Figure 3.30. Microscopic images of F*IS*H-labeled cells of *P. veronii* MT4 in the 5-CS grown consortium. Panels: **(a-b)** after 24 h; **(c-d)** after 48 h; **(e-f)** after 72 h; **(g-h)** after 96 h; **(i-j)** after 120 h; **(k-l)** after 144 h. MT4 cells stained with F*IS*H probe depicted in the panels **a**, **c**, **e**, **g**, **i**, and **k**. Total bacteria counterstained with DAPI presented in the panels **b**, **d**, **f**, **h**, **j**, and **l**. The bar represents 10 µm.

The MT consortium grew on 5-CS with a maximum specific growth rate of $\mu = 0{,}05\ h^{-1}$ that is almost twice as fast as with 4-CS as substrate ($\mu = 0{,}028\ h^{-1}$) but still much slower than the previously reported value of $0{,}16\ h^{-1}$ recorded for a pure culture of MT1 growing on 5-CS (Nikodem *et al.*, 2003). The fact that bacteria in the inoculum were not adapted to chlorinated substrate could be the reason for observed relatively low growth rate of the consortium. The maximum 5-CS degradation rate recorded during the course of experiment equalled to 0,67 mM/h·unit of OD_{600} and was nearly twice as high as the rate of 0,35 mM/h·unit of OD_{600} observed for 4-CS degradation under identical conditions. Addition of 4 mM of 5-chlorosalicylate slightly perturbed the degradative activity as indicated by a decrease in the degradation rate. Degradation of every portion of 5-CS was accompanied by peaks of accumulating protoanemonin (up to 12 μM) and *cis*-dienelactone (up to 31 μM). 4-Chlorocatechol (3 μM) could only be detected at minor concentrations after the culture was fed with 4 mM of 5-CS where its presence coincided with the observed decrease in the degradative activity of consortium.

In terms of its quantitative structure, MT consortium evolved during cultivation on 5-CS in the fed-batch mode (Fig. 3.26b). For instance, the initial 15% share of MT1 in the community increased up to 73% after 72 h of incubation. The temporary disruption of the degradative activity of the consortium was reflected by a drop in the content of MT1 to 8% of total bacteria. When the culture resumed its degradative activity the content of MT1 increased again to the level of 38% of all bacteria. These oscillations could have also been seen in the sequence of microphotographs (Fig. 3.27).

MT3 accounted for approx. 50% of total bacteria in the inoculating material but its content in the consortium gradually decreased to 24% during the first 96 h of incubation. Nevertheless, in the consortium showing degradative activity towards 5-CS this strain was the second most abundant member, similarly to that observed during growth on 4-CS. High loads of 5-CS (4 mM) affected the content of MT3 in the community that was reduced to 7% after 120 h but not to the extent recorded for MT1. Similarly as in the case of MT1, the number of MT3 cells was on the increase when the consortium resumed its degradative activity (Fig. 3.26b and Fig. 3.29).

The population of MT4 accounted for 20% of total bacteria in the inoculum and decreased rapidly to the value below 1% after 48 h and remained on the level of 0,1-0,2% during the whole course of experiment (Fig. 3.30). The content of MT2 in the consortium diminished likewise but in the less severe fashion from 9% in the inoculum to 2% after 72 h and to 0,5% for the rest of experiment (Fig. 3.26b and Fig. 3.28).

Comparison of growth rates of the MT consortium cultivated on 4-CS and 5-CS shows that the latter substrate is by far the preferred one. This agrees with the data for the pure culture of MT1 that grew on 5-CS with a rate of 0,16 h^{-1}, more than three times higher than 0,05 h^{-1} measured during growth on 4-CS (Nikodem *et al.*, 2003). Taking into account that similar k_{cat} values were observed for the transformation of 4-CS and 5-CS by salicylate hydroxylase, it seems that cultivation on 5-CS resulted in a more efficient and more balanced expression of catabolic enzymes. These in turn led to the faster growth, but also to the excretion of notably lower levels of 4-chlorocatechol into the medium.

3.5.2.3. Growth of the RW consortium on 4-chlorosalicylate

Some chlorosalicylate degrading bacteria have been described in the literature, and typically, they degrade chlorosalicylates *via* chlorocatechols and a chlorocatechol pathway (Rubio *et al.*, 1986, Schindowski *et al.*, 1991). As described above, *P. reinekei* MT1 harbours a novel route of chlorosalicylate degradation, where auxiliary organisms such as *E. brevis* MT2, *A. xylosoxidans* MT3 and *P. veronii* MT4 are supporting the performance of MT1. *P. moorei* strain RW10 was isolated from an enrichment culture using 3-chlorodibenzofuran as carbon source (Wittich *et al.*, 1999). Like MT1, RW10 is capable of utilizing 4- or 5-chlorosalicylate without involvement of the chlorocatechol pathway, probably by a metabolic route similar to the one elucidated in MT1. Here it was thus verified, in how far *P. moorei* RW10 can replace MT1 in the community.

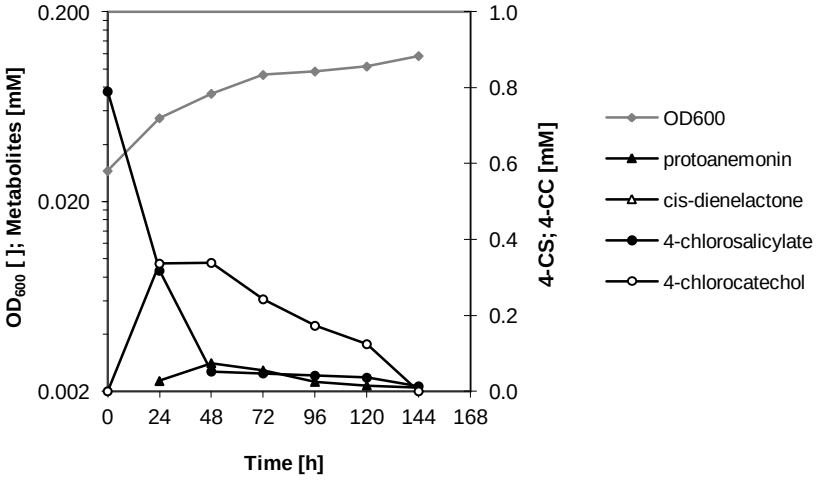

Figure 3.31. Degradation of 4-chlorosalicylate by the RW consortium.

Inoculating material for this experiment was prepared as previously described (3.5.2.1.) with individual strains grown in mineral medium on 8 mM acetate as sole carbon source at

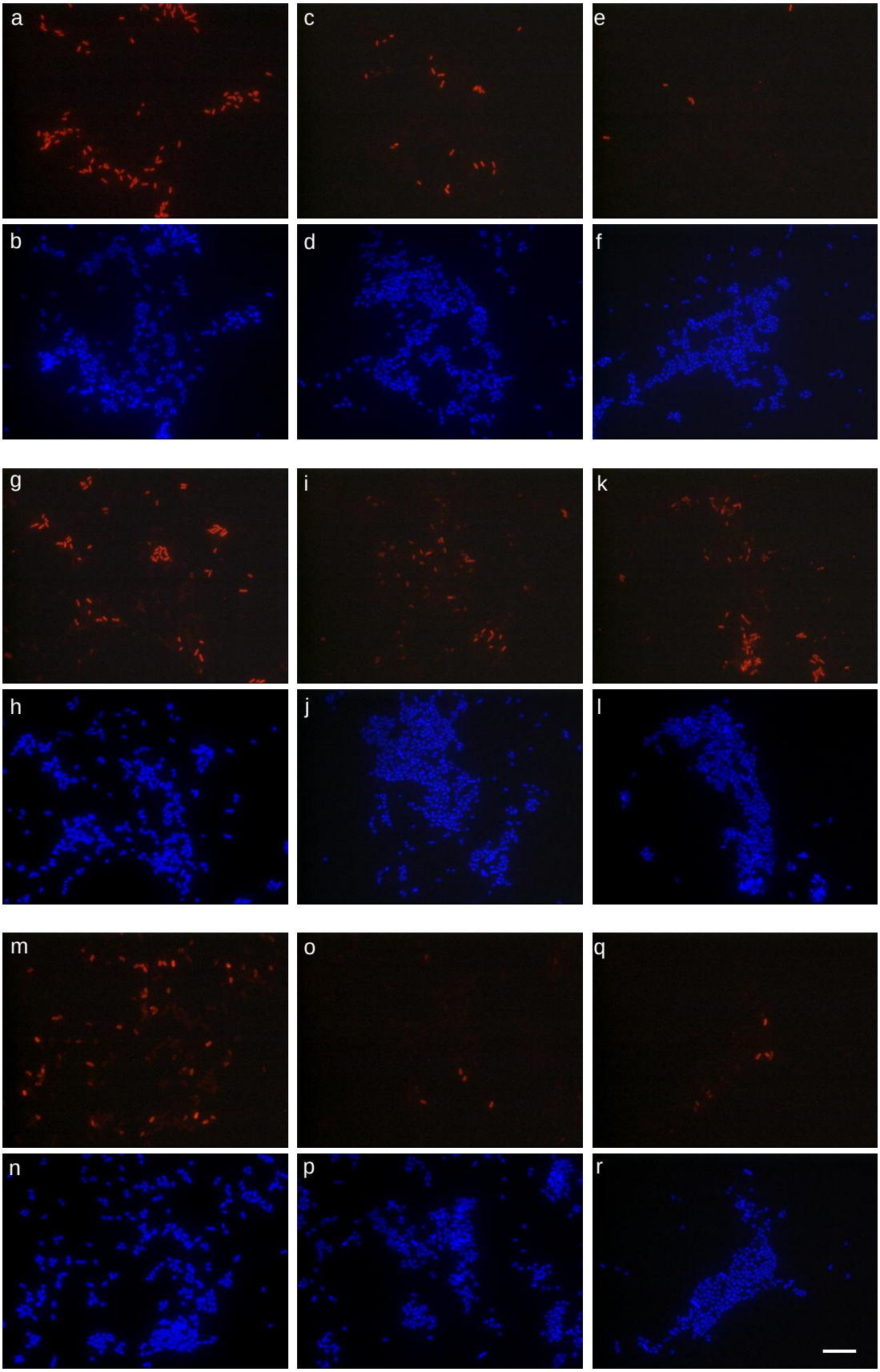

Figure 3.32. Microscopic images of F*IS*H-labeled *E. brevis* MT2 (**a-f**), *A. xylosoxidans* MT3 (**g-l**) and *P. veronii* MT4 (**m-r**) in the RW consortium degrading 4-CS after 24 h (**a-b, g-h, m-n**), after 72 h (**c-d, i-j, o-p**) and after 144 h (**e-f, k-l, q-r**) of incubation. The bar represents 10 µm.

30ºC to the late exponential phase. The cultures of *P. moorei* RW10, MT2, MT3 and MT4 were combined in a volumetric ratio of 1:1:1:1 and cultivated in the mineral medium containing 1 mM of 4-CS at 30ºC on the orbital shaker (120 rpm). The growth of the biomass was determined by measuring the optical density and the concentration of 4-CS and metabolites was measured by HPLC (Fig. 3.31). The rate of 4-CS degradation by the consortium was calculated from the depletion of substrate in the unit of time per OD_{600} unit of biomass. Presence of MT2, MT3 and MT4 in the community was analysed by F*IS*H and microscopic observations (Fig. 3.32).

The RW consortium grew on 4-chlorosalicylate with a specific growth rate of 0,027 h^{-1} that is almost equal to the growth rate of 0,028 h^{-1} determined for the MT consortium under identical conditions. The maximum 4-CS degradation rate of 0,47 mM/h·unit of OD_{600} was slightly higher in case of RW community than 0,35 mM/h·unit of OD_{600} for the MT community. However, growth on 4-CS of the RW consortium resulted in the accumulation of higher amounts of 4-chlorocatechol in the culture medium (338 µM) compared to the MT community (6 µM). In addition to 4-chlorocatechol, the RW consortium accumulated protoanemonin (up to 3 µM) and *cis*-dienelactone (up to 2 µM) at similar concentrations as the MT consortium. This metabolite profile observed during degradation of 4-CS by the RW community supports the view that *P. moorei* RW10 breaks down chlorosalicylates *via* a pathway similar to the one observed in MT1.

All three members of the original MT consortium – MT2, MT3 and MT4 coexisted with strain RW10 in the new RW community when grown on 4-CS in batch culture. From the microscopic analysis it seems that, like in the original MT consortium, the share of MT3 remained relatively stable during the entire period of cultivation (Fig. 3.32g-l) while the content of MT2 (Fig. 3.32a-f) and MT4 (Fig. 3.32q-r) decreased over time.

In the RW consortium *P. moorei* RW10 not only successfully took over the function of 4-CS degradation from MT1 but it also proved to be capable to form a community with strains MT2, MT3 and MT4 at least for the short time of the cultivation experiment.

3.5.2.4. Growth of the RW consortium on 5-chlorosalicylate in fed-batch culture

The mixture of RW10, MT2, MT3 and MT4 prepared as described previously (3.5.2.3.) was used as inoculum for cultivating the RW community on 1 mM 5-CS at 30ºC on the orbital shaker (120 rpm). After depletion of the substrate, the culture was successively supplemented with increasing doses of 5-CS (2 mM, 3 mM, and 4 mM). Bacterial growth was measured as the increase of the optical density and the concentration of both substrate and metabolites were measured by HPLC (Fig. 3.33). The 5-CS degradation rate was calculated from the depletion of substrate per unit of time per OD_{600} unit of biomass. The presence of MT2, MT3 and MT4 was observed using F*IS*H and epifluorescent microscopy (Fig. 3.34).

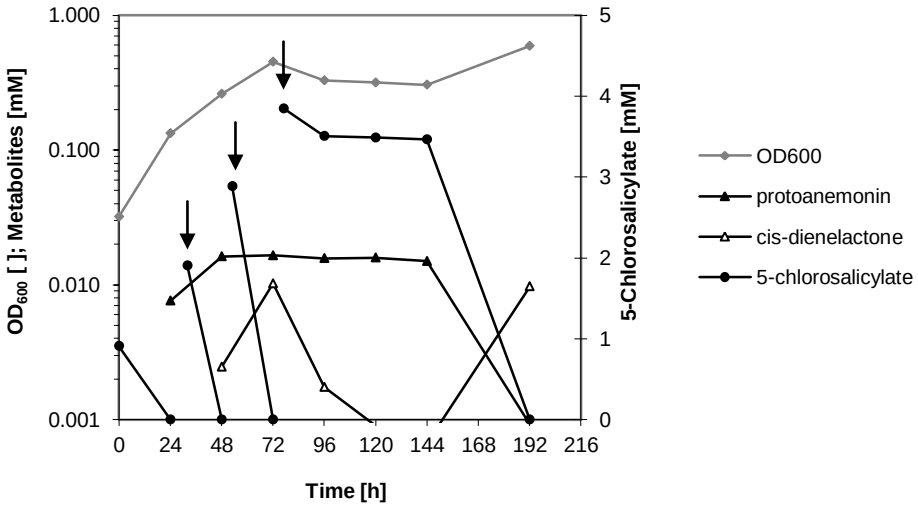

Figure 3.33. Degradation of 5-chlorosalicylate by the RW consortium in fed-batch mode. Arrows on the graph indicate time points when the culture was fed with 5-CS.

With a specific growth rate $\mu = 0{,}059\ h^{-1}$ the RW consortium grew on 5-CS twice as fast as on the 4-CS ($\mu = 0{,}027\ h^{-1}$). However, this growth rate was similar to that of the MT consortium under identical conditions ($\mu = 0{,}050\ h^{-1}$ see: 3.5.2.2.). The 5-CS degradation rate by the RW consortium was 0,60 mM/h·unit of OD_{600} and, thus, higher than the rate of 4-CS degradation (0,47 mM/h·unit of OD_{600}) but similar to the 5-CS degradation rate by the MT consortium (0,67 mM/h·unit of OD_{600}). The profile of metabolites that accumulated in the medium during 5-CS breakdown by the RW community was also similar to the one observed for the MT community with protoanemonin (up to 17 µM) and *cis*-dienelactone (up to 10 µM) as the only compounds detected. Feeding the RW consortium culture with high doses of 5-CS (4 mM) resulted, as observed for the MT consortium, in interrupted degradation. However, following 72 h of lag phase, the community resumed its degradative activity.

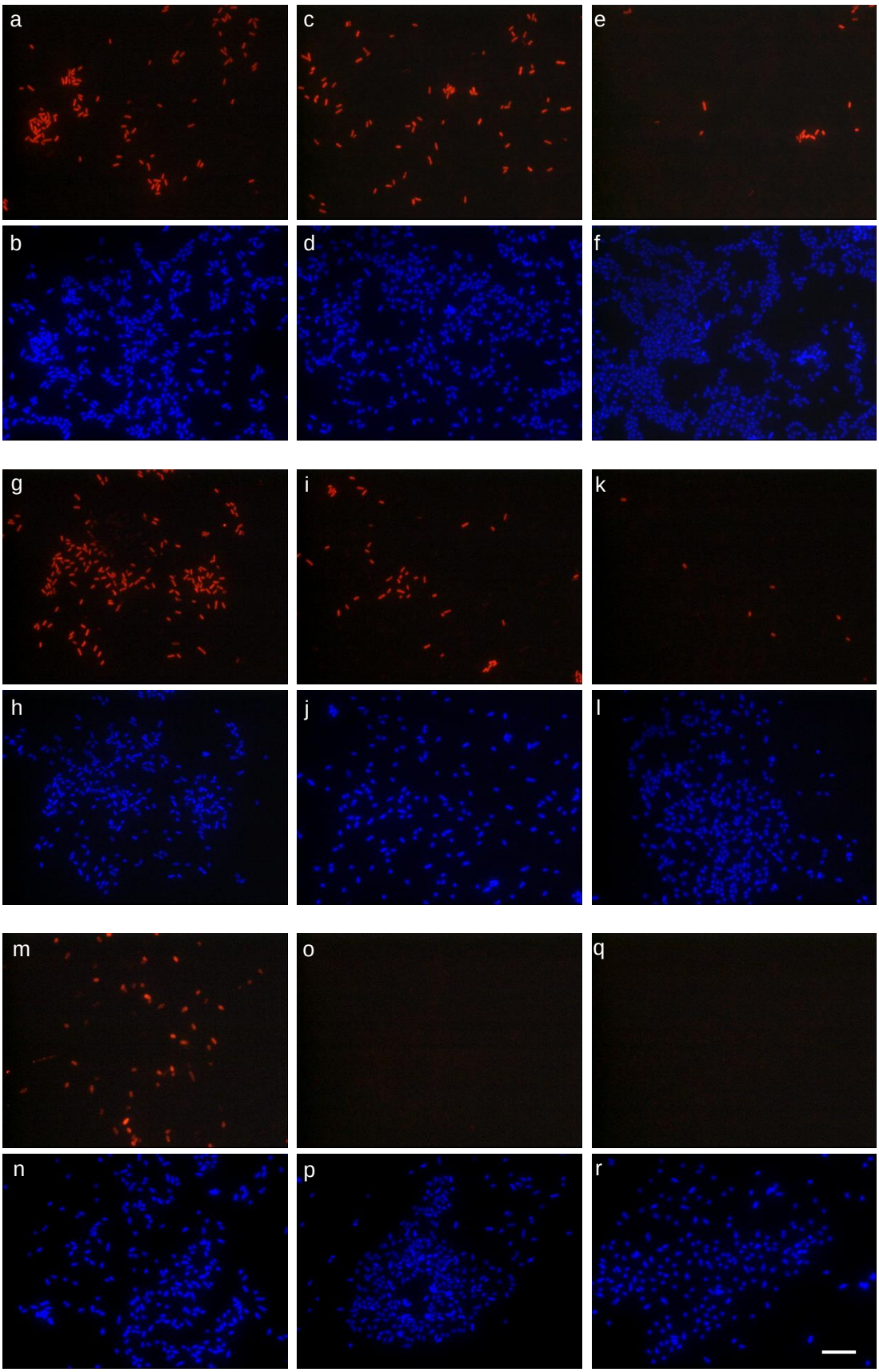

Figure 3.34. Microscopic images of F*IS*H-labeled cells of *E. brevis* MT2 (**a-f**), *A. xylosoxidans* MT3 (**g-l**) and *P. veronii* MT4 (**m-r**) in the RW concortium grown on 5-CS after 24 h (**a-b, g-h, m-n**), after 72 h (**c-d, i-j, o-p**) and after 144 h (**e-f, k-l, q-r**) of incubation. The bar represents 10 µm.

Strains MT2, MT3 and MT4 in the RW community during growth on 5-CS behaved in a similar manner as in the MT consortium (Figs. 3.30-3.32). The relative abundance of MT2 and MT3 in the mixed culture showed a strong tendency to decrease over time while the initially abundant population of MT4 fell below the detection limit of 0,1% (Fig. 3.34) after 48 h of cultivation.

Comparison of the MT and RW consortia, which differed only in the chlorosalicylate degrading strain, showed close similarities in substrate degradation rates, profiles of accumulating metabolites, and population dynamics of the three auxiliary strains (MT2, MT3 and MT4). These may be indicative of similar interspecies interactions in both consortia. However, the ability of MT2, MT3 and MT4 to form a bacterial community with chlorosalicylate degraders like MT1 and RW10 might depend on the utilization of the specific catabolic pathway for breakdown of 4-CS and 5-CS by those strains. Thus, it would be interesting to test if and how MT2, MT3 and MT4 strains could coexist in a community with other chlorosalicylate degrading bacteria that use different routes for mineralization of substrate, such as with *Pseudomonas* sp. WR4016 that degrades 4-CS *via ortho*-cleavage and a subsequent chlorocatechol pathway (Rubio *et al.*, 1986).

3.5.3. Perturbations of the consortium grown on 4-chlorosalicylate in the chemostat

The continuous consortium culture described in detail in 3.4.1. was subjected to a series of perturbations which included alterations in the dilution rate and transient anaerobiosis. Responses of the consortium to the applied perturbations were followed by monitoring optical density of the culture (biomass), concentration of 4-CS and metabolites in the culture supernatant and the composition of the bacterial community.

3.5.3.1. Response of the consortium growing on 4-chlorosalicylate in the chemostat to an increased dilution rate

The content of biomass in a continuous culture is proportional to the amount of substrate provided into the chemostat vessel, if the dilution rate remains below the maximum growth rate of the cells (μ_{max}). A step-wise increase of the dilution rate was performed in order to achieve specific growth rates of the consortium close to the μ_{max} and to identify bottlenecks of 4-CS degradation by following metabolites that accumulate in the medium (Fig. 3.35a). Responses of individual subpopulations within the consortium to such an increase in the dilution rate were analysed by monitoring the community composition of the mixed culture (Fig. 3.35b).

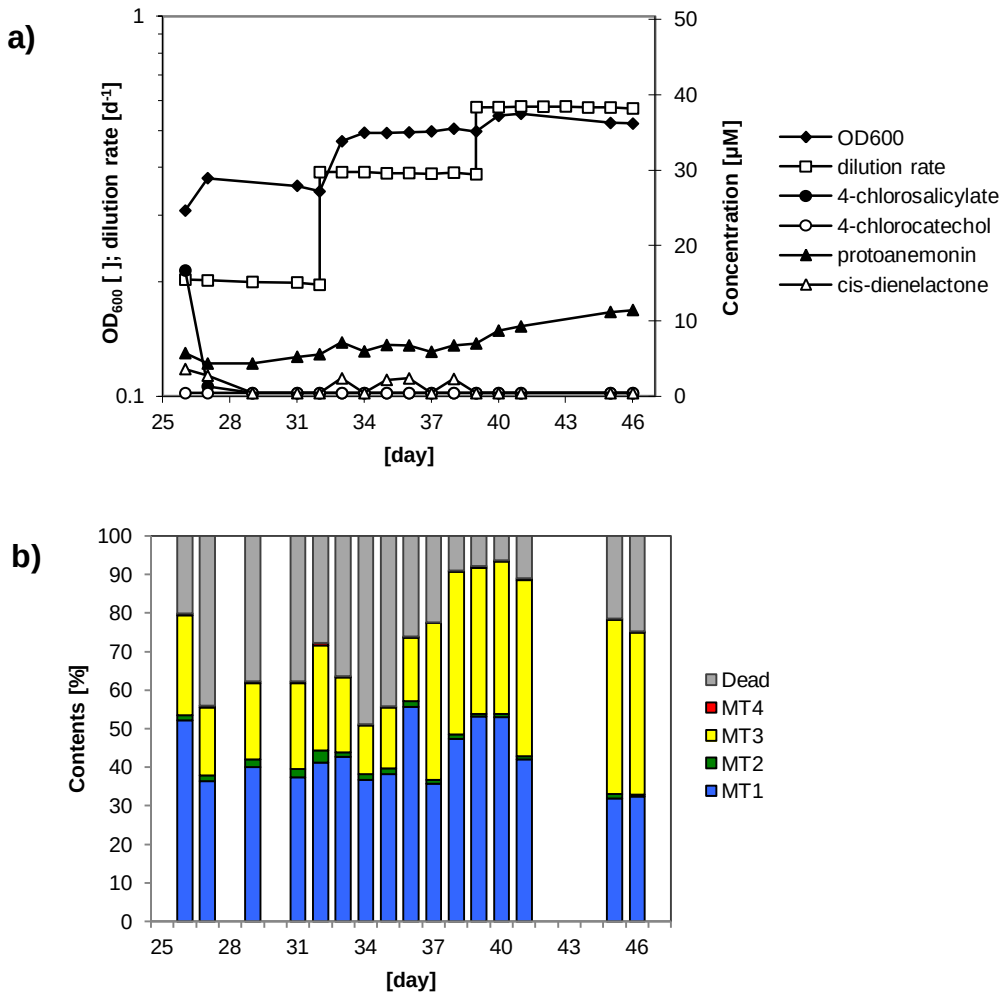

Figure 3.35. Response of the 4-CS degrading consortium to increased dilution rates: (**a**) dilution rate, optical density and metabolite profile; (**b**) community structure.

The consortium culture was capable of growing at dilution rates of at least up to 0,6 d^{-1} (10 mM of 4-CS). Depletion of 4-CS was complete at all three dilution rates tested (0,2; 0,4 and 0,6 d^{-1}). Protoanemonin was identified as the major accumulating metabolite. Its concentration was positively correlated with dilution rate and increased from 4-5 µM at 0,2 d^{-1} to 6-7 µM at 0,4 d^{-1} and to 8-11 µM at 0,6 d^{-1}. The concentration of *cis*-dienelactone remained low at all dilution rates and has never exceeded 3 µM.

Unexpectedly, the optical density of the culture increased with an increased dilution rate from 0,308-0,375 at 0,2 d^{-1} to 0,469-0,506 at 0,4 d^{-1} and then to 0,522-0,554 at 0,6 d^{-1}. This observation contradicts the theoretical principle of the chemostat where the biomass in the vessel should increase with increasing concentration of growth-limiting substrate in the medium but not with an increased dilution rate.

However, the dilution rate in the 4-chlorosalicylate supplied chemostat clearly influenced also the consortium structure (Fig. 3.35b). At a dilution rate of 0,2 d^{-1} MT1 was the dominant

member of consortium while cultivation at 0,4 d^{-1} resulted in approximately similar numbers of MT1 and MT3 in the community. After a further increase in the dilution rate to 0,6 d^{-1} MT3 became the predominant member of the consortium. The increase in the optical density observed for higher dilution rates seems, thus, to be correlated with an increased relative abundance of MT3. It may, therefore be speculated, that at higher dilution rates, a majority of substrate, processed by MT1 is further metabolized by MT3, and that MT3 is capable of more effectively using the processed substrate. However, if such cross-feeding occurs, as previously suggested, at the stage of 4-chlorocatechol (Pelz ez al., 1999), or at the stage of *cis*-dienelactone, where indications have been accumulated in the current work, remains to be elucidated.

As for MT1, the relative abundance of MT4 has also decreased with increasing dilution rate. Interestingly, the decrease in abundance of MT4 correlates with an increase in the concentration of protoanemonin, where MT4 was previously assumed to feed on (Pelz *et al.*, 1999), and may indicate the failure of MT4 to deal adequately with even low concentrations of this compound.

3.5.3.2. Response of consortium grown in 4-CS-fed chemostat to disrupted aeration

Insufficient aeration is known to impede many bioremediation processes that occurr in the environment. Oxygen is necessary for bacteria in the 4-chlorosalicylate degrading consortium as a terminal acceptor of electrons in respiration but specifically as substrate for oxidative reactions in the breakdown of the substrate. The importance of oxygen for the consortium and its 4-CS-degrading activity was tested by disrupting aeration in the chemostat culture for a period of 1-3 h. After the air-flow through the reactor vessel was reinstalled, the response of the consortium to the perturbation was followed on the level of its biomass, degradative activity and microbial composition (Fig. 3.36.). The dilution rate of the continuous culture was reduced in the post-stress period proportionally to the severity of the observed symptoms so as to minimise the probability of an irreversible breakdown and to ensure recovery of the culture.

Interrupted aeration over a period of 3 h (Fig. 3.36a-c) triggered a powerful response of the consortium. The optical density after the first day was reduced from 0,522 to 0,202, that is lower than the value of 0,357 calculated assuming wash-out of non-growing bacteria. Degradation of 4-CS by the consortium obviously stopped immediately in response to oxygen-limiting conditions (Fig. 3.36b) and after one day of anaerobiosis, 3,45 mM of 4-CS accumulated in the medium. This value is lower than theoretically calculated 4,23 mM for assumed complete lack of degradative activity. The oxygen supplied after resuming the

aeration was mainly used to transform part of the supplied 4-CS to 4-chlorocatechol (373 μM), the autoxidation of which resulted in a dark brown coloration of the medium. Only part of intermediate 4-chlorocatechol was obviously transformed further, as indicated by the slightly increasing amounts of protoanemonin and *cis*-dienelactone. After one day, the dilution rate was significantly reduced and the consortium resumed its full 4-CS degradative activity only after all accumulated 4-chlorocatechol was removed from the medium.

The 3 h-long period of anaerobiosis acted detrimentally predominantly towards MT1. The relative abundance of this strain in the consortium declined from 43% to 2,6% of viable bacteria. The interrupted aeration had similar effect on the content of MT4 that decreased from average 0,31% to 0,18% of viable bacteria. In contrast, the content of MT2, that is probably living on cellular debris that became more abundant as a result of perturbation, increased from from 0,75% to 6,3% of active cells in the community. Whereas the interrupted aeration exerted a significant negative effect on the viability of MT1, which is probably due to the toxic effect of accumulating 4-chlorocatechol, the total number of viable MT3 cells remained constant, and only declined slightly during the exposition to 4-chlorocatechol. Consequently, the relative abundance of MT3 among the viable bacteria increased from 56% to 96%. Although the alterations observed in the consortium structure were tremendous, they were at least partially reversible when the 4-chlorocatechol was washed out from the medium. When the oxygen supply was reinstalled and the dilution rate reduced, the consortium culture was capable to recover from stress. A new steady-state after recovery was indicated by the complete removal of accumulated 4-CS, 4-chlorocatechol and *cis*-dienelactone from the medium and a stabilized optical density.

In case of a period of anaerobiosis lasting for only 1 h, the overall response of the consortium was very similar (Fig. 3.36d-f) and included a reduction in the optical density (from 0,348 to 0,148) exceeding the wash-out rate, a period of ceased 4-CS degrading activity, accumulation of metabolites and shifts in the community structure similar to those described above.

Short periods of oxygen limitation in the 4-chlorosalicylate-fed chemostat affected both the degradative activity and the microbial structure of the consortium. The consortium, however, showed a remarkable capacity to restore its functional and structural characteristic after the aerobic conditions were reinstated. Perhaps this feature enables the consortium to compete successfully with other indigenous microorganisms in a natural habitat.

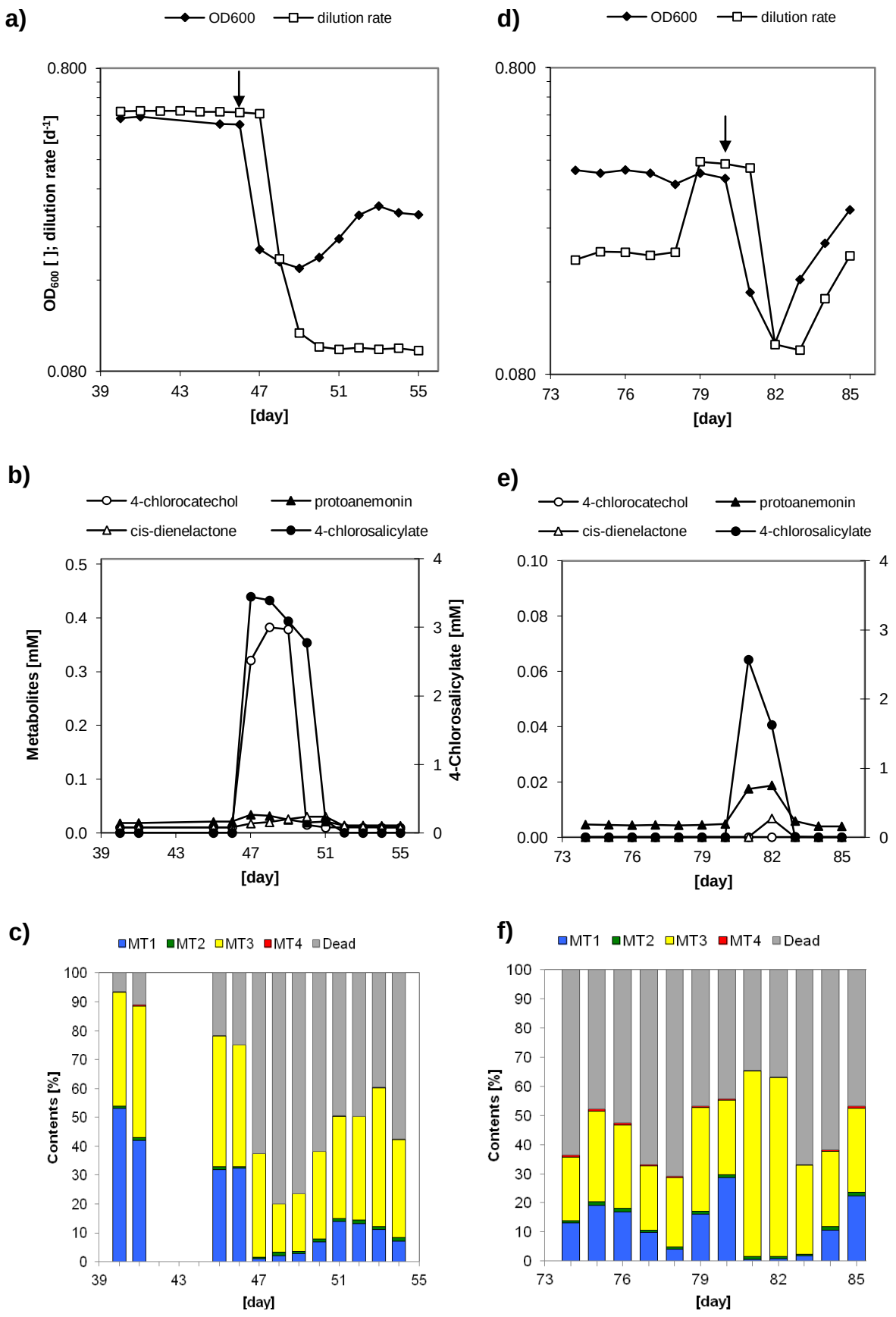

Figure 3.36. Effect of a 3 h-long **(a-c)** and a 1 h-long **(d-f)** anaerobiosis on the chemostat consortium culture: **(a** and **d)** dilution rate and cellular density, **(b** and **e)** concentration of substrate and metabolites, **(c** and **f)** consortium structure.

4. DISCUSSION

Until very recently microbial communities from the environment were often treated as useful catalytic 'black boxes' e.g. in the processes of bioremediation or bioleaching. Characterisation of these complex systems was frequently restricted to describing their taxonomic diversity and sometimes their quantitative structure. Consortia or communities that could be cultivated in the laboratory conditions were often seen as a curiosity but with their usefulness limited to providing complex biological material that display the desired physiological or enzymatic potential. Recent advances in molecular biology methods and especially in the development of genomics, transcriptomics, proteomics and metabolomics resulted in focusing more attention on understanding how these complex microbial systems really work. This knowledge on the functioning of microbial communities will not only contribute to a better understanding of various ecosystems but will also provide rational guidelines for designing mixed cultures with potential usefulness in the processes of bioremediation.

In this work, a 4-CS-degrading bacterial community was studied with the main aim of characterising its responses to abiotic perturbations likely to occurr in the environment. The first part of the study focused on gaining basic information on the physiology, biochemistry and genetics of individual consortium strains. In the second part, a series of experiments were carried out that included cultivating bacteria in various mixed culture set-ups as well as following responses of the consortium culture to different temperature condition, altered supply of substrate and periodic anaerobiosis. On the basis of collected evidence 'a portrait' of the 4-CS-degrading consortium might be drawn, that, although imperfect, may serve as a framework to understand how this particular mixed culture functions under environmental conditions.

4.1. Metabolic potential of individual consortium strains

Simple growth tests in mineral medium with a range of compounds used as sole source of carbon and energy may provide indications about physiological capabilities of a microorganism, although they are not fully informative about the involved pathways.

P. reinekei MT1 was shown to grow at the expense of benzoate, salicylate and protocatechuate but not gentisate. Out of two hitherto known pathways for aerobic degradation of benzoate that leads *via* catechol or alternatively *via* benzoyl-CoA, the first one

seems more likely to exist in MT1. Even though the corresponding Rieske non-heme iron benzoate dioxygenase that transforms benzoate into benzoate dihydrodiol (Reiner & Hegeman, 1971) has not yet been identified in this strain, the presence of catechol branch of 3-oxoadipate pathway for channeling this dihydroxylated intermediate is well known (Nikodem *et al.*, 2003). Additionally, a phylogenomic study of the microbial genomes revealed that the pathway for degradation of benzoate through its CoA-derivative is frequent in β-Proteobacteria but has not been found in any of the sequenced γ-Proteobacteria yet (Perez-Pantoja *et al.*, 2010b). On the other hand, genes for the mineralization of benzoate through its initial dioxygenation are relatively common in *Pseudomonadaceae* (Perez-Pantoja *et al.*, 2010b). Pseudomonads usually break down protocatechuate through intradiol ring-cleavage catalyzed by protocatechuate 3,4-dioxygenase leading to 3-carboxymuconate that is further channeled into the 3-oxoadipate pathway rather than through extradiol cleavage by protocatechuate 4,5-dioxygenase (Perez-Pantoja *et al.*, 2010b). As the whole *pca* gene cluster encoding the complete set of enzymes for the protocatechuate branch of 3-oxoadipate pathway has been identified in MT1 (see: 3.2.2.3.; Fig.3.11 & 3.14; Tab. 3.7), it is likely that this route is also used by strain MT1. Metabolism of salicylate by MT1 was characterised previously as involving a decarboxylating salicylate 1-hydroxylase yielding catechol, which is further metabolized through the catechol branch of the 3-oxoadipate pathway (Nikodem *et al.*, 2003; Camara *et al.*, 2007). Interestingly, neither salicylate 1-hydroxylase nor salicylate 5-hydroxylase encoding genes were found in any *Pseudomonas* genome sequenced up to date (Perez-Pantoja *et al.*, 2010b). However, numerous observations indicate that the degradation of salicylate by pseudomonads proceeds preferentially *via* catechol and subsequent intradiol ring-cleavage, such as in the napththalene-degrading *P. putida* PpG7 (Dunn & Gunsalus, 1973), in MT1 (Nikodem *et al.*, 2003) or in *P. moorei* RW10 (Pieper, personal comm.) rather than *via* gentisate.

A. xylosoxidans MT3 utilized benzoate, salicylate and gentisate as sole carbon and energy substrate but not protocatechuate. It seems likely that in this strain gentisate is the first intermediate of the salicylate degradation pathway and formed by a salicylate 5-hydroxylase as described for *Ralstonia* sp. U2 (Zhou *et al.*, 2002). In fact, phylogenomic analysis of aromatic degradation pathways in Burkholderiales revealed the presence of genes encoding salicylate 5-hydroxylases not only in many bacteria belonging to the *Commamonadaceae*, but also in two *Achromobacter* strains sequenced thus far (*Achromobacter piechaudii* ATCC43553 and *A. xylosooxidans* A8) (Pérez-Pantoja *et al.*, 2011). The presence of a gentisate 1,2-dioxygenase activity in MT3 is also in agreement with the observed relatively high frequency of this catabolic marker in β-proteobacterial genomes (Perez-Pantoja *et al.*,

2010b). Genes encoding benzoate dioxygenases are among members of the Burkholderiales (Perez-Pantoja *et al.*, 2011) only wide-spread in *Burkolderiaceae*, whereas out of the 8 *Alcaligenaceae* members, only *Bordetella petrii* has a homologue, and specifically, they are absent from both *Achromobacter* genomes sequenced thus far. In contrast, genes for the degradation of benzoate *via* benzoyl-CoA are present in six of the sequenced *Alcaligenaceae* genomes, and among them in both *Achromobacter* genomes. This may suggest that benzoate is degraded *via* benzoyl-CoA in MT3, however, the presence of this route in MT3 remains still to be elucidated.

P. veronii MT4 showed the capability to grow with benzoate and protocatechuate as sole carbon source but could not sustain its growth neither with salicylate nor gentisate. The presence of a protocatechuate degradation pathway in this strain is not surprising if one takes into account that genes encoding enzymes of this route are, among all 36 *Pseudomonas* strains sequenced so far, only absent from *Pseudomonas mendocina* ymp and *Pseudomonas* sp. UK4 (Perez-Pantoja *et al.*, 2010b). Similarly, as benzoate dioxygenase encoding genes are widespread in *Pseudomonas* strains (Perez-Pantoja *et al.*, 2010b) whereas genes encoding benzoyl-CoA oxygenase have not been observed in any of the thus far 36 sequenced *Pseudomonas* genomes, it is reasonable to assume that benzoate is degraded by strain MT4 *via* initial dioxygenation and catechol as central intermediate.

4.2. Genetics of the 4-chlorosalicylate degradation by consortium

Complete degradation of 4-chlorosalicylate by the MT consortium requires the action of numerous enzymes. Considerable effort was undertaken in order to identify genes involved in the 4-CS breakdown in the genomes of MT1, MT3 and MT4. The role of different gene clusters from strain MT1 in the breakdown of aromatic and chloroaromatic compounds is discussed below.

A gene cluster termed *mar* was discovered in the genome of MT4 and identified as encoding, among other proteins, enzymes responsible for the channeling hydroxybenzoquinol into the central metabolism. The presence of a hydroxybenzoquinol degradation pathway comprising the intradiol ring cleavage by a hydroxybenoquinol dioxygenase to maleylacetate followed by maleylacetate reductase catalyzed reduction to 3-oxoadipate was already observed in the genomes of various bacteria belonging to the *Pseudomonadaceae* although it is not common among the members of this family of γ-Proteobacteria (Perez-Pantoja *et al.*, 2010b).

Mining of the MT3 genome for enzymatic activities expressed from the phage library identified a putative *cis*-dienelactone hydrolase homologue. This finding was in accordance with enzyme activities detected in the cellular extract from this strain (Tab. 3.3.) and with the ability of MT3 to transform *cis*-dienelactone in the whole cell assay (Fig. 3.1). Unfortunately, due to the technical limitations of the screening procedure retrieval of its DNA sequence was not possible.

4.2.1. Degradation of salicylate and its derivatives by P. reinekei MT1 is encrypted by complex genetic system

P. reinekei MT1 is capable of degrading salicylate, 4- and 5-chlorosalicylate as well as 4- and 5-methylsalicylate. A search in the MT1 genome revealed that genes encoding enzymes involved in the breakdown of salicylate and its chloro-/methyl-derivatives are dispersed in several clusters. Further detailed and painstaking studies helped to associate particular genes or gene clusters with the degradation of different salicylate derivatives. A gene cluster encoding salicylate hydroxylase (*sal* cluster) initiating the degradation of various salicylates was initially observed in the course of the present work and further characterised by Camara *et al.* (2007). The gene cluster encodes also a catechol 1,2-dioxygenase ($C12O_{salD}$) and a muconate cycloisomerase (MCI_{salC}), which, despite being phylogenetically closely related to enzymes of *Pseudomonas* strains, are specifically adapted to the transformation of 4-methylcatechol and 3-methylmuconate, respectively. Both of these gene products are, when compared to archetype catechol 1,2-dioxygenases and muconate cycloisomerases, to a certain extent also adapted for the transformation of 4-chlorocatechol and 3-chloromuconate, respectively. However, like archetype muconate cycloisomerases, MCI_{salC} catalyzes the formation of predominantly 4-chloromuconolactone, which spontaneously decomposes to protoanemonin (Camara *et al.*, 2007, Nikodem *et al.*, 2003). Whereas the archetype *cat* gene cluster of *P. reinekei* MT1 encoding catechol 1,2-dioxygenase ($C12O_{catA}$), muconate cycloisomerase (MCI_{catB}) and muconolactone isomerase (MCI_{catC}) are not involved in the degradation of substituted salicylates, specific gene clusters encode enzymes necessary to process metabolites formed by the action of enzymes encoded by the *sal* cluster. Enzymes processing 4-methylmuconolactone, the cycloisomerization product of 3-methylmuconate are located in the *mml* cluster (Marin *et al.*, 2010). The *cca* gene cluster encodes, apart from a novel (chloro)catechol 1,2-dioxygenase, $C12O_{ccaA}$, a novel (chloro)muconate cycloisomerase, MCI_{ccaB}, which showed features not yet reported. This cycloisomerase, which was practically inactive with muconate, evolved for the turnover of 3-substituted muconates and transforms 3-chloromuconate into equal amounts of *cis*-dienelactone and protoanemonin, suggesting that

it is a functional intermediate between chloromuconate cycloisomerases and muconate cycloisomerases. Phylogenetic analysis showed that $C12O_{ccaA}$ and MCI_{ccaB} are only distantly related to previously described catechol 1,2-dioxygenases and muconate cycloisomerases. Kinetic analysis indicated that MCI_{ccaB} and $C12O_{salD}$, rather than $C12O_{ccaA}$, are crucial for 5-chlorosalicylate degradation. Genes encoding *trans*-dienelactone hydrolase (*ccaC*) preventing formation of protoanemonin by transforming intermediate 4-chloromuconolactone into maleylacetate, and a maleylacetate reductase (*ccaD*), are also encoded in the *cca* gene cluster. Thus, this region includes genes sufficient to enable MT1 to transform 4-chlorocatechol to 3-oxoadipate. However, compared to typical chlorocatechol 1,2-dioxygenases, neither $C12O_{salD}$ nor $C12O_{ccaA}$ were specifically adapted to 4-chlorocatechol turnover, suggesting the turnover of this intermediate as a possible bottleneck in the degradation. However, the most important enzymatic step in chlorosalicylate degradation by MT1 is the transformation of 3-chloromuconate. A sole action of MCI_{salC} would result in the formation of 4-chloromuconolactone followed by spontaneous decomposition to dead-end protoanemonin. Expression of *trans*-dienelactone hydrolase will prevent protoanemonin formation to a significant extent, by forming maleylacetate. However, expression of MCI_{ccaB} encoded in the same gene cluster as *trans*-dienelactone hydrolase not only allows a better flux through the pathway, but probably increases the formation of *cis*-dienelactone, which is a dead-end metabolite for MT1. Moreover, the ratio between 3-chloromuconate cycloisomerising and 4-chloromuconolactone transforming activities significantly determines the amount of spontaneous formation of protoanemonin. Thus, small difference in the expression of *sal* versus *cca* cluster encoded enzymes will significantly change the flux through the parallel pathways and the ratio by which dead-end intermediates are excreted.

Enzymes encoded by the described above *sal* and *cca* gene clusters allow the transformation of 4- and 5-chlorosalicylate to 3-oxoadipate. In this work, an additional gene cluster termed *pca* was identified encompassing genes encoding enzymes for the further metabolism of 3-oxoadipate, as well as genes encoding enzymes for transformation of protocatechuate to 3-oxoadipate, the so-called protocatechuate branch of the 3-oxoadipate pathway (Fig. 3.11, 3.12, Tab. 3.7).

Although the precise function of proteins encoded by *pca* genes has to be further elucidated several premises exist that indicate their possible involvement in the degradation of salicylate derivatives by strain MT1. First of all, some of the *pca*-encoded enzymes like carboxymuconate cycloisomerase and 3-oxoadipate:succinyl-CoA transferase were significantly overexpressed during growth of MT1 on 4-CS when compared to the growth on acetate (Bobadilla, 2006).

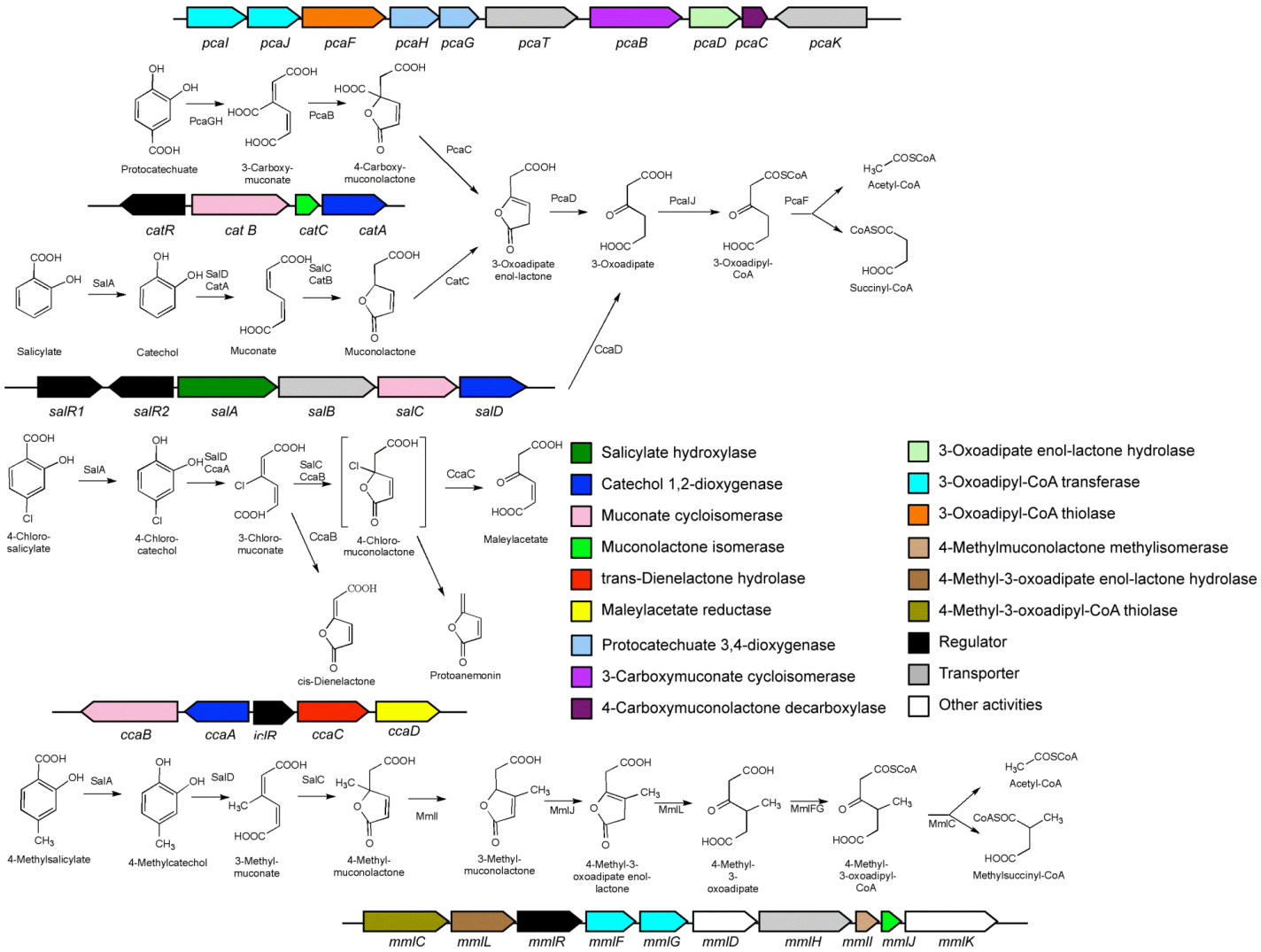

Figure 4.1. The role of proteins encoded in the *pca*, *cat*, *sal*, *cca*, and *mml* gene clusters in *P. reinekei* MT1 in the degradation of aromatic, chloroaromatic and methylaromatic compounds.

Second, the gene encoding 3-oxoadipate enol-lactone hydrolase, which is essential for both the catechol and protocatechuate branch of the 3-oxoadipate pathway, was found encoded within the *pca* cluster. Overall, the whole organization of the *pca* cluster is identical to that observed in *P. fluorescens* Pf01 and *P. fluorescens* Pf-5, with the exception of the localization of the *pcaK* gene, which in these *Pseudomonas* strains is localized upstream of *pcaI*. A comparison of genetic environments of 3-oxoadipate enol-lactone hydrolase encoding genes in *Pseudomonas* shows that they are usually localized in catabolic gene clusters comprising further genes of the protocatechuate branch of the 3-oxoadipate pathway. They are never clustered with genes encoding enzymes of the catechol branch, which in *Pseudomonas* strains, including strain MT1, are organized in a *catRBCA* gene cluster encoding transcriptional regulator, muconate cycloisomerase, muconolactone isomerase and catechol 1,2-dioxygenase, respectively. It is thus reasonable to assume that the *pca* gene cluster in MT1 is recruited for further degradation of 3-oxoadipate enol-lactone formed from salicylate. Finally, 3-oxoadipate:succinyl-CoA transferase and 3-oxoadipyl-CoA thiolase are also both encoded by the *pca* cluster enabling the channeling of 3-oxoadipate into the TCA cycle. Expression of 3-oxoadipate:succinyl-CoA transferase in response to 4-CS actually shows that the *pca* gene cluster is involved also in 4-CS degradation and that the *pcaIJF* gene products have their role in the conversion of 3-oxoadipate into succinyl-CoA and acetyl-CoA. This contrasts the degradation of methylsubstituted salicylates, where a specific gene cluster could be identified encoding proteins for the conversion of 4-methylmuconolactone to TCA cycle intermediates (Marin *et al.*, 2010).

4.3. Dissecting the quantitative structure of bacterial mixed cultures with F*IS*H-flow cytometry

The complexity of mixed culture constitutes one of the fundamental challenges in studying the behavior of microbial communities. In this work, Fluorescent *In Situ* Hybridisation (F*IS*H) was deployed to discriminate cells of specific strains in the consortium and subsequently successfully combined with high-throughput flow cytometric quantification of fluorescent bacteria. The consortium structure as determined by enumeration using F*IS*H-flow cytometry was comparable to estimates obtained by F*IS*H-microscopy and immunofluorescence but characterised by lower values of experimental errors. This increased accuracy helped to reveal more subtle variations in the consortium structure.

It could be observed that for exponentially growing cells, the quantitative structure of mixed bacterial populations as determined by indirect fluorescent techniques were in good agreement with the direct colony counts after plating serial dilutions on LB agar. However, when the F*IS*H-flow cytometry was used for following population dynamics in various continuous mixed cultures on a daily basis over the period of several weeks, a relatively large fraction of bacteria were not fluorescing upon addition of any MT-specific probe but still showed the DNA-conferred fluorescence from propidium iodide (Figs. 3.14c, 3.17c, and 3.18c). The presence of invading microorganisms potentially contaminating the cultures was analysed both by direct microscopic observations and by F*IS*H using an Eubacteria-specific probe (EUB338). However, none of the tests revealed any abnormalities in the mixed cultures and the number of bacteria counted post hybridisation with EUB338 probe generally was in good agreement with the sum of counts for individual populations in a given culture. Interestingly, similar phenomenon of lowered total counts was reported for bacterial community dynamics in the fermentor and in the trickle-bed bioreactor degrading aromatic compounds (Stoffels *et al.*, 1998). In contrast to the exponential growth phase in the batch, it could be anticipated that the chemostat due to its substrate-limiting principle contains relatively large fraction of physiologically inactive bacteria that contain only small number of ribosomes which constitute primary targets for F*IS*H probes. Obviously, bacteria containing relatively low number of ribosomes that are often termed 'viable but not cultivable' (VBNC) would still fluoresce upon the addition of DNA-binding dyes such as propidium iodide or ethidium bromide. Consequently, for the purpose of this work, bacteria showing fluorescence upon binding DNA-specific dye and not showing F*IS*H-conferred fluorescence were deemed inactive.

Successful application of F*IS*H-flow cytometry in determining the dynamic structure of the mixed culture marks the progress in understanding behaviour of microbial consortia. Compatibility of F*IS*H with other molecular techniques make it a valuable tool for the future studies over complex bacterial systems including the investigated 4-CS degrading consortium.

4.4. Comparison of different mixed culture set-ups wih the pure culture of MT1 under chemostat conditions

Both *A. xylosoxidans* MT3 and *P. veronii* MT4 strains were found to form stable binary communities with *P. reinekei* MT1 during continuous cultivation on 4-CS. The ability of these binary cultures to degrade 4-CS, the profiles of metabolites excreted to the medium and

the yield (biomass) were compared with the corresponding values obtained for both the consortium and the pure MT1 culture (Strocchi, unpublished) grown under identical conditions (Fig. 4.2ab). Community structures observed in the binary set-ups were compared to the structure of entire four-membered MT consortium (Fig. 4.2c).

Under continuous conditions using the standard dilution rate of 0,2 d^{-1} and 10 mM 4-CS as carbon source, all four cultures showed complete degradation of substrate. However, only in the pure culture of MT1 residual amounts of 4-chlorocatechol (2,0 ± 1,5 µM) could be observed in the supernatant. This observation is in agreement with the hypothesis of Pelz *et al.* (1999) that strain MT3 is responsible for the detoxification of 4-chlorocatechol excreted by MT1. Comparison of the average metabolite profiles indicated that mixed cultures containing strain MT3 (the four membered consortium and the MT1/MT3 binary set-up) accumulate lower amounts of *cis*-dienelactone. The ability of this strain for efficient assimilation of this compound, confirmed by a resting cell assay (Fig. 3.1.) and an observed dienelactone hydrolase activity (Tab. 3.3.), is congruent with the suggestion of Nikodem (2004) that *cis*-dienelactone excreted by MT1 is also cross-fed to MT3. Unfortunately, it was not possible to determine any correlation between the average content of protoanemonin in culture supernatants and the community composition of the culture and for instance the highest concentration of this metabolite was unexpectedly detected in the MT1/MT4 binary set-up (up to 11 µm). However, the amount of 4-CS converted into protoanemonin and thus being excreted by MT1 depends on both the relative and absolute activities of muconate cycloisomerases and *trans*-dienelactone hydrolase, where only a high relative acivity of *trans*-dienelactone hydrolase will be capable to transform most of 4-chloromuconolactone generated before its spontaneous decomposition, and a high concentration of *trans*-dienelactone hydrolase will reduce the decomposition rate. It is known, that the genome of *P. reinekei* MT1 encodes at least three different muconate cycloisomerases – MCI_{ccaB} (Camara *et al.*, 2009), MCI_{catB} and MCI_{salC} (Camara et at. 2007), two of which (MCI_{ccaB} and MCI_{salC}) are involved in 4-CS degradation. Thus, it might be expected that slightly different levels of protein expression of these muconate cycloisomerases and *trans*-dienelactone hydrolase will result in different amounts of protoanemonin accumulating in the culture medium.

Continuous cultures growing at the same dilution rate of 0,2 d^{-1} showed different efficiencies in converting 4-CS into biomass. The observed average optical density increased in the following order: MT1 ≤ MT1/MT4 < MT1/MT3 < consortium. It seems that efficiency of 4-CS assimilation by consortium bacteria increases with increasing complexity of the community. From the comparison of two binary cultures MT1/MT3 and MT1/MT4 it is

evident that the presence of strain MT3 has a more profound effect on the level of overall biomass reached in the chemostat than the presence of strain MT4. For the mixed cultures, the yield of biomass also correlated positively with the content of metabolically active bacteria as analysed by F*IS*H-flow cytometry (Fig. 4.2c).

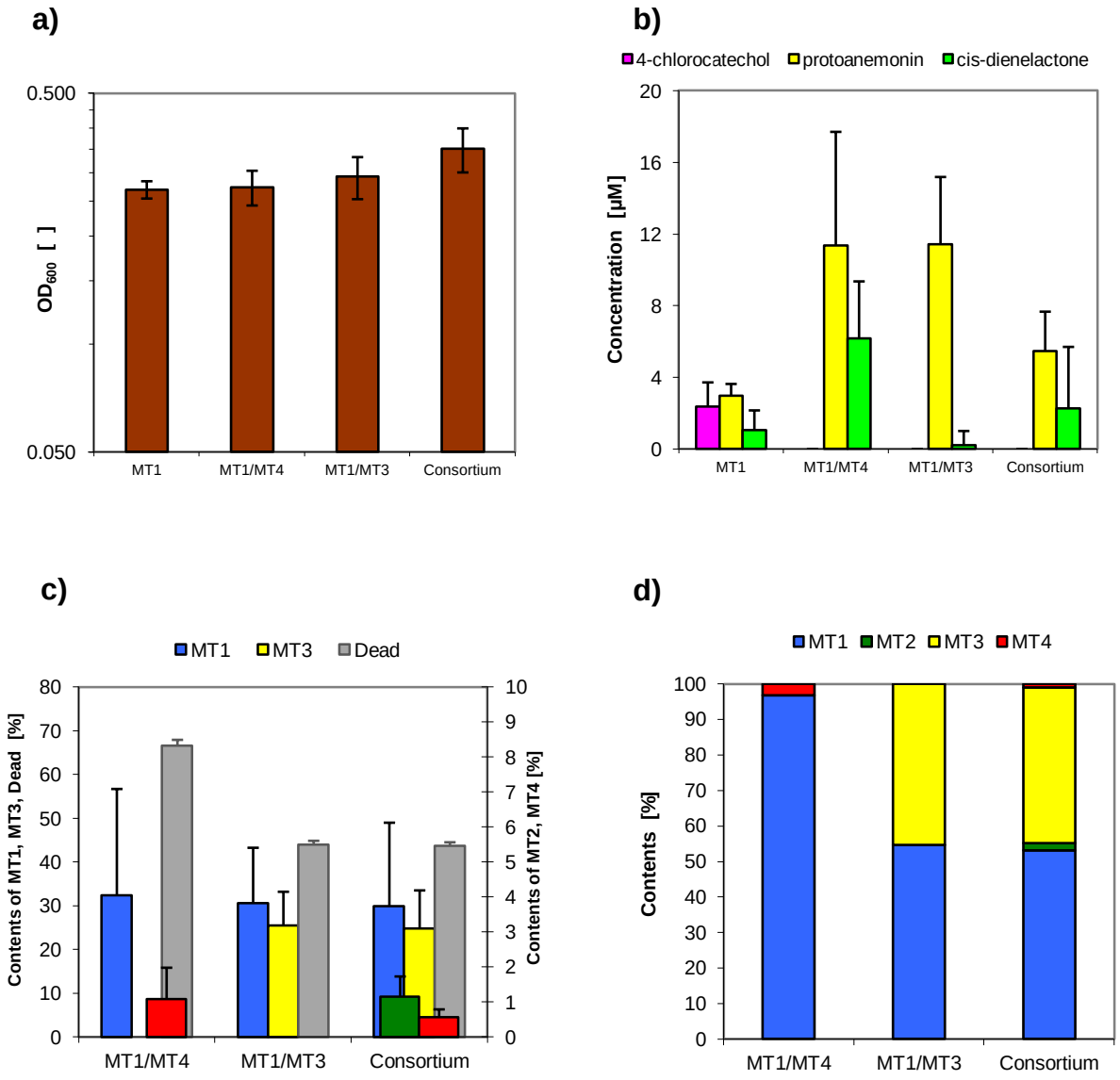

Figure 4.2. Comparison of main parameters for continuous cultures grown on 4-CS: **(a)** optical density (biomass), **(b)** metabolite profile, **(c)** community structure, and **(d)** community structure of metabolically active bacteria. Data for MT1 chemostat culture from Strocchi (unpubl.).

Interestingly, the relative content of MT3 cells in the MT1/MT3 binary set-up and in the consortium culture were similar. Similarly, the content of MT4 in the MT1/MT4 binary setup and in the consortium did not differ significantly (Fig. 4.2c). These observations indicate that the content of strains MT3 and MT4 in the consortium is not influenced by the presence of

other community members but is mainly determined by the amount of 4-CS metabolites that are released by MT1 as previously suggested (Pelz *et al.*, 1999).

The fact that *P. reinekei* MT1 can coexist with the other γ-proteobacterial strains of the *Pseudomonadaceae* family (MT4) and with β-Proteobacteria (MT3) both in the complex community, as well as in the binary setup, is an intriguing observation that may have practical importance. A survey of the literature shows that many microbial consortia obtained by selective enrichment for the degradation of aromatic and diverse other pollutants, consisted mainly of γ- (mainly *Pseudomonas*) and β-Proteobacteria (often *Alcaligenaceae*). For instance, a bacterial mixed culture able to mineralize molinate contained two members of the genus *Pseudomonas* (*P. chlororaphis*, and *P. nitroreducens*), *A. xylosoxidans*, *Stenotrophomonas maltophilia* and *Gulosibacter molinatovorans* (Barreiros *et al.*, 2003). Another microbial consortium isolated to degrade the herbicide Mecoprop comprised two species of *Pseudomonas*, an *Alcaligenes* species, a *Flavobacterium* species and *Acinetobacter calcoaceticus* (Lappin *et al.*, 1985). A stable enrichment culture with triclosan as sole carbon and energy substrate consisted of six strains, namely *P. mendocina*, *P. aeruginosa*, *A. xylosoxidans*, *Sphingomonas sanguis*, *Rhodanobacter lindanoclasticus*, and *Agrobacterium radiobacter* (Hay *et al.*, 2001). Two other cases of stable mixed cultures including members of β- and γ-Proteobacteria are binary cultures of *P. fluorescens* and *C. acidovorans* degrading cocaine (Lister *et al.*, 1996) and *Burkholderia* sp. LB400 and *P. putida* degrading low-chlorinated biphenyls (Potrawfke *et al.*, 1998). As the high potential of β- and γ-Proteobacteria for the aerobic breakdown of aromatics is well recognized (Perez-Pantoja *et al.*, 2010b), the often observed co-isolation of members of β- and γ-Proteobacteria creates a basis for the rational design of communities displaying desired degradative features.

4.5. Influence of substrate, temperature and oxygen concentration on functioning of the 4-chlorosalicylate degrading bacterial consortium

The simulation of challenges that microbial consortia would meet in the environment was performed by comparative analysis of its growth at different conditions in batch cultures and by monitoring responses of chemostat cultures to inflicted perturbations. The preference of consortium towards two different chlorosalicylate isomers (4-CS and 5-CS) as sole carbon and energy substrate and the influence of temperature on the rate of growth and 4-CS degradation were determined in fed-batch and batch cultures, respectively. The impact of

aeration and increased substrate flow (higher dilution rate) on the 4-CS breakdown and the community structure were assessed in continuous culture.

4.5.1. Substrate preference of the consortium culture

Similarly to MT1, only the 4- and 5-chlorosalicylate isomers could be used by the microbial consortium as substrates for growth. However, the growth rate of the consortium with 5-CS (0,050 h^{-1}) was considerably faster than with 4-CS (0,028 h^{-1}), which was also reflected in the higher substrate degradation rates. Interestingly, strain MT1 was previously reported to grow on 5-CS more than three times faster than on 4-CS however, with μ equaling 0,16 h^{-1} and 0,05 h^{-1} (Nikodem *et al.*, 2003), and thus, with faster rates than reported here. However, it may be suggested that MT1 used in that study was adapted for growth on chlorosalicylates by permanent subcultivation on the substrate.

A similar substrate preference was also observed for the artificially composed community with strain *P. moorei* RW10 replacing MT1, with growth rates of 0,059 h^{-1} on 5-CS and 0,027 h^{-1} on 4-CS. This is hardly surprising as the chlorosalicylate degradation routes in strains MT1 and RW10 are probably identical (Pieper, personal comm.) and may indicate the presence of similar salicylate hydroxylases with similar substrate preferences in both strains.

4.5.2. Growth of consortium at various temperature conditions

The bacterial consortium could grow and degrade 4-CS at temperature ranging from 12ºC up to 30ºC, which is consistent with the temperature optimum for growth displayed by the main consortium member MT1. Interestingly, even though the specific growth rate of strain MT1 in mineral medium with acetate was highest at 30ºC, the whole consortium on 4-CS showed fastest growth and substrate degradation at 25ºC. During cultivation of the consortium on 4-CS at 30ºC the growth and substrate degradation rates were reduced. From the comparison of profiles of metabolites accumulating in the culture media (Fig. 3.18c-f) it is evident that the toxicity of 4-chlorocatechol (Schweigert *et al.*, 2001) is responsible for the observed effect rather than the toxicity of protoanemonin (Blasco *et al.*, 1995).

Despite the obvious differences in growth and substrate degradation rates the structure of the consortium at the end of exponential phase and beginning of stationary growth phase was very similar under the tested temperature conditions (Fig. 4.3.).

The development of the consortium in batch culture on 4-CS could be divided into two stages. In the first one, when 4-CS substrate is in plentiful supply, strain MT1 dominates the community accounting for more than 90% of total cells. In the second stage, after 4-CS

available in the medium becomes exhausted, strain MT3 shows rapid growth and establishes itself as the second most abundant consortium member.

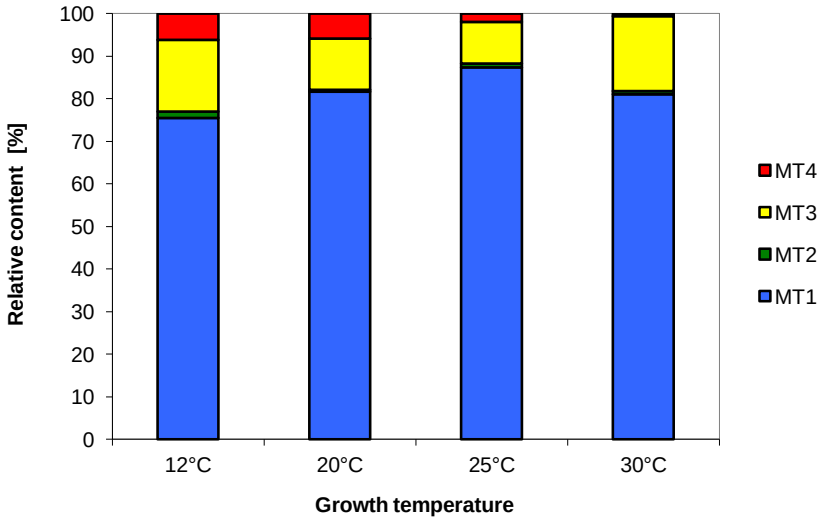

Figure 4.3. Consortium structure during late exponential/early stationary growth in batch culture with 4-CS at different temperatures.

The consortium structure observed in this work during growth on 4-CS at different temperatures both in batch and continuous cultures was compared in Tab. 4.1. with previously reported data (Pelz *et al.*, 1999; Tillmann 2004; Rabenau 2004). In this work a negative correlation between the growth temperature and the content of MT4 in the community was found for the batch cultures. Similarly, the content of MT2 in the bacterial community grown in batch decreased with increasing cultivation temperature. These effects, however, were not observed for continuous cultures, thus, they are probably derived from the growth phase effect during cultivation in batch.

Within the range between 12ºC and 30ºC, that is the growth optimum for the 4-CS degrading strain MT1, the temperature obviously influences the rate of breakdown of substrate by four-membered consortium. However, the impact of growth temperature on the composition of microbial community is only negligible. It might be speculated that the synergistic way of 4-CS degradation by consortium is not affected during cultivation at temperature between 12ºC and 30ºC. This relative stability, displayed by the 4-CS degrading consortium within certain range of thermal conditions may give it a competitive advantage in its natural habitat.

Table 4.1. Community composition during growth on 4-CS in the continuous and batch culture according to various authors.

Culture	Relative abundance [%]			
	MT1	**MT2**	**MT3**	**MT4**
chemostat, 12°C (Pelz *et al.*, 1999)	84 ± 3	0,7 ± 0,3	7,5 ± 3,8	8,0 ± 4,2
chemostat, 12°C [1]	70 ± 2	0,7 ± 0,2	28,7 ± 4,7	0,3 ± 0,1
chemostat, 12-20°C (Rabenau, 2004) [2]	76 ± 1	2,0 ± 0,7	19,0 ± 1,2	3,0 ± 1,2
chemostat, 20°C [1]	77 ± 3	0,8 ± 0,2	21,9 ± 3,6	0,4 ± 0,1
chemostat A, 30°C (Tillmann, 2004)	81 ± 7	1,7 ± 0,7	16,8 ± 0,7	0,9 ± 0,4
chemostat B, 30°C (Tillmann, 2004)	70 ± 7	0,8 ± 0,7	28,8 ± 4,4	0,9 ± 0,2
chemostat, 30°C [1]	58 ± 4	0,6 ± 0,2	40,6 ± 6,6	0,5 ± 0,1
batch culture, 12°C (Rabenau, 2004) [4]	74 ± 1	2,0 ± 0,7	16,0 ± 2,3	7,0 ± 1,0
batch culture, 12°C [1,3]	78 ± 3	3,3 ± 0,8	12,2 ± 2,0	7,0 ± 0,8
batch culture, 20°C [1,3]	81 ± 3	2,2 ± 0,5	10,4 ± 1,7	6,0 ± 0,7
batch culture, 25°C [1,3]	91 ± 3	1,3 ± 0,3	4,4 ± 0,7	3,5 ± 0,4
batch culture, 30°C [1,3]	89 ± 3	1,1 ± 0,2	6,9 ± 1,1	3,1 ± 0,4

[1] the sum of viable cells taken as 100%; [2] average of n = 35 experiments carried out at 12ºC and 20ºC; [3] average across the whole growth cycle in the periodic culture; [4] average of n = 9 experiments.

4.5.3. Responses of consortium chemostat culture to perturbations

The consortium grown in the 4-CS-fed chemostat was subjected to perturbations of two different kinds: (i) step-wise increase of the dilution rate which equals the specific growth rate (μ), and (ii) transiently disrupted oxygen supply. A step-wise increase of the dilution rate acted as mild stressor that did not induce a dramatic response of the consortium. However, the observed increasing biomass in the culture and the altered community structure with a growing share of strain MT3 in response to the increased flow rate of medium through the reactor indicates better efficiency of the consortium in utilizing the available carbon substrate. It is likely that MT3 is largely responsible for this effect and that it might play an important role in stabilizing the consortium against environmental challenges. On the other hand, a short period of anaerobiosis triggered a powerful response, that if left unattended, could result in an irreversible breakdown of the system.

4.5.3.1. MT1 is primarily affected by oxygen deprivation in the consortium culture

The process of 4-chlorosalicylate breakdown by the consortium is strictly aerobic with two oxygen-dependent enzymatic steps. A transiently disrupted aeration interrupted the degradation of 4-CS and reduced the content of MT1 cells by more than 30-fold. It is most likely that the accumulation of 4-chlorocatechol had a severe impact on the viability of MT1. Observed accumulation of 4-chlorocatechol in the medium coincided with relative increase in the number of MT3 that became the dominant member of the consortium. This increase might be due to MT3 being more resistant than MT1 to the exposure on toxic 4-chlorocatechol. If the *A. xylosoxidans* MT3 possess the 4-chlorocatechol detoxification mechanism as proposed previously (Pelz *et al.*, 1999; Pawelczyk *et al.*, 2008) this observation is hardly surprising. Although, the community is obviously well-protected against 4-chlorocatechol poisoning by the presence of strain MT3, the efficient degradation of 4-CS requires conditions that are optimal for its main degrader MT1. Consequently, any strategy designed for the use of MT consortium in bioremediation has to take this factor into account.

4.5.3.2. Consortium recovery from stress is independent on the nature of stressor

A typical response of the consortium to stress caused by perturbation was manifested in the accumulation of 4-chlorocatechol and other metabolites of 4-CS breakdown by MT1 (protoanemonin and *cis*-dienelactone). Secondary symptoms of a functional breakdown included darkening of the culture medium due to the oxidative polymerization of chlorocatechol, reduced biomass and a decreased content of active bacteria. However, the consortium showed a remarkable capacity to recover its structure and function under favourable conditions and this feature was independent of the nature of perturbation (excessive load of substrate or periodic oxygen limitation). Recovery of the consortium culture was marked by the removal of excessively accumulated metabolites of 4-CS breakdown from the culture medium, stabilization of the cellular density and restoration of the characteristic functional structure of the bacterial community.

REFERENCES

Aas, J. A., B. J. Paster, L. N. Stokes, I. Olsen, and F. E. Dewhirst (2005). Defining the normal bacterial flora of the oral cavity. J. Clin. Microbiol. **43:** 5721-5732.

Altenschmidt, U., and G. Fuchs (1992). Novel aerobic 2-aminobenzoate metabolism. Purification and characterization of 2-aminobenzoate-CoA ligase, localization of the genes on a 8-kbp plasmid, and cloning and sequencing of the genes from a denitrifying *Pseudomonas* sp. Eur. J. Biochem. **205**: 721-727.

Altenschmidt, U., B. Oswald, E. Steiner, H. Herrmann, and G. Fuchs (1993). New aerobic benzoate oxidation pathway *via* benzoyl-Coenzyme A and 3-hydroxybenzoyl-Coenzyme A in a denitrifying *Pseudomonas* sp. J. Bacteriol. **175**: 4851-4858.

Altschul, S. F., W. Gish, W. Miller, E. W. Myers, and D. J. Lipman (1990). Basic local alignment search tool. J. Mol. Biol. **215**: 403-410.

Altschul, S. F., T. L. Madden, A. A. Schäffer, J. Zhang, Z. Zhanh, W. Miller, and D. J. Lipman (1997). Gapped BLAST and PSI-BLAST: a new generation of protein database search programs. Nucl. Acids Res. **25**: 3389-3401.

Amann, R. I., B. J. Binder, R. J. Olson, S. W. Chisholm, R. Devereux and D. A. Stahl (1990a). Combination of 16S rRNA-targeted oligonucleotide probes with flow cytometry for analyzing mixed microbial populations. Appl. Environ. Microbiol. **56**: 1919-1925.

Amann, R. I., L. Krumholz, and D. A. Stahl (1990b). Fluorescent-oligonucleotide probing of whole cells for determinative, phylogenetic, and environmental studies in microbiology. J. Bacteriol. **172**: 762-770.

Amann, R. I., W. Ludwig, and K.-H. Schleifer (1995). Phylogenetic identification and *in situ* detection of individual microbial cells without cultivation. Microbiol. Rev. **59**: 143-169.

Arfmann, H.-A., K. N. Timmis, and R.-M. Wittich (1997). Mineralization of 4-chlorodibenzofuran by a consortium consisting of *Sphingomonas* sp. strain RW1 and *Burkholderia* sp. strain JWS. Appl. Environ. Microbiol. **63**: 3458-3462.

Armengaud, J., K. N. Timmis and R. M. Wittich (1999). A functional 4-hydroxysalicylate/ hydroxyquinol degradative pathway gene cluster is linked to the initial dibenzo-p-dioxin pathway genes in *Sphingomonas* sp. strain RW1**.** J. Bacteriol. **181**: 3452-3461.

Assinder, S. J., and P. A. Williams (1990). The TOL plasmids: determinants of the catabolism of toluene and the xylenes. Adv. Microb. Physiol. **31**: 1-69.

Avignone-Rosa, C., J. White, A. Kuiper, P. W. Postma, M. Bibb, and M. J. Teixeira de Mattos (2002). Carbon flux distribution in antibiotic-producing chemostat cultures of *Streptomyces lividans*. Metab. Eng. **4**: 138-150.

Bailey, J. E., J. Fazel-Madjlessi, D. N. McQuitty, L. Y. Lee, J. C. Allred, and J. A. Oro (1977). Characterization of bacterial growth by means of flow microfluorometry. Science **198**: 1175-1176.

Ballou, D. P., B. Entsch, and L. J. Cole (2005). Dynamics involved in catalysis by single-component and two-component flavin-dependent aromatic hydroxylases. Biochem. Biophys. Res. Commun. **338**: 590-598.

Barreiros, L., B. Nogales, C. M. Manaia, A. C. S. Ferreira, D. H. Pieper, M. A. Reis, and O. C. Nunes (2003). A novel pathway for mineralization of the thiocarbamate herbicide molinate by a defined bacterial mixed culture. Environ. Microbiol. **5**: 944-953.

Blasco, R., R.-M. Wittich, M. Mallavarapu, K. N. Timmis, and D. H. Pieper (1995). From xenobiotic to antibiotic, formation of protoanemonin from 4-chlorocatechol by enzymes of the 3-oxoadipate pathway. J. Biol. Chem. **270**: 29229-29235.

Bobadilla, R. A. (2006). Proteomics and kinetic modeling analysis of a 4-chlorosalicylate degrading bacterial community. PhD Thesis, TU Braunschweig.

Boer, V. M., J. H. de Winde, J. T. Pronk, and M. D. W. Piper (2003). The genome-wide transcriptional responses of *Saccharomyces cerevisiae* grown on glucose in aerobic chemostat cultures limited for carbon, nitrogen, phosphorus, or sulfur. J. Biol. Chem. **278**: 3265-3274.

Bos, R., H. C. van der Mei, H. J. Busscher (1996). Co-adhesion of oral microbial pairs under flow in the presence of saliva and lactose. J. Dent. Res. **75**: 809-815.

Bosch, R., E. R. B. Moore, E. Garcia-Valdez, and D. H. Pieper (1999). NahW, a novel, inducible salicylate hydroxylase involved in mineralization of naphthalene by *Pseudomonas stutzeri* AN10. J. Bacteriol. **181**: 2315-2322.

Bradshaw, D. J., A. S. McKee, and P. D. Marsh (1989). Effects of carbohydrate pulses and pH on population shifts within oral microbial communities *in vitro*. J. Dent. Res. **68**: 1298-1302.

Bradshaw, D. J., P. D. Marsh (1994). Effect of sugar alcohols on the composition and metabolism of a mixed culture of oral bacteria grown in a chemostat. Caries Res. **28**: 251-256.

Brilon, C., W. Beckmann, M. Hellwig, and H.-J. Knackmuss (1981). Enrichment and isolation of naphthalenesulfonic acid-utilizing Pseudomonads. Appl. Environ. Microbiol. **42**: 39-43.

Bryson, V., and W. Szybalski (1952). Microbial selection. Science **116**: 45-51.

Bundy, M., A. L. Campbell, and E. L. Neidle (1998). Similarities between the *antABC*-encoded anthranilate dioxygenase and the *benABC*-encoded benzoate dioxygenase of *Acinetobacter* sp. strain ADP1. J. Bacteriol. **180**: 4466-4474.

Buswell, J. A., and D. W. Ribbons (1988). Vanillate *o*-demethylase from *Pseudomonas* species. Methods Enzymol. **161**: 294-301.

Cafaro, V., V. Izzo, R. Scognamiglio, E. Notomista, E. Capasso, A. Casbarra, P. Pucci, A. Di Donato (2004). Phenol hydroxylase and toluene/*o*-xylene monooxygenase from *Pseudomonas stutzeri* OX1: interplay between two enzymes. Appl. Environ. Microbiol. **70**: 2211-2219.

Camara, B. (2006). Genetic and biochemical characterisation of a metabolic route observed in *Pseudomonas* sp. MT1 for the degradation of chlorosalicylates. PhD Thesis, TU Braunschweig.

Camara, B., P. Bielecki, F. Kaminski, V. M. Dos Santos, I. Plumeier, P. Nikodem and D. H. Pieper (2007). A gene cluster involved in degradation of substituted salicylates via *ortho* cleavage in *Pseudomonas* sp. strain MT1 encodes enzymes specifically adapted for transformation of 4-methylcatechol and 3-methylmuconate**.** J. Bacteriol. **189**: 1664-1674.

Camara, B., M. Marin, M. Schlömann, H.-J. Hecht, H. Junca, and D. H. Pieper (2008). *trans*-Dienelactone hydrolase from *Pseudomonas reinekei* MT1, a novel zinc-dependent hydrolase. Biochem. Biophys. Res. Comm. **376**: 423-428.

Camara, B., P. Nikodem, P. Bielecki, R. Bobadilla, H. Junca, and D. H. Pieper (2009). Characterization of a gene cluster involved in 4-chlorocatechol degradation by *Pseudomonas reinekei* MT1. J. Bacteriol. **191**: 4905-4915.

Chain, P. S. G., V. J. Denef, K. T. Konstantinidis, L. M. Vergez, L. Agullo, V. L. Reyes, L. Hauser, M. Cordova et al. (2006). *Burkholderia xenovorans* LB400 harbors a multi-replicon, 9,73-Mbp genome shaped for versatility. Proc Natl Acad Sci USA **103**: 15280-15287.

Chikindas, M. L., J. Novak, A. J. Driessen, W. N. Konings, K. M. Schilling, and P. W. Caufield (1995). Mutacin II, a bactericidal antibiotic from *Streptococcus mutans*. Antimicrob. Agents Chemother. **39**: 2656-2660.

Contzen, M., and A. Stolz (2000). Characterization of the genes for two protocatechuate 3,4-dioxygenases from the 4-sulfocatechol-degrading bacterium *Agrobacterium radiobacter* strain S2. J. Bacteriol. **182**: 6123-6129.

Crawford, R. L., S. W. Hutton, and P. J. Chapman (1975). Purification and properties of gentisate 1,2-dioxygenase from *Moraxella osloensis*. J. Bacteriol. **121**: 794-799.

Daubaras, D. L., C. D. Hershberger, K. Kitano and A. M. Chakrabarty (1995). Sequence analysis of a gene cluster involved in metabolism of 2,4,5-trichlorophenoxyacetic acid by *Burkholderia cepacia* AC1100**.** Appl. Environ. Microbiol. **61**: 1279-1289.

Dean, A. C. R., and C. N. Hinshelwood (1966). Growth, function and regulation in bacterial cells. Clarendon Press, Oxford, UK.

DeLong, E. F., G. S. Wickham, N. R. Pace (1989). Phylogenetic stains: ribosomal RNA-based probes for the identification of single cells. Science **243**: 1360-1363.

Diaz, P. L., P. S. Zilm, and A. H. Rogers (2002). *Fusobacterium nucleatum* support the growth of *Porphyromonas gingivalis* in oxygenated and carbon dioxide-depleted environments. Microbiology 148: 467-472.

DiMarco, A. A., B. A. Averhoff, and L. N. Ornston (1993). Identification of the transcriptional activator *pobR* and characterization of its role in the expression of *pobA*, the structural gene for p-hydroxybenzoate hydroxylase in *Acinetobacter calcoaceticus*. J. Bacteriol. **175**: 4499-4506.

Dorn, E., and H.-J. Knackmuss (1978). Chemical structure and biodegradability of halogenated aromatic compounds. Two catechol 1,2-dioxygenases from 3-chlorobenzoate-grown Pseudomonad. Biochem J. **174**: 73-84.

Dunn, N. W., and I. C. Gunsalus (1973). Transmissible plasmid coding enzymes for early enzymes of naphthalene oxidation in *Pseudomonas putida*. J. Bacteriol. **114**: 974-979.

Dykhuizen, D. E., and D. L. Hartl (1983). Selection in chemostats. Microbiol. Rev. **47**: 150-168.

Endo, R., M. Kamakura, K. Miyauchi, M. Fukuda, Y. Ohtsubo, M. Tsuda and Y. Nagata (2005). Identification and characterization of genes involved in the downstream degradation pathway of gamma-hexachlorocyclohexane in *Sphingomonas paucimobilis* UT26**.** J. Bacteriol. **187**: 847-853.

Faude, U. C. (1996). Immunochemische Analyse mikrobieller Lebensgemeinschaften. Fakultät für Biowissenschaften, Pharmazie und Psychologie. PhD Thesis, University Leipzig, Leipzig.

Feigel, B. J., and H.-J. Knackmuss (1993). Syntrophic interactions during degradation of 4-aminobenzenesulfonic acid by a two species bacterial culture. Arch. Microbiol. **159**: 124-130.

Fetzner, S., R. Müller, and F. Lingens (1992). Purification and some properties of 2-halobenzoate 1,2-dioxygenase, a two component enzyme system from *Pseudomonas cepacia* 2CBS. J. Bacteriol. **174**: 279-290.

Fuchs, B. M., G. Wallner, W. Beisker, I. Schwippl, W.Ludwig, and R. Amann (1998). Flow cytometric analysis of the *in situ* accessibility of *Escherichia coli* 16S rRNA for fluorescently labeled oligonucleotide probes. Appl. Environ. Microbiol. **64**: 4973-4982.

Fuchs, B. M., M. V. Zubkov, K. Sahm, P. H. Burkill, and R. Amann (2000). Changes in community composition during dilution cultures of marine bacterioplankton as assessed by flow cytometric and molecular biological techniques. Environ. Microbiol. **2**: 191-201.

Gaetti-Jardim, E., and M. J. Avila-Campos (1999). Bacteriocin-like activity of oral *Fusobacterium nucleatum* isolated from human and non-human primates. Rev. Microbiol. **30**: 342-346.

Gersdorf, H., A. Meissner, K. Pelz, G. Krekeler, and U. B. Göbel (1993). Identification of *Bacteroides forsythus* in subgingival plaque from patients with advanced periodontitis. J. Clin. Microbiol. **31**: 941-946.

Gescher, J., W. Eisenreich, J. Worth, A. Bacher, and G. Fuchs (2005). Aerobic benzoyl-CoA catabolic pathway in *Azoarcus evansii*: studies on the non-oxygenolytic ring cleavage enzyme. Mol. Microbiol. **56**: 1586-1600.

Gibson, D. T., and R. E. Parales (2000). Aromatic hydrocarbon dioxygenases in environmental biotechnology. Curr. Opin. Biotechnol. **11**: 236-243.

Glöckner, F. O., R. Amann, A. Alfreider, J. Pernthaler, R. Psenner, K. Trebesius and K.-H. Schleifer (1996). An in situ hybridization protocol for detection and identification of planktonic bacteria. Syst. Appl. Microbiol. **19**: 403-406.

Göbel, M., K. Kassel-Cati, E. Schmidt and W. Reineke (2002). Degradation of aromatics and chloroaromatics by *Pseudomonas* sp. strain B13: cloning, characterization, and analysis of sequences encoding 3-oxoadipate:succinyl-coenzyme A (CoA) transferase and 3-oxoadipyl-CoA thiolase**.** J. Bacteriol. **184**: 216-223.

Grenier, D., and D. Mayrand (1986). Nutritional relationships between oral bacteria. Infect. Immun. **53**: 616-620.

Gucker, F. T., C. O'Konski, H. B. Pickard, and J. N. Pitts (1947). A photoelectric counter for colloidal particles. Am. J. Chem. **69**: 2422-2431.

Hahn, D., R. I. Amann, W. Ludwig, A. D. L. Akkermans, and K.-H. Schleifer (1992). Detection of microorganisms in soil after *in situ* hybridization with rRNA-targeted, fluorescently labelled oligonucleotides. J. Gen. Microbiol. **138**: 879-887.

Haigler, B. E., S. F. Nishino, and J. C. Spain (1988). Degradation of 1,2-dichlorobenzene by a *Pseudomonas* sp. Appl. Environ. Microbiol. **54**: 294-301.

Hall, T. A. (1999). BioEdit: a user-friendly biological sequence alignment editor and analysis program for Windows 95/98/NT. Nucleic Acids Symposium Series **41**: 95-98.

Haller, H. D., and R. K. Finn (1979). Biodegradation of 3-chlorobenzoate and formation of black color in the presence and absence of benzoate. Eur. J. Appl. Microbiol. Biotechnol. **8**: 191-205.

Hammond, B. F., S. E. Lillard, and R. H. Stevens (1987). A bacteriocin of *Actinobacillus actinomycetemcomitans*. Infect. Immun. **55**: 686-691.

Hartl, D., and D. Dykhuizen (1979). A selectively driven molecular clock. Nature **281**: 230-231.

Hartnett, C., E. L. Neidle, K. L. Ngai and L. N. Ornston (1990). DNA sequences of genes encoding *Acinetobacter calcoaceticus* protocatechuate 3,4-dioxygenase: evidence indicating shuffling of genes and of DNA sequences within genes during their evolutionary divergence. J. Bacteriol. **172**: 956-966.

Harwood, C. S., N. N. Nichols, M. K. Kim, J. L. Ditty and R. E. Parales (1994). Identification of the *pcaRKF* gene cluster from *Pseudomonas putida*: involvement in chemotaxis, biodegradation, and transport of 4-hydroxybenzoate**.** J. Bacteriol. **176**: 6479-6488.

Harwood, C. S., and R. E. Parales (1996). The β-ketoadipate pathway and the biology of self-identity. Annu. Rev. Microbiol. **50**: 553-590.

Havarstein, L. S., P. Gaustad, I. F. Nes, and D. A. Morrison (1996). Identification of the streptococcal competence-pheromone receptor. Mol. Microbiol. **21**: 863-869.

Hay, A. G., P. M. Dees, and G. S. Sayler (2001). Growth of bacterial consortium on triclosan. FEMS Microb. Ecol. **36**: 105-112.

Hayes, A., N. Zhang, J. Wu, P. R. Butler, N. C. Hauser, J. D. Hoheisel, F. L. Lim, A. D. Sharrocks, and S. G. Oliver (2002). Hybridization array technology coupled with chemostat culture: tools to interrogate gene expression in *Saccharomyces cerevisiae*. Methods **26**: 281-290.

Herbert, D. (1961). A theoretical analysis of continuous culture systems. Soc. Chem. Ind. Monograph (London) **12**: 21-53.

Hoskisson, P. A., and G. Hobbs (2005). Continuous culture – making a comeback? Microbiol. **151**: 3153-3159.

Huang, Y., K. X. Zhao, X. H. Shen, M. T. Chaudhry, C. Y. Jiang, and S. J. Liu (2006). Genetic characterization of the resorcinol catabolic pathway in *Corynebacterium glutamicum*. Appl. Environ. Microbiol. **72**: 7238-7245.

Ihalin, R., V. Loimaranta, M. Lenander-Lumikari, and J. Tenuovo (2001). The sensitivity of *Porphyromonas gingivalis* and *Fusobacterium nucleatum* to different (pseudo)halide-peroxidase combinations compared with mutans streptococci. J. Med. Microbiol. **50**: 42-48.

Ishiyama, D., D. Vujaklija, and J. Davies (2004). Novel pathway of salicylate degradation by *Streptomyces* sp. strain WA46. Appl. Environ. Microbiol. **70**: 1297-1306.

Jain, R. K., J. H. Dreisbach, and J. C. Spain (1994). Biodegradation of *p*-nitrophenol *via* 1,2,4-benzenetriol by an *Arthrobacter* sp. Appl. Environ. Microbiol. **60**: 3030-3032.

Jannasch, H. W. (1974). Steady state and the chemostat in ecology. Limnol & Oceanogr. **19**: 716-720.

Jannasch, H. W., and T. Egli (1993). Microbial growth kinetics: a historical perspective. Antonie van Leeuwenhoek **63**: 213-224.

Jimenez, J. I., B. Minambres, J. L. Garcia, and E. Diaz (2002). Genomic analysis of the aromatic catabolic pathways from *Pseudomonas putida* KT2440. Environ. Microbiol. **4**: 824-841.

Jimenez, L., A. Breen, N. Thomas, T. W. Federle, and G. S. Sayler (1991). Mineralization of linear alkylbenzene sulfonate by a four-membered aerobic bacterial consortium. Appl. Environ. Microbiol. **57**: 1566-1569.

Kaschabek, S. R., and W. Reineke (1992). Maleylacetate reductase of *Pseudomonas* sp. strain B13: dechlorination of chloromaleylacetates, metabolites in the degradation of chloroaromatic compounds. Arch. Microbiol. **158**: 412-417.

Katsivela, E., V. Wray, D. H. Pieper, and R.-M. Wittich (1999). Initial reactions in the biodegradation of 1-chloro-4-nitrobenzene by a newly isolated bacterium, strain LW1. Appl. Environ. Microbiol. **65**: 1405-1412.

Kaulmann, U., S. R. Kaschabek, and M. Schlömann (2001). Mechanism of chloride elimination from 3-chloro and 2,4-dichloro-*cis*,*cis*-muconate: new insight obtained from analysis of muconate cycloisomerase variant CatB-K169A. J. Bacteriol. **183**: 4551-4561.

Keil, H., S. Keil, R. W. Pickup and P. A. Williams (1985). Evolutionary conservation of genes coding for meta pathway enzymes within TOL plasmids pWW0 and pWW53**.** J. Bacteriol. **164**: 887-895.

Kenzaka, T., N. Yamaguchi, K. Tani, and M. Nasu (1998). rRNA-targeted fluorescent *in situ* hybridization analysis of bacterial community structure in river water. Microbiology **144**: 2085-2093.

Khalameyezer, V., I. Fischer, U. T. Bornscheuer, and J. Altenbucher (1999). Screening, nucleotide sequence, and biochemical characterization of an esterase from *Pseudomonas fluorescens* with high activity towards lactones. Appl. Environ. Microbiol. **65**: 477-482.

Kinniment, S. L., J. W. T. Wimpenny, D. Adams, and P. D. Marsh (1996). The effect of chlorhexidine on defined, mixed culture oral biofilms grown in a novel model system. J. Appl. Microbiol. **81**: 120-125.

Kirk, T. K., and R. L. Farrell (1987). Enzymatic "combustion": the microbial degradation of lignin. Annu. Rev. Microbiol. **41**: 465-505.

Kolenbrander, P. E. (2000). Oral microbial communities: biofilms, interactions, and genetic systems. Ann. Rev. Microbiol. **54**: 413-437.

Kolenbrander, P. E., R. N. Andersen, and L. V. Moore (1989). Coaggregation of *Fusobacterium nucleatum*, *Selenomonas flueggei*, *Selenomonas infelix*, *Selenomonas noxia*, and *Selenomonas sputigena* with strains from 11 genera of oral bacteria. Infect. Immun. **57**: 3194-3203.

Kolenbrander, P. E., R. N. Andersen, L. V. Moore (1990). Intrageneric coaggregation among strains of human oral bacteria: potential role in primary colonization of the tooth surface. Appl. Environ. Microbiol. **56**: 3890-3894.

Kolkman, A., M. M. A. Olsthoorn, C. E. M. Heeremans, A. J. R. Heck, and M. Slijper (2005). Comparative Proteome Analysis of *Saccharomyces cerevisiae* grown in chemostat cultures limited for glucose or ethanol. Mol. Cell. Proteom. **4**: 1-11.

Kovarova, K., A. Käch, V. Chaloupka, A. J. B. Zehnder, and T. Egli (1997). Cultivation of *Escherichia coli* with mixtures of 3-phenylpropionic acid and glucose: steady-state kinetics. Appl. Environ. Microbiol. **63**: 2619-2624.

Kovarova-Kovar, K., and T. Egli (1998). Growth kinetics of suspended microbial cells: from single-substrate-controlled growth to mixed-substrate kinetics. Microbiol. Mol. Biol. Rev. **62**: 646-666.

Kowalchuk, G. A., G. B. Hartnett, A. Benson, J. E. Houghton, K. L. Ngai and L. N. Ornston (1994). Contrasting patterns of evolutionary divergence within the *Acinetobacter calcoaceticus pca* operon. Gene **146**: 23-30.

Kreth, J., J. Merritt, W. Shi, and F. Qi (2005). Competition and coexistence between *Streptococcus mutans* and *Streptococcus sanguinis* in the dental biofilm. J. Bacteriol. **187**: 7193-7203.

Kroes, I., P. W. Lepp, and D. A. Relman (1999). Bacterial diversity within the human subgingival crevice. Proc. Natl. Acad. Sci. USA. **96**: 14547-14552.

Kuramitsu, H. K., X. He, R. Lux, M. H. Anderson, W. Shi (2007). Interspecies interactions within oral microbial communities. Microbiol. Mol. Biol. Rev. **71**: 653-670.

Lange, J. L., P. S. Thorne, and N. Lynch (1997). Application of flow cytometry and fluorescent in situ hybridization for assessment of exposure to airborne bacteria. Appl. Environ. Microbiol. **63**: 1557-1563.

Lappin, H. M., M. P. Greaves, and J. H. Slater (1985). Degradation of the herbicide Mecoprop [2-(2-Methyl-4-chlorophenoxy)propionic acid] by a synergistic microbial community. Appl. Environ. Microbiol. **49**: 429-433.

Leahy, J. G., P. J. Batchelor, and S. M. Morcomb (2003). Evolution of the soluble diiron monooxygenases. FEMS Microbiol. Rev. **27**: 449-479.

Leder, P., D. Tiemeier, and L. Enquist (1977). EK2 derivatives of bacteriophage lambda useful in the cloning of DNA from higher organisms: the lambdagtWES system. Science **196**: 175-177.

Lee, N., P. H. Nielsen, K. H. Andreasen, S. Juretschko, J. L. Nielsen, K.-H. Schleifer, and M. Wagner (1999). Combination of fluorescent in situ hybridization and microautoradiography – A new tool for structure-function analyses in microbial ecology. Appl. Environ. Microbiol. **65**: 1289-1297.

Leininger, S., T. Urich, M. Schloter, L. Schwark, J. Qi, G. W. Nicol, J. I. Prosser, S. C. Schuster and C. Schleper (2006). Archaea predominate among ammonia-oxidizing prokaryotes in soil. Nature **442**: 806-809.

Li, Y.-H., P. C. Y. Lau, J. H. Lee, R. P. Ellen, and D. G. Cvitkovitch (2001). Natural genetic transformation of *Streptococcus mutans* growing in biofilms. J. Bacteriol. **183**: 897-908.

Liang, Q., M. Takeo, M. Chen, W. Zhang, Y. Xu and M. Lin (2005). Chromosome-encoded gene cluster for the metabolic pathway that converts aniline to TCA-cycle intermediates in *Delftia tsuruhatensis* AD9. Microbiology **151**: 3435-3446.

Licht, T. R., T. Tolker-Nielsen, K. Holmstrøm, K. A. Krogfelt, and S. Molin (1999). Inhibition of *Escherichia coli* precursor-16S rRNA processing by mouse intestinal contents. Environ. Microbiol. **1**: 23-32.

Lister, D. L., R. F. Sproule, A. J. Britt, C. R. Lowe, and N. C. Bruce (1996). Degradation of cocaine by a mixed culture of *Pseudomonas fluorescens* MBER and *Comamonas acidovorans* MBLF. Appl. Environ. Microbiol. **62**: 94-99.

Liu, A. M. F., N. A. Somers, R. J. Kazlauskas, T. S. Brush, F. Zocher, M. M. Enzelberger, U. T. Bornscheuer et al. (2001). Mapping the substrate selectivity of new hydrolases using colorimetric screening: lipases from *Bacillus thermocatenulatus* and *Ophiostoma piniferum*, esterases from *Pseudomonas fluorescens* and *Streptomyces diastatochromogenes*. Tetrahedron: Asymmetry **12**: 545-556.

Lovley, D. (2003). Cleaning up with genomics: applying molecular biology to bioremediation. Nat. Rev. Microbiol. **1**: 35-44.

Lunsford, R. D., (1998). Streptococcal transformation: essential features and applications of a natural gene exchange system. Plasmid **39**: 10-20.

Lykidis, A., D. Perez-Pantoja, T. Ledger, K. Mavromatis, I. J. Anderson, N. N. Ivanova, S. D. Hooper, A. Lapidus, S. Lucas, B. Gonzalez, and R. C. Kyrpides (2010). The complete multipartite genome sequence of *Cupriavidus necator* JMP134, a versatile pollutant degrader.PLoS ONE **5**: e9729

Manz, W., U. Szewczyk, P. Eriksson, R. Amann, K.-H. Schleifer, and T. A. Stenström (1993). *In situ* identification of bacteria in drinking water and adjoining biofilms by hybridization with 16S and 23S rRNA-directed fluorescent oligonucleotide probes. Appl. Environ. Microbiol. **59**: 2293-2298.

Marin, M., D. Perez-Pantoja, R. Donoso. V. Wray, B. Gonzalez, and D. H. Pieper (2010). Modified 3-oxoadipate pathway for the biodegradation of methylaromatics in *Pseudomonas reinekei* MT1. J. Bacteriol. **192**: 1543-1552.

Marsh, P. D. (2005). Dental plaque: biological significance of a biofilm and community life-style. J. Clin. Periodontol. **32**: 7-15.

Marsh, P. D., D. J. Bradshaw (1990). The effect of fluoride on the stability of oral bacterial communities *in vitro*. J. Dent. Res. **69**: 668-671.

Martin, G. A., and W. P. Hempfling (1976). A method for the regulation of microbial population density during continuous culture at high growth rates. Arch. Microbiol. **107**: 41-47.

Matsumoto-Nakano, M., and H. K. Kuramitsu (2006). Role of bacteriocin immunity proteins in the antimicrobial sensitivity of *Streptococcus mutans*. J. Bacteriol. **188**: 8095-8102.

McFall, S. M., S. A. Chugani, and A. M. Chakrabarty (1998). Transcriptional activation of the catechol and chlorocatechol operons: variations on a theme. Gene **223**: 257-267.

McLeod, M. P., R. L. Warren, W. W. L. Hsiao, N. Araki, M. Myhre, C. Fernandes, D. Miyazawa, W. Wong et al. (2006). The complete genome of *Rhodococcus* sp. RHA1 provides insights into a catabolic powerhouse. Proc. Natl. Acad. Sci. USA **103**: 15582-15587.

Mercer, D. K., K. P. Scott, C. M. Melville, L. A. Glover, and H. J. Flint (2001). Transformation of an oral bacterium via chromosomal integration of free DNA in the presence of human saliva. FEMS Microbiol. Lett. **200**: 163-167.

Mercer, D. K., K. P. Scott, W. A. Bruce-Johnston, L. A. Glover, and H. J. Flint (1999). Fate of free DNA and transformation of the oral bacterium *Streptococcus gordonii* DL1 by plasmid DNA in human saliva. Appl. Environ. Microbiol. **65**: 6-10.

Mikx, F. H., and J. S. van der Hoeven (1975). Symbiosis of *Streptococcus mutans* and *Veillonella alcalescens* in mixed continuous culture. Arch. Oral Microbiol. **20**: 407-410.

Miyauchi, K., S. K. Suh, Y. Nagata, and M. Takagi (1998). Cloning and sequencing of a 2,5-dichlorohydroquinone reductive dehalogenase gene whose product is involved in degradation of gamma-hexachlorocyclohexane by *Sphingomonas paucimobilis*. J. Bacteriol. **180**: 1354-1359.

Molin, S., M. Givskov (1999). Application of molecular tools for *in situ* monitoring of bacterial growth activity. Environ. Microbiol. **1**: 383-391.

Monod, J. (1950). La technique de culture continue, theorie et applications. Ann. Inst. Pasteur **79**: 390-410.

Moonen, M. J. H., S. A. Synowsky, W. A. M. van den Berg, A. H. Westphal, A. J. R. Heck, R. H. H. van den Heuvel, M. W. Fraaije, and W. J. H. van Berkel (2008a). Hydroquinone dioxygenase from *Pseudomonas fluorescens* ACB: a novel member of the family of nonheme-iron(II)-dependent dioxygenases. J. Bacteriol. **190**: 5199-5209.

Moonen, M. J. H., N. M. Kamerbeek, A. H. Westphal, S. A. Boeren, D. B. Janssen, M. W. Fraaije, and W. J. H. van Berkel (2008b). Elucidation of the 4-hydroxyacetophenone catabolic pathway in *Pseudomonas fluorescens* ACB. J. Bacteriol. **190**: 5190-5198.

Moore, E. R. B., M. Mau, A. Arnscheidt, E. C. Böttger, R. A. Hutson, M. D. Collins, Y. van de Peer, R. de Wachter, and K. N. Timmis (1996). The determination and comparison of the 16S rRNA gene sequences of species of the genus *Pseudomonas* (sensu stricto) and estimation of the natural intrageneric relationships. System. Appl. Microbiol. **19**: 478-492.

Nagata, Y., R. Endo, M. Ito, Y. Ohtsubo, and M. Tsuda (2007). Aerobic degradation of lindane (gamma-hexachlorocyclohexane) in bacteria and its biochemical and molecular basis. Appl. Microbiol. Biotechnol. **76**: 741-752.

Nakai, C., H. Uyeyama, H. Kagamiyama, T. Nakazawa, S. Inouye, F. Kishi, A. Nakazawa and M. Nozaki (1995). Cloning, DNA sequencing, and amino acid sequencing of catechol 1,2-dioxygenases (pyrocatechase) from *Pseudomonas putida* mt-2 and *Pseudomonas arvilla* C-1. Arch. Biochem. Biophys. **321**: 353-362.

Nakazawa, T., and E. Hayashi (1978). Phthalate and 4-hydroxyphthalate metabolism in *Pseudomonas testosteroni*: purification and properties of 4,5-dihydroxyphthalate decarboxylase. Appl. Environ. Microbiol. **36**: 264-269.

Nebe-von-Caron G., P. J. Stephens, C. J. Hewitt, J. R. Powell, and R. A. Badley (2000). Analysis of bacterial function by multi-colour fluorescence flow cytometry and single cell sorting. J. Microbiol. Methods **42**: 97-114.

Nelson, K. E., C. Weinel, I. T. Paulsen, R. J. Dodson, H. Hilbert, V. A. P. Martins dos Santos, D. E. Fouts, S. R. Gill et al. (2002). Complete genome sequence and comparative analysis of the metabolically versatile *Pseudomonas putida* KT2440. Environ. Microbiol. **4**: 799-808.

Nes, I. F., D. B. Diep, and H. Holo (2007). Bacteriocin diversity in *Streptococcus* and *Enterococcus*. J. Bacteriol. **189**: 1189-1198.

Nicholson, M. L., M. Gaasenbeek and D. E. Laudenbach (1995). Two enzymes together capable of cysteine biosynthesis are encoded on a cyanobacterial plasmid. Mol. Gen. Genet. **247**: 623-632.

Nikodem, P., V. Hecht, M. Schlömann and D. H. Pieper (2003). New bacterial pathway for 4- and 5-chlorosalicylate degradation via 4-chlorocatechol and maleylacetate in *Pseudomonas* sp. strain MT1. J. Bacteriol. **185**: 6790-6800.

Nikodem, P. (2004). New bacterial pathway of 4- and 5-chlorosalicylate degradation via 4-chlorocatechol and maleylacetate in a *Pseudomonas* strain. PhD Thesis, TU Braunschweig.

Nojiri, H., K. Maeda, H. Sekiguchi, M. Urata, M. Shintani, T. Yoshida, H. Habe and T. Omori (2002). Organization and transcriptional characterization of catechol degradation genes involved in carbazole degradation by *Pseudomonas resinovorans* strain CA10**.** Biosci. Biotechnol. Biochem. **66**: 897-901.

Nordin, K., M. Unell, and J. K. Jansson (2005). Novel 4-chlorophenol degradation gene cluster and degradation route *via* hydroxyquinol in *Arthrobacter chlorophenolicus* A6. Appl. Environ. Microbiol. **71**: 6538-6544.

Notley-McRobb, L., and T. Ferenci (1999). The generation of multiple co-existing *mal*-regulatory mutations through polygenic evolution in glucose-limited populations of *Escherichia coli*. Environ. Microbiol. **1**: 45-52.

Novick, A., and L. Szilard (1950a). Description of the chemostat. Science **112**: 715-716.

Novick, A., and L. Szilard (1950b). Experiments with the chomstat on spontaneous mutations of bacteria. Proc. Natl. Acad. Sci. USA **36**: 708-719.

Nyvad, B., M. Kilian (1987). Microbiology of the early colonization of human enamel and root surfaces *in vivo*. Scand. J. Dent. Res. **95**: 369-380.

Olivera, E. R., B. Minambres, B. Garcia, C. Muniz, M. A. Moreno, A. Ferrandez, E. Diaz, J. L. Garcia, and J. M. Luengo (1998). Molecular characterization of the phenylacetic acid catabolic pathway in *Pseudomonas putida* U: the phenylacetyl-CoA catabolon. Proc. Natl. Acad. Sci. USA **95**: 6419-6424.

Overhage, J., H. Priefert, and A. Steinbuchel (1999). Biochemical and genetic analyses of ferulic acid catabolism in *Pseudomonas* sp. strain HR199. Appl. Environ. Microbiol. **65**: 4837-4847.

Park, W., P. Padmanabhan, S. Padmanabhan, G. J. Zylstra and E. L. Madsen (2002). *NahR*, encoding a LysR-type transcriptional regulator, is highly conserved among naphthalene-degrading

bacteria isolated from a coal tar waste-contaminated site and in extracted community DNA**.** Microbiology **148**: 2319-2329.

Paster, B. J., I. Olsen, J. A. Aas, and F. E. Dewhirst (2006). The breadth of bacterial diversity in the human periodontal pocket and other oral sites. Periodontology 2000. **42**: 80-87.

Paster, B. J., S. K. Boches, J. L. Galvin, R. E. Ericson, C. N. Lau, V. A. Levanos, A. Sahasrabudhe, and F. E. Dewhirst (2001). Bacterial diversity in human subgingival plaque. J. Bacteriol. **183**: 3770-3783.

Pawelczyk, S., D. Bumann, and W.-R. Abraham (2010). Kinetics of carbon sharing in a bacterial consortium revealed by combining stable isotope probing with fluorescence-activated cell sorting. J. Appl. Microbiol. **110**: 1065-1073.

Pelz, O. (1999). Functional characterization of a 4-chlorosalicylate-degrading bacterial community by $\delta^{13}C$ labeling biomarkers. PhD Thesis, TU Braunschweig.

Pelz, O., M. Tesar, R.-M. Wittich, E. R. B. Moore, K. N. Timmis and W.-R. Abraham (1999). Towards elucidation of microbial community metabolic pathway: unravelling the network of carbon sharing in a pollutant degrading bacterial consortium by immunocapture and isotopic ratio mass spectrometry. Environ. Microbiol. **1**: 167-174.

Peng, X., N. Misawa, and S. Harayama (2003). Isolation and characterization of thermophilic *Bacilli* degrading cinnamic, 4-coumaric, and ferulic acids. Appl. Environ. Microbiol. **69**: 1417-1427.

Perez-Pantoja, D., R. De la Iglesia, D. H. Pieper, and B. Gonzalez (2008). Metabolic reconstruction of aromatic compounds degradation from the genome of the amazing pollutant-degrading bacterium *Cupriavidus necator* JMP134. FEMS Microbiol. Rev. **32**: 736-794.

Perez-Pantoja, D., R. Donoso, L. Agullo, M. Cordova, M. Seeger, D. H. Pieper, and B. Gonzalez (2011). Genomic analysis of the potential for aromatic compounds biodegradation in *Burkholderiales*. Environ. Microbiol. doi:10/1111/j.1462-2920.2011.02613.x.

Perez-Pantoja, D., B. Gonzalez, and D. H. Pieper (2010a). Aerobic degradation of aromatic hydrocarbons. In: K. N. Timmis (ed.) Handbook of hydrocarbon and lipid microbiology. Springer Verlag Berlin Heidelberg, pp. 799-837.

Perez-Pantoja, D., R. Donoso, H. Junca, B. Gonzalez, and D. H. Pieper (2010b). Phylogenomics of aerobic bacterial degradation of aromatics. In: K. N. Timmis (ed.) Handbook of hydrocarbon and lipid microbiology. Springer Verlag Berlin Heidelberg, pp. 1355-1397.

Pieper, D. H., B. Gonzalez, B. Camara, D. Perez-Pantoja, and W. Reineke (2010). Aerobic degradation of chloroaromatics. In: K. N. Timmis (ed.) Handbook of hydrocarbon and lipid microbiology. Springer Verlag Berlin Heidelberg, pp. 839-864.

Pieper, D. H., K. Pollmann, P. Nikodem, B. Gonzalez, and V. Wray (2002). Monitoring key reactions in degradation of chloroaromatics by in situ ^{1}H nuclear magnetic resonance: solution structures of metabolites formed from *cis*-dienelactone. J. Bacteriol. **184**: 1466-1470.

Piper, M. D. W., P. Daran-Lapujade, C. Bro, B. Regenberg, S. Knudsen, J. Nielsen, and J. T. Pronk (2002). Reproducibility of oligonucleotide microarray transcriptome analyses. J. Biol. Chem. **277**: 37001-37008.

Porter, K. G., and Y. S. Feig (1980). The use fo DAPI for identifying and counting aquatic microflora. Limnol. Oceanogr. **25**: 943-948.

Qi, F., P. Chen, and P. W. Caufield (1999). Purification of mutacin III from group III *Streptococcus mutans* UA787 and genetic analysis of mutacin III biosynthesis genes. Appl. Environ. Microbiol. **65**: 3880-3887.

Qi, F., P. Chen, and P. W. Caufield (2001). The group I strain of *Streptococcus mutans*, UA140, produce both the lantibiotic mutacin I and a nonlantibiotic bacteriocin, mutacin IV. Appl. Environ. Microbiol. **67**: 15-21.

Rabenau, A. (2004). Influence of biotic and abiotic factors on the composition and function of a 4-chlorosalicylate degrading consortium. PhD Thesis, TU Braunschweig.

Ramos, J. L., E. Duque, P. Godoy and A. Segura (1998). Efflux pumps involved in toluene tolerance in *Pseudomonas putida* DOT-T1E. J. Bacteriol. **180**: 3323-3329.

Reineke, W. (1998). Development of hybrid strains for the mineralization of chloroaromatics by patchwork assembly. Annu. Rev. Microbiol. **52:** 287-331.

Reineke , W. (2001). Aerobic and anaerobic biodegradation potentials of microorganisms. In: O. Hutzinger (ed.) The handbook of environmental chemistry. Springer Verlag Berlin, pp: 1-161.

Reineke, W., and H.-J. Knackmuss (1984). Microbial metabolism of haloaromatics: isolation and properties of a chlorobenzene-degrading bacterium. Appl. Environ. Microbiol. **47**: 395-402.

Reiner, A., and G. Hegeman (1971). Metabolism of benzoic acid by bacteria. Accumulation of (-)-3,5-cyclohexadiene-1,2-diol-1-carboxylic acid by mutant strain of *Alcaligenes eutrophus*. Biochemistry **10**: 2530-2536.

Romero-Steiner, S., R. E. Parales, C. S. Harwood, and J. E. Houghton (1994). Characterization of the *pcaR* regulatory gene from *Pseudomonas putida*, which is required for the complete degradation of p-hydroxybenzoate. J. Bacteriol. **176:** 5771-5779.

Rubio, M. A., K.-H. Engesser, and H.-J. Knackmuss (1986). Microbial metabolism of chlorosalicylates: accelerated evolution by natural genetic exchange. Arch. Microbiol. **145**: 116-122.

Sambrook, J., E. Fritsch, and T. Maniatis (1989). Molecular Cloning. A Laboratory Manual (2nd Ed.). Cold Spring Harbor Laboratory Press, New York.

Schell, U., S. Helin, T. Kajander, M. Schlömann, and A. Goldman (1999). Structural basis for the activity of two muconate cycloisomerase variants toward substituted muconates. Prot. Struct. Funct. Genet. **34**: 125-136.

Schindowski, A., R.-M. Wittich, and P. Fortnagel (1991). Catabolism of 3,5-dichlorosalicylate by *Pseudomonas* sp. strain JWS. FEMS Microbiol. Lett. **84**: 63-69.

Schleheck, D., T. P. Knepper, K. Fisher, and A. M. Cook (2004). Mineralization of individual congeners of linear alkylbenzenesulfonate by defined pairs of heterotrophic bacteria. Appl. Environ. Microbiol. **70**: 4053-4063.

Schlömann, M., P. Fischer, E. Schmidt, and H.-J. Knackmuss (1990a). Enzymatic formation, stability, and spontaneous reactions of 4-fluoromuconolactone, a metabolite of bacterial degradation of 4-fluorobenzoate. J. Bacteriol. **172**: 5119-5129.

Schlömann, M., E. Schmidt, and H.-J. Knackmuss (1990b). Different types of dienelactone hydrolase in 4-fluorobenzoate-utilizing bacteria. J. Bacteriol. **172**: 5112-5118.

Schmidt, E., and H.-J. Knackmuss (1980). Chemical structure and biodegradability of halogenated aromatic compounds. Conversion of chlorinated muconic acids into maleoylacetic acid. Biochem J. **192**: 339-347.

Schramm, A., L. H. Larsen, N. P. Revsbech, N. B. Ramsing, R. Amann, and K.-H. Schleifer (1996). Structure and function of a nitrifying biofilm as determined by in situ hybridization and the use of microelectrodes. Appl. Environ. Microbiol. **62**: 4641-4647.

Schweigert, N., A. J. B. Zehnder, and R. I. L. Eggen (2001). Chemical properties of catechols and their molecular modes of toxic action in cells, from microorganisms to mammals. Environ. Microbiol. **3**: 81-91.

Seibert, V., K. Stadler-Fritzsche, and M. Schlömann (1993). Purification and characterization of maleylacetate reductase from *Alcaligenes eutrophus* JMP134(pJP4). J. Bacteriol. **175**: 6745-6754.

Senn, H., U. Lendenmann, M. Snozzi, G. Hamer, and T. Egli (1994). The growth of *Escherichia coli* in glucose-limited chemostat cultures: a reexamination of the kinetics. Biochim. Biophys. Acta **1201**: 424-436.

Shen, W., W. Liu, J. Zhang, J. Tao, H. Deng, H. Cao, and Z. Cui (2010). Cloning and characterization of a gene cluster involved in the catabolism of *p*-nitrophenol from *Pseudomonas putida* DLL-E4. Bioresour. Technol. **101**: 7516-7522.

Shimura, M., G. MukerjeeDhar, K. Kimbara, H. Nagato, H. Kiyohara, and T. Hatta (1999). Isolation and characterization of a thermophilic *Bacillus* sp. JF8 capable of degrading polychlorinated biphenyls and naphthalene. FEMS Microbiol. Lett. **178**: 87-93.

Smits, T. H. M, M. Röthlisberger, B, Witholt, and J. B. van Beilen (1999). Molecular screening for alkane hydroxylase genes in Gram-negative and Gram-positive strains. Environ. Microbiol. **1**: 307-317.

Sørensen, S. R., Z. Ronen, and J. Aamand (2002). Growth in coculture stimulates metabolism of the phenylurea herbicide isoproturon by *Sphingomonas* sp. strain SRS2. Appl. Environ. Microbiol. **68**: 3478-3485.

Spence, E. L., M. Kawamukai, J. Sanvoisin, H. Braven and T. D. Bugg (1996). Catechol dioxygenases from *Escherichia coli* (MhpB) and *Alcaligenes eutrophus* (MpcI): sequence analysis and biochemical properties of a third family of extradiol dioxygenases. J. Bacteriol. **178**: 5249-5256.

Sperl, G. T., and G. J. Harvey (1988). Microbial adaptation to bromobenzene in a chemostat. Curr. Microbiol. **17**: 99-103.

Steen, H. B., and T. M. Lindmo (1979). Flow cytometry: a high resolution instrument for everyone. Science **204**:403-404.

Stoffels, M., R. Amann, W. Ludwig, D. Hekmat, and K.-H. Schleifer (1998). Bacterial community dynamics during start-up of a trickle-bed bioreactor degrading aromatic compounds. Appl. Environ. Microbiol. **64**: 930-939.

Takahashi, N., (2003). Acid-neutralizing activity during amino acid fermentation by *Porphyromonas gingivalis, Prevotella intermedia* and *Fusobacterium nucleatum*. Oral Microbiol. Immunol. **18**: 109-113.

Tay, S. T.-L., V. Ivanov, S. Yi, W.-Q. Zhuang, and J.-H. Tay (2002). Presence of anaerobic *Bacteroides* in aerobically grown microbial granules. Mirob. Ecol. **44**: 278-285.

Teanpaisan, R., A. M. Baxter, and C. W. Douglas (1998). Production and sensitivity of bacteriocin-like activity among *Porphyromonas gingivalis, Prevotella intermedia* and *Pr. nigrescens* strains isolated from periodontal sites. J. Med. Microbiol. **47**: 585-589.

Tesar, M., C. Hoch, E. R. B. Moore, and K, N, Timmis (1996). Westprinting: development of a rapid immunochemical identification for species within the genus *Pseudomonas* sensu stricto. Syst. Appl. Microbiol. **19**: 577-588.

Thiel, M., and M. Schlömann (2000). Detection and characterization of genes of chlorocatechol pathways in strains growing on chloroaromatic compounds. Biospektrum VAAM Jahrestagung abstr. 13.P.1.42.

Tillmann, S. (2004). Abschätzung des Abbaupotentials mikrobieller Biozönosen und Identifizierung der am organischen Abbau beteiligten Bakteriengruppen mittels Isotopenmassenspektrometrie (IRMS). PhD Thesis, TU Braunschweig.

van der Hoeven, J. S., A. I. Toorop, and F. H. Mikx (1978). Symbiotic relationship of *Veilllonella alcalescens* and *Streptococcus mutans* in dental plaque in gnobiotic rats. Caries. Res. **12**: 142-147.

van der Kooji, D., J. P. Oranje, and W. A. M. Hijnen (1982). Growth of *Pseudomonas aeruginosa* in tap water in relation to utilization of substrates at concentrations of few micrograms per liter. Appl. Environ. Microbiol. **44**: 1086-1095.

van der Meer, J. R., R. I. Eggen, A. J. Zehnder and de W. M. Vos (1991). Sequence analysis of the *Pseudomonas* sp. strain P51 *tcb* gene cluster, which encodes metabolism of chlorinated catechols: evidence for specialization of catechol 1,2-dioxygenases for chlorinated substrates**.** J. Bacteriol. **173**: 2425-2434.

van der Meer, J. R., W. Roelofsen, G. Schraa, and A. J. B. Zehnder (1987). Degradation of low concentrations of dichlorobenzenes and 1,2,4-trichlorobenzene by *Pseudomonas* sp. strain P51 in nonsterile soil columns. FEMS Microbiol. Lett. **45**: 333-341.

Venter, J. C., K. Remington, J. F. Heidelberg, A. L. Halpern, D. Rusch, J. A. Eisen, D. Wu, I. Paulsen, K. E. Nelson, W. Nelson, D. E. Fouts, S. Levy, A. H. Knap, M. W. Lomas, K. Nealson, O. White, J. Peterson, J. Hoffman, R. Parsons, H. Baden-Tillson, C. Pfannkoch, Y.-H. Rogers, H. O. Smith (2004). Environmental genome shotgun sequencing of the Sargasso Sea. Science **304**: 66-74.

Verwoert, I. I., E. C. Verbree, K. H. van der Linden, H. J. Nijkamp and A. R. Stuitje (1992). Cloning, nucleotide sequence, and expression of the *Escherichia coli fabD* gene, encoding malonyl coenzyme A-acyl carrier protein transacylase. J. Bacteriol. **174**: 2851-2857.

Wagner, M., R. Amann, H. Lemmer and K.-H. Schleifer (1993). Probing activated sludge with oligonucleotides specific for Proteobacteria: inadequacy of culture-dependent methods for describing microbial community structure. Appl. Environ. Microbiol. **59**: 1520-1525.

Wagner, M., R. Erhart, W. Manz, R. Amann, H. Lemmer, D. Wedi, and K.-H. Schleifer (1994). Development of an rRNA-targeted oligonucleotide probe specific for the genus *Acinetobacter* and its application for *in situ* monitoring in activated sludge. Appl. Environ. Microbiol. **60**: 792-800.

Wallner, G., R. Erhart, and R. I. Amann (1995). Flow cytometric analysis of activated sludge with rRNA-targeted probes. Appl. Environ. Microbiol. **61**: 1859-1866.

Wang, B.-Y., and H. K. Kuramitsu (2005). Interactions between oral bacteria: inhibition of *Streptococcus mutans* bacteriocin production by *Streptococcus gordonii*. Appl. Environ. Microbiol. **71**: 354-362.

Watanabe, K., M. Teramoto, H. Futamata, and S. Harayama (1998). Molecular detection, isolation and physiological characterization of functionally dominant phenol-degrading bacteria in activate sludge. Appl. Environ. Microbiol. **64**: 4396-4402.

Whittaker, C. J., C. M. Klier, P. E. Kolenbrander (1996). Mechanism of adhesion by oral bacteria. Annu. Rev. Microbiol. **50**: 513-552.

Wiebe, M. G., G. D. Robson, S. G. Oliver, and A. P. J. Trinci (1994). Evolution of *Fusarium graminearum* A3/5 grown in a glucose-limited chemostat culture at a slow dilution rate. Microbiol. **140**: 3023-3029.

Wittich, R-M., C. Strömpl, E. R. B. Moore, R. Blasco, and K. N. Timmis (1999). Interactions of *Sphingomonas* and *Pseudomonas* strains in the degradation of chlorinated dibenzofurans. J. Ind. Microbiol. Biot. **23**: 353-358.

Woese, C. R. (1987). Bacterial evolution. Microbiol. Rev. **51**: 221-271.

Woese, C. R., E. Stackebrandt, T. J. Macke, and G. E. Fox (1985). A phylogenetic definition of the major eubacterial taxa. Syst. Appl. Microbiol. **6**: 143-151.

Wu, J., N. Zhang, A. Hayes, K. Panoutsopoulou, and S. G. Oliver (2004). Global analysis of nutrient control of gene expression in *Saccharomyces cerevisiae* during growth and starvation. Proc. Natl. Acad. Sci USA **101**: 3148-3153.

Yamamoto, S., M. Katagiri, H. Maeno, and O. Hayashi (1965). Salicylate hydroxylase, a monooxygenase requiring flavin adenine dinucleotide. I. Purification and general properties. J. Biol. Chem. **240**: 3408-3413.

You, I. S., D. Ghosal and I. C. Gunsalus (1988). Nucleotide sequence of plasmid NAH7 gene *nahR* and DNA binding of the nahR product. J. Bacteriol. **170**: 5409-5415.

You, I. S., D. Ghosal and I. C. Gunsalus (1991). Nucleotide sequence analysis of the *Pseudomonas putida* PpG7 salicylate hydroxylase gene (*nahG*) and its 3'-flanking region**.** Biochemistry **30**: 1635-1641.

You, I. S., R. I. Murray, D. Jollie and I. C. Gunsalus (1990). Purification and characterization of salicylate hydroxylase from *Pseudomonas putida* PpG7. Biochem. Biophys. Res. Commun. **169**: 1049-1054.

Zaar, A., J. Gescher, W. Eisenreich, A. Bacher, and G. Fuchs (2004). New enzymes involved in aerobic benzoate metabolism in *Azoarcus evansii*. Mol. Microbiol. **54**: 223-238.

Zhou, N.-Y., J. Al-Dulayymi, M. S. Baird, and P. A. Williams (2002). Salicylate 5-hydroxylase from *Ralstonia* sp. strain U2: a monooxygenase with close relationships to and shared electron transport proteins with naphthalene dioxygenase. J. Bacteriol. **184**: 1547-1555.

Zoetendal, E. G., K. Ben-Amor, H. J. M. Harmsen, F. Schut, A. D. L. Akkermans, and W. M. de Vos (2002). Quantification of uncultured *Ruminococcus obeum*-like bacteria in human fecal samples by fluorescent in situ hybridization and flow cytometry using 16S rRNA-targeted probes. Appl. Environ. Microbiol. **68**: 4225-4232.

Zylstra, G. J., R. H. Olsen and D. P. Ballou (1989). Genetic organization and sequence of the *Pseudomonas cepacia* genes for the alpha and beta subunits of protocatechuate 3,4-dioxygenase. J. Bacteriol. **171**: 5915-5921.

APPENDIX

Table A.1. List of sequencing primers used in this study.

Primer	Sequence (5'→3')	Primer	Sequence (5'→3')
MT1:mci-1B_T3a	ATT GGC TGC TAA CTT AGG CG	MT4:diox-B_T7b	GAT CTC AGC AAT CGA GCA G
MT1:mci-1B_T3b	GCA GCA ACA CTT GCT GGT G	MT4:diox-B_T7c	GTA TTG ATA CGC TGT AGC G
MT1:mci-1B_T3c	GCA TCA TCA GTG TAT CCG CT	MT4:mr-1_T3b	CGA TAG ACA GTT GGC AAG G
MT1:mci-1B_T3d	CAG TTC CAT GGT TAC GCT CT	MT4:mr-1_T3c	GGC AAT ATC ATC CAA TCG GC
MT1:mci-1B_T7a	GAT TGG CAC CTA TCT TCA C	MT4:mr-1_T7b	TGC AAC ACA AGA TTG CGT TG
MT1:mci-1B_T7b	CGA ATC AGG AAC AGT CCG AT	MT4:mr-1_T7c	TCG GTT GAA ATC ATC AGC GG
MT1:mci-1B_T7c	GCA GCT GGC TGA CCA ACA G	MT4:mr-1_T7d	ACT GTG CTT TCA AGC TCG GC
MT1:mci-1B_T7d	GGT TTG AGC GCA GAC GAT CA	MT4:mr-1_UPb	ATT TCC GAA CCG GCA TAG G
MT1:mci-1K_T3a	TGA TCT TGT CCA GAC GCT GG	MT4:mr-1_UPc	TTC GTC GGT ACT GAA TCG C
MT1:mci-1K_T3b	CTG CTC TAC AAA CGG AAC AG	MT4:mr-1_UPd	GTC ATC AAC TCG ACG ATG CG
MT1:mci-1K_T7a	TGA TCG TTC TCA ACC AGA C	MT4:mr-1_UPe	TCG GTG ACT TCG GTG TGC A
MT1:mci-1K_T7b	CGC GAC AAC CTG ATC GAC A	MT4:mr-1_DWb	ATC CAA ATG ACC CGC AAG CC
MT1:mci-1O_T3a	ATT GCA AAC CGA CGA TAG GC	MT4:mr-1_DWc	CAA GCA GAT CAT GCA AAG CC
MT1:mci-1O_T7a	CTG TCA AGT AAG CCT CGC	MT1:carb-1A_T3b	GTA TGC TTC GTA GGC ATC G
MT1:mci-3E_T3a	CCT CTT GTT GTT GAT AGT CG	MT1:carb-1A_T3c	CTT GCG TGA TCT CGA AGC
MT1:mci-3E_T3b	GTT GCT TTC TTT AAC TCC AGG	MT1:carb-1A_T3d	CAA CGT TGC GGA CGA TTA C
MT1:mci-3M_T3a	GAT GCG CTG TAT GAG CAT AC	MT1:carb-1A_T3e	TCT GGT GCT GAC TGC GAT G
MT1:mci-3V_T3a	TTG ATC TGT CCA CAC CAT GG	MT1:carb-1A_T7b	CGA TGA CAG CAG CAT GGA C
MT1:mci-3V_T3b	GCG TTT ACC GAG CGA TAC G	MT1:carb-1A_T7c	GCG ACT ACA GCA ACA ACG
MT1:mci-3V_T7a	AGC CAC ATG AGG TAC TGT AG	MT1:carb-1B_T3b	GTC CAG CAG ATG ATC CAG
MT1:mci-1A9_T3b	TGC TGT TCT GGG TGT ATG G	MT1:carb-1D_T3b	ATC CGT TGC TCG AAT GCG
MT1:mci-1A9_T3c	AGC GCT TGA ACC AGA GCT G	MT1:carb-2A_T3b	CGA GTT GAA CGA AAG CCA C
MT1:mci-1A9_T3d	GCC ATC ATG CAG GTG TTC G	MT1:carb-2A_T7b	TGA TGC CGA AAC GGT GTT C
MT1:mci-1A9_DWb	CTG ACC TTG AAG AAG CTG G	MT1:carb_UP	CGT TTT CGA TCA GTT CCA GC
MT1:mci-1A9_DWc	ATG GCA GTG AAG ATG ACG TC	MT1:carb_UPb	CAC GTT CTT CAG GCT CAG
MT1:mci-1A9_DWd	GAT GCT CGT TAA CGA TGA CG	MT1:carb_UPc	GGA ACA GCG AAA TCA ACG
MT4:diox-A_T3b	ACA GCG TCA AGG TGA GCA TG	MT1:carb_UPd	TGC GTT TGC TGC GTT CTT C
MT4:diox-A_T3c	CAC GCT GGA GAT TTC CAG	MT1:carb_DW	TGC TGT CGA CGC TGT TCA G
MT4:diox-A_T7b	TCG GCC AAT ACG GCA ACA G	MT1:carb_DWb	TGT CCA ACT CAC TGG GTA C
MT4:diox-A_T7c	GCG ATG GCG ATC AAC AAC	MT1:carb_DWc	TCA TTC AGG AAC ATG TGC C
MT4:diox-B_T3b	CGG ATT TCT GAC AGC ACT G	MT1:carb_DICARB	ACC CAG CAC GGT GAT GAA C
MT4:diox-B_T3c	TTA CCG AAC GTA GTC CAG	MT1:carb_PDIOX	AGG CCG ATG TGG TAG TAC
		MT1:carb_PDIOX2	AGG TCG TTG TCC TTC TCG

```
          10        20        30        40        50        60        70        80
     ....|....|....|....|....|....|....|....|....|....|....|....|....|....|....|
MT1  TCCCGAAGGTTA-GACTAGCTACTTCTGGTGCAACCCACTCCCATGGTGTGACGGGCGGTGTGTACAAGGCCCGGGAACG
MT4  -CCCGAAGGTTA-GACTAGCTACTTCTGGTGCAACCCACTCCCATGGTGTGACGGGCGGTGTGTACAAGGCCCGGGAACG
MT3  CCCTTGCGGTTA-GGCTAACTACTTCTGGTAAAACCCACTCCCATGGTGTGACGGGCGGTGTGTACAAGACCCGGGAACG
MT2  CCGCTCCTTTTACGGTCACCGACTTCAGGTACCCCCAGCTTCCATGGCTTGACGGGCGGTGTGTACAAGGCCCGGGAACG

          90       100       110       120       130       140       150       160
     ....|....|....|....|....|....|....|....|....|....|....|....|....|....|....|
MT1  TATTCACCGCGACATT-CTGATTCGCGATTACTAGCGATTCCGACTTCACGCAGTCGAGTTGCAGACTGCGATCCGGACT
MT4  TATTCACCGCGACATT-CTGATTCGCGATTACTAGCGATTCCGACTTCACGCAGTCGAGTTGCAGACTGCGATCCGGACT
MT3  TATTCACCGCGACATG-CTGATCCGCGATTACTAGCGATTCCGACTTCACGCAGTCGAGTTGCAGACTGCGATCCGGACT
MT2  TATTCACCGCATCATGGCTGATATGCGATTACTAGCGATTCCAGCTTCATAGAGTCGAGTTGCAGACTCCAATCCGAACT

         170       180       190       200       210       220       230       240
     ....|....|....|....|....|....|....|....|....|....|....|....|....|....|....|
MT1  ACGATCGGTTTTATGGGATTAGCTCCACCTCGCGGCTTGGCAACCCTCTGTACCGACCATTGTAGCACGTGTGTAGCCCA
MT4  ACGATCGGTTTTCTGGGATTAGCTCCACCTCGCGGCTTGGCAACCCTCTGTACCGACCATTGTAGCACGTGTGTAGCCCA
MT3  ACGATCGGGTTTCTGGGATTGGCTCCCCCTCGCGGGTTGGCGACCCTCTGTCCCGACCATTGTATGACGTGTGAAGCCCT
MT2  GAGATAAGTTTTC-GAGATTCGCATCTTGTTGCCAAGTAGCTGCCCTCTGTACTTACCATTGTAGCACGTGTGTAGCCCA

         250       260       270       280       290       300       310       320
     ....|....|....|....|....|....|....|....|....|....|....|....|....|....|....|
MT1  GGCCGTAAGGGCCATGATGACTTGACGTCATCCCCACCTTCCTC-CGGTTTGTCACCGGCAGTCTCCTTAGAGTGCCCAC
MT4  GGCCGTAAGGGCCATGATGACTTGACGTCATCCCCACCTTCCTC-CGGTTTGTCACCGGCAGTCTCCTTAGAGTGCCCAC
MT3  ACCCATAAGGGCCATGAGGACTTGACGTCATCCCCACCTTCCTC-CGGTTTGTCACCGGCAGTCTCATTAGAGTGCCC--
MT2  AGACGTAAGGGCCGTGATGACTTGACGTCGTCCCCACCTTCCTCGCGGTTTG-CACCGGCAGTCTCATTAGAGTCCCCGT

         330       340       350       360       370       380       390       400
     ....|....|....|....|....|....|....|....|....|....|....|....|....|....|....|
MT1  CATAACGTGCTGGTAACTAAGGACAAGGGTTGCGCTCGTTACGGGACTTAACCCAACATCTCACGACACGAGCTGACGAC
MT4  CATTACGTGCTGGTAACTAAGGACAAGGGTTGCGCTCGTTACGGGACTTAACCCAACATCTCACGACACGAGCTGACGAC
MT3  --TTTCGT---AGCAACTAATGACAAGGGTTGCGCTCGTTGCGGGACTTAACCCAACATCTCACGACACGAGCTGACGAC
MT2  CTTTAAACGCTGGCAACTAATGATAGGGGTTGCGCTCGTTGCAGGACTTAACCTAACACCTCACGGCACGAGCTGACGAC

         410       420       430       440       450       460       470       480
     ....|....|....|....|....|....|....|....|....|....|....|....|....|....|....|
MT1  AGCCATGCAGCACCTGTCT--CAATGTTCCCGAAGGCACCAATCCATCTCTGGAAAGTTCATTGGATGTC-AAGGCCTGG
MT4  AGCCATGCAGCACCTGTCT--CAATGTTCCCGAAGGCACCAATCTATCTCTAGAAAGTTCATTGGATGTC-AAGGCCTGG
MT3  AGCCATGCAGCACCTGTGTTCCGGTTCTCTTGCGAGCACTTCCAAATCTCTTCGGAATTCCAGACATGTC-AAGGGTAGG
MT2  AGCCATGCAGCACCTTG----CATTCTGTCCGAAGAAA--AATCTATTTCTAGATCTGTCAAATTGCATTTAAGCCTTGG

         490       500       510       520       530       540       550       560
     ....|....|....|....|....|....|....|....|....|....|....|....|....|....|....|
MT1  TAAGGTTCTTCGCGTTGCTTCGAATTAAACCACATGCTCCACCGCTTGTGCGGGCCCCCGTCAATTCATTTGAGTTTTAA
MT4  TAAGGTTCTTCGCGTTGCTTCGAATTAAACCACATGCTCCACCGCTTGTGCGGGCCCCCGTCAATTCATTTGAGTTTTAA
MT3  TAAGGTTTTTCGCGTTGCATCGAATTAATCCACATCATCCACCGCTTGTGCGGGTCCCCGTCAATTCCTTTGAGTTTTAA
MT2  TAAGGTTCCTCGCGTATCATCGAATTAAACCACATGCTCCACCGCTTGTGCGGGCCCCCGTCAATTCCTTTGAGTTTCAT

         570       580       590       600       610       620       630       640
     ....|....|....|....|....|....|....|....|....|....|....|....|....|....|....|
MT1  CCTTGCGGCCGTACTCCCCAGGCGGTCAACTTAATGCGTTAGCTGCGCCACTAAGAGCTCAAGGCTCCCAACGGCTAGTT
MT4  CCTTGCGGCCGTACTCCCCAGGCGGTCAACTTAATGCGTTAGCTGCGCCACTAAGAGCTCAAGGCTCCCAACGGCTAGTT
MT3  TCTTGCGACCGTACTCCCCAGGCGGTCAACTTCACGCGTTAGCTGCGCTACCAAG-GCCCGAAGGCCCCAACAGCTAGTT
MT2  TCTTGCGAACGTACTCCCCAGGTGGGATACTTATAACTTTCGCTTAGCCACTGAG---TCCGAAAACCCAACAGCAAGTA

         650       660       670       680       690       700       710       720
     ....|....|....|....|....|....|....|....|....|....|....|....|....|....|....|
MT1  GACATCGTTTACGGCGTGGACTACCAGGGTATCTAATCCTGTTTGCTCCCCACGCTTTCGCACCTCAGTGTCAGTATCAG
MT4  GACATCGTTTACGGCGTGGACTACCAGGGTATCTAATCCTGTTTGCTCCCCACGCTTTCGCACCTCAGTGTCAGTATCAG
MT3  GACATCGTTTAGGGCGTGGACTACCAGGGTATCTAATCCTGTTTGCTCCCCACGCTTTCGTGCATGAGCGTCAGTGTTAT
MT2  TCCATCGTTTACGGCGTGGACTACCAGGGTATCTAATCCTGTTCGCTCCCCACGCTTTCGTCCATCAGCGTCAGTTGAGA

         730       740       750       760       770       780       790       800
     ....|....|....|....|....|....|....|....|....|....|....|....|....|....|....|
MT1  TCCAGGTGGTCGCCTTCGCCACTGGTGTTCCTTCCTATATCTACGCATTTCACCGCTACACAGGAAATTCCACCACCCTC
MT4  TCCAGGTGGTCGCCTTCGCCACTGGTGTTCCTTCCTATATCTACGCATTTCACCGCTACACAGGAAATTCCACCACCCTC
MT3  CCCAGGAGGCTGCCTTCGCCATCGGTGTTCCTCCGCATATCTACGCATTTCACTGCTACACGCGGAATTCCACCTCCCTC
MT2  CTTAGTGACCTGCCTTCGCAATTGGTGTTCTGCGTAATATCTAAGCATTTCACCGCTACACTACACATTCCAGCCACTTC
```

```
          810       820       830       840       850       860       870       880
     ....|....|....|....|....|....|....|....|....|....|....|....|....|....|....|
MT1  TACCATACTCTAGCTTGTCAGTTTTGAATGCAGTTCCCAGGTTGAGCCCGGGGATTTCACATCCAACTTAACAAACCACC
MT4  TACCATACTCTAGTCAGTCAGTTTTGAATGCAGTTCCCAGGTTGAGCCCGGGGATTTCACATCCAACTTAACTAACCACC
MT3  TGACACACTCTAGCTCGGTAGTTAAAAATGCAGTTCCAAAGTTAAGCTCTGGGATTTCACATCTTTCTTTCCGAACCGCC
MT2  AAACTCACTCAAGACTAACAGTATCAATGGCAGTTTCATAGTTAAGCTATGAGATTTCACCACTGACTGATTAATCCGCC

          890       900       910       920       930       940       950       960
     ....|....|....|....|....|....|....|....|....|....|....|....|....|....|....|
MT1  TACGCGCGCTTTACGCCCAGTAATTCCGATTAACGCTTGCACCCTCTGTATTACCGCGGGCTGCTGGCACAGAGTTAGCC
MT4  TACGCGCGCTTTACGCCCAGTAATTCCGATTAACGCTTGCACCCTCTGTATTACCGCGG-CTGCTGGCACAGAGTTAGCC
MT3  TGCGCACGCTTTACGCCCAGTAATTCCGATTAACGCTTGCACCCTACGTATTACCGCGG-CTGCTGGCACGTAGTTAGCC
MT2  TACGGACCCTTTAAACCCAATAAATCCGGATAACGCTTGCACCCTCCGTATTACCGCGG-CTGCTGGCACGGAGTTAGCC

          970       980       990       1000      1010      1020      1030      1040
     ....|....|....|....|....|....|....|....|....|....|....|....|....|....|....|
MT1  GGTGCTTATTCTGTCGGTAACGTCAAAATTGCAGAGTATTAATCTACAACCCTTCCTCCCAACTTAAAGTGCTTTACAAT
MT4  GGTGCTTATTCTGTCGGTAACGTCAAAACAATCACGTATTAGGTAACTGCCCTTCCTCCCAACTTAAAGTGCTTTACAAT
MT3  GGTGCTTATTCTGCAGGTACCGTCAGTTTCACGGGGTATTAACCCATGACGTTTCTTTCCTGCCAAAAGTGCTTTACAAC
MT2  GGTGCTTATTCTTCTGGTACCTTCAGCTACTTA------CACGTAAGTAGGTTTATCCCCAGATAAAAGTAGTTTACAAC

          1050      1060      1070      1080      1090      1100      1110      1120
     ....|....|....|....|....|....|....|....|....|....|....|....|....|....|....|
MT1  CCG-AAGACCTTCTTCACACACGCGGCATGGCTGGATCAGGCTTTCGCCCATTGTCCAATATTCCCCACTGCTGCCTCCC
MT4  CCG-AAGACCTTCTTCACACACGCGGCATGGCTGGATCAGGCTTTCGCCCATTGTCCAATATTCCCCACTGCTGCCTCCC
MT3  CCG-AAGGCCTTCATCGCACACGCGGGATGGCTGGATCAGGGTTTCCCCCATTGTCCAAAATTCCCCACTGCTGCCTCCC
MT2  CCATAAGGCCGTCATCCTACACGCGGGATGGCTGGATCAGGCTTCCACCCATTGTCCAATATTCCTCACTGCTGCCTCCC

          1130      1140      1150      1160      1170      1180      1190      1200
     ....|....|....|....|....|....|....|....|....|....|....|....|....|....|....|
MT1  GTAGGAGTCTGGACCGTGTCTCAGTTCCAGTGTGACTGATCATCCTCTCAGACCAGTTACGGATCGTCGCCTTGGTGAGC
MT4  GTAGGAGTCTGGACCGTGTCTCAGTTCCAGTGTGACTGATCATCCTCTCAGACCAGTTACGGATCGTCGCCTTGGTGAGC
MT3  GTAGGAGTCTGGGCCGTGTCTCAGTCCCAGTGTGGCTGGTCGTCCTCTCAAACCAGCTACGGATCGTCGCCTTGGTGAGC
MT2  GTAGGAGTCTGGTCCGTGTCTCAGTACCAGTGTGGGGGTTCACCCTCTCAGGCCCCCTAAAGATCATCGTCTTGGTGAGC

          1210      1220      1230      1240      1250      1260      1270      1280
     ....|....|....|....|....|....|....|....|....|....|....|....|....|....|....|
MT1  CATTACCTCACCAACTAGCTAATCCGACCTAGGCTCATCTGATAGCGCAAGGCCCG--AAGGTCCCCTGCTTTCTCCCGT
MT4  CATTACCTCACCAACTAGCTAATCCGACCTAGGCTCATCTGATAGCGCAAGGCCCG--AAGGTCCCCTGCTTTCTCCCGT
MT3  CNTTACCCCACCAACTAGCTAATCCGATATCGGCCGCTCTAATAGTGCAAGGTCTT--GCGATCCCCTGCTTTCCCCCGT
MT2  CGTTACCTCACCAACTAACTAATCTTACGCATGCCTATCCTACTGCGATAAATCTTTCAAAATTTCATGATGCCATGAAT

          1290      1300      1310      1320      1330      1340      1350      1360
     ....|....|....|....|....|....|....|....|....|....|....|....|....|....|....|
MT1  AGGACGTATGCGGTATTAGCGTTCCTTTCGAAACGTTGTCCCCCACTANCAGGCAGATTCC-TAGGCATTACTCACCCGT
MT4  AGGACGTATGCGGTATTAGCGTCCGTTTCCGAACGTTATCCCCCACTACCAGGCAGATTCC-TAGGCATTACTCACCCGT
MT3  AGGGCGTATGCGGTATTAGCCACGCTTTCGCGTAGTTATCCCCCGCTACTAGGCACGTTCC-GATACATTACTCACCCGT
MT2  TCTAT-TATAAAGTATTAATCCTCCTTTCGAAGGGCTATCCTTTTCAGTAGGGCAAGTTGCATACGCGTTACGCACCCGT

          1370      1380      1390      1400      1410      1420      1430      1440
     ....|....|....|....|....|....|....|....|....|....|....|....|....|....|....|
MT1  CCGCCGCTGAATTCAGGAGCAAGCTCCTGTCATCCGCTCGACTTGCATGTGTTAGGCCTGCCGCCAGCGTTCAATCTGAG
MT4  CCGCCGCTCTCAAGAGAAGCAAGCTTCTCTCTACCGCTCGACTTGCATGTGTTAGGCCTGCCGCCAGCGTTCAATCTGAG
MT3  TCGCCACTCGCCACCAGACCGAAGTCCGTGCTGCCGTTCGACTTGCATGTGTAAGGCATCCCGCTAGCGTTCAATCTGAG
MT2  GCGCCGGTCTCTATCTCCCGAAAGA--AATATACCCCTCGGCTTGCATGTGTTAGGCCTCCCGCTAGCGTTCATCCTGAG

          1450
     ....|....|....|..
MT1  CCATGATNAAAACTCT-
MT4  CCATGATCAAAANCTCT
MT3  CCATGATCAAAACTCT-
MT2  CCATGATCAAAACTCT-
```

Figure A.1. Alignment of 16S rDNA sequence fragments from consortium bacteria (reverse complement shown). Highlighted sequences correspond to strain-specific FISH oligoprobes.

Lebenslauf

Filip Jakub Kamiński

Geboren: 24 August 1974 in Łódź, Polen

Ausbildung und berufliche Tätigkeit:

2008-jetzt	**Technisches Assistent** am Centre for Novel Agricultural Products (CNAP), York, Groβbritannien im Bereich Pflanzliches Molekular Biologie
2006-2008	**Vaterschaftsurlaub**
2002-2005	**Anfertigung der Promotion im Fach Mikrobiologie** Gesellschaft für Biotechnologische Forschug – GBF (heute HZI) in der Arbeitsgruppe Mikrobiologie (betreut zuerst durch Dr. Vitor dos Santos, dann durch Prof. Dr. Dietmar H. Pieper)
2001-2002	**Stipendiat der DBU und Nowicki Stiftung** in GBF GmbH, Braunschweig, Deutschland im Bereich Mikrobiologie
1993-2000	**Diplom in Biotechnologie** Politechnika Łódzka, Łódź, Polen
1989-1993	**Abitur** XXI Allgemeinbildende Oberschule, Łódź, Polen

Veröffentlichungen:

Cámara B, Bielecki P, **Kaminski F**, Santos VD, Plumeier I, Nikodem P and Pieper DH. A gene cluster involved in degradation of substituted salicylates via ortho cleavage in Pseudomonas sp. strain MT1 encodes enzymes specifically adapted for transformation of 4-methylcatechol and 3-methylmuconate. Journal of Bacteriology. 2007. 189: 1664-1674.

Schneiker S, Martins dos Santos VAP, Bartels D, Bekel T, Brecht M, Buhrmester J, Chernikova TN, Denaro R, Ferrer M, Gertler C, Goesmann A, Golyshina OV, **Kaminski F**, Khachane AN, Lang S, Linke B, McHardy AC, Meyer F, Nechitaylo T, Pühler A, Regenhardt D, Rupp O, Sabirova JS, Selbitschka W, Yakimov MM, Timmis KN, Vorhölter FJ, Weidner S, Kaiser O, and Golyshin PN. Genome sequence of the ubiquitous hydrocarbon-degrading marine bacterium *Alcanivorax borkumensis*. Nature Biotechnology. 2006. 24: 997-1004.

Kaminski F, Polak J, Kwapisz E, Bielecki S. Plasmids of bacteria degrading hydrocarbons of petroleum oil. Zeszyty Naukowe Politechniki Śląskiej, Seria: Inżynieria Środowiskowa. 2000, 45: 161-170.

Präsentationen und Teilnahme an Internationalen Kongressen:

Kaminski F. Molecular tools for monitoring bacterial populations. Potential and limitations of different methods. Molecular Biology Workshop, Universidade Catholica Portuguesa, Porto, Portugalien. 2003 (Vortrag).

Polak J, Kwapisz E, **Kaminski F**, Bielecki S. Degraders of petroleum hydrocarbons and their plasmids. 10th European Congress on Biotechnology. Biotechnological Challenges in the New Millennium, Madrid, Spanien. 2001 (Poster Präsentation).

Kaminski F, Polak J, Kwapisz E, Bielecki S. Analysis of plasmids in microorganisms degrading hydrocarbons of petroleum oil. 50th Congress of Polish Chemical Society, Łódź, Polen. 2000 (Poster Präsentation).

Kaminski F, DNA analysis in bacteria degrading petroleum hydrocarbons by means of PFGE. Environmental Biotechnology Seminar, Wisła-Jarzębata, Polen. 2000 (Vortrag).